USDA

EPA

United States
Department of
Agriculture

Northeast Watershed Research
Center
University Park PA 16802

United States
Environmental Protection
Agency

Office of Environmental
Processes and Effects Research
Washington DC 20460

EPA-600/7-84-044
March 1984

Research and Development

Hydrology and Water Quality on Stripmined Lands

Interagency Energy/Environment R&D Program Report

Do not remove. This document should be retained in the EPA Region 5 Library Collection.

HYDROLOGY AND WATER QUALITY ON STRIPMINED LANDS

by

A. S. Rogowski and H. B. Pionke
U.S. Department of Agriculture, ARS
Northeast Watershed Research Center
University Park, Pennsylvania 16802

EPA-IAG-D5-E763

Project Officer

Clinton W. Hall
Office of Energy, Minerals and Industry
Washington, D.C. 20250

Office of Research and Development
U.S. Environmental Protection Agency
Washington, D. C. 20250

U.S. Environmental Protection Agen
Region 5, Library (5PL-16)
230 S. Dearborn Street, Room 1670
Chicago, IL 60604

DISCLAIMER

This report has been reviewed by the Office of Energy, Minesoils and Industry, U.S. Environmental Protection Agency, and approved for publication. Approval does not signify that the contents necessarily reflect the views and policies of the U.S. Environmental Protection Agency, nor does mention of trade names or commercial products constitute endorsement or recommendation for use.

FOREWORD

The Federal Water Pollution Control Act Amendments of 1972, in part, stress the control of nonpoint source pollution. Sections 102 (C-1), 208 (b-2,F) and 304(e) authorize basin scale development of water quality control plans and provide for area-wide waste treatment management. The act and the amendments include, when warranted, waters from agriculturally and silviculturally related nonpoint sources, and requires the issuance of guidelines for both identifying and evaluating the nature and extent of nonpoint source pollutants and the methods to control these sources. Research program at the Northeast Watershed Research Center contributes to the aforementioned goals. The major objectives of the Center are to:

- study the major hydrologic and water-quality associated problems of the Northeastern U.S. and
- develop hydrologic and water quality simulation capability useful for land-use planning. Initial emphasis is on the hydrologically most severe land uses of the Northeast.

Within the context of the Center's objectives, stripmining for coal ranks as a major and hydrologically severe land use. In addition, once the site is reclaimed and the conditions of the mining permit are met, stripmined areas revert legally from point to nonpoint sources. As a result, the hydrologic,

physical, and chemical behavior of the reclaimed land needs to be understood directly and in terms of control practices before the goals of Sections 102, 208 and 304 can be fully met.

Signed:

H. B. Pionke

H. B. Pionke
Director
Northeast Watershed
Research Center

ABSTRACT

Studies were conducted to evaluate physical properties of spoils resulting from surface-coal mining and reclamation operations in Clearfield County, Pennsylvania. Bulk density, evapotranspiration, water retention, infiltration, and hydraulic conductivity values were determined at 10 sites randomly located within a 4-ha experimental area. Average bulk density of the surface 0.5-m layer of minesoil was 1,763 kg/m^3 while specific surface at most sites averaged 31 m^2/g. Microlysimeter data indicated that evapotranspiration (ET) on minesoil could be approximated by class-A pan evaporation or by model results. A large amount of spatial variation was observed in infiltration, water retention and hydraulic conductivity values. In the uppermost 0.75 m of the profile most minesoils on the average retained 35 mm of water, between 10 and 1,500 kPa, compared to 136 mm for the adjoining soils. When water was available ET approached potential, however, hydraulic properties of the minesoil would likely lead to droughty conditions and extended periods of plant stress.

Two, 3.6-m deep, 2.4-m diameter caissons were used to measure water movement in reconstituted spoil profile. In here we present details of instrumentation and propose methods for determining spoil-water-retentivity curve and hydraulic conductivity as a function of water content and/or tensiometer pressure including a correction for coarse fragment content. This correction may be significant when modeling flows in spoil materials. During water application we found that on spoil alone, water infiltrated faster and less of it was retained in the profile after drainage than on topsoiled spoil. More sediment moved with

infiltrating water in the topsoiled profile, and oxygen concentrations after application of water were lower than on spoil alone. Similar situations may prevail in the field. During the initial wetting, settlement was considerable and changes in temperature and bulk density were good indicators of water movement within the spoil and topsoiled spoil profiles. However, flow through larger channels did contribute significant amounts of water to the water table in the spoil without being detected by radioactive probes, temperature probes, or tensiometers.

Total acidity provides a reasonable estimate of other major chemical parameters contained in spoil drainage. In caisson percolate, good linear correlations existed between total acidity and Al, total soluble Fe, Mg, and SO_4 concentrations. These exclude the lowest concentrations (<10 meq/L) which normally do not represent the important acid contributing spoils. The relationship between total acidity and Ca, Fe^{+2}, Mn and pH was much less precise.

A partially weathered spoil, containing both pyrite and acid products, exerts the primary control on the concentration of acid products in percolate. Normal variations in hydrology appear less important. This was apparent from analyses of data taken over several caisson runs as well as within one run. Except for extreme hydrologic conditions or the "first flush" of total acidity observed initially, the maximum and stabilized total acidity in percolate increased with spoil depth or as other chemically related spoil properties increased.

The total acidity of percolate appeared related to both the spoil depth in the caisson and to the total acidity of spoil extract. If the total acidity from a spoil layer extract, compared to that of the overlying spoil layers, is substantially greater (about 1 order of magnitude), this spoil layer will

distinctly and identifiably influence percolate quality. Where total acidity is not substantially greater, the spatial and hydrologic variability will tend to mask the contributions from each layer into what appears as a total acidity increase with depth. A substantial increase of total sulfate and pyrite content in the spoil profile (about 1 order of magnitude) corresponded with a similar increase in the total acidity of percolate. Extreme total pyrite or SO_4 concentrations in the spoil profile can be used to delineate the primary total acidity contributing zones.

The concentrations of Cd, Cr, total soluble Fe, Hg, Mn and Zn in spoil extracts exceeded EPA water quality drinking standards from one (Cr) to all (Mn) spoil layers. The standards for Pb and Cu were not exceeded. Generally, trace metal concentrations in the spoil layer extracts agree closely with those observed in the corresponding spoil percolate. The Cu and Zn concentrations in the percolate were considerably higher. In caisson 2, the trace metal concentrations in the spoil layer extract, caisson percolate, and the caisson well agree closely. This suggested that reduction in trace metal concentrations caused by dilution or other processes occurs primarily after entry into the groundwater or stream system rather than in the spoil profile. Concentration of Cu, Zn and Mn in spoil extract could be approximated from the SO_4 concentration.

Potentially there are several chemical and hydrologic problems associated with placement of acid spoil materials. The rational for a deep placement well below the soil surface, and preferably below a water table, is to prevent or minimize oxidation of pyrite to sulfuric acid and associated salts by reducing the supply of oxygen. If, however, substantial sulfuric acid or associated salts are already contained within the spoil because of present or previous mining, handling and reclamation operations (or if large supplies of

indigenous salts exist, placement below a water table) may actually increase the rate of acid and salt leaching. Specific placement of acid- and salt-containing spoil should be aimed at preventing contact with percolating water or rising water tables. We recommend placement based on chemical and physical spoil properties that may affect water percolation and O_2 diffusion rates in the profile. Both the deeper placement of acid spoil and coarser particle size can substantially reduce the amount of acid drainage. Placement above the water table with emphasis on percolate control may be better for high sulfate spoils, while placement below the non-fluctuating water table may be better for pyrite spoils.

CONCLUSIONS

Federal and State surface coal mining reclamation laws have set water quality effluent standards both explicitly and implicitly. To achieve some of these explicit standards, the emphasis is on effluent treatment. In contrast, the groundwater quality standards are not explicit, but instead require that practices or technologies be applied that minimize the degradation in groundwater quality. Essentially, this calls for the proper application of an often nonexistent technology to achieve minimum degradation. From the economic and aesthetic viewpoint the onsite control methods often appear most attractive. If necessary, when used in conjunction with the more expensive offsite effluent treatment processes, onsite controls may help to achieve effluent standards at a substantially reduced cost.

Selecting the onsite control technology to optimize relatively long-term effluent and groundwater quality while minimizing short-term erosion may prove complex and very difficult. By law or necessity, these decisions and their continual updating fall to the appropriate State or Federal agencies, who must designate acceptable technologies or guidelines for selecting these technologies. Part of the problem is that the processes controlling acid production and salt or trace metal losses are not sufficiently well understood on a large enough scale for adequate design of appropriate control technologies. Control methods such as those described here are based on assumptions, and they contain limitations that often make them inappropriate for a particular site. Hence, there is a great need for improved understanding of the systems, and for

innovative application of this understanding to better and more efficiently reclaimed surface coal mines.

Studies dealing with the physical and hydraulic properties of minesoils indicated that surface mining and reclamation operations have resulted in minesoils at 31 m^2/g specific surface and 1,763 kg/m^3 bulk density. On minesoils studied, the bulk density first decreased and then increased with depth. Between 10 and 1,500 kPa tensiometer pressure, most minesoils retained about one-fourth as much water as did natural soils (35 vs. 136 mm). Evapotranspiration from the minesoils could be approximated by class-A pan evaporation results or modeled using an ET model.

Single ring infiltrometer data results and saturated hydraulic conductivity of minesoils were variable. Exposure to the elements for 4 months lowered the mean value of hydraulic conductivity for the minesoils at the site but increased the variability.

The findings of this study have the following hydrologic implications. Where geology is similar to that of the study area, surface mining will generally result in a minesoil with low infiltration rates (high density and low porosity). While evapotranspiration may approach potential rates when water is available, hydraulic properties of minesoil may result in droughty conditions and periods of plant stress. However, hydrologic changes resulting from mining can be highly variable from site to site and will also vary over time as a result of weathering processes.

Investigations were conducted to compare changes in soil morphology and chemistry before and after surface coal mining and reclamation operations in Clearfield County, Pennsylvania. Four minesoil pits located within a disturbed area and four natural soil pits located in adjacent undisturbed areas were described and sampled. The minesoils were classified as Udorthents, three of

the natural soils were classified as Typic Dystrochrepts and one as an Aquic Fragiudult. The most prominent feature of the minesoils was their high degree of coarseness and high rock fragment content; their roots tended to concentrate along soil coarse fragment interface. In general, the chemical constituents of the minesoils were similar to those of the natural soils. However, as a result of extended weathering more total bases have been leached from the natural soils and significantly more extractable aluminum was found in them than in the minesoils. The high content of carboniferous shale and coal fragments in the minesoils affected organic carbon and nitrogen determinations, while comparison of mineralogy suggested that the minesoils studied were derived from the same materials from which the natural soils had originally developed.

Preliminary results of instrumenting two large caissons filled with strip mine-spoil and applying water indicated that on the spoil alone, water initially infiltrated faster and carried much less sediment with it than it did on top-soiled profile. As we applied water to the caissons we also observed the pressure buildup within the profiles. After wetting, oxygen concentrations recovered faster in spoil alone than in topsoiled spoil. In both caissons, infiltrating water reached the water table faster than expected from observing the movement of the wetting front, this was attributed to flow through larger channels.

Two-probe gamma density probe was well suited to measuring the rate of wetting front advance in the spoil, while response time of porous cup tensiometers was delayed. When there was a difference in temperature between the applied water and spoil, thermocouple output registered temperature changes within the profile caused by the wetting-front passage. Water redistribution profiles indicated fast drainage on spoil alone and delayed drainage in the topsoiled profile. Water table data showed that in both caissons more than 50 percent of applied water drained from the profiles studied within 24 h.

Spoil hydraulic properties were obtained experimentally in the laboratory and successfully compared with water content and tensiometer pressure values measured in the caissons. Large corrections appear necessary to adjust spoil retentivity curves for the coarse fragment contents present in most Pennsylvania spoils. This could be significant in simulation and model building.

In a larger context of reclamation and management of spoils this study suggests that total reliance on radioactive probes to monitor water content and movement in the spoil materials may not be warranted. Rapid drainage through large channels can easily go undetected unless water table behavior is monitored closely at the same time.

A number of spoil properties need to be considered before deciding where and how to place acid spoils. Generally these properties relate to and often control percolation and O_2 diffusion rates into the spoil bank. These include porosity, water retention, and particle size distribution of the topsoil, the layer below the topsoil, and the worst acid spoil layer. Depth below surface and differences in particle size distributions can substantially reduce the amount of percolate or slow the amount of O_2 delivered. Analysis of both SO_4 and pyrite concentrations in spoil can identify the worst acid spoil layer for subsequent isolation and can indicate whether placement should be above or below the water table. Placement above the water table with emphasis on percolate control may be a better method for highly SO_4-contaminated spoil, whereas placement below nonfluctuating water table may be best for highly pyritic spoils low in SO_4. In addition, the rate of acid production and loss from spoil can potentially be controlled by increasing the spoil particle size.

We have concluded that the spoil percolate quality is generally stable. The maximum or stabilized total acidity in caisson percolate increased with

spoil depth or other chemically related spoil parameters except for extreme hydrologic conditions. More normal variations in hydrology do not appear to dominate percolate quality.

The spoil percolate quality appears related to both the spoil depth in the caisson, and the quality of the spoil or the spoil extract. If the total acidity of a spoil layer extract is substantially greater than that from overlying layers, this spoil layer will exert an identifiable and dominating influence on percolate quality. Where not substantially greater, the spatial and hydrologic variability will tend to mask the contributions from each layer into what appears as a total acidity increase with depth. A substantial increase of total sulfate and pyrite content of the spoil matrix (about or above 1 order of magnitude) corresponded to similar increases in the total acidity of spoil extract and caisson percolate. Soil layers with extremely high total pyrite or SO_4 matrix concentrations can also be used to delineate the primary total acidity contributing zones in the spoil profile.

We found that the concentration of Cd, Cr, total soluble Fe, Hg, Mn and Zn in spoil extracts exceeded EPA water quality drinking standards from one (Hg) to all (Mn) spoil layers. The standards for Pb and Cu were not exceeded. Generally, the trace metal concentration in the spoil extracts agreed closely with those observed in the corresponding spoil percolate. The Cu and Zn concentrations in the percolate were considerably higher. In caisson 2, the trace metal concentrations in the spoil extract, caisson percolate and the caisson well agreed closely. This suggests that reduction in trace metal concentrations achieved by dilution or other processes occurs primarily after entry into the groundwater or stream system rather than within the spoil profile.

The major chemical controls on acid products loss to groundwater from the spoil particle are the acid products diffusion and the acid production rates. The waters percolating to the groundwater table dissolve and remove acid products from the surface of the spoil particle. The concentration of acid products at that surface is likely controlled by either the diffusion rate of acid products from interior oxidation or storage sites, or the acid production rate controlled by either the kinetics of pyrite oxidation or the diffusion of O_2 to pyrite oxidation sites within the particle.

Pyrite oxidation in the spoil particle, potentially the most important process, appears primarily controlled by either the pyrite oxidation or O_2 diffusion rate. For new, unweathered spoil, the experimentally determined pyrite oxidation rate compared reasonably well with published values. The rate of 0.16 mg SO_4 generated/g pyrite/hour remained undiminished following approximately a 1500 hour incubation period in 20 percent O_2. Thus, pyrite oxidation rather than the O_2 diffusion rates appeared to be controlling. As weathering removes the shallow pyrites, the O_2 diffusion or acid product diffusion rate appears to be controlling.

Because the spoil particles used contain substantial concentrations of acid products (3.1%) as well as pyrite (3.8%), the initial acid product losses to groundwater can be very large, even in the absence of O_2, especially where submerged or frequently flushed. As particle leaching progresses, diffusion rather than percolation or groundwater flow rates becomes potentially controlling because of the very low diffusion coefficient of these acid products. The acid product contributing zone was 0.022 cm depth for a 0.5 cm diameter assumed cylindrical spoil particle which amounted to 17 percent of the total particle volume. Thus, 83 percent of the spoil particle volume was noncontributing.

In cases where diffusion is limiting, the basic spoil particle size is important in controlling the rate of salt and acid loss to groundwaters since this reduces the acid contributing volumes relative to the total spoil mass.

Total acidity provides a reasonable estimate of other major chemical parameters contained in spoil drainage. In caisson percolate, good linear correlations existed between total acidity and Al, total soluble Fe, Mg, and SO_4 concentrations. These exclude the lowest concentrations (<10 meq/l) which normally do not represent the important acid contributing spoils. The relationship of total acidity with Ca, ferrous Fe, Mn and pH was much less precise. Concentration of Cu, Zn and Mn in spoil extract could be better approximated from the sulfate concentration than from the pH values.

CONTENTS

Foreword iii
Abstract v
Conclusions. ix
Figures. xviii
Tables xxiii

1. Introduction. 1
References 12

2. Site Description. 19
Chemical Properties. 19
Natural Soils 22
Minesoils 25
Root Density and Particle Size Distributions. 26
Chemical Properties 28
Organic Carbon. 31
Clay Mineralogy 33
Sulfur (S). 33
Spectrometric Analyses. 34
Spectrographic Analyses 35
Physical Properties. 36
Specific Surface. 39
Bulk Density. 42
Minesoil Water 45
Moisture characteristic 45
Water retention 47
Hydraulic conductivity. 50
Infiltration. 51
Evapotranspiration. 54
References 56

3. Caisson Studies 61
Monitoring Water Movement Through Strip Mine Spoil Profiles 61
Instrumentation 65
Methods 67
Results and Discussion. 69
Modeling Water Flux on Strip-Mined Land. 79
The Caissons. 80
Flow Models 83
Model 1. 83
Model 2. 85
Results and Discussion. 87

CONTENTS (continued)

Chemical Considerations 93
Analysis, Sampling and Storage Methods 93
Chemical Properties of the Spoil 96
Chemical Properties of the Spoil Percolate 100
Chemical Interrelationships of Spoil and Spoil Percolate. 104
Processes Controlling Acid Product and Acid Losses from the Spoil Particle. 109
Laboratory Setup and Procedure 111
Calculation Method 115
Experimental Results 122
Diffusion of Acid Products to the Particle Surface or O_2 into the Particle as the Controlling Process. 124
Rate of Pyrite Oxidation as the Controlling Process 126
Interpretation of Results. 127
Chemical Parameter Interrelationships. 128
References. 135

4. Field Studies. 140
Physical and Hydrologic Setting 140
Chemical Setting. 146
Water Quality 148
Site Response in Time. 148
Controlling Processes. 156
Site Response in Space. 159
Mean values. 159
Conclusions 162
References. 164

5. Recommendations. 165
Introduction. 165
What Was Done 167
Subsidence of Materials and Changes in Density and Porosity. 168
Water Movement in the Profile 170
Chemical Effects of Atmospheric and Hydrologic Isolation 173
Intraparticle Diffusion Processes Affecting Acid Production and Loss 178
References. 182

FIGURES

Number		Page
2.1	Schematic diagram of study area and location of experimental pits P1-P4 for the soils and P5-P8 for the minesoils	19
2.2	Cation exchange capacity on the <2 mm material (clear) and total volume (shaded), base saturation, pH and total acidity for the natural soils and the minesoils.	29
2.3	Study area and location of minesoil pits, lysimeter sites, and infiltration sites.	39
2.4	Determination of bulk density by a modified excavation technique (Bertram, 1973)	43
2.5	Water retentivity curve (gravimetric) for a minesoil corrected and not corrected for coarse fragments.	47
2.6	A microlysimeter site	51
2.7	Cumulative ET values during the study as determined by model results, changes in lysimeter weight, and evaporation from the class A pan	55
3.1	Backhoe excavates successive layers of spoil at Kylertown	62
3.2	Research staff assembles boxes for transport of Kylertown spoil by truck to the experimental facility	62
3.3	Boxes are unloaded at the experimental research facility.	63
3.4	Caissons at the experimental research facility to be filled with Kylertown spoil.	63
3.5	Numbered boxes are positioned near the appropriate caisson preparatory to reconstituting the field profile	64
3.6	Inside of caisson 1 showing the 2.5' depth of spoil in place, access tubes for measuring density and moisture and a lysimeter for collecting the effluent, ladder was used by personnel who rebuilt the field profile layer by layer.	64
3.7	Caisson instrumentation description	65

FIGURES (continued)

Number		Page
3.8	Caisson profile density before (original) and after (new) water application	70
3.9	Water redistribution profiles for caissons 1 and 2 for indicated times	74
3.10	Comparison among tensiometer pressures at 0.3-, 0.6- and 0.9-m depths on caisson 1 and 2 for 27 and 15 days after water was applied	75
3.11	(a) Water retentivity curves averaged for all depths for spoil profile corrected and uncorrected for coarse fragments and specific retention; (b) matched (Green and Corey, 1971) hydraulic conductivity values as a function of water, corrected for coarse fragments and specific retention; (c) hydraulic conductivity as a function of tensiometer pressure; curves labeled 1a refer to caisson 1, they were matched at K_{sat} = 0.13 m/hr, curves labeled 2 were for spoil material in caisson 2 and were matched at K_{sat} = 1.89 m/hr. . .	76
3.12	Schematic representation of the two caissons.	81
3.13	Moisture characteristic (a) and hydraulic conductivity (b) as a function of tensiometer pressure.	82
3.14	Moisture and pressure profiles simulated with model 1 on a hypothetical topsoiled spoil (a), natural soil (b), and nontopsoiled spoil (c). The numbers on the curves indicate time in minutes from the beginning of water application at the surface.	88
3.15	Comparison of experimental (caisson 1) water contents obtained on a topsoiled minesoil during the run with a moisture profile at 0.8 h predicted by model 1 (3.15a); comparison of experimental water contents taken 1 day (3.15b) and 1 month after the run (3.15c) with moisture profiles at 1 day and at 1 month predicted by model 1. Solid circles (●) are experimental (caisson 1) values at indicated times; open circles (○) in (3.15c) show profile water content 44 days after the run	89
3.16	Comparison of experimental water contents obtained on non-topsoiled spoil profiles 2 h (●) and 30 days (▲) after the water application ceased with simulated profiles.	91

FIGURES (continued)

Number		Page
3.17	Comparison of experimental water contents on nontopsoiled spoil for two intermittent rain periods (● and ▲) 41 h apart with water content profiles simulated using model 2	92
3.18	Relation of total acidity from lysimeter drainage with spoil and spoil extract analyses for corresponding spoil layers. . .	104
3.19	Relation of total acidity from lysimeter drainage with spoil and spoil extract analyses for corresponding spoil layers. . .	105
3.20	Total acidity as related to flow duration on caissons 1 (7/18/78) and 2 (8/23/78).	107
3.21	Total acidity as related to quantity of leachate under saturated conditions for spoil 21.	109
3.22	Relationship of total salts (TS) with electrical conductivity (EC) for selected column leachates	113
3.23	Relationship of total salts (TS) with electrical conductivity (EC) for selected column leachates (expanded).	114
3.24	Relationship of SO_4 with electrical conductivity (EC) for selected column leachates.	114
3.25	Relationship of SO_4 with electrical conductivity (EC) for selected column leachates (expanded)	115
3.26	Assumed geometry and labelling of individual spoil particle. . .	117
3.27	Example of column leaching sequence following N_2 incubation. . .	117
3.28	Relationship between O_2 availability, incubation time and the acid product concentration in leachate (extrapolated to zero dilution)	119
3.29	Expanded scale relationship between O_2 availability, incubation time and the acid product concentration in leachate (extrapolated to zero dilution).	120
3.30	Relationship of acid production rate for different incubation periods under air and N_2 atmospheres	122
3.31	Relationship between two measures of total acidity	129
3.32	Relationship between total acidity and sulfate concentration . .	130
3.33	Relationship of calcium, magnesium, manganese and aluminum with total acidity	131

FIGURES (continued)

Number		Page
3.34	Relationship between total soluble iron and total acidity	131
3.35	Relationship of log Zn, Cu and Mn concentrations with pH.	132
3.36	Relationship of Zn, Cu and Mn concentrations with sulfate concentrations.	134
4.1	Schematic diagram of the experimental site.	140
4.2	Vegetative cover density (T/ha) at the experimental site.	142
4.3	Relative distribution of infiltration at 60 minutes for a 65 mm Summer storm (200 = 43 mm, 150 = 38 mm, 100 = 31 mm, 50 = 23 mm)	143
4.4	Water content at the surface (a) and at 0.3 m (b) and water table evaluations during a monitoring period in the summer, site scales are in meters	144
4.5	Characteristic distribution pattern of solar radiation (a) and of precipitation (b) at the experimental site	145
4.6	Site response to a spring storm	145
4.7	Typical oxygen profiles in August (a), and October (b) at the experimental site	148
4.8a	Overall response of the experimental site during the study period: Water levels	149
4.8b	Overall response of the experimental site during the study period: Iron (Fe) concentration.	150
4.8c	Overall response of the experimental site during the study period: Aluminum (Al) concentration.	151
4.8d	Overall response of the experimental site during study period: Sulfate (SO_4) concentration.	152
4.9	Water table elevations (solid line) and SO_4 concentrations (dashed line) during 500-700 day time segment, points represent experimental values of SO_4 concentration.	159
4.10	Average changes in pH (units), and iron (Fe), manganese (Mn), magnesium (Mg), aluminum (Al), and sulfate (SO_4) in mg/l, outside scale is in meters.	160

FIGURES (continued)

Number		Page
5.1	Water profiles in the topsoiled spoil prior to and following ponding	170
5.2	Water profiles (a) in nontopsoiled spoil following wetting, and (b) corresponding elevations of water table and amounts of water applied.	172
5.3	Total acidity as a function of (a) leachate, and (b) percolate quantity at 1.2 m (●), 2 m (△), and 2.5 m (○) below the spoil surface	176
5.4	Assumed structure of cylindrical spoil particle	179
5.5	Contributing spoil volume as a function of cylindrical particle radius	180

TABLES

Number		Page
2.1	Morphological Properties of Soils and Minesoils	23
2.2	Roots and Particle Size Distributions for Soils (Pit 1-4) and Minesoils (Pit 5-8)	27
2.3	Iron Oxide and Extractable Aluminum in Minesoils (Pit 5-8) and Contiguous Natural Soils (Pit 1-4).	30
2.4	Percentage of Organic Carbon, Nitrogen, C/N Ratio and Clay Mineral Content of Minesoils (Pit 5-8) and Contiguous Natural Soils (Pit 1-4).	32
2.5	Total Sulfate, Pyritic and Organic Sulfur Contents of Selected Horizons	34
2.6	Quantitative Spectrometric Analysis of Selected Horizons (Presented in Percentages).	35
2.7	Semiquantitative Spectrographic Analysis of Selected Horizons (Presented in PPM)	36
2.8	Coarse Fragment Content (By Weight) of the Minesoil Horizons. . .	41
2.9	Organic Matter (OM), 1500 kPa Water Content (W) and Specific Surface (SS) of Minesoils	41
2.10	Surface Bulk Density (Mean), and Coefficient of Variation (C.V.) of Minesoils Determined by Various Methods	44
2.11	Depth Bulk Density Distributions on the Minesoil, and the Site Mean, Standard Deviation (SD) and Coefficient of Variation (C.V.).	45
2.12	Minesoil Moisture Characteristics	46
2.13	Water Content of Minesoils (Sample) After 2 Days of Drainage, of Clods Desorbed at 30 kPa, and Moisture Characteristic Values (MC) at 10 kPa for Surface Horizons.	48
2.14	Water Retained between 10 and 1500 kPa Tensiometer Pressure at Four Minesoil Sites and at One Natural Soil Site.	49

TABLES (continued)

Number		Page
2.15	Saturated Hydraulic Conductivity at 10 Lysimeter Sites (L-1 to L-10) Before (Initial) and After 4 Months of Field Exposure (Final) Corrected to 20°C	52
2.16	Infiltration Velocities on Natural Soil, Topsoiled, and Nontopsoiled Minesoil	53
3.1	Location of Instruments Caisson 1 and 2	66
3.2	Sediment Concentration in the Well and in the Effluent from Lysimeters at Different Times After Water was Applied	70
3.3	Oxygen Concentration at Selected Depths After Water Application	71
3.4	Depth of Water Infiltration with Time After Application	72
3.5	Distribution of Total Available Pore Space (TPS) and of Spoil Water in Caissons with Depth	78
3.6	Water Depth, Seepage Flux, and Contained Volume in the Saturated Zone After Water was Applied to Caissons	79
3.7	Selected Average Physical and Hydrologic Properties of Caisson Materials	82
3.8	Experimental Values of Seepage Flux and Antecedent Moisture Content (θ)	86
3.9	Simulated Amounts, Duration and Intensities of Applied Rain and Antecedent Water Content	86
3.10	Experimental and Simulated Profile Water Content Values, Matching Factors and Their Reciprocals	91
3.11	Spoil Pyrite Analysis	97
3.12	Values of pH, Electrical Conductivity (EC), Total Acidity, Ca, Mg, and SO_4 for Twenty-One Layers of Reconstructed Spoil Profile	98
3.13	Trace Metal Concentration of Spoil Extract	99
3.14	Chemical Characteristics of Spoil Drainage at Selected Depths within Caissons 1 and 2	101
3.15	Trace Metal Contamination of Caisson Percolate and Well Waters Taken from Caisson 1 and 2 for Run 1	103

TABLES (continued)

Number		Page
3.16	Incubation Sequences, Time and Composition of Eluant Gas by Column	112
3.17	The Weathered Volume (Contributing) and Depth (Δr) as Related to Different Diffusion Coefficients	125
3.18	Effect of Spoil Particle on Contributing Volume	125
3.19	Relationship of the Total Acidity Determined at pH 8.2 (y) to Different Chemical Parameters (x)	129
4.1	Time of Occurrence of Major Storms and Associated Well Elevation Minima and Maxima	154
4.2	Controlling Processes Affecting Groundwater Quality on Stripmines	157
4.3	Acidity, pH, and Concentration of Selected Chemical Constituents in Well Water on a Mine and Reclaimed Site Measured During High and Low Water Levels	161
4.4	Average Water Levels, Acidity and Concentrations of SO_4, Fe and Al at High and Low Water Levels for Grouped Wells	163
5.1	The Sulfate, Sulfide and Organic Sulfur Content for Unmined Coal Overburden	174

SECTION 1

INTRODUCTION

Current literature contains numerous studies of acid generation, neutralization, and transformation in strip-mine spoil materials, yet we do not understand well the rate-determining processes on the field scale. We know even less about the spoil water flow, oxygen diffusion, surface runoff, erosion, evapotranspiration, and temperature distributions within the spoil banks.

Prevailing economics, and the concerted national effort towards energy self-sufficiency, virtually ensure strip mining of our shallow coal deposits. This activity will cause considerable changes in the amount, distribution, and quality of water in mined areas, and change the temperature and evapotranspiration (ET) regimes. The oxidation of pyrite, and subsequent flushing of oxidation products, could result in acid discharges from some areas. Modern methods of strip mining and reclamation (Grim and Hill, 1974) are likely to alleviate many of the problems by judicious placement and isolation of acid-producing materials, topsoiling, liming, and rapid revegetation. Nevertheless, at present we have no single technique available to assess beforehand the degree of impact and the long-range effects of strip mining on a given area. Extensive bibliographies, with abstracts on the subjects of strip mining, mine drainage reclamation, and interstate water compacts are readily available (NTIS, 1975; Bituminous Coal Research, Inc., 1964 through 1975; Maloney, 1975; Frawley, 1971). For clues to changes expected in soil profiles before and after strip mining, we should look closely at the status of nitrogen, weatherable minerals, and available water (Ahmad, 1971). Some conventional hydrologic studies (Collier et al., 1970) showed, as expected, that past strip-mining activities

significantly increased acidity and mineralization of surface water and ground water. In other studies, Corbett (1965) and Agnew (1971) pointed out beneficial effects, such as increased infiltration and water-storage capacity, as well as delayed runoff and extended base flow, particularly during the dry periods. Corbett and Agnew (1968) identified the "flushout" phenomenon common to many strip-mine locations. Flushouts result from intense rains during periods of low flow and drought, and may account for a large proportion of acid-loading of streams (Corbett, 1969). Smith et al. (1974) also pointed out the positive effects of strip mining, as in the control of slope and grade, and the possible management of root-zone depth and weatherable mineral content. However, at the same time, temporary organic matter deficiencies and weak soil structure will probably prevail. If we know the properties of overburden in advance, we may reconstruct soils by altering their physical and chemical characteristics to suit better the growth of plants. Destruction of compact soil layers, apt to impede movement of water and growth of roots (McCormack, 1974), has sometimes led to improvement of soil environment for plant growth. Nevertheless, the continuous long-term and recurring problem of pyrite weathering, and concurrent transport of oxidation products still defies solution. The transport, in general, is accomplished by percolating, seeping, or flowing water that feeds streams, drains the area, or recharges the ground water. Although modern methods in strip mining (Grim and Hill, 1974; USEPA, 1973) can minimize these effects, long-term impact and legal aspects and implications (Goldberg, 1971; Goldberg and Power, 1973) are still largely unknown. Smith et al. (1971), in studies of 70- to 130-year-old weathered iron-ore spoil, suggested that reclaimed sites may have a higher density, lower porosity, continuing lack of structure, and lower N and organic matter contents, as well as poorer infiltration rates, than adjacent undisturbed soils. However, their results also showed that properly placed mine soils provide

increased water-holding capacity, greater root depth, and a more weatherable mineral matrix.

Lysimeter studies (Lowry and Finney, 1962) have shed some light on the oxidation of pyrite and leaching rates of the oxidation products within a small portion of the profile under vertical flow conditions. Recently, Smith et al. (1974) adapted selected chemical, physical, and mineralogical measurements, used to classify natural soils, to coal overburden sections and strip-mine spoil in West Virginia. Improved classification of mine soils, based on observable properties of mine soil profiles, will most certainly provide the needed basis for more precise management.

The actual acid production and the quality of spoil water are due to modification of the potential acid production by neutralizing or the rate-limiting factors. We could estimate potential acid production by leaching spoil samples, by the analysis of total pyrite (VonDemfange and Warner, 1975), or by classifying spoils to estimate the available or total pyrite. Analogously, we can determine the neutralization potential by mineralogically based estimates of the quantity of CO_3 materials.

Leaching study provides directly an estimate of readily available pyrite. It is, however, a laborious site specific procedure. The total pyrite analysis estimates potential acid production, but does not give a measure of availability. Some use it directly as input to equations for determining the acid or neutralization potential (Caruccio, 1973; VonDemfange and Warner, 1975). The surface area exposed affects pyrite availability (OSU, 1970). Classification of potential acid production, according to pyrite particle-size and amount associated with selected strata, is currently under active investigation (Caruccio, 1973).

We can classify the dominant chemical processes according to acid generation, neutralization, and transformation reactions. According to Singer and Stumm

(1968), the summary reactions for the acid generation by oxidation of pyrite minerals are:

$$FeS_2(s) + 3.5\ O_2 + H_2O = 2SO_4^{2-} + Fe^{2+} + 2H^+, \tag{1.1}$$

$$Fe^{2+} + 0.25\ O_2 + H^+ = Fe^{3+} + 0.5\ H_2O, \tag{1.2}$$

$$Fe^{3+} + 3\ H_2O = Fe(OH)_3\downarrow + 3H^+, \text{ and} \tag{1.3}$$

$$FeS_2(s) + 14\ Fe^{3+} + 8\ H_2O = 15\ Fe^{2+} + 2SO_4^{2-} + 16H^+. \tag{1.4}$$

In these reactions, four moles of H^+ are being generated for each mole of FeS_2 consumed, two moles of H^+ each eventually resulting from oxidation of $2S^- \rightarrow 2SO_4^{2-}$ and $Fe^{2+} \rightarrow Fe^{3+}$. The challenge is to relate the pertinent characteristics of these reactions to acid production on a spoil bank scale.

Under certain conditions, laboratory tests show that reaction rate [1] depends on water concentration, pH, texture of pyritic materials, and temperature. Apparently, the concentration build-up of oxidation products, which would slow acid production, does not occur when humidity is near 100%. Condensation of gaseous H_2O on the reactant sites causes solubilization, and then reaction product removal by dripping (Shumate et al., 1971). Laboratory-derived, simple relationships between the reaction rates and pH, temperature, dissolved O_2, and relative humidity are referenced in OSU (1971), and specifically described in Smith et al. (1968), OSU (1970), and Clark (1966).

Estimating acid production by reaction (1.4), which is directly dependent on reaction (1.2), is much more complex. According to the literature, this requires an estimate of Fe^{3+} concentrations and the Fe^{3+}/Fe^{2+} ratio as input to reaction

(1.4) (Smith et al., 1968). Under conditions of low Fe^{3+}/Fe^{2+} ratios (<0.3) and high O_2 (15% in atmosphere), pyrite oxidation by reaction (1.1) greatly exceeds the pyrite oxidation rate by reaction (1.4) (Shumate et al., 1971), and the practical assumption that acid production depends directly on the dissolved O_2 concentration is reasonable. At low Fe^{3+}/Fe^{2+} ratios (20% ferric or lower), experimental data have also shown (OSU, 1971) that microbially induced oxidation is small and, consequently, acid drainage produced is small, as compared with that produced independently of microbial activity. Several authors have argued that, in the presence of O_2, acid generation is related to O_2 consumption, regardless of whether chemically or microbially induced oxidation dominates (Harvard University, 1970; Shumate et al., 1971; Smith, 1974).

Additional simplification is given by Morth[1], who predicted acid production reasonably well by relating the experimental rate of acid generation to the O_2 concentration (in terms of partial pressure), rather than dissolved O_2. If this can be done, then the calculated or observed O_2 in the spoil atmosphere, and its distribution down through the spoil bank, can relate directly to acid production. In a laboratory study (NUS Corporation, 1971), acid, Fe, and conductivity resulting from pyrite oxidation were all noted as a function of O_2 concentration (to 40%) in a carrier gas, indicating that partial pressure of O_2, rather than dissolved O_2, could be used directly to predict acid production.

The amount, reactivity, and distribution of CO_3 minerals affects the extent of neutralization of acid effluent from the pyritic reaction sites. The CO_3

---

[1]A. H. Morth. 1971. Acid mine drainage: a mathematical model. Ph.D. Thesis. Ohio State University, Columbus, Ohio.

minerals can be calcite (Ca), dolomite (Ca, Mg), or siderite (Fe). However, if siderite breaks down, the amount of H^+ from Fe will be greater than the HCO_3^- from siderite. The question remains to be answered whether siderite can in fact produce significant alkalinity. Drainage waters will generally increase in pH with a corresponding increase in Ca^{2+}, Mg^{2+}, or possibly Fe^{2+} content, unless Ca^{2+} concentration exceeds the solubility of $CaSO_4$, or unless Fe^{2+} is oxidized and exceeds the solubility of the appropriate Fe^{3+} compounds.

"Spoil" water behaves similarly to soil water to the extent that a given spoil material corresponds to original soil. For example, for Pottsville series and Lower Kittanning bed of the Allegheny series, the percentage of material <2 mm (the soil-size fraction) varies between 17-64% in spoils, as compared with 35-95% in the original soils (Plass and Vogel, 1973). Data of Ciolkosz et al. (1983) also show wide variations in textures of mine soils. When larger sizes predominate, spoil is no longer analogous to soil, and may have to be treated as rockfill (Leps, 1973, p. 91). Frequently, mine spoils have many air pockets (large voids), these may contribute to the non-Darcy behavior of the spoil. Under those circumstances Darcy's Law would not hold, and for saturated conditions turbulent flows could prevail. Although Coleman[2] does not explicitly indicate the amount of >25-mm materials in the spoils that he tested for infiltration, close examination of his Figure 13 suggests that these materials compose about 60% of the total.

Coleman[2] also found that the dark carbonaceous spoil banks in central Pennsylvania had an infiltration rate about 10 times higher than the forest soil

---

[2]G. B. Coleman. 1951. A study of water infiltration into spoil banks in central Pennsylvania. M.S. Thesis. The Pennsylvania State University, University Park, Pennsylvania.

nearby. However, spoil material, derived from the yellow thick-bedded shales and sandstones, had infiltration rates four to five times lower than wooded soil. In strip-mining literature, soil is commonly considered as material <2 mm in diameter. Coleman[2] concluded that higher soil contents (39%) decrease the air space in the yellow shale and mixed spoils, causing a decreased rate of infiltration, while the lower soil content (20%) of the dark shales had the opposite effect. He also showed that frost, compaction, and erosion decreased infiltration rates on the spoils.

Brown[3] obtained analytical flow nets for the three vertically separated flow systems in Clearfield County, PA. He found an "upper" system present in the interval between the topographic highs and the roofs of the deep mines. This system controlled the amount of water entering the deep mines through the roof and along the stripped outcrop. Vertical permeabilities were generally increased by fracturing and collapse of the mine roofs.

Brown[3] also found that the "middle" flow system was the most complex, with discharge occurring to both the stream valley and into the top of the Connoquenessing Sandstone formation. This flow system seemed to reflect local topographic features. Finally, he found that the "lower" flow system was more regional in extent and, generally, ignored local topography. He believed discharge occurred along the deeply incised streams. In some areas, ground water flow seemed to be controlled predominantly by fractures and joints. Brown[3] concluded that by defining the density, orientation, and permeabilities of these fractures for each

---

[3]R. L. Brown. 1971. Shallow groundwater flow systems beneath strip and deep coal mines at two sites, Clearfield County, PA. Ph.D. Thesis. The Pennsylvania State University, University Park, Pennsylvania.

rock type, and by relating the occurrence of fractures to structural features, ground water flow systems could be defined, and unique flow solutions could be obtained. Emrich and Merritt (1969) concluded that acid drainage from coal mines may often pollute underlying aquifers through joints, fractures, and abandoned oil and gas wells. Moving down the hydraulic gradient, it may discharge as Fe-rich springs or flowing wells, or may pollute domestic or municipal water supplies.

Thames et al. (1974) assumed Darcian flow to model water transfer in Arizona's Black Mesa spoil. Considering the heterogeneity of our spoil materials, this approach may be open to question. Other than the work of Davis et al. (1964), ElBoushi and Davis (1969), and ElBoushi (1975) on infiltration into rock piles, not specifically related to strip mines, there seems to be no information in the literature on infiltration and unsaturated flow in strip-mine spoil. The problem is further complicated by the current practice of spreading topsoil over the coarser spoil material. Thus, in any consideration of these flows, the fingering process, due to the wetting front instability (Hill and Parlange, 1972), may need to be taken into account.

Two sources of heat exist in spoil materials, one at the surface due to solar radiation, the other within the spoil bank as a result of internal exothermic chemical reactions. These include oxidation of pyrite, condensation of H_2O, and possibly solubilization of acid-generated by-products. Solar heat can increase the surface temperature to as much as 80°C on the dark organic shale and bituminous coal (Deely and Borden, 1969). The high surface temperatures (particularly above 50°C) in spoils hinder the establishment of vegetative cover. Mulching with organic materials has been somewhat successful in lowering the temperature and conserving moisture (Kusko and Hutnik, 1974). The coarseness of the spoil materials acts like a gravel mulch, tending to minimize the temperature fluctuations. Ahmad and Ghosh (1971) found that diurnal fluctuations of temperature in the spoil at a

60-cm depth were insignificant. From the standpoint of evapotranspiration (ET), tops of plants growing on the spoil can experience extreme moisture stress, while roots remained reasonably cool. In the literature there is no mention of an ET-model developed for, and operating on, strip-mined soils. Possibly, the Blackland ET-model (Ritchie, 1972; Richardson and Ritchie, 1973) can be adapted for this purpose.

Lovering (1948) first studied geothermal gradients. He showed that pyrite oxidizing above a water table in rocks undisturbed by mining operations caused noticeable inflections in the temperature gradient at a 200-m depth. Ahmad and Ghosh (1971), used the differences in temperature to map acid-producing areas in Ohio, and concluded that maximum ground temperatures at 60-cm depth corresponded to a high percentage of pyrite content and low pH. The ground temperature gradient seemed higher in acid-producing areas relative to nonacid-producing areas. Their observations suggest a qualitative partitioning of a strip-mine watershed based on detailed temperature surveys into acid-contributing and acid noncontributing zones.

The term *modeling*, when used in strip-mining literature, has different meanings for different individuals. For example, Caruccio and Ferm (1974) discussed a conceptual sedimentary model for coal. They concluded that, by identifying the environment of deposition for a particular stratum, they could forecast the occurrence and the mode of distribution of S in coal and associated rocks.

Miller and Thompson (1974) examined the effects of coal barrier width, using the work of Cedergren (1967) on application of flow nets to seepage flows. They concluded that compared to a 6-m coal barrier, a 15-m barrier decreased the restricted flow 53%, and a 30-m barrier decreased it 75%.

Herricks et al. (1975) used the Stanford Watershed Model (SWM) to generate streamflow sequences for areas with no recorded historical record, based on the

sequences for an instrumented subwatershed. He also used simulated SO_4 concentrations in a conservative stream-loading model to provide an indication of the amount and intensity of acid-mine drainage, and in addition obtained an indication of the erosive action of selected storm discharges through the use of sediment transport theory.

Sternberg and Agnew (1968) suggested a general analytical model of surface-mine drainage. They obtained solutions for changes in ground water level and flow that would occur in response to a uniform rate of seepage.

By far the most practical approach to modeling has come from Ohio State University, and is best summarized in Shumate et al. (1971), Morth[1], Morth et al. (1972), and Ricca and Chow (1974). In Shumate et al. (1971), a conceptual model for pyrite oxidation was proposed, physical, chemical, and biological systems involved were discussed, and some abatement techniques were considered.

Morth[1] used Shumate's conceptual model to produce a mathematical model of acid-mine drainage for a drift mine. The key assumption of this model, based on a review of pertinent laboratory data, was that the oxidation rate was proportional to the O_2 concentration. Thus, Morth developed a program to predict O_2 concentration within small channels of coal or shale. The output of the program was a set of O_2 gradients for a given set of channel lengths and atmospheric pressures. The hydrologic aspects of this program are somewhat less sophisticated. The program is based on a simple material balance (In-Out = Accumulation) using precipitation amount and estimates of infiltration capacity and evapotranspiration. It is the hydrologic system of essentially undisturbed overburden, with water seeping through "cracks and crannies" to reappear in an established water table, that may at times intersect parts of mined-out areas. In strip mines, however, the graded overburden is in a form of rubble and the acid-forming material may be either buried deeply, distributed randomly, or placed otherwise through the spoil.

The current literature survey suggests that much work has been done on the basic chemical reactions of acid generation, neutralization, and transformation; yet, the rate-determining chemical processes on the field scale are not well defined. Even less has been done on the subject of water flow, air and O_2 diffusion, evapotranspiration, temperature distribution, and possible surface runoff. It is the purpose of this study to remedy the situation.

We plan in what follows to examine the impact of strip mining on the hydrology of a mined area. In doing so we will examine experimental results obtained from our laboratory and field studies and attempt to draw general conclusions applicable to other areas.

Ricca and Chow (1974) combined Morth's[1] Acid Drainage Model with the Ohio State version of Stanford Watershed Model (SWM) to produce daily mine-water outflow and daily acid load from a watershed, on which the experimental mine modeled by Morth[1] and Morth et al. (1972) was located. They found that, generally, the agreement between simulated and observed values was quite satisfactory. The concept of using SWM to predict the impact of strip mining on an area has apparently not yet been tested. Unmined watersheds, however, have been modeled extensively, and now some mined watersheds are being modeled. Because the calibration of SWM requires abundant data, extension of other areas generally is based on the assumption of similarity, which may not always be valid.

REFERENCES

1. Agnew, A. F. Coal Mining Hydrology and the Environment, Or Give the Devil His Due. In: AIME Environmental Quality Conference, June 7-9, Am. Inst. Min., Metall. Pet. Eng., New York, N.Y., 1971. pp. 157-164.
2. Ahmad, M. U. Summary of the Proceedings of the Acid Mine Drainage Workshop. Acid Mine Drainage Workshop, Athens, Ohio, August 2-6. Department of Geology, Ohio University, Athens, Ohio, 1971. pp. 1-6.
3. Ahmad, M. U., and B. A. Ghosh. Temperature Survey of Coal Mines Producing Acid Water. In: Proceedings, Seventh International Symposium on Remote Sensing of Environment, 2:1109-1154. Willow Run Laboratory, University of Michigan, Ann Arbor, Mich., 1971.
4. Bituminous Coal Research, Inc. Mine Drainage Abstracts, A Bibliography. Bituminous Coal Research, Inc., Monroeville, Pa., 1964.
5. Bituminous Coal Research, Inc. 1965-1974 Supplements. Mine Drainage Abstracts, A Bibliography. Bituminous Coal Research, Inc., Monroeville, Pa.,
6. Bituminous Coal Research, Inc. Reclamation of Coal-Mined Land, A Bibliography with Abstracts. Bituminous Coal Research, Inc., Monroeville, Pa., 1975.
7. Caruccio, F. T. Characterization of Strip-Mine Drainage by Pyrite Grain Size and Chemical Quality of Existing Groundwater. In: Ecology and Reclamation of Devastated Land, Volume 1, R. J. Hutnik and C. David, eds. Gordon and Breach Publishers, New York, 1973. pp. 193-226.
8. Caruccio, F. T., and J. C. Ferm. Paleoenvironment Predictor of Acid Mine Drainage Problems. In: Fifth Symposium on Coal Mine Drainage Research, Louisville, Ky. National Coal Association, Washington, D.C., 1974. pp. 5-10.
9. Cedergren, H. T. Seepage, Drainage, and Flow Nets. John Wiley and Sons, Inc., New York, 1967.

10. Ciolkosz, E. J., R. L. Cunningham, G. W. Petersen, and R. C. Cronce. Characteristics Interpretations and Uses of Pennsylvania Minesoils. Progress Report 381. The Pennsylvania State University, Agricultural Experiment Station, University Park, Pa., 1983. 88 pp.

11. Clark. C. S. Oxidation of Coal Mine Pyrite. J. Sanit. Eng. Div., Am. Soc. Civ. Eng. 92:127-145, 1966.

12. Collier, C. R., R. J. Pickering, and J. J. Munsen, eds. Influences of Strip Mining on the Hydrologic Environment of Parts of Beaver Creek Basin, Kentucky, 1955-66. Geological Survey Prof. Paper No. 427C. U.S. Government Printing Office, Washington, D.C., 1970. pp. 1-58.

13. Corbett, D. M. Runoff Contributions from Cast Overburdens of Surface Mining Operations for Coal, Pike County, Indiana. Water Resources Research Center, Rep. No. 1 (1965). Indiana University, Bloomington, Ind., 1965. pp. 1-67.

14. Corbett, D. M. Acid Mine Drainage Problems of the Patoka River Watershed. Southwestern Indiana Water Resources Research Center, Rep. of Invest. No. 4. Indiana University, Bloomington, Ind., 1969. pp. 1-173.

15. Corbett, D. M., and A. F. Agnew. Coal Mining Effect on Busseron Creek Watershed, Sullivan County, Indiana. Water Resources Research Center, Rep. of Invest. No. 2. Indiana University, Bloomington, Ind., 1968. pp. 1-187.

16. Davis, S. N., R. D. Bernard, M. K. Botz, and C. N. Cullimare. Some Hydrogeologic Factors in Water Contamination by Nuclear Cratering. U.S. Atomic Energy Comm. HNS-1229-49, Las Vegas, Nev., 1964.

17. Deely, D. J., and F. Y. Borden. High Surface Temperatures on Stripmine Spoils. In: Ecology and Reclamation of Devastated Land, R. J. Hutnik and G. Davis, eds. Gordon and Breach Publishers, New York, 1969. pp. 69-79.

18. ElBoushi, I. M. Amount of Water Needed to Initiate Flow in Rubbly Rock Particles. J. Hydrol., 27:275-289, 1975.

19. ElBoushi, I. M., and S. N. Davis. Water Retention Characteristics of Coarse Rock Particles. J. Hydrol., 8:431-441, 1969.

20. Emrich, C. H., and G. L. Merritt. Effects of Mine Drainage on Groundwater. Ground Water, 7(3):27-32, 1969.

21. Frawley, M. L. Surface Mined Areas: Control and Reclamation of Environmental Damage, A Bibliography. PB-203-448. U.S. Department of Interior, Washington, D.C., 1971. 67 pp.

22. Goldberg, E. F. The Legal Framework of Acid Mine Drainage Control. Acid Mine Drainage Workshop, August 2-6, Athens, Ohio. Department of Geology, Ohio University, Athens, Ohio, 1971. pp. 76-85.

23. Goldberg, E. F., and G. Power. Legal Problems of Coal Mine Reclamation. Water Pollution Control Research Series. EPA-14010 FZU 03/72, U.S. Environmental Protection Agency, Raleigh, NC, 1973.

24. Grim, E. C., and R. D. Hill. Environmental Protection in Surface Mining of Coal. EPA-670/2-74-093, U.S. Environmental Protection Agency, Cincinnati, Ohio, 1974. pp. 1-277.

25. Harvard University. Oxygenation of Ferrous Iron. 14010-06169, Contract PH 36-66-107, Federal Water Quality Administration, U.S. Department of Interior, Washington, D.C., 1970.

26. Herricks, E. E., V. O. Shanholtz, and D. N. Contractor. Models to Predict Environmental Impact of Mine Drainage on Streams. Trans. ASAE 18(4): 657-663, 1975.

27. Hill, D. E., and J.-Y. Parlange. Wetting Front Instability in Layered Soils. Soil Sci. Soc. Am. Proc., 36(5):697-702, 1972.

28. Kusko, M., Jr., and R. J. Hutnik. Effect of Mulches and Amendments on the Survival and Growth of Vegetation Planted on Anthracite Processing Wastes. Special Research Report SR-101. Pennsylvania State University, University Park, Pa., 1974.

29. Leps, T. M. Flow through Rock Fill. In: Embankment-Dam Engineering. Casagrande Volume, R. C. Hirshfield and S. J. Poules, eds. John Wiley and Sons, Inc., New York, 1973. pp. 87-107.

30. Lovering, T. S. Geothermal Gradients, Recent Climatic Changes, and Rate of Sulfide Oxidation in the San Manuel District, Arizona. Econ. Geol., 43(1):1-20, 1948.

31. Lowry, G. L., and J. H. Finney. A Lysimeter for Studying the Physical and Chemical Changes in Weathering Coal Spoils. Ohio Agricultural Experiment Station Research Circular 113, Wooster, Ohio, 1962.

32. McCormack, D. E. Soil Reconstruction: For the Best Soil After Mining. In: Second Res. and Appl. Technol. Symposium on MIned Land Reclamation, October 22-24, Louisville, Ky. National Coal Association, Washington, D.C., 1974. pp. 150-162.

33. Maloney, F. E., ed. Interstate Water Compacts, A Bibliography. Water Resources Sci. Inf. Center, Office of Water Research and Technol. OWRT/WRSIC 75-205. U.S. Department of Interior, Washington, D.C., 1975.

34. Miller, J. T., and D. R. Thompson. Seepage and Mine Barrier Width. In: Fifth Symposium on Coal Mine Drainage Research, October 22-24, Louisville, Ky. National Coal Association, Washington, D.C., 1974. pp. 103-127.

35. Morth, A. H., E. E. Smith, and K. S. Shumate. Pyritic Systems: A Mathematical Model. EPA Technol. Series 14010 EAH, Contract No. 14-12-589, Report No. 665771. U.S. Environmental Protection Agency, Washington, D.C., 1972. 171 pp.

36. National Technical Information Service. Strip Mining, A Bibliography with Abstracts. U.S. Department of Commerce, Springfield, Va., 1975.

37. NUS Corporation. The Effects of Various Gas Atmospheres on the Oxidation of Coal Mine Pyrites. Water Pollution Control Research Series 14010 ECC-08/71. U.S. Environmental Protection Agency, Washington, D.C., 1971.

38. Ohio State University Research Foundation. Sulfide to Sulfate Reaction Mechanism. Water Pollution Control Research Series 14010 FPS-02/70. Federal Water Quality Administration, U.S. Department of Interior, Washington, D.C., 1970.

39. Ohio State University Research Foundation. Pilot Scale Study of Acid Mine Drainage. Water Pollution Control Research Series 14010 EXA-03/71. U.S. Environmental Protection Agency, Washington, D.C., 1971. 84 pp.

40. Plass, W. T., and W. G. Vogel. Chemical Properties and Particle Size Distribution of 39 Surface-Mine Spoils in Southern West Virginia. USDA Forest Service Research Paper NE-273. Northeastern Forest Experiment Station, Upper Darby, Pa., 1973.

41. Ricca, V. T., and K. Chow. Acid Mine Drainage Quantity and Quality Generation Model. Trans. Soc. Min. Eng., Amer. Institute of Mining Eng., 256(4):328-336, 1974.

42. Richardson, C. W., and J. T. Ritchie. Soil Water Balance for Small Watershed. Trans. ASAE, 16:72-77, 1973.

43. Ritchie, J. T. Model for Predicting Evaporation from a Row Crop with Incomplete Cover. Water Resour. Res., 8(5):1204-1213, 1972.

44. Shumate, K. S., E. E. Smith, P. R. Dugan, R. A. Brant, and C. I. Randles. Acid Mine Drainage Formation and Abatement. Water Pollution Control Research Series Program 14010 FPR. U.S. Environmental Protection Agency, Washington, D.C., 1971.

45. Singer, P. C., and W. Stumm. Kinetics of the Oxidation of Ferrous Iron. In: Proceedings, Second Symposium on Coal Mine Drainage Research, May 14-15, Pittsburgh, Pa. Coal Industry Advisory Comm. to Ohio River Valley Sanitation Commission, 1968. pp. 12-34.

46. Smith, E. E., K. Svanks, and K. Shumate. Sulfide to Sulfate Reaction Studies. In: Proceedings, Second Symposium on Coal Mine Drainage Research, May 14-15, Pittsburgh, Pa. Coal Industry Advisory Comm. to Ohio River Valley Sanitation Commission, 1968. pp. 1-11.

47. Smith, J. J. Acid Production in Mine Drainage Systems. In: Extraction of Minerals and Energy: Today's Dilemma, R. A. Deju, ed. Ann Arbor Science Publishers, Inc., Ann Arbor, Mich., 1974. pp. 57-75.

48. Smith, R. M., W. E. Grube, Jr., T. Arkle, Jr., and A. Sobek. Mine Spoil Potentials for Soil and Water Quality. EPA-670/2-74-070, Environmental Protection Technol. Series, U.S. Environmental Protection Agency, Cincinnati, Ohio, 1974. 303 pp.

49. Smith, R. M., E. H. Tryon, and E. H. Tyner. Soil Development on Mine Spoil. Bull. 604T. West Virginia University, Agricultural Experiment Station, Morgantown, W. Va., 1971.

50. Sternberg, Y. M., and A. F. Agnew. Hydrology of Surface Mining, A Case Study. Water Resour. Res., 4(2):363-368, 1968.

51. Thames, J. L., E. J. Crompton, and R. T. Patten. Hydrologic Study of a Reclaimed Surface Mined Area on the Black Mesa. In: Second Research and Appl. Technol. Symposium on Mined Land Reclamation, October 22-24, Louisville, Ky. National Coal Association, Washington, D.C., 1974.

52. U.S. Environmental Protection Agency. Processes, Procedures and Methods to Control Pollution from Mining Activities. EPA-430/0-73-011, U.S. Environmental Protection Agency, Washington, D.C., 1973. pp. 1-390.

53. VonDemfange, W. C., and D. L. Warner. Vertical Distribution of Sulfur Forms in Surface Coal Mine Spoils. In: Third Symposium on Surface Mining and Reclamation, October 21-23, Louisville, Ky. National Coal Association, Washington, D.C., 1975. 1:135-147.

SECTION 2

SITE DESCRIPTION

CHEMICAL PROPERTIES

The experimental site (Figure 2.1) selected was a reclaimed 4 ha strip mine adjoining undisturbed land and located near Kylertown in Clearfield County, Pennsylvania, within the Pittsburgh Plateau section of the Appalachian Plateau Province. The geologic system (Pennsylvanian) was characterized by cyclic

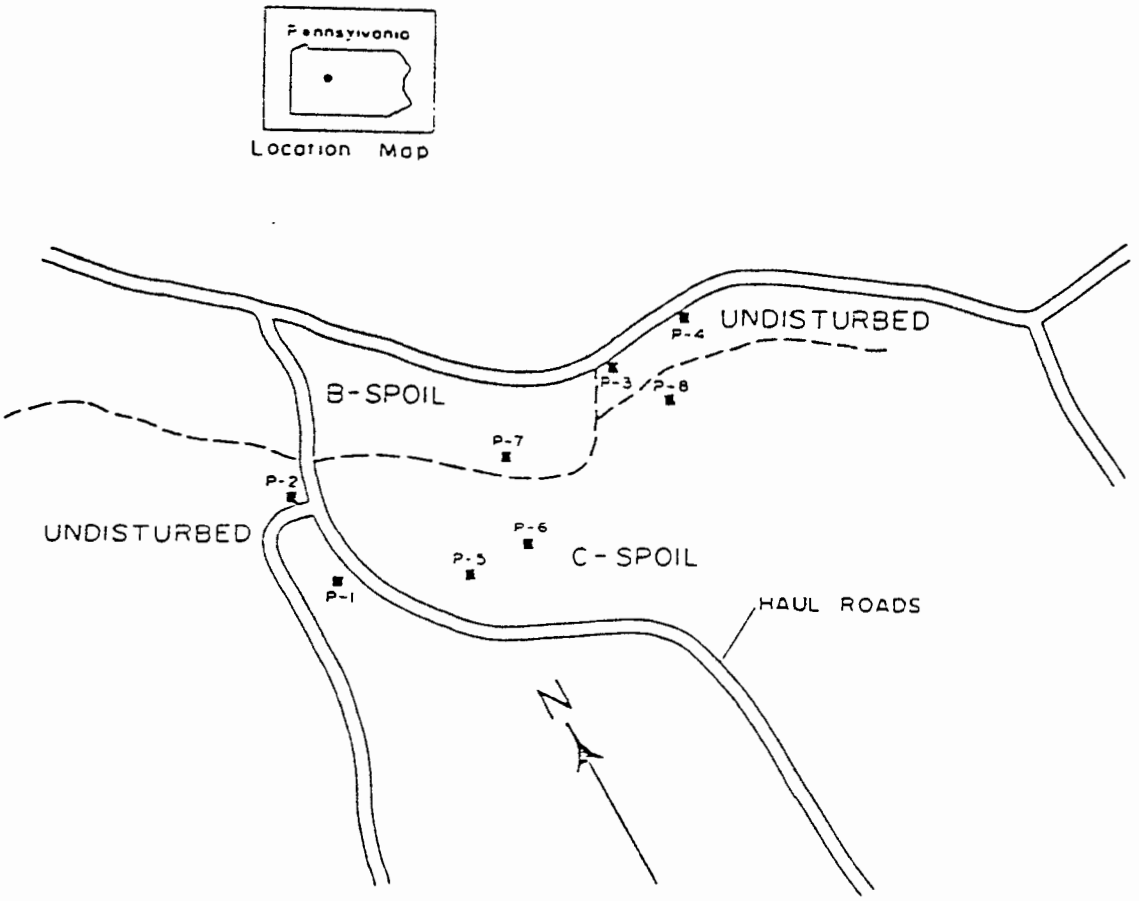

Figure 2.1. Schematic diagram of study area and location of experimental pits P1-P4 for the soils and P5-P8 for the minesoils.

sequences of sandstone, shale, coal and clay, and underlain by flat-lying to gently folded reddish, yellowish and brownish clay shale and yellowish brownish sandstone, shale and siltstone. The coal strata included the middle and lower Kittanning seams (C and B) of the Allegheny group, Millstone Run and Mineral Creek formations. In general, sandstones overlay the middle Kittanning C-seam, with siltstones and shales predominating above the lower Kittanning B-seam. The general topography of the area was broad with rounded divides separated by narrow V-shaped valleys (Glass, 1972). The mean elevation of the site was about 450 m with a northern to northeastern aspect.

Before stripping, the vegetation of the area was hardwood forest, grasses, legumes and trees have since become established on the site following reclamation. The lower portion of the experimental site (B-spoil in Figure 2.1) was mined and reclaimed in 1969 before passage of the Pennsylvania legislation requiring topsoiling and burial of acid materials. Although the area has been contoured, topsoil was not spread over the spoil. Beech, pine, and aspen have been planted on this area. The upper portion of the area (C-spoil in Figure 2.1) was mined and reclaimed in 1974 after passage of the stripmine legislation. As a direct consequence, 15 to 20 cm of topsoil was spread over the spoil, the site was limed and planted to grass and legumes. The eastern half of the area (pit 8) was also heavily manured resulting in a good stand of clover. On the mined area, the disturbed material extends to a depth of about 10 m, and small pockets and larger tracts of original undisturbed soil surround the area. Pit sampling was done in 1976, 7 years (B-spoil) and 2 years (C-spoil) after reclamation.

Four pits (pit 1-4) about 2 m deep, 3 m long and 1.5 m wide were sited around the periphery of the mined land on soils originally present in the area, and four pits (pit 5-8) were randomly located within the reclaimed area (Figure 2.1). Detailed morphological descriptions of the profiles were made according to the Soil

Survey Manual (Soil Survey Staff, 1951), and the pedons were classified according to the recent system of soil taxonomy (Soil Survey Staff, 1975). Root distribution descriptions were made using the procedure outlined in Appendix II of Soil Taxonomy (Soil Survey Staff, 1975). Four square decimeters outlined on an acetate sheet was placed over the horizons and the number of roots were counted and averaged.

Bulk samples (~5 kg) were obtained from each horizon of the natural soils and minesoils. Coarse fragments (>19 mm diameter) were sieved from the bulk samples and weighed in the field. The material <19 mm was air dried and retained for further analyses. Particle-size analyses of the samples from each horizon were made by sieving and by the pipette method after dispersion with sodium metaphosphate ($NaPO_3$) and sodium carbonate (Na_2CO_3) (Kilmer and Alexander, 1949). Chemical analyses were made on that fraction which passed through a 2-mm sieve. Soil reaction (pH) was determined with a pH meter and glass electrode on three 1:1 (by weight) soil solution suspensions, with distilled water, 1N KCl, and 0.01 M $CaCl_2$, respectively. The basic cations (Ca, Mg, K and Na) were extracted with 1N NH_4OAc solution at pH 7 (Peech et al., 1947). Ca and Mg levels were determined by atomic absorption spectrophotometry, and K and Na contents were determined by flame emission spectrophotometry. Extractable acidity was determined by titration of a $BaCl_2$-triethanolamine soil extract at pH 8.1 (Yuan, 1959). The Aluminon method (Yuan, 1959) was used to determine Al. Free iron oxides, extracted by Na dithionite-citrate-bicarbonate, were analyzed for using orthophenanthroline. Organic carbon content was determined by ignition with a Fischer induction furnace (Young and Lindbeck, 1964) and by the Walkley-Black method (U.S. Salinity Laboratory, 1954). Total nitrogen was determined by the Kjeldahl method (Jackson, 1958).

Quantitative spectrometric and semiquantitative spectrographic analyses, as well as sulfur analyses on samples from representative horizons of soils and minesoils were performed by the Mineral Constitution Laboratory, The Pennsylvania

State University, University Park, Pennsylvania. Total sulfur was determined using the high temperature combustion method (LECO furnace). When total sulfur exceeded 0.05% of the sample by weight, pyritic, sulfate, and organic forms were analyzed separately. Depending on the amount present, pyritic sulfur was determined either by atomic absorption spectroscopy or by the Eschka method (D271-70), and sulfate sulfur was obtained by precipitation with $BaCl_2$ (D2492-68) (ASTM, 1971).

Samples from each horizon were prepared for X-ray diffraction by removing free iron oxides and organic matter (Anderson, 1963). Clay material (<2μ) was removed by centrifugation and two subsamples were obtained. One subsample was saturated with Mg and the other with K. X-ray diffraction patterns were run on the room temperature (25°C) Mg saturated slides and again after solvation with ethylene glycol at 80°C. Patterns were also obtained from the room temperature (25°C) K saturated slides, and after 2 hours of heat treatment at both 300 and 500°C.

The undisturbed Hazleton and Dekalb soils, at pits 1 and 2, respectively, are within a forested area. Trees had been removed from the site on which the Cookport and Hazleton soils were located (pits 3 and 4). The pedogenetic features common to well developed soils were expressed in the soils at these four locations. In contrast, soils at pits 5 through 8 are located within the area which has been stripmined and reclaimed, and consequently exhibit characteristics of minimal pedogenetic development.

Natural Soils

Pit 1. Structural development and horizon differentiation were evident in this soil (Table 2.1). Clay films have accumulated in the B22t and B23t horizons due to pedogenetic processes, however, the clay content does not qualify either of these as diagnostic argillic horizons.

TABLE 2.1. MORPHOLOGICAL PROPERTIES OF SOILS AND MINESOILS

Pit	Horizon	Depth (cm)	Moist Color		Texture*	Structure†	Consistence		Boundary¶
			Matrix	Mottles			Moist‡	Wet§	
1	A1	0-3	10 YR 3/2		sil	gr	fr	ns,np	cw
	A2	3-10	10 YR 5/4		sil	pl&sbk	fr	ns,np	cs
	B21	10-41	10 YR 5/4		l	pl&sbk	fr	ns,sp	gs
	B22t	41-74	7.5 YR 5/4						
			& 4/4		cnl	sbk	fr	ns,np	cw
	B23t	74-109	7.5 YR 5/8						
			& 4/4		cnsil	sbk	fi	ns,np	gw
	C	109-176	7.5 YR 6/6		vcnsil	sbk	fi	ns,np	gw
2	A1	0-10	10 YR 3/2		sil	gr	fr	ns,np	cs
	B21	10-33	10 YR 5/6		l	sbk	fr	ns,np	gw
	B22	33-51	10 YR 5/6		cnl	sbk	fr	ns,np	gw
	B23	51-71	7.5 YR 5/6		cnl	sbk	fr	ns,np	cw
	C	71-74	7.5 YR 6/6		vcnl	m	fi-fr	ns,np	cw
3	A1	0-15					vfi		di
	A2	15-43	10 YR 6/4		cnl	abk	fr	ns,np	gw
	B1	43-66	10 YR 5/6		cnl	abk	fr	ss,sp	cw
	Bx1t	66-91	7.5 YR 4/4		cnl	pr&abk	fi	ss,p	gw
	Bx2t	91-117	7.5 YR 4/4	10 YR 6/2	cl	pr&sbk	fi	ss,sp	gw
	Bx3t	117-135	10 YR 5/4	7.5 YR 5/6					
				& 10 YR 6/2	sil	pr&sbk	fi	s,p	cw
	Bx4t	135-167+	10 YR 3/3	10 YR 6/2	vcnl	pr&sbk	vfi	ns,sp	
4	A1	0-8	10 YR 4/2		cnsil	pl&gr	fr	ss,p	cw
	A2	8-20	10 YR 5/4		cnsil	pl&sbk	fr	s,p	cw
	B21t	20-48	10 YR 5/8		cnsil	sbk	fr	s,p	gi
	B22t	48-74	10 YR 4/4		cnsil	sbk	fi	ss,sp	gi
	B23t	74-94	10 YR 5/8		cnsil	sbk	fr	ss,sp	aw
	IIC1	94-125	N 2/0		vcnsil	m	fr	ns,np	ai
	IIC2	125-183+	10 YR 6/1						
			& 6/4		vcnsil	m	vfr	ns,np	
5	Ap	0-20	10 YR 5/6						
			& 4/4		vcnl	pl&sbk	fr-fi	ss,sp	aw
	C1	20-36	10 YR 3/3		vcnsl	m	fr	ss,np	gw
	C2	36-56	10 YR 3/3		vcnsl	m	fr	ss,np	gw
	C3	56-74	10 YR 3/3		vcnsl	m	fr	ss,np	ds
	C4	74-114	10 YR 3/3		vcnsl	m	fi	ss,np	cw
	C5	114-152	10 YR 4/3		vcnls	m	fr	ns,np	
6	Ap	0-13	10 YR 5/4		vcnsil	gr&sbk	fr	ss,sp	aw
	AC	13-28	10 YR 4/3		vcnsl	sbk&m	fr-fi	ss,sp	gw
	C1	28-53	10 YR 4/4		vcnsl	m	fi	ss,sp	cw
	C2	53-84	7.5 YR 5/4		vcnls	m	fr	ns,np	gi
7	Ap1	0-10	7.5 YR 3/2		vshl	sbk	fr	ss,sp	ab
	Ap2	10-31	10 YR 4/3		vshsl	sbk&m	fr-fi	ss,sp	ab
	C1	31-51	10 YR 4/2		vshsl	m	fi	ss,np	gw
	C2	51-66	10 YR 3/2		vshls	m	fr	ns,np	cw
	C3	66-127				100% rock fragment			cw
	C4	127-154	10 YR 3/1						
			& N 2/0		vshls&ls	m	fr	ns,np	
8	AC	0-18	10 YR 5/4		vshsl	gr&sbk	fr	ss,sp	as
	C1	18-36	10 YR 4/3		vshsl	m	fr-fi	ss,np	gw
	C2	36-58	10 YR 3/3		vshsl	m	fi	ss,np	gw
	C3	58-102	10 YR 4/2		vshsl	m	fi	ss,np	gw
	C4	102-145	10 YR 3/2						
			& 4/4		vshl	m	fi	ss,sp	ci
	C5	145-183+	10 YR 4/2						
			& 4/4		vshl	m	fi	ns,np	

*sil=silt loam, l=loam, cnl=channery loam, cnsil=channery silt loam, vcnsil=very channery silt loam, vcnl=very channery loam, cl=clay loam, vcnsl=very channery sandy loam, vcnls=very channery loamy sand, vshl=very shaly loam, vshsl=very shaly sandy loam, vshls=very shaly loamy sand, ls=loamy sand.

†gr=granular, pl=platy, sbk=subangular blocky, m=massive, abk=angular blocky, pr=prismatic

‡fr=friable, fi=firm, vfi=very firm, vfr=very friable.

§ns=nonsticky, np=nonplastic, ss=slightly sticky, sp=slightly plastic, p=plastic, s=sticky.

¶cw=clear wavy, cs=clear smooth, gs=gradual smooth, gw=gradual wavy, di=diffuse irregular, gi=gradual irregular, aw=abrupt wavy, ai=abrupt irregular, ds=diffuse smooth, ab=abrupt broken, as=abrupt smooth, ci=clear irregular.

Pit 2. This soil is similar to that of pit 1 except that it is shallower in depth to bedrock. This pedon is well drained and moderately deep. Both pedons had characteristics common to the Hazleton and Dekalb series (loamy-skeletal, mixed, mesic). In both, the particle size control sections (25-100 cm) contain less than 35% rock fragments by volume, and consequently the pedons do not fit the modal concept of their respective series and are considered taxadjunct to those series. They are both classified as coarse loamy, mixed, mesic Typic Dystrochrepts.

Pit 3. The A1 horizon consisted of depositional material that had eroded from adjacent stripmined areas. The very firm, thick, platy structure showed evidence of compaction. The soil in pit 3 was also the only one with a fragipan (Bx horizons). Clay films were evident in the Bx1t through the Bx4t horizons, and the Bx1t horizon had sufficient illuvial clay to qualify as an argillic horizon. The mottles in the Bx2t through Bx4t horizons was indicative of the impeded drainage. The fragipan extended from 66 cm to the bottom of the pit at 167 cm.

This soil is moderately well drained. It differs slightly from the Cookport series in having less clay in the particle size control section (25-100 cm). The pedon is classified a coarse-loamy, mixed, mesic, Aquic Fragiudult.

Pit 4. The surface horizon has received erosional deposits resulting from stripmining and reclamation of adjacent areas. Beneath this horizon the soil was undisturbed.

The soil was similar to that encountered in pit 1, except for a higher percentage of channers in the particle size control section (coarse-loamy, mixed, mesic Typic Dystrochrept). In addition, a weathered coal seam (coal blossom) was found at a 94 cm depth (IIC1) in this profile overlying a mottled underclay layer (IIIC2). As in pit 1, this pedon contained less than 35% rock fragments by volume in the particle-size-control section (25-100 cm) and did not fit the modal concept of the Hazleton series.

Minesoils

Pit 5. The surface horizon had moderate medium platy structure parting to weak very fine subangular blocky structure indicating that soil forming processes have occurred. The abrupt color change from the Ap horizon to the C horizons is due to the topsoiled nature of this profile.

Pit 6. The Ap horizon had granular and weakly developed subangular blocky structure. Vegetation has exerted its effect enhancing this development. The transitional (AC) horizon had subangular blocky structure grading to structureless, massive soil material. The C3 horizon was composed almost entirely of rock fragments with about 15 to 20% void space.

Pit 7. The surface horizons, Ap1 and Ap2, had weakly developed fine subangular blocky structure grading to massive material at about 30 cm. The color of Ap horizons in this profile was lithochromic. In the C3 horizon, no fine material was present. The horizon was composed mainly of large rock fragments with 20% void space.

Pit 8. A weak fine granular and a weak very fine subangular blocky structure was present in the Ap horizon. Bands of different colored soil were present in the C4 and C5 horizons. The C5 horizon (145 cm) was composed primarily of rock fragments.

The minesoils in pits 5 through 8 are loamy skeletal, mixed, mesic members of the Udorthent great group. The minesoils do not fit into any of the established Udorthent subgroups. Some modifications in Soil Taxonomy criteria are necessary in order to be applied to minesoils. The epipedons of the minesoils were the only horizons that exhibited any pedogenetic development. The C horizons were always structureless and massive with wavy horizon boundaries. Pits 5, 6, and 8 were located in C-spoil material. Consequently, their A to C horizon color changes were primarily due to the soil material spread over the spoil during

reclamation. Minesoil at pit 7 was located on the B-spoil, it did not have abrupt color change, since no topsoil had been spread over this area during reclamation.

Root Density and Particle Size Distributions

Sieve analysis data (Table 2.2) show that a majority of materials in minesoils (>75 percent on the average by weight) were coarse fragments. About 30% of the coarse fragments in minesoils were larger than 76 mm (Pedersen et al., 1978). In their fine earth fraction (<2 mm), most minesoils had significantly less silt and more sand than the natural soils. The clay content, however, for both soils and minesoils did not vary significantly from horizon to horizon nor from pit to pit.

Root penetration in soils (pit 1-4) was limited either by bedrock or a fragipan. In pit 3, roots were numerous to 43 cm, below which they significantly decreased in number and size to the fragipan (Bx) horizon. Few roots penetrated the fragipan, some seemed to grow laterally along the upper boundary, and those that penetrated the fragipan were located along prism walls. In pit 4, most of the roots were located in the A horizon, and roots did not penetrate beneath the coal blossom horizon (94-125 cm). The forested profiles (pit 1 and 2) contained roots throughout the solum.

In the minesoils, many very fine grass roots were present in the topsoiled portion of the profile. These roots, at times tended to grow parallel to the soil surface or spread on plates and ped surfaces. As the spoil became coarser, fine fibrous roots were flattened on coarse fragments and between structural units. Tap-roots were contorted, and there were fewer roots on the shale than on the sandstone fragments. Few roots penetrated the massive C-horizons of the minesoils. Thus, even though the minesoil profiles generally offer a deeper medium for root proliferation, their coarse, structureless nature and resulting rapid drainage, and low water retention capacity may limit root proliferation drastically.

TABLE 2.2. ROOTS AND PARTICLE SIZE DISTRIBUTIONS FOR SOILS (PIT 1-4) AND MINESOILS (PIT 5-8)

Depth (cm)	Horizon	Roots*	% Coarse Fragments†	Particle Size Distribution (mm) Sand 2.0-0.05 (% <2 mm)	Silt 0.05-0.002	Clay < 0.002
Pit 1						
0	A1		23.2	34.8	55.6	9.6
3	A2	Many	23.1	37.3	51.1	11.6
10	B21	Many	32.2	43.9	42.0	14.1
41	B22t	Many	33.9	45.6	40.3	14.1
74	B23t	Few	14.3	58.7	29.7	11.7
109	C	None	57.4	62.5	23.4	14.1
Pit 2						
0	A1		41.7	39.1	46.7	14.1
10	B21	Many	37.7	47.3	38.8	13.8
33	B22	Many	38.3	47.9	39.0	13.1
51	B23	Few	40.5	46.2	40.9	12.9
71	C	None	45.8	48.4	41.4	10.2
Pit 3						
0	A1		55.7	47.1	37.5	15.4
15	A2	Many	38.5	42.7	44.0	13.3
43	B1	Common	44.7	45.1	42.2	12.7
66	Bx1t	Few	49.6	41.4	44.3	14.3
91	Bx2t		36.5	38.4	43.4	18.2
117	Bx3t		29.0	32.6	47.4	20.0
135	Bx4t		49.5	38.2	44.4	17.6
Pit 4						
0	A1	Many	34.1	25.7	58.0	16.3
8	A2	Many	35.5	25.6	57.1	17.3
20	B21t	Few	34.2	27.8	54.3	17.9
48	B22t		38.8	35.4	46.7	17.8
74	B23t		34.5	38.0	47.2	14.8
94	IIC1		31.2	42.5	47.4	10.1
125	IIIC2	None	35.1	21.4	53.7	24.9
Values for Pits 1-4: Average			37.4	40.5	44.7	14.8
Standard Deviation			9.8	9.7	8.0	3.4

Depth (cm)	Horizon	Roots*	% Coarse Fragments†	Particle Size Distribution (mm) Sand 2.0-0.05 (% <2 mm)	Silt 0.05-0.002	Clay < 0.002
Pit 5						
0	Ap	Many	64.4	45.5	38.3	16.3
20	C1	Common/Few	84.6	61.4	26.6	12.0
36	C2	None	79.7	62.3	27.2	10.5
56	C3		79.4	62.1	25.4	12.4
74	C4		80.4	62.3	24.3	13.3
114	C5		90.0	64.6	22.2	13.2
Pit 6						
0	Ap	Many	73.3	47.6	35.7	16.7
13	AC	Many/Common	71.1	53.0	31.0	16.0
28	C1	Few	79.3	58.8	26.1	15.2
53	C2		92.8	66.5	20.3	13.2
Pit 7						
0	Ap1	Many	82.2	51.7	31.9	16.4
10	Ap2	Common	54.1	53.6	28.9	17.5
31	C1	None	86.4	53.5	32.7	13.8
51	C2		88.9	61.4	28.1	10.5
66	C3		66.0	65.7	25.5	8.8
127	C4		80.9	64.6	26.1	9.3
Pit 8						
0	AC	Many	67.8	55.1	35.1	9.8
18	C1	Few	76.5	54.8	33.1	12.1
36	C2	None	81.0	50.6	37.1	12.3
58	C3		81.4	50.0	38.9	11.1
102	C4	Few	71.6	48.0	41.7	10.3
145	C5		69.9	41.1	46.5	12.4
Values for Pits 5-8: Average			77.3	56.1	31.0	12.9
Standard Deviation			9.3	7.3	6.7	2.6

*None = 0, few = (<1,000/m²), common = 1,000-10,000/m²; many = (≥10,000/m²).
†Fragments > 2 mm.

Chemical Properties

Cation exchange capacity (CEC), cation exchange capacity corrected for coarse fragment content, base saturation, pH, and total acidity for different horizons of soils (pit 1-4) and minesoils (pit 5-8) are presented in Figure 2.2. The CEC ranged from 8.5 to 61.2 meq/100 g in the natural soils and from 7.3 to 22.4 meq/100 g in the minesoils. The high absorptive capacity of the carbonaceous matter (coal blossom) in the IIC1 horizon accounted for the high CEC value of this horizon. Whereas, the high CEC's of the A1 horizons of pits 1 and 2 are attributed to the high organic carbon contents. Most of the exchange sites on the soils studied were occupied by H^+ and Al^{+3} ions. Although the average CEC of the minesoils (17 meq/100 g) was higher than in the natural soils (14 meq/100 g), the differences were not significant at the 5% level. However, when the CEC values in component horizons were corrected for the coarse fragment content the differences became pronounced. A 3 meq/100 g nutrient content of corrected minesoils was low when compared to that for the A and B horizons of the adjacent contiguous soils (13 meq/100 g). Therefore, on coarse slowly weathering spoils nutrients availability may limit vegetative growth in the absence of supplemental fertilization.

The pH values of the natural soils and minesoils appeared similar. Total acidity of the natural soils was generally higher due to leaching of bases over time. The high total acidities of the A1 horizons of pits 1 and 2 are attributed to the high organic matter content of these horizons and the effects of an overlying leaf litter, whose decomposition causes acidic conditions. The large differences in total acidity for the AC horizon of minesoil in pit 8 resulted from heavy liming and manuring of that part of the site.

In the natural soils, total acidity generally decreased with depth, whereas in most minesoils (pits 6, 7, 8) it increased. On the average the natural soils and minesoil in pit 7 had a greater percentage of iron oxides and extractable Al

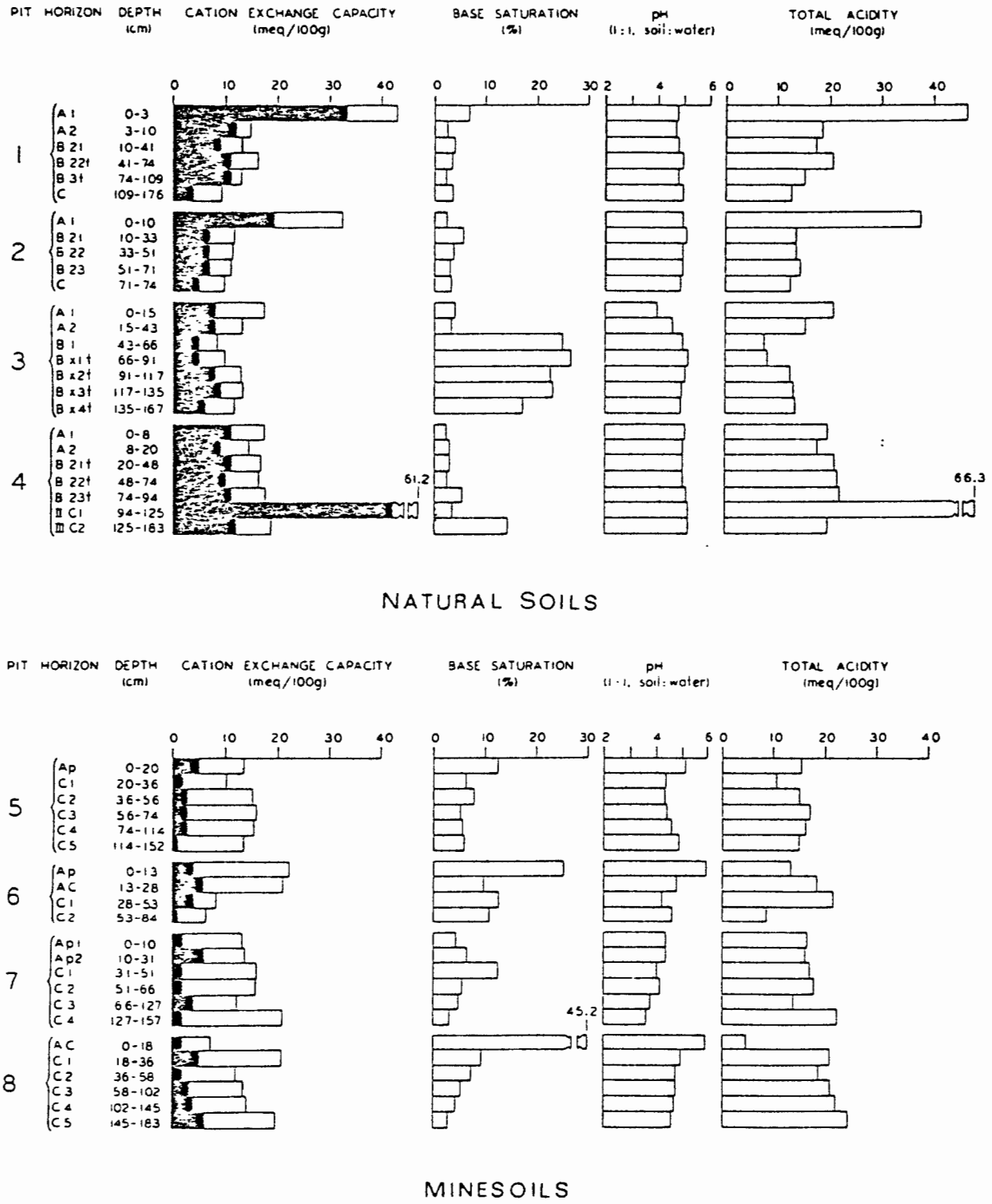

Figure 2.2. Cation exchange capacity on the <2 mm material (clear) and total volume (shaded), base saturation, pH and total acidity for the natural soils and the minesoils.

(Table 2.3). Presence of iron oxides and extractable Al is related to the weathering. It appears that the natural soil horizons, because of their more weathered conditions, contained significantly more iron oxides and extractable Al than the minesoils in pits 5, 6, and 8. Minesoil in pit 7 which has been weathering for only seven years also followed the same trend. The observed levels (Table 2.3) of Al could be toxic to some plant species (Al > 1 to 2 meq/100 g).

TABLE 2.3. IRON OXIDE AND EXTRACTABLE ALUMINUM IN MINESOILS (PIT 5-8) AND CONTIGUOUS NATURAL SOILS (PIT 1-4)

Horizon cm		Iron Oxide %	Extractable Aluminum meq/100 g	Horizon cm		Iron Oxide %	Extractable Aluminum meq/100 g
Pit 1				Pit 5			
0	A1	3.3	6.2	0	Ap	1.7	3.5
3	A2	2.8	4.2	20	C1	1.9	1.4
10	B21	3.1	5.0	36	C2	2.1	1.0
41	B22t	3.2	5.1	56	C3	1.8	1.3
74	B23t	2.6	3.6	74	C4	1.8	1.3
109	C	2.2	3.8	114	C5	1.8	0.7
Pit 2				Pit 6			
0	A1	2.4	6.2	0	Ap	1.2	0.1
10	B21	2.1	2.8	13	AC	1.7	1.7
33	B22	1.9	2.8	28	C1	1.6	2.6
51	B23	1.8	3.5	53	C2	2.2	1.3
71	C	1.9	3.0				
Pit 3				Pit 7			
0	A1	4.1	4.2	0	Ap1	2.3	3.6
15	A2	2.2	2.8	10	Ap2	2.2	3.1
43	B1	2.7	1.0	31	C1	2.3	2.6
66	Bx1t	3.0	1.1	51	C2	1.9	2.8
91	Bx2t	3.3	2.6	66	C3	2.4	2.1
117	Bx3t	3.7	3.0	127	C4	3.1	1.8
135	Bx4t	4.5	3.5				
Pit 4				Pit 8			
0	A1	3.0	3.0	0	AC	1.2	0.1
8	A2	3.3	3.8	18	C1	1.6	1.9
20	B21t	3.4	5.0	36	C2	1.8	2.6
48	B22t	3.8	5.9	58	C3	1.8	2.8
74	B23t	4.0	5.4	102	C4	1.8	3.6
94	IIC1	1.7	7.1	145	C5	1.9	5.1
125	IIIC2	4.0	3.5				
Average		3.0	3.9			1.9	2.1
Standard Deviation		0.8	1.5			0.4	1.2

Organic Carbon

In general, organic carbon content decreased with depth in the natural soils and increased with depth in the minesoils (Table 2.4). Organic carbon contents were highest in the partially decomposed coal seam (IIC1) of pit 4 and in the horizons above B23t, and below (IIIC2) this seam. Whereas, in natural soils the A1 horizons in pits 1 and 2 have accumulated most organic matter from the forest vegetation. The minesoil in pit 7 which was derived from carboniferous shale also had a very high organic carbon content. Thus, the high carbon values of minesoils are attributed to the presence of partly weathered coal or carboniferous shale fragments rather than to vegetation remains.

The Walkley-Black method seemed to agree in general with the ignition method values for the surface horizons of the natural soils, but gave lower values for subsurface horizons. The values obtained by the Walkley-Black method for the minesoils did not agree with those determined by ignition. The values obtained by ignition were 1/3 to 6 times higher than those obtained by the Walkley-Black method; however, this relationship was not constant and the AC horizon of pit 8 had higher organic C when determined by Walkley-Black method.

Apparently the organic C in minesoils cannot be accurately determined by either of these methods when shale and coal fragments are present. Alternate methods should be sought, which could give more reliable determinations.

The C/N ratios for three of the natural soil profiles decreased with depth (pits 1, 2, and 3). However, high values of C in the coal blossom (IIC1) and underclay (IIIC2) were responsible for higher C/N ratios in pit 4. The C/N ratios obtained on the minesoils were very erratic because of high C values, and were generally higher than could be attributed to either plant or animal residues.

TABLE 2.4. PERCENTAGE OF ORGANIC CARBON*, NITROGEN, C/N RATIO AND CLAY MINERAL CONTENT OF MINESOILS (PIT 5-8) AND CONTIGUOUS NATURAL SOILS (PIT 1-4)

Horizon (cm)	C	N	C/N	Clay Minerals M	V	I	K	Q
Pit 1								
0 A1	6.27	0.346	18.1		45	15	40	tr
3 A2	2.13	0.064	33.3		40	20	35	5
10 B21	0.42	0.040	10.5	5	30	25	35	5
41 B22t	0.32	0.037	8.7	15	20	30	35	tr
74 B23t	0.10	0.048	2.1	5	15	35	45	
109 C	0.09	0.026	3.5					
Pit 2								
0 A1	3.64	0.170	21.4	tr	50	20	30	tr
10 B21	0.56	0.037	15.1		55	15	30	tr
33 B22	0.43	0.030	14.3		55	15	25	5
51 B23	0.22	0.021	10.5	tr	50	20	30	tr
71 C	0.17	0.029	5.9	tr	35	30	35	tr
Pit 3								
0 A1	1.53	0.123	12.4	10	15	35	40	tr
15 A2	1.52	0.057	26.7	10	20	25	45	tr
43 B1	0.23	0.030	7.7	10	20	30	40	tr
66 Bx1t	0.24	0.022	10.9	10	15	30	45	tr
91 Bx2t	0.20	0.029	6.9	15	15	35	35	tr
117 Bx3t	0.34	0.027	12.6	20	15	30	35	tr
135 Bx4t	0.35	0.037	9.5	15	15	30	40	tr
Pit 4								
0 A1	6.25	0.101	61.9	15	25	20	40	tr
8 A2	0.85	0.058	14.7	15	25	20	40	tr
20 B21t	0.67	0.058	26.2	10	25	25	40	tr
48 B22t	0.34	0.047	7.2	10	20	30	40	
74 B23t	1.51	0.057	26.5	10	10	40	40	
94 IIC1	12.59	0.347	36.3	5	5	40	50	
125 IIIC2	2.03	0.059	34.4	5		40	55	
Average	1.72	0.076	—	11	27	27	39	5
Standard Deviation	2.85	0.088	—	4	15	8	7	0

Horizon (cm)	C	N	C/N	Clay Minerals M	V	I	K	Q
Pit 5								
0 Ap	0.39	0.037	10.5	10	15	35	40	tr
20 C1	1.81	0.068	26.6		10	45	40	5
36 C2	1.68	0.062	27.1		10	40	45	5
56 C3	1.87	0.049	38.2	5	10	45	40	tr
74 C4	1.51	0.053	28.5	5	5	40	45	5
114 C5	1.43	0.052	27.5	5	5	45	40	5
Pit 6								
0 Ap	0.78	0.058	13.5	10	15	30	40	5
13 AC	1.80	0.048	37.5		10	40	45	5
28 C1	1.64	0.059	27.8	tr	5	50	45	tr
53 C2	0.95	0.026	36.5		10	40	50	
Pit 7								
0 Ap1	4.37	0.110	39.7	tr	10	40	50	tr
10 Ap2	2.49	0.059	42.2	5	10	40	45	tr
31 C1	6.88	0.185	37.2	tr	5	45	45	5
51 C2	11.40	0.285	40.0	5	5	40	45	5
66 C3	19.90	0.576	34.6	5	10	40	40	5
127 C4	22.83	0.644	70.0	5	5	40	40	10
Pit 8								
0 AC	0.69	0.050	13.8	5	30	20	35	10
18 C1	0.53	0.070	7.6	5	10	45	40	
36 C2	2.85	0.112	25.5	10	15	35	40	tr
58 C3	2.76	0.075	36.8	5	15	35	40	5
102 C4	3.00	0.101	29.7	5	20	35	35	5
145 C5	2.74	0.112	24.5	10	15	30	40	5
Average	4.29	0.131	—	6	11	39	42	6
Standard Deviation	6.06	0.166	—	2	6	7	4	2

*By ignition method.
C=Organic carbon
N=Nitrogen
M=Montmorillonite
V=Vermiculite
I=Illite
K=Kaolinite
Q=Quartz

Clay Mineralogy

The conversion of illite to vermiculite (Ciolkosz, 1978) is one of the principal clay weathering transformations in Pennsylvania soils. Vermiculite and kaolinite were the dominant clay minerals in the natural soils (pit 1-4), while illite and kaolinite were dominant in the minesoils (pit 5-8) (Table 2.4). The illite in the natural soils has been weathered to vermiculite while in the minesoils much illite remains. Mineralogical data indicates that minesoils are similar to the contiguous natural soils. However, the minesoils studied, all weathering for less than 10 years, have not been exposed to as intensive weathering as the natural soils.

The large amount of montmorillonite in pit 3 is attributed to the impeded drainage (fragipan) in that profile, while topographic position of pit 4, and to a certain extent 8, is probably responsible for the higher montmorillonite content.

Sulfur (S)

The discussion covering S and the following two sections on spectrometric and spectrographic analyses may be regarded as somewhat speculative in nature. We do not know the extent of natural variation associated with the elements considered. Quite possibly some random degree of stratification in minesoils could be responsible for higher or lower contents of certain elements as compared to natural soils. Consequently, considerable caution should be exercised when ascribing any of the reported results directly to the soil forming processes.

The total S content (Table 2.5) of natural soils was not high enough to warrant component analyses into sulfate S, pyritic S, and organic S. The high sulfate S content of the C2 horizon of pit 7 (0.16%) may be a result of the longer weathering of this profile (7 years compared to 3 years for other minesoils) or due to the

TABLE 2.5. TOTAL SULFATE, PYRITIC AND ORGANIC SULFUR CONTENTS OF SELECTED HORIZONS

Pit	Depth (cm)	Horizon	Total*	Sulfate	Pyritic	Organic
1	3-10	A2	0.03			
	41-74	B22t	0.03			
2	0-10	A1	0.04			
	33-51	B22	0.03			
3	15-43	A2	0.04			
	46-66	B1	0.03			
	117-135	Bx3t	0.04			
4	0-20	A2	0.03			
	48-74	B22t	0.03			
	94-125	IIC1	0.19	0.01	0.03	0.15
5	0-10	Ap	0.03			
	74-114	C4	0.13	0.05	0.07	0.01
6	0-13	Ap	0.03			
	58-84	C2	0.13	0.05	0.08	0.00
7	10-31	Ap2	0.10	0.05	0.02	0.03
	51-66	C2	0.38	0.16	0.07	0.15
8	0-18	AC	0.04			
	58-102	C3	0.08	0.04	0.04	0.00

*Total sulfur≤0.05%, no further analysis.

random stratification of the spoil material. Greater amounts of organic S forms were found in the IIIC1 horizon of pit 4 and C2 horizon of pit 7. Pyritic S, the principal component in the formation of acid mine drainage, was low in all of the minesoil horizons yet higher than in the natural soils. Since highly acid materials have been buried well below the sampling depth considered in this study, they are not considered to be a major problem at this site.

Spectrometric Analyses

Quantitative spectrometric analyses (Table 2.6) reveal some trends, however, little difference is noted between soil and minesoil.

The SiO_2 contents of the natural soils and minesoils are similar. The higher values of SiO_2 in the C4 horizon of pit 5 indicated that weathering at this depth possibly has not exerted as much an affect as in the overlying horizons or may be

TABLE 2.6. QUANTITATIVE SPECTROMETRIC ANALYSIS OF SELECTED HORIZONS (PRESENTED IN PERCENTAGES)

Pit	Depth (cm)	Horizon	Wt. Ash	SiO_2	Al_2O_3	TiO_2	Fe_2O_3	MgO	CaO	MnO	Na_2O	K_2O	Total
1	3-10	A2	94.03	79.0	12.0	0.92	4.75	0.78	0.11	0.061	0.33	1.96	99.9
	41-74	B22t	94.81	76.5	13.8	0.89	5.75	0.61	0.14	0.076	0.27	2.24	100.3
2	0-10	A1	90.05	84.0	9.0	0.80	2.92	0.76	0.12	0.039	0.29	1.43	99.4
	33-51	B22	96.12	86.0	8.7	0.74	2.71	0.39	0.12	0.039	0.24	1.46	100.4
3	15-43	A2	95.22	84.0	9.3	0.79	2.65	0.39	0.09	0.039	0.25	1.63	99.1
	43-66	B1	96.47	83.0	10.0	0.79	3.30	0.49	0.17	0.049	0.28	1.85	99.9
	117-135	Bx3t	95.76	81.5	12.1	0.79	4.58	0.75	0.17	0.075	0.47	2.25	102.7
4	8-20	A2	94.35	78.5	14.1	1.04	4.55	0.69	0.11	0.069	0.37	2.35	101.8
	48-74	B22t	94.10	74.0	15.8	1.02	5.95	0.91	0.08	0.046	0.40	2.67	100.9
	94-125	IIC1	70.12	71.0	18.9	1.19	5.30	0.68	0.32	0.067	0.03	3.10	100.9
Average			92.10	79.75	12.37	0.40	4.25	0.65	0.14	0.056	0.24	2.09	
Standard Deviation			7.93	4.84	3.33	0.14	1.26	0.17	.07	0.015	0.12	0.54	
5	0-10	Ap	95.43	82.0	12.6	0.87	4.22	0.53	0.18	0.046	0.26	2.09	102.8
	74-114	C4	94.27	90.5	11.7	0.63	5.62	0.49	0.11	0.058	0.12	2.23	101.5
6	0-13	Ap	95.03	82.0	11.2	0.82	3.93	0.48	0.40	0.074	0.24	1.87	101.0
	53-84	C2	94.07	79.0	12.6	0.69	6.80	0.54	0.15	0.055	0.12	2.39	102.4
7	10-31	Ap2	92.96	78.5	13.3	0.77	5.23	0.51	0.09	0.088	0.14	2.40	101.0
	51-66	C2	77.09	73.0	15.5	0.92	8.75	0.72	0.19	0.074	0.19	2.66	102.0
8	0-18	AC	95.54	86.0	8.3	0.64	3.85	0.37	0.27	0.064	0.20	1.37	101.1
	58-102	C3	91.80	77.5	14.2	0.91	6.55	0.69	0.10	0.102	0.30	2.53	102.9
Average			92.02	81.06	12.42	0.78	5.62	0.54	0.19	0.070	0.20	2.19	
Standard Deviation			6.17	5.40	2.15	0.12	1.70	0.11	0.12	0.018	0.07	0.42	

due again to the random stratification of spoil material. Lower SiO_2 values in C2 horizon of pit 7 indicate lower content of sandstone, in the mixture of sandstone and shale of the B-spoil. The higher values of Fe_2O_3 for the deeper horizons of minesoils may have resulted from the dissolution and redistribution of iron sulfides. The greater proportion of K_2O in the minesoils as compared with the natural soil horizons may indicate a more active weathering of illite.

Spectrographic Analyses

Semiquantitative spectrographic analysis of select horizon material was confirmatory showing little difference between trace elements of soils and minesoils (Table 2.7).

TABLE 2.7. SEMIQUANTITATIVE SPECTROGRAPHIC ANALYSIS OF SELECTED HORIZONS* (PRESENTED IN PPM)

Pit	Depth (cm)	Horizon	Ba	Be	Ce	Co	Cr	Cu	Ga	La	Ni	Sc	Sr	V	Y	Zr
1	3-10	A2	350	<3	120	<20	74	23	23	40	25	12.0	41	96	31	420
	41-74	B22t	380	<3	<100	<20	100	31	25	32	32	15.0	47	100	33	390
2	0-10	A1	390	<3	<100	<20	74	16	15	33	<25	6.6	35	66	33	440
	33-51	B22	310	<3	<100	<20	56	16	18	30	<25	8.0	30	62	26	290
3	15-43	A2	380	<3	<100	<20	70	15	19	30	26	8.4	50	72	26	340
	43-66	B1	320	<3	<100	<20	66	18	18	31	<25	10.0	43	74	36	340
	117-135	Bx3t	350	<3	<100	<20	84	24	21	38	31	12.0	50	100	29	340
4	8-20	A2	410	<3	<100	<20	100	20	25	48	25	12.0	64	110	35	340
	48-74	B22t	430	<3	<100	<20	100	32	28	52	33	17.0	86	130	40	410
	94-125	IIC1	300	4	120	39	120	54	39	60	74	25.0	160	150	60	330
Average			362	<3	<104	<22	84	25	23	39	<32	13.6	61	96	35	364
Standard Deviation			43				20	12	7	11		5.6	38	29	10	48
5	0-10	Ap	340	<3	100	<20	76	22	22	43	<25	13.0	42	110	32	340
	74-114	C4	300	<3	<100	<20	80	26	23	34	44	13.0	46	100	22	250
6	0-13	Ap	340	<3	120	<20	86	21	23	50	<25	12.0	45	100	33	490
	53-84	C2	270	<3	<100	<20	60	30	22	43	27	13.0	45	100	35	310
7	10-31	Ap2	390	<3	<100	50	96	35	26	43	27	14.0	64	110	30	240
	51-66	C2	440	<3	110	<20	110	50	26	44	40	18.0	120	120	37	370
8	0-18	AC	290	<3	<100	<20	50	12	16	29	<25	5.4	41	120	30	380
	58-102	C3	430	<3	<100	43	100	50	29	40	46	16.0	80	120	39	310
Average			350	<3	<104	<27	82	31	23	41	<32	13.0	60	110	32	336
Standard Deviation			64				20	14	4	7		3.6	28	9	5	80

*Not detected in all samples: Ag, Bi, Ge, Mo, Nb, Pb, Sn, Yb.

Where coarse shale fragments predominated in the deeper horizons of minesoils (pits 7 and 8), the Cu content was slightly higher than that of natural soils, whereas the Co content of the Ap2 of pit 7 and C3 of pit 8, attributed to higher shale content in these profiles, exceeded the 1-40 ppm range reported for soils (Baker and Chesnin, 1975). The Ba, Cr, V, Be, and Ni contents of the minesoils and associated soils were within ranges expected for natural soils which indicates that heavy metal toxicities would not be encountered on these minesoils.

PHYSICAL PROPERTIES

Typically, minesoils in Appalachia are low in organic matter and high in coarse fragments, with weakly developed structure. Their surface horizons contain the

greatest amounts of fine soil material, <2 mm in diameter. Large boulders and fragmented rock pieces are common. During the mining operation, overburden rock is shattered by blasting, and as a result many "fines" essentially consist of pulverized unweathered rock materials (Rogowski et al., 1977).

Here we will discuss the effects of surface mining and reclamation operations on some physical properties of resultant minesoil. The objectives were to determine the moisture characteristics and specific surface of minesoils, to establish the range and variation in bulk density, to determine the hydraulic conductivity, and to estimate initial evapotranspiration at the reclaimed site.

Bulk densities of minesoils especially at the surface are usually greater than those of undisturbed soils because of their compacted state, lack of structure, immature pedogenetic nature, and higher coarse fragment content (Ciolkosz et al., 1983). Natural soils tend to be more porous with an intricately developed system of cracks and fissures. Although, in general, the total porosity is lower, pores in minesoils are typically larger.

Physical and morphological properties of both natural soils and minesoils influence water retention and movement within a profile. Water retention depends mainly on the amount of the <2 mm fraction and on structure. The degree of tension with which the water is held determines its availability to plants. Specific retention decreases with an increase in particle size (Farmer and Richardson, 1976), resulting from a decrease in surface area and an increase in pore size; however, it does not seem to be changed significantly by the shape or type of fragments, nor by the time allowed for drainage (ElBoushi, 1966)[1].

---

[1] I. M. ElBoushi. 1966. Geologic interpretations of recharge through coarse gravel and broken rock. Ph.D. Thesis. Stanford University, Stanford, California.

It is difficult to obtain undisturbed samples of minesoils for determination of hydraulic properties because of the large percentage of coarse fragments and weak structural development of these materials. Sieved samples, particularly when corrected for coarse-fragments content, may however give a useful estimate of hydraulic properties, like moisture characteristic and hydraulic conductivity. Bruce (1972) concluded that sieving of coarse-textured, organic-matter deficient materials did not significantly modify their water retention properties. In general, research results (Bruce, 1972; Unger, 1975) have indicated that if natural structure is present, any type of sample disturbance will disrupt it, modifying pore-size distribution and pore volume. However, in materials with little or no structural development, like minesoils, this effect should either be minor or absent.

In the Appalachian minesoils we expect the storage of plant available water to be significantly reduced because of their coarser texture, greater rock fragment content and larger pores. Rates of infiltration and hydraulic conductivity usually increase as the materials become coarser textured. The coarser texture, however, restricts unsaturated moisture movement within the profile due to a decrease in area for flow and increase in tortuosity (Mehuys et al., 1975). At times minesoils may occupy up to 25% greater volume than the natural material (Van Voast, 1974), frequently including randomly distributed large channels which allow rapid drainage. Therefore, values for water movements into and through minesoils are highly variable. ElBoushi (1966)[1] has shown that water infiltrating through loose granular material (similar to subsurface horizons of many minesoils) tends to concentrate into discrete paths. Similar flows, but due to wetting front instability, have been discussed by Hill and Parlange (1972), and more recently by Raats (1973) and Philip (1975).

The experimental site (Figure 2.3) shows location of instrumentation, and measurement sites. When sampling minesoils at pits 5, 6, 7, and 8 we could only

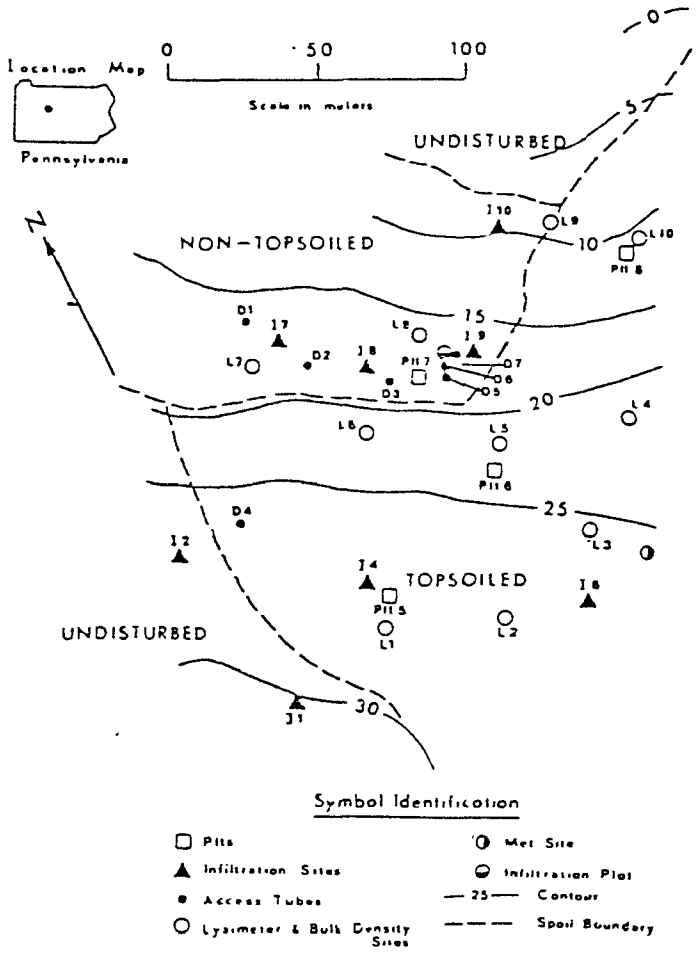

Figure 2.3. Study area and location of minesoil pits, lysimeter sites, and infiltration sites.

obtain a few clods near the surface at pits 5 and 7, and none at all below the 0.2 m depth and at the other two pits. In addition to clods, bulk samples (about 5 kg) were collected from each horizon down to a depth of 1.5 to 2.0 m.

Specific Surface

Specific surface area (SS) of the mineral fraction of minesoils in meters squared per gram was calculated, using an equation of Young and Onstad (1976)

$$SS = -2.36 + 7.96\ (W) - 4.49\ (OM) \qquad (2.1)$$

In equation (2.1), W is the percent gravimetric water content at 1,500 kPa corrected for coarse fragments and OM is the percentage of organic matter estimated by multiplying percentage C (Walkley-Black) by a factor of 2.5, as suggested by Broadbent (1953) for subsoil materials also corrected for coarse fragments.

In general, the correction for coarse fragments of properties such as organic matter involved multiplying the value obtained by the percentage of material <2 mm, while correction of water retention values such as 1,500 kPa values (W) involved multiplying them by percentage of material <2 mm and adding a correction factor. Correction factors were in turn obtained by determining experimentally (ElBoushi, 1966)[1] the amount of water retained by coarse fragments and multiplying these values by percentage of material >2 mm. This amount of water retained by sandstones (pits 5, 6, and 8) was 0.0282 g/g and for shale (pit 7) it was 0.0687 g/g. Thus, the convections for sandstone (CSD) and shale (CSH) coarse fragments may be written

$$CSD = U\ (1-B) + 0.0282B \qquad (2.2)$$

$$CSH = U\ (1-B) + 0.0687B$$

where U is the uncorrected value of water retention determined in the laboratory on the <2 mm material and B are the amounts of coarse fragments >2 mm present in the respective horizon (Table 2.8) of the minesoil.

Table 2.9 lists organic matter, 1,500-kPa water content, and specific surface values for the minesoils. Relatively high organic matter values reported for the C horizons of minesoils may in part be due to inclusion of coal fragments (pit 7), or to mixing in of plant debris during reclamation (pit 5, 6, and 8). Originally the area was forested. While the tree trunks were removed during land preparation before mining commenced, much of the rest was mixed with the material later comprising upper layers discussed here. Organic matter contents exhibited much larger variation among sites and horizons as measured by CV values than did 1,500

TABLE 2.8. COARSE FRAGMENT CONTENT (BY WEIGHT) OF THE MINESOIL HORIZONS

Horizon	Coarse fragments	Horizon	Coarse fragments
	g/g		g/g
	Pit 5		Pit 7
Ap	0.644	Ap1	0.822
C1	0.846	Ap2	0.541
C2	0.797	C1	0.864
C3	0.794	C2	0.889
	Pit 6		Pit 8
Ap	0.733	AC	0.678
AC	0.711	C1	0.765
C1	0.793	C2	0.812
C2	0.928	C3	0.814

TABLE 2.9. ORGANIC MATTER (OM)*, 1,500 kPa WATER CONTENT (W)†, AND SPECIFIC SURFACE (SS)‡ OF MINESOILS

Horizon	OM	W	SS
	--------- % ---------		m^2/g
		Pit 5	
Ap	0.16	4.38	31.8
C1	0.22	3.29	22.8
C2	0.30	3.45	26.4
C3	0.29	3.62	25.2
		Pit 6	
Ap	0.48	4.09	28.0
AC	0.70	3.90	25.5
C1	0.42	3.47	23.3
C2	0.08	3.00	21.2
		Pit 7	
Ap1	0.90	6.83	47.9
Ap2	1.40	6.94	46.6
C1	0.73	6.86	49.0
C2	0.65	6.91	49.7
		Pit 8	
AC	0.75	3.66	23.4
C1	0.69	3.70	24.0
C2	0.61	3.58	23.4
C3	0.51	3.56	23.7
Mean	0.56	4.45	30.7
C.V.	58.9%	33.3%	35.0%

*Walkley-Black OM = 2.5C, corrected for coarse fragments.
†Gravimetric, corrected for coarse fragments.
‡SS from equation (4.1).

kPa values. The values of specific surface obtained for the minesoils appear to be typical of the materials low in montmorillonite. Comparison of the A horizons of the minesoils with the A horizons of the adjoining natural soils (not listed in Table 2.9) showed them to be somewhat less (33.9 vs. 38.3 m^2/g), while a comparison of C horizons suggested values on minesoils to be about two-third of those on adjoining natural soils.

Pit 7 values were the highest primarily because of a higher water content at 1,500 kPa. This results since more water was found experimentally to be retained on shale (0.0687 g/g) than on sandstone fragments (0.0282 g/g) used in the correction factor (equations (2.2) and (2.3)) computations. On the average, values for other pits were about the same. Both the organic matter values and the 1,500-kPa values were corrected for the coarse fragment content. Thus, the results represent specific surface area of the minesoil as a whole. Somewhat higher values for minesoils (36.7 vs. 31.0 m^2/g) would be reported if this correction has not been applied. Young and Onstad (1976) concluded that equation (2.1) when compared with measured values of specific surface could explain about 86% of the variation.

Bulk Density

Bulk density near the minesoil surface was measured at 10 lysimeter sites randomly located within the reclaimed area (Figure 2.3). Five replicate readings around each site were made with a direct transmission gamma probe (Blake, 1965; Troxler, 1970), at 0.15- and 0.30-m depth. Bulk density was determined on clods collected near lysimeter sites and bulk density was also determined gravimetrically using a modified excavation technique (Bertram, 1973). In this technique, we placed a steel ring (1 m in diam.) on the spoil surface at each of the 10 sites and removed loose stones and excessive vegetation (Figure 2.4). A pliable rubber liner was then fitted inside the ring and the volume of water needed to fill the ring was determined. The minesoil within the ring was then removed to about the

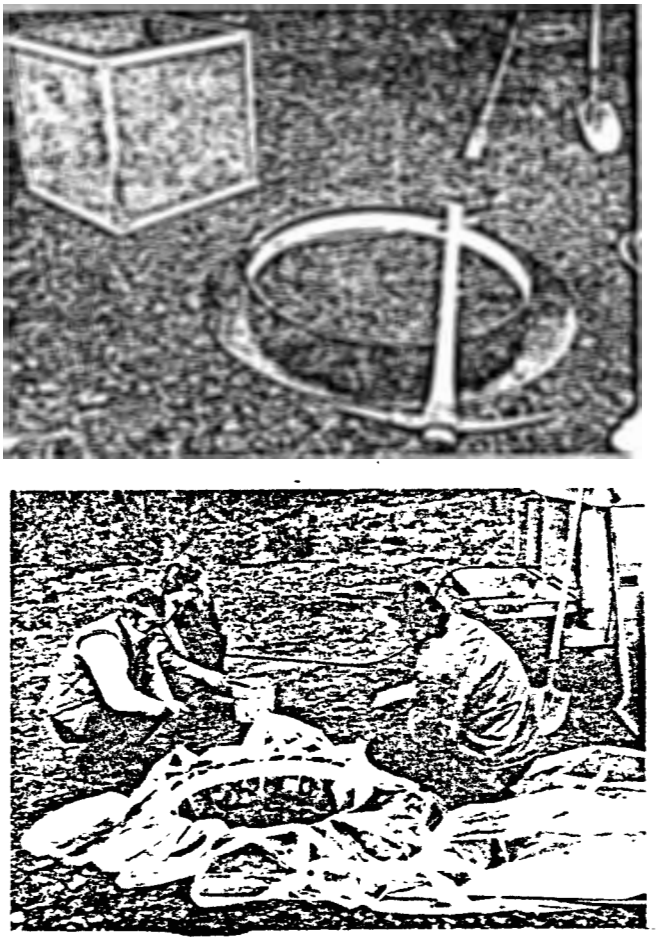

Figure 2.4. Determination of bulk density by a modified excavation technique (Bertram, 1973).

0.5-m depth and weighed. Small grab samples were taken to determine gravimetric water content. The rubber liner was then replaced in the excavation and water added to the same level as before. From volume differences and soil weight, corrected for water content, dry bulk density was determined.

In addition, minesoil density to 1.5 m was determined at seven locations (Figure 2.3) with the depth density gamma probe and corrected for water content obtained with neutron scatter equipment. Access tube installation (Figure 2.3) in the stony minesoil materials followed Rawitz (1969).

The average surface bulk densities obtained by various methods (Table 2.10) were not significantly different from each other at the 5% level. The excavation technique had the highest coefficient of variation, whereas the clods had the lowest. Results also showed that the means of the sites did not vary significantly from one another. It appears that the direct transmission gamma probe method is well suited to non-destructive measurement of minesoil bulk density. It is by far the most convenient and rapid of the methods tried. However, where very large fragments prevail, the excavation method could prove superior.

TABLE 2.10. SURFACE BULK DENSITY (MEAN), AND COEFFICIENT OF VARIATION (C.V.) OF MINESOILS DETERMINED BY VARIOUS METHODS

Method	Mean	C.V.
	kg/m^2	%
Excavation	1.810	13.3
Gamma probe	1.700	11.2
Clods*	1.780	6.7

*Desaturated at 30-kPa tensiometer pressure.

In Table 2.11 depth bulk density measurements of minesoil at seven sites are given. On the average the density in the 2-m profiles increases with depth and the degree of variation (as measured by the coefficient of variation) appears to decrease. Low density values (<1,000 kg/m^3) are probably indicative of large spaces and cavities within the spoil, while higher densities may imply proximity to solid shale or sandstone fragments, or degree of equipment compaction at shallow depth. Despite the diversity of locations, there was little apparent difference in bulk density between the sites both on the topsoiled and nontopsoiled profiles when low values were excluded.

TABLE 2.11. DEPTH BULK DENSITY DISTRIBUTIONS ON THE MINESOIL, AND THE SITE MEAN, STANDARD DEVIATION (SD) AND COEFFICIENT OF VARIATION (C.V.)

Depth	D1	D2	D3	D4	D5	D6	D7	Mean	SD	C.V.
m	kg/m^2									%
0.305	1.730	1.360	1.240	1.740	1.390	1.400	1.630	1.499	199	13
0.610	1.670	1.210	890*	1.680	1.590	1.590	1.450	1.532	178	12
0.914	1.650	1.610	1.600	1.130	1.600	1.610	1.600	1.543	183	12
1.219	1.720	1.660	1.510	670*	1.530	1.580	1.530	1.588	84	5
1.524	1.060*	1.660	1.510	730*	1.580	1.600	1.650	1.600	54	3
1.829	640*	1.620	1.530	760*	1.580	1.550	1.650	1.586	44	3
2.134	1.790	1.630	1.590	1.590	1.630	1.540	1.570	1.620	81	5

*Value not included in computation of mean.

Minesoil Water--

Moisture characteristic--Gravimetric moisture characteristics of sieved (<2 mm) materials from each horizon of the minesoils was obtained experimentally in triplicate by desorption (Richards, 1965). Subsequently, these values were corrected for coarse fragments. Since clods could not be obtained at the pits on all but two horizons of the minesoils, we have no measure of profile bulk density other than gamma probe readings at different sites. The moisture data are therefore presented on the gravimetric basis. Indeed, because of high coarse fragment content, with many fragments being of boulder proportions, we may question advisability of presenting the moisture data on other than gravimetric basis. Under conditions of abundant rainfall minesoils can supply ample water to plants (Plass and Vogel, 1973). At times it even appears that minesoils have greater amounts of available water in comparison to natural soils (Verma and Thames, 1975). This apparent increase in availability often results because water in minesoils is normally held at lower tensions than in corresponding natural soils.

The textural differences and organic matter deficiencies of minesoils account in general for their lower water holding capacities, and when corrected for coarse fragments, the minesoils actually retain substantially less water than comparable natural soil horizons. Table 2.12 gives moisture characteristic data (gravimetric) at four pits corrected and uncorrected for coarse fragments. Figure 2.5 shows

TABLE 2.12. MINESOIL MOISTURE CHARACTERISTICS

Depth	Horizon	Tensiometer pressure (kPa) 0	1	2	4	6	8	10	15	24	33	100	1,500
m		g/g											
							Pit 5						
0	Ap	0.4205*	0.3494	0.3337	0.2975	0.2766	0.2650	0.2569	0.2265	0.2122	0.1797	0.1667	0.0719
		0.1678†	0.1425	0.1369	0.1241	0.1166	0.1125	0.1096	0.0988	0.0937	0.0821	0.0775	0.0438
0.20	C1	0.3271	0.2856	0.2727	0.2337	0.2208	0.2128	0.2098	0.1890	0.1715	0.1452	0.1370	0.0590
		0.0734	0.0678	0.0658	0.0598	0.0579	0.0566	0.0562	0.0530	0.0503	0.0462	0.0449	0.0329
0.36	C2	0.3267	0.2786	0.2650	0.2249	0.2158	0.2017	0.1989	0.1799	0.1686	0.1396	0.1338	0.0592
		0.8888	0.0790	0.0762	0.0681	0.0663	0.0634	0.0628	0.0590	0.0567	0.0508	0.0496	0.0345
0.56	C3	0.3483	0.2828	0.2696	0.2289	0.2141	-	0.1999	0.1792	0.1772	0.1684	0.1621	0.0671
		0.0931	0.0798	0.0771	0.0688	0.0658	-	0.0629	0.0593	0.0589	0.0570	0.0557	0.0362
							Pit 6						
0	Ap	0.4250	0.3777	0.3577	0.3115	0.2892	-	0.2687	0.2331	0.2273	0.2155	0.1956	0.0759
		0.1341	0.1215	0.1162	0.1038	0.0979	-	0.0924	0.0829	0.0813	0.0782	0.0729	0.0409
0.13	AC	0.3457	0.2900	0.2716	0.2343	0.2081	0.1983	0.1930	0.1816	0.1678	0.1632	0.1524	0.0657
		0.1200	0.1039	0.0985	0.0878	0.0802	0.0774	0.0758	0.0725	0.0685	0.0672	0.0641	0.0390
0.28	C1	0.3409	0.2852	0.2801	0.2564	0.2193	0.2084	0.1999	0.1780	0.1483	0.1290	0.1207	0.0594
		0.0929	0.0814	0.0803	0.0754	0.0677	0.0647	0.0637	0.0592	0.0530	0.0491	0.0473	0.0347
0.53	C2	0.2921	0.2270	0.2255	0.1930	0.1690	0.1492	0.1426	0.1312	0.1201	0.1133	0.1017	0.0528
		0.0472	0.0425	0.0424	0.0400	0.0383	0.0369	0.0364	0.0356	0.0348	0.0343	0.0335	0.0300
							Pit 7						
0	Ap1	0.3087	0.2668	0.2568	0.2328	0.2007	0.1930	0.1876	0.1786	0.1677	0.1661	0.1544	0.0662
		0.1114	0.1039	0.1022	0.0979	0.0922	0.0908	0.0898	0.0882	0.0863	0.0860	0.0839	0.0683
0.10	Ap2	0.3309	0.2954	0.2779	0.2498	0.2134	0.2005	0.1946	0.1900	0.1815	0.1772	0.1641	0.0776
		0.1890	0.1727	0.1647	0.1518	0.1351	0.1292	0.1265	0.1244	0.1205	0.1185	0.1125	0.0694
0.31	C1	0.3815	0.3092	0.2972	0.2525	0.2244	0.2084	0.1999	0.1865	0.1749	0.1769	0.1615	0.0661
		0.1112	0.1014	0.0998	0.0937	0.0899	0.0877	0.0865	0.0847	0.0831	0.0834	0.0813	0.0686
0.51	C2	0.3680	0.3034	0.2970	0.2509	0.2156	0.1924	0.1875	0.1774	0.1587	0.1573	0.1440	0.0721
		0.1019	0.0947	0.0940	0.0889	0.0850	0.0824	0.0819	0.0807	0.0787	0.0785	0.0770	0.0691
							Pit 8						
0	AC	0.4277*	0.3954	0.3523	0.3102	0.2921	0.2757	0.2559	0.2403	0.2313	0.2209	0.2053	0.0542
		0.1843†	0.1739	0.1600	0.1465	0.1406	0.1354	0.1290	0.1240	0.1211	0.1177	0.1127	0.0366
0.18	C1	0.3912	0.3558	0.3261	0.2899	0.2676	0.2515	0.2349	0.2085	0.1993	0.1612	0.1538	0.0655
		0.1445	0.1362	0.1292	0.1207	0.1155	0.1117	0.1078	0.1016	0.0994	0.0900	0.0887	0.0370
0.36	C2	0.3969	0.3621	0.3276	0.2890	0.2708	0.2592	0.2386	0.2192	0.2025	0.1927	0.1771	0.0681
		0.1310	0.1244	0.1179	0.1105	0.1071	0.1048	0.1009	0.0973	0.0941	0.0922	0.0892	0.0358
0.58	C3	0.3779	0.3503	0.3206	0.2835	0.2692	0.2569	0.2421	0.2278	0.2212	0.2078	0.1876	0.0684
		0.1262	0.1211	0.1155	0.1086	0.1060	0.1037	0.1009	0.0983	0.0970	0.0946	0.0908	0.0356

*Uncorrected.
†Corrected for coarse fragments.

typical retentivity curves of one horizon, corrected and uncorrected for coarse fragments. While uncorrected data both in Table 2.12 and Figure 2.5 are similar to that for a fine-grained soil, corrected data shows what can be expected on the minesoil when coarse fragment content is included. In reality, some sorting of coarse fragments and fines does probably take place within the minesoil profiles. Pockets of fines could well exhibit moisture characteristics much like the uncorrected curves shown, while aggregations of coarse fragments from which the fines have been washed out would essentially be unaffected by internal gradients other than gravity.

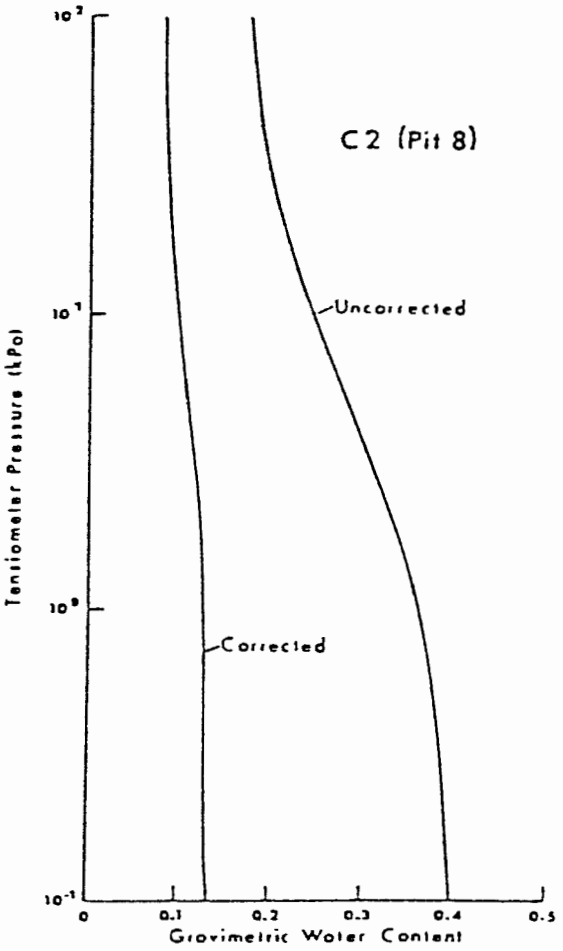

Figure 2.5. Water retentivity curve (gravimetric) for a minesoil corrected and not corrected for coarse fragments.

The corrected curves may not be actually realized anywhere within the spoil profile, they do however represent an average between the two extremes discussed above.

Water retention--Unlike natural soils which may drain slowly in response to gravity and matrix gradients within the structured profiles, coarse textured, structureless, minesoils of Appalachia often drain rapidly through discrete large pores or channels in response to gravity alone. Some water may be retained in the form of films on the surface of the particles and some at the contact points. Alternatively, if weathering of surface materials or deposition of fines forms a

slowly permeable crust, infiltration and redistribution become greatly inhibited (Crosby et al., 1977). At times, if a small head (0.1 m) is imposed on such slowly permeable areas, piping results and new channels open up.

Water retention on the minesoils was estimated in two ways. First, water retention was studied in the field. Two days after a 38-mm rainfall, which effectively saturated the minesoil, gravimetric samples were obtained from the surface and subsurface in close proximity to each of the lysimeter sites. Water content was determined on the dried and weighed samples and water retention was calculated. Second, clods sampled from the vicinity of lysimeter sites were desorbed at 30 kPa dried, weighed, and moisture content was calculated.

In Table 2.13 the amount of water retained by minesoils 2 days after a 38-mm rainfall is compared with that retained by clods desorbed at 30-kPa tensiometer pressure. If field-gravity drainage were to correspond to 30-kPa desorption, the values for clods and samples would be the same, however, the clods in all cases retained less water than the field samples. Comparing this data with corrected values of moisture characteristic suggests a limit at about 10 kPa for these minesoils should be used rather than the conventional 30 kPa value for estimating

TABLE 2.13. WATER CONTENT OF MINESOILS (SAMPLE) AFTER 2 DAYS OF DRAINAGE, OF CLODS DESORBED AT 30 kPa, AND MOISTURE CHARACTERISTIC VALUES (MC) AT 10 kPa FOR SURFACE HORIZONS

Site	Water content		
	Sample	30 kPa clods	10 kPa MC
	g/g		
L-1	0.106	0.084	0.110
L-2	0.088	-	-
L-3	0.082	-	-
L-4	0.082	0.058	-
L-5	0.091	0.062	0.092
L-6	0.092	0.066	-
L-7	0.105	0.068	-
L-8	0.079	0.053	0.090
L-9	0.062	0.047	-
L-10	0.121	-	0.129
Mean	0.091	0.063	0.105
C.V.	18.3	19.1	17.3

water availability. Taking 10 kPa as the lower limit, and assuming average profile density shown in Table 2.11 the amount of water available to plants in spoil profiles between 10 kPa and 1500 kPa is estimated in Table 2.14.

TABLE 2.14. WATER RETAINED BETWEEN 10 AND 1500 kPa TENSIOMETER PRESSURE AT FOUR MINESOIL SITES AND AT ONE NATURAL SOIL SITE

Site		Water retained			
	Thickness,	Uncorrected		Corrected *	
Horizon	mm	wt, g	mm	wt, g	mm
			Pit 5		
Ap	200	0.185	56.0	0.066	20.0
C1	160	0.151	37.0	0.023	5.7
C2	200	0.140	43.1	0.028	8.7
C3	180	0.133	37.4	0.027	7.5
Total	740		173.5(23.5) †		41.9(5.7)
			Pit 6		
Ap	130	0.193	37.9	0.052	10.1
AC	150	0.127	29.2	0.036	8.5
C1	250	0.141	54.5	0.025	11.2
C2	310	0.090	43.9	0.006	3.1
Total	840		165.5(19.7)		32.9(3.9)
			Pit 7		
Ap1	100	0.121	18.3	0.022	3.3
Ap2	210	0.117	37.7	0.057	18.4
C1	200	0.134	41.5	0.018	5.5
C2	150	0.115	26.9	0.013	3.0
Total	660		124.4(18.9)		30.2(4.6)
			Pit 8		
AC	180	0.207	55.1	0.092	25.3
C1	180	0.169	46.6	0.071	19.6
C2	220	0.171	58.3	0.065	22.3
C3	440	0.174	121.6	0.065	45.8
Total	1.020		282.0(27.7)		113.0(11.1)
			Hazleton sil		
A1	30	0.476	12.6	0.366	9.7
A2	70	0.226	22.0	0.174	16.9
B21	310	0.135	74.5	0.092	50.5
B22t	330	0.141	89.1	0.093	58.9
Total	740		198.2(26.8)		136.0(18.4)

* Corrected for coarse fragments

† Values in brackets are expressed as percentage of total thickness, i.e. (23.5) = 100(173.5/740).

Compared to values on natural soil and on minesoil uncorrected for coarse fragments, retention on corrected minesoils (except at pit 8) is very low (Table 2.14). Topsoiled profiles (pits 5 and 6) retain most plant-available water near the surface. On a nontopsoiled profile (pit 7) higher retention in the Ap2 may indicate a zone of illuviation, fines having been washed down from the minesoil surface. Compared with other profiles, the minesoil at pit 8 shows retention similar to that of the natural soil. This pit is situated on a lower slope adjoining nontopsoiled materials, and contains more montmorillonite and vermiculite than minesoils at other pits. Very low amounts of water retained in spoil profiles in general will lead to low water availability and limited plant growth.

Retention values for natural soils are included for comparison only. Since the analysis was performed on sieved <2-mm material and the profile does exhibit structural development the results should be treated with caution (Bruce, 1972; Unger, 1975).

Hydraulic conductivity--Using the spoil material packed into microlysimeters (Figure 2.6), saturated hydraulic conductivity of minesoil before and after an ET study was determined in the laboratory by a constant head method (Klute, 1965). Field exposure of microlysimeters for 4 months resulted in some fines being lost through piping and some scaling of the surface.

Results of the hydraulic conductivity experiment performed before and after 4 months of field exposure are presented in Table 2.15. Large variability (as measured by CV values) existed between the lysimeters, particularly during the second run. High values of conductivity obtained for the second run (L-6 and L-8) were due to washing out of fine material from the lysimeters. Such occurrences may be quite representative of field conditions, when piping and internal erosion are common. The conductivities generally were lower after microlysimeters were exposed to the elements. Compared to initial results, field exposure seems to have

Figure 2.6. A microlysimeter site.

decreased the magnitude and increased the variability of the average hydraulic conductivity values. The values obtained represent unconsolidated spoil material. No attempt was made to plug any channels which developed when fines were washed out during drainage and subsequent exposure. The results may be indicative of minesoil conductivity immediately following reclamation.

Infiltration--In contrast to the hydraulic conductivity measurement on disturbed and repacked minesoils, infiltration was determined in the field on

TABLE 2.15. SATURATED HYDRAULIC CONDUCTIVITY AT 10 LYSIMETER SITES (L-1 TO L-10) BEFORE (INITIAL) AND AFTER 4 MONTHS OF FIELD EXPOSURE (FINAL) CORRECTED TO 20°C

Lysimeter site no	Saturated hydraulic conductivity	
	Initial	Final
	mm/hour	
L-1	39	4
L-2	303	20
L-3	89	28
L-4	126	22
L-5	7.425	2.024
L-6	1.707	43.590
L-7	1.925	3.049
L-8	3.303	19.391
L-9	1.608	142
L-10	667	153
Mean*	640	298
C.V., %	9	80

*Logarithmic mean, and coefficient of variation (C.V.).

undisturbed sites using a 0.5 m diam cylinder infiltrometer (Coleman, 1951)[2]. Half of the infiltrometer (0.1 m) was imbedded in the spoil and the opening made by the cylinder walls was sealed with bentonite clay. Five-liter increments (25 mm) of water were added to the cylinder repeatedly and allowed to infiltrate. During the first addition we measured the initial infiltration rate as calculated from the lowering of water level, while in the subsequent runs we looked for the rate to stabilize and eventually decline. Field determined final infiltration capacities were expected to be less than the hydraulic conductivity values determined on the microlysimeters in the laboratory (Talsma, 1969). Less disturbance, larger area, and possibly some surface crusting could be responsible for the decreased rates. But even these lower rates were likely to overestimate

[2]G. B. Coleman. 1951. A study of water infiltration into spoil banks in central Pennsylvania. M.S. Thesis. The Pennsylvania State University, University Park, Pennsylvania.

the true infiltration capacity by about 14% (Tricker, 1978). Infiltration rates were also measured on a 2.5 by 2.5 m infiltration plot cased to the depth of 1 m and situated in the area that has not been topsoiled.

Table 2.16 shows results of the preliminary infiltration study on topsoiled and nontopsoiled minesoil, on adjacent natural soil, and on the infiltration plot. The infiltration rates generally were lower than the hydraulic conductivity values given in Table 2.15. This is because of differences in methods of measurement and basic hydraulic properties of materials. In general, hydraulic conductivity values are expected to be higher than the final infiltration rate (Talsma, 1969). Values determined using a constant head method (Klute, 1965) are generally obtained on fully saturated disturbed and repacked materials. In contrast, ponding of water during the infiltration measurements does not necessarily result in a fully saturated flow; because of surface crusting slower unsaturated flows and fingering are often more likely (Hill and Parlange, 1972; Raats, 1973; Philip, 1975). Comparison of results for the infiltrometers and infiltration plot shows the values also to decrease with increase in size.

TABLE 2.16. INFILTRATION VELOCITIES ON NATURAL SOIL, TOPSOILED, AND NONTOPSOILED MINESOIL

Site	Water applied	$\bar{I}$	C.V.	Initial	Steady	Final
	mm	mm/hour	%	mm/hour		
Natural soil						
I-1	75	53	4	140	40	27
I-2	450	421	4	-	-	-
Topsoiled material						
I-4	75	11	34	190	19	3
I-6	75	28	11	343	19	5
Nontopsoiled materials						
I-7	75	17	17	286	19	3
I-8	25	3 3	42			
I-9	75	14	12	21	19	11
I-10	50	7.3	22	10	6	3
Infiltration plot	140	2.0	47	7	2	1

Hydraulic properties such as moisture characteristic will also materially influence the rate of water transfer within the minesoil profiles. The steepness of the corrected retentivity curves (Figure 2.5) will be complemented (Rogowski and Jacoby, 1979) by a corresponding steepness in the hydraulic conductivity--water content curves (not shown). Thus a change in water content of as little as three percentage points (from 0.20 to 0.17 g/g) may result in a hydraulic conductivity change of three orders of magnitude (from 10^3 to 10^0 mm/hr). While hydraulic conductivity values (Table 2.15) depict an unusual situation of complete saturation, using final field infiltration rate values likely will lead to a better first estimate of minesoil conductivity.

Infiltration values on minesoils also appear lower than on natural soils. This is despite the fact that at I-1 the surface horizon had been eroded and at site I-2 the litter layer has been removed. Both these sites are in an area where trees have been recently removed. Consequently, large amount of decaying roots and old root channels are present which could be responsible for higher rates.

Evapotranspiration-- At each lysimeter site some of the excavated minesoil was repacked into small microlysimeters (0.2 by 0.3 m) (Rogowski and Jacoby, 1977) to approximate measured field bulk density. The microlysimeters (Figure 2.6) were seeded with ryegrass (*Lolium perenne* L.) and set on collecting pans in the excavations. Acrylic liners were placed around each microlysimeter, and the minesoil was returned to its original level. Vegetation was reestablished at each site, and an evapotranspiration (ET) study was initiated. The amount of water seeping through the minesoil and the weight of each cylinder was recorded twice weekly. Rainfall, evaporation, maximum-minimum temperature, and solar radiation data were also monitored during this time.

Figure 2.7 shows preliminary cumulative ET values during the study as determined by model results, changes in lysimeter weight, and evaporation from the class

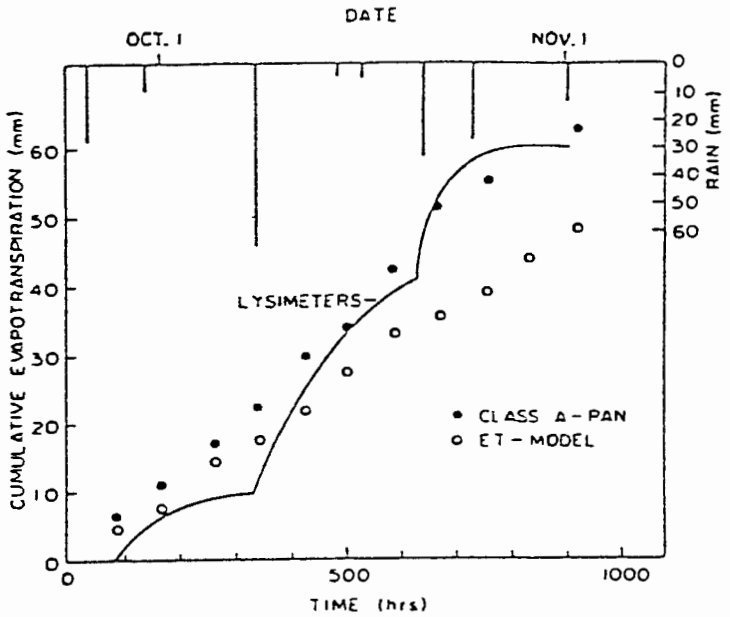

Figure 2.7. Cumulative ET values during the study as determined by model results, changes in lysimeter weight, and evaporation from the class A pan.

A pan. Although the model data appear lower, the results showed that ET from minesoil in the microlysimeters (2.4 mm/day average) could be approximated either by class A pan evaporation (1.8 mm/day) or the model (Ritchie, 1972) (1.3 mm/day). Linear regression of the lysimeter and the A pan data gave an r^2 value of 0.984; comparison with model data an r^2 value of 0.950; and comparison of the model data with the class A pan data an r^2 value of 0.987. Under the conditions of the experiment, lysimeters retained more water than would be expected under normal conditions since downward seepage was prevented by a liner and contact with underlying minesoil was not maintained. Other studies (Rogowski, 1978; Rogowski and Jacoby, 1979) and careful consideration of hydraulic properties suggests that droughty conditions can easily occur. Small changes in moisture content (Figure 2.5) lead to large changes in the tensiometer pressure. Consequently, little water is readily available (Table 2.14) for plant use on most minesoils as compared to natural soils.

REFERENCES

1. Anderson, J. L. An Improved Pretreatment for Mineralogical Analysis of Samples Containing Organic Matter. Clays and Clay Minerals, 10:380-388, 1963.
2. ASTM. Standard Methods of Coal Analysis. American Society for Testing Materials, Philadelphia, Pa., 1971.
3. Baker, D. E., and L. Chesnin. Chemical Monitoring of Soils for Environmental Quality and Animal and Human Health. Adv. Agron., 27:305-374, 1975.
4. Bertram, G. E. Field Tests for Compacted Rockfill. In: Embankment-dam Engineering, Casagrande Volume, R. C. Hirshfield and S. J. Poules, eds. John Wiley and Sons, Inc., New York, 1973. pp. 1-20.
5. Blake, G. R. Bulk Density. In: Methods of Soil Analysis, Part 1, C. A. Black, ed. American Society of Agronomy, Madison, Wis. Agronomy, 9:374-390, 1965.
6. Broadbent, F. E. The Soil Organic Fraction. Adv. Agron., 5:153-183, 1953.
7. Bruce, R. R. Hydraulic Conductivity Evaluation of the Soil Profile from Soil Water Retention Relations. Soil Sci. Soc. Am. Proc., 36:555-561, 1972.
8. Ciolkosz, E. J., G. W. Petersen, R. L. Cunningham, and R. P. Matelski. Soils Developed from Colluvium in the Ridge and Valley Area of Pennsylvania. In: Proceedings of the International Geobotany Conference, University of Tennessee Press, Knoxville, Tenn., 1978.
9. Ciolkosz, E. J., R. L. Cunningham, G. W. Petersen, and R. C. Cronce. Characteristics Interpretations and Uses of Pennsylvania Minesoils. Progress Report 381. The Pennsylvania State University, Agricultural Experiment Station, University Park, Pa., 1983. 88 pp.

10. Crosby, E. C., D. E. Overton, and R. A. Minear. A Simulation Model of Spoil Bank Hydrology. In: Surface Mining and Fish/Wildlife Needs in the Eastern U.S., D. E. Samuel, J. R. Stauffer, C. H. Hocutt, and W. T. Mason, Jr., eds. Proceedings, Fifth Symposium on Surface Mining and Reclamation, NCA/BCR Coal Conference and Expo IV, October 18-20, Louisville, Ky., 1977. pp. 28-31.

11. Farmer, E. E., and B. Z. Richardson. Hydrologic and Soil Properties of Coal Mine Overburden Piles in Southeastern Montana. In: Proceedings, Fourth Symposium on Surface Mining and Reclamation, NCA/BCR Coal Conference and Expo III, October 19-21, Louisville, Ky., 1976. pp. 120-130.

12. Glass, G. B. Geology and Mineral Resources of the Philipsburg 7-1/2 Minute Quadrangle, Centre and Clearfield Counties, Pennsylvania. Pennsylvania Geological Survey, 4th Series, Department of Environmental Resources, Harrisburg, Pa., 1972.

13. Hill, D. E., and J.-Y. Parlange. Wetting Front Instability in Layered Soils. Soil Sci. Soc. Am. Proc., 36(5):697-702, 1972.

14. Jackson, M. L. Soil Chemical Analysis. Prentice Hall, Englewood Cliffs, New Jersey, 1958.

15. Kilmer, V. J., and L. T. Alexander. Methods of Making Mechanical Analyses of Soils. Soil Sci., 68:15-24, 1949.

16. Klute, A. Laboratory Measurement of Hydraulic Conductivity of Saturated Soil. In: Methods of Soil Analysis, Part 1, C. A. Black, ed. American Society of Agronomy, Madison, Wis. Agronomy, 9:214-215, 1965.

17. Mehuys, G. R., L. H. Stolzy, J. Letey, and L. V. Weeks. Effect of Stones on the Hydraulic Conductivity of Relatively Dry Desert Soils. Soil Sci. Soc. Am. Proc., 39:37-42, 1975.

18. Pedersen, T. A., A. S. Rogowski, and R. Pennock, Jr. Comparison of Some Properties of Minesoils and Contiguous Natural Soils. EPA-600/7-78-162, U.S. Environmental Protection Agency, Research and Development Series, Cincinnati, Ohio, 1978. 141 pp.

19. Peech, M. L., L. T. Alexander, L. A. Dean, and J. F. Reed. Methods of Soil Analysis for Soil Fertility Investigations. U.S. Department of Agriculture Circular 757, Government Printing Office, Washington, D.C., 1947.

20. Philip, J. R. Stability Analysis of Infiltration. Soil Sci. Soc. Am. Proc., 39:1042-1049, 1975.

21. Plass, W. T., and W. G. Vogel. Chemical Properties and Particle Size Distribution of 39 Surface-Mine Spoils in Southern West Virginia. Northeast Forest Experiment Station Research Paper NE-276, 1973.

22. Raats, P. A. C. Unstable Wetting Fronts in Uniform and Nonuniform Soils. Soil Sci. Soc. Am. Proc., 37:681-685, 1973.

23. Rawitz, E. Installation and Field Calibration of Neutron Scatter Equipment for Hydrologic Research in Heterogeneous and Stony Soils. Water Resour. Res., 5(2):519-523, 1969.

24. Richards, L. A. Physical Conditions of Water in Soil. In: Methods of Soil Analysis, Part 1, C. A. Black, ed. American Society of Agronomy, Madison, Wis. Agronomy, 9:128-152, 1965.

25. Ritchie, J. R. Model for Predicting Evaporation from a Row Crop with Incomplete Cover. Water Resour. Res., 8(5):1204-1213.

26. Rogowski, A. S. Water Regime in Stripmine Spoil. In: Surface Mining and Fish/Wildlife Needs in the Eastern U.S., D. E. Samuel, J. R. Stauffer, C. H. Hocutt, and W. T. Mason, Jr., eds., Proceedings of a Symposium, December 3-6, Morgantown, West Va., 1978. pp. 137-145.

27. Rogowski, A. S., and E. L. Jacoby, Jr. Assessment of Water Loss Patterns with Microlysimeters. Agron. J., 69:419-424, 1977.

28. Rogowski, A. S., and E. L. Jacoby, Jr. Monitoring Water Movement through Strip Mine Spoil Profiles. Trans. ASAE 22:104-109, 114, 1979.

29. Soil Survey Staff. Soil Survey Manual. U.S. Department of Agriculture Handbook 18, U.S. Government Printing Office, Washington, D.C., 1951.

30. Soil Survey Staff. Soil Taxonomy: A Basic System of Classification for Making and Interpreting Soil Surveys. U.S. Department of Agriculture Handbook 436, U.S. Government Printing Office, Washington, D.C., 1975.

31. Talsma, T. In Situ Measurement of Sorptivity. Aust. J. Soil Res., 7:269-276, 1969.

32. Tricker, A. S. The Infiltration Cylinder, Some Comments on its Use. J. Hydrol., 36:383-391, 1978.

33. Troxler Electronic Laboratories, Inc. 2400 Series COMPAC, Surface Moisture-Density Gauge Manual. Raleigh, N.C., 1970.

34. Unger, P. W. Water Retention by Core and Sieved Samples. Soil Sci. Soc. Am. Proc., 39:1197-1200, 1975.

35. U.S. Salinity Laboratory. Diagnosis and Improvement of Saline and Alkali Soils. U.S. Department of Agriculture Handbook 60, U.S. Government Printing Office, Washington, D.C., 1954.

36. Van Voast, W. A. Hydrologic Effects of Strip Coal Mining in Southeastern Montana--Emphasis: One Year Mining Near Decker. Montana College of Mineral Science and Technology, Butte, Montana, 1974.

37. Verma, T. R., and J. L. Thames. Rehabilitation of Land Disturbed by Surface Mining Coal in Arizona. J. Soil Water Conserv., 30:129-132, 1975.

38. Young, J. L., and M. R. Lindbeck. Carbon Determination in Soils and Organic Materials with a High Frequency Induction Furnace. Soil Sci. Soc. Am. Proc., 28:377-381, 1964.

39. Young, R. A., and C. A. Onstad. Predicting Particle-Size Composition of Eroded Soil. Trans. ASAE, 19:1071-1075, 1976.

40. Yuan, T. L. Determination of Exchangeable Hydrogen in Soils by Titration Method. Soil Sci., 88:164-167, 1959.

SECTION 3

CAISSON STUDIES

MONITORING WATER MOVEMENT THROUGH STRIP MINE SPOIL PROFILES

The methods of measuring and simulating water flow on disturbed land are scarce. The purpose of this study was to develop suitable instrumentation and adapt existing methodology to the assessment of water flow on stripmined lands. The experimental studies, described in this and the following section, are confined to the measurement and modeling of water flow in reconstructed spoil profiles.

The spoil profile chosen for study and described in detail in Section 2 was situated on a site near Kylertown, Pa. This site had been stripmined seven years before for Lower Kittanning coal (B-seam), and two years before for Middle Kittanning coal (C-seam). The regraded spoil, underlain by an undisturbed clay layer, consisted of a mixture of grey shale and light colored sandstone covered in part (C-spoil only) with topsoil material (loamy skeletal, mixed, mesic, Udorthents). The area was planted in trees, grass and legumes and part of it had been limed, fertilized and manured. The site was surrounded by wooded and cultivated patches of original soils.

A 6-m spoil profile was excavated (Figures 3.1, 3.2) with a large backhoe, in 20 almost equal depth increments, transported to a research facility, and placed by hand in two 2.4 m diameter caissons (Figures 3.3, 3.4, 3.5, 3.6) duplicating the field order. A 15 kg sample from each box was used for analyses of particle size, physical and chemical properties. The caissons, constructed from 14 gage, corrugated, galvanized steel culverts, were placed under roof on a concrete pad, and were precoated with 12 mil layer of NEXON--a commercially available thermoplastic, corrosion resistant, coal-tar-based resin.

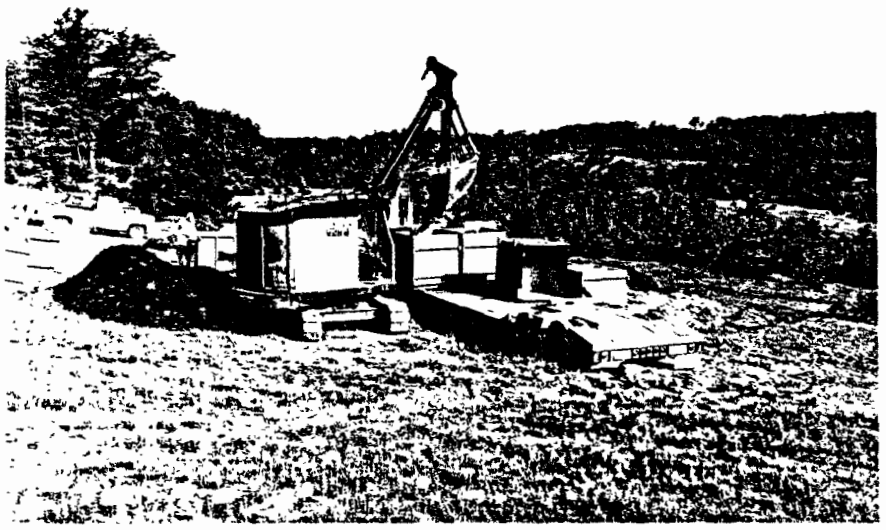

Figure 3.1. Backhoe excavates successive layers of spoil at Kylertown.

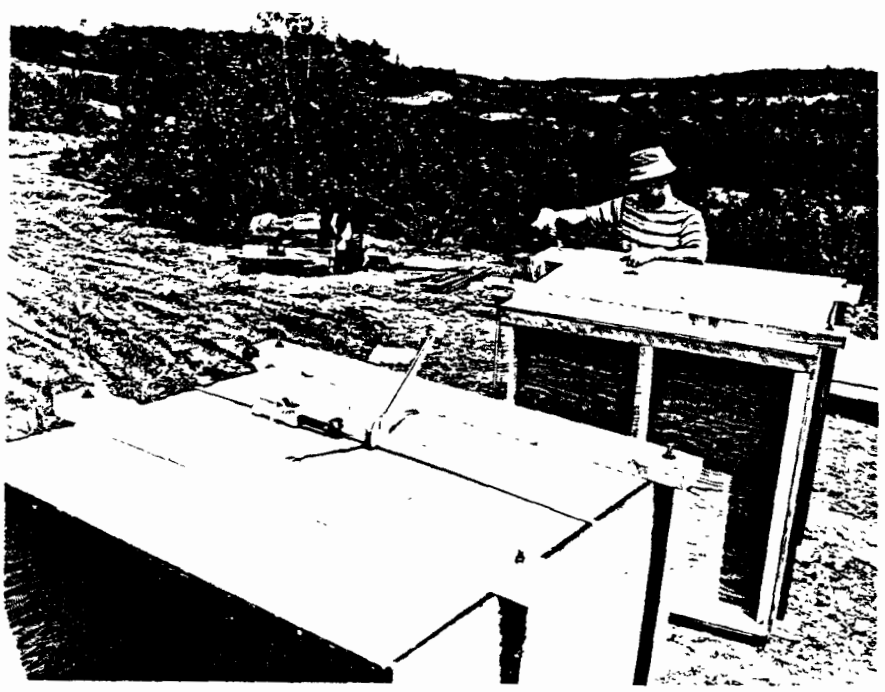

Figure 3.2. Research staff assembles boxes for transport of Kylertown spoil by truck to the experimental facility.

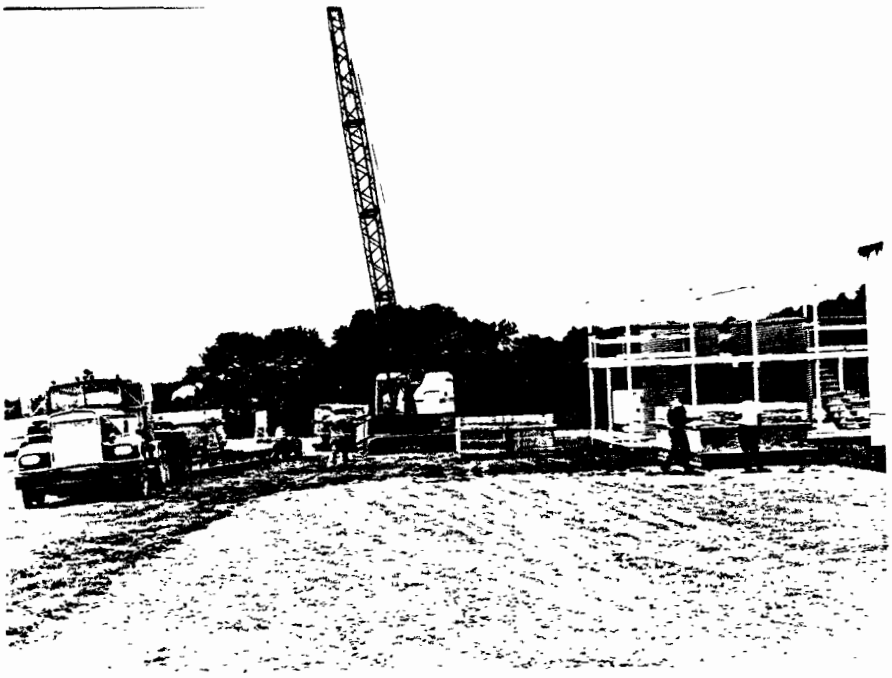

Figure 3.3. Boxes are unloaded at the experimental research facility.

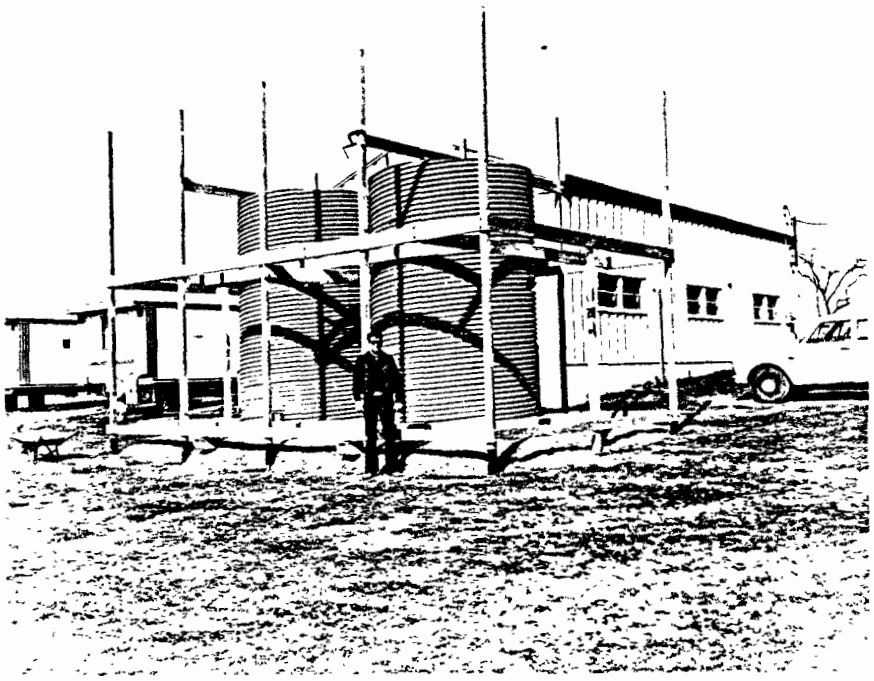

Figure 3.4. Caissons at the experimental research facility to be filled with Kylertown spoil.

Figure 3.5. Numbered boxes are positioned near the appropriate caisson preparatory to reconstituting the field profile.

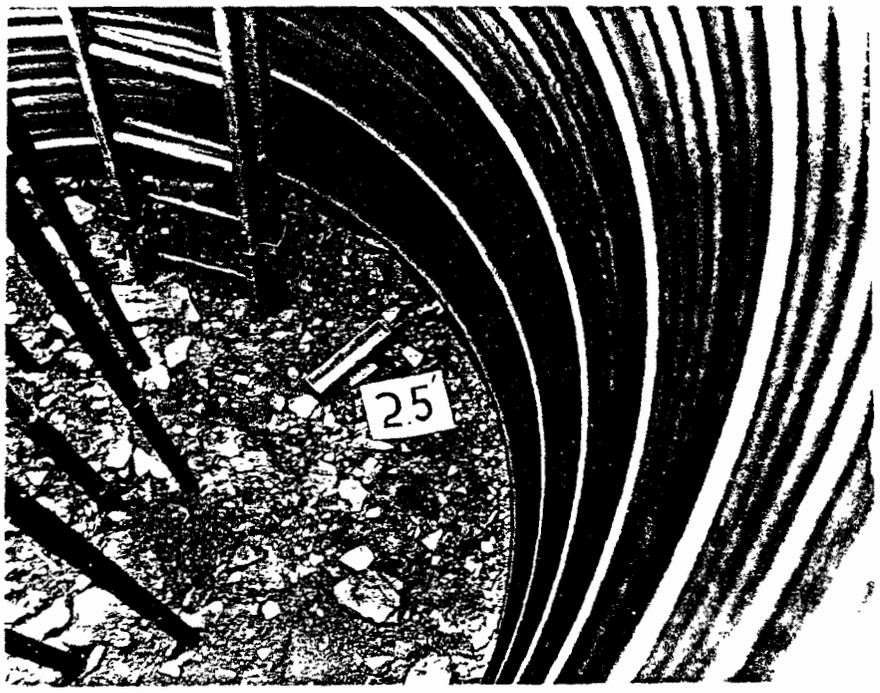

Figure 3.6. Inside of caisson 1 showing the 2.5' depth of spoil in place, access tubes for measuring density and moisture and a lysimeter for collecting the effluent, ladder was used by personnel who rebuilt the field profile layer by layer.

To ensure uniform drainage, 0.6 m of inert quartz sand of a compatible particle-size distribution with the spoil was placed at the bottom of each caisson. The reassembled spoil profile was covered in caisson 1 with 0.5 m of topsoil, while in caisson 2 a dark acid shale layer (0.4 m) taken from just above the B-coal seam was placed below the reassembled profile and on top of the sand.

Instrumentation

Figure 3.7 shows the cross section of an instrumented caisson, and Table 3.1 gives the location of different types of instrumentation in both caissons.

A central well for measurement of water levels consisted of a rigid PVC (polyvinyl chloride) pipe with a 0.6 m long stainless steel screen at the bottom. Four aluminum access tubes, for measurement of density and water content with gamma and neutron probes, respectively, were coated with a corrosion resistant paint. The access tubes were placed 0.3 m apart to accommodate a two-probe density probe besides a standard neutron moisture gage.

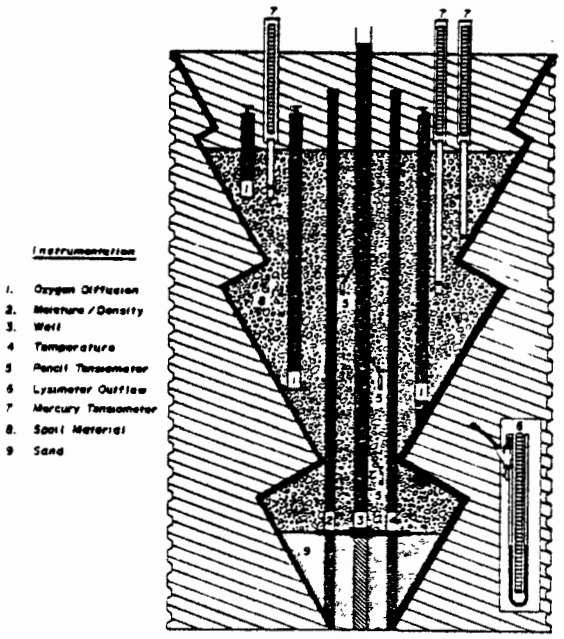

Figure 3.7. Caisson instrumentation description.

TABLE 3.1. LOCATION OF INSTRUMENTS* CAISSON 1 AND 2

Location		
Caisson 1	Caisson 2	Type
(cm)		
0	0	Old surface
18	31	New surface
30	38	L, Tr, D, TC(2)
61	69	L, Tg, TC(2)
90	98	Tr
122	130	L, Tp, D, TC(2)
183	191	L, Tp, TC(1)
244	252	L, Tp, D, TC(2)
274	282	L, TC(1)
274	282	Bottom of spoil
274	282	Top of screen and sand
335	343	Bottom, well casing, access tubes

*L = lysimeter; Tr = mercury tensiometer; D = diffusion chamber; TC = thermocouple; Tg = gage tensiometer; Tp = pencil tensiometer.

Changes in moisture content and density were measured using neutron and gamma probes, respectively. Organic C was determined by a Walkley Black method (Allison, 1965). Total S was obtained by a high temperature combustion, while standard tests (ASTM, 1971) were used to evaluate sulfate, pyritic and organic S in each layer of the spoil.

We measured leaching potential of the reassembled profile on a 10-kg subsample of each excavated layer by placing it in a 20 cm diameter PVC cylinder and leaching with 1000 ml of water. The leachate was filtered and on the filtrate pH, total acidity, electrical conductivity, Ca, Mg, and SO_4 were determined. The results of these analyses are discussed in detail elsewhere in this report.

Rainwater needed for application to the caissons was collected from the roof of the research facility and stored in large tanks.

Using values of bulk density, we also calculated the total available pore space (TPS) from the equation

$$TPS = 1 - (\text{Bulk Density}/2650)$$

where 2650 was the assumed particle density in kg/m^3.

In addition to the 4 access tubes for measurement of density and water we filled two other access tubes with ethylene glycol, and placed copper-constantan thermocouples inside at selected depths to measure small changes in temperature during water application. The method was similar to that used in borehole geophysics (Keys and MacCary, 1971), except we used stationary thermocouples, instead of a mobile probe, and added ethylene glycol to water to prevent freezing.

We installed porous cup tensiometers, by excavating a hole in the spoil and filling the bottom part around the porous cup with a fine spoil slurry.

We also installed tension free lysimeters (Jordan, 1966), made a PVC and stainless steel to prevent corrosion, at selected depths at a 10° slope while the caissons were being filled and connected each one to its own manometer-outflow assembly. The manometer-outflow assembly served a dual purpose: air pressure changes could be read as we applied the water at the surface and we could measure and sample water intercepted by the lysimeters for subsequent chemical analysis.

Oxygen diffusion chambers similar to those described by Raney (1949), allowed ambient spoil air to diffuse into a space previously swept clear with nitrogen. Diffused oxygen was measured with an oxygen analyzer, and oxygen concentration in the spoil was computed using appropriate calibration procedures.

Methods

In topsoiled caisson 1, we applied the stored rainwater at the average rate of 300 mm/h (1.4 m^3/h) for 92 min, using a pump and sprinkler system. The pump was

operated during 0 to 70 min and 102 to 124 min time intervals. This rate caused some surface ponding. In caisson 2, we applied the stored rainwater at the rate of 1890 mm/h (8.8 m^3/h) for 16 min (following the initial 5 min application at the same rate as in caisson 1). The pump was operated during 0 to 5 min and 47 to 63 min time intervals. Even at the high application rate no noticeable ponding was evident. The total amounts applied were 455 and 483 mm of water (2115 and 2246 L) to caissons 1 and 2, respectively. After water application we left caisson 2 uncovered but covered caisson 1 with a plastic sheet and allowed it to drain for 17 days. We then uncovered it, and on the 23rd day after water application raked the surface to break the crust.

To determine a water retentivity curve of the spoil profiles we used the following system. We cleaned and de-aired 80 mm diameter, 25 kPa (250 mb) fast-flow retainer ceramic plates. Rings, the same size as the plates and 40 mm high were placed on the retainer plates and filled with <2-mm fraction of spoil material. We used the <2-mm fraction in accordance with soil taxonomy textural gropings for soils (Soil Survey Staff, 1975). The ring and retainer assemblies were then placed on an extractor plate (25 kPa ceramic) in the pressure cooker apparatus. Water was added and samples were allowed to saturate overnight. The next day excess water was wiped off; samples were weighed, and their volume measured. Subsequently, samples were desaturated at 1, 4, 8, 15 and 24 kPa (10, 40, 80, 150 and 240 mb) dried and weighed. To express water content on a total volume basis, calculated values for a water retentivity curve were multiplied by a factor equal to the fractional amount of spoil material <2 mm in a given sample. Specific retention for spoil particles >2 mm was then measured, adjusted for the amount of >2-mm material present, and added as a constant to the recalculated values. The procedure for measuring specific retention, adapted from ElBoushi (1966), consisted of wetting a known

volume of particles, allowing it to drain briefly (30 min), and computing water retained from weight changes.

The Green and Corey (1971) model with Millington and Quirk (1960) pore size interaction factor was used to calculate the hydraulic conductivity as a function of tensiometer pressure and soil water content from corrected and uncorrected values of water-retentivity curve. The factor of 4/3 was more suitable for the coarse materials (Rogowski, 1972) than other factors commonly used in the basic Marshall (1958) model. The model was matched at the saturated conductivity corresponding to average conductivity measured on the topsoiled and nontopsoiled portions of the experimental site.

Results and Discussion

We observed considerable settling, 0.18 m (6%) on caisson 1 and 0.31 m (10%) on caisson 2, during the water application. The settling corresponded closely to the field behavior of the freshly reclaimed spoil.

The results showed that the profile density increased in both caissons after water was applied and spoil had settled (Figure 3.8). The density in caisson 1 increased most near the surface and progressively less with depth, while in caisson 2, except for the acid shale layer, the increase in density was least near the surface becoming progressively more with depth. The acid shale layer changed little in density after water application, probably because of the many large rock fragments.

Spoil settling and changes in density following water application may indicate internal sediment movement. Table 3.2 shows sediment concentration values in the effluent from lysimeters for different times after water was applied to each caisson. Higher concentrations of sediment in effluent from caisson 1 compared with those from caisson 2 suggests a possibility of greater internal erosion (piping) on topsoiled areas. Such mass movement of soil may also transport into the profile iron- and sulfur-oxidizing bacteria associated with the sediment.

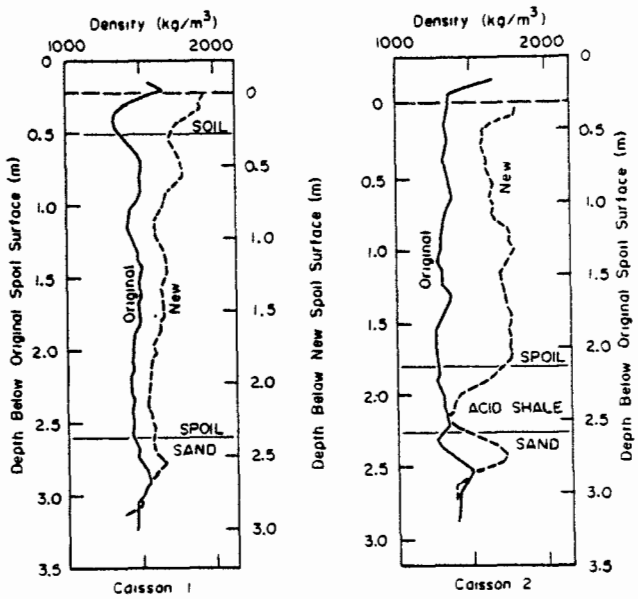

Figure 3.8. Caisson profile density before (original) and after (new) water application.

TABLE 3.2. SEDIMENT CONCENTRATION IN THE WELL AND IN THE EFFLUENT FROM LYSIMETERS AT DIFFERENT TIMES AFTER WATER WAS APPLIED

Caisson 1			Caisson 2		
Time	Depth*	Sediment	Time	Depth	Sediment
min	m	ppm	min	m	ppm
34	0.30	90138	60	0.38	7828
46	0.61	50604	60	0.69	1160
46	1.83	6952	60	1.30	7504
47	1.22	6746	60	1.91	2212
62	2.44	3578	60	2.52	2292
			60	2.82	1960
90	0.61	15702	75	1.30	1388
111	1.83	2370	75	2.52	888
128	1.22	3090	75	2.82	592
130	0.30	16062			
133	2.44	758	125	2.52	548
			125	2.82	332
			155	3.43	108
			185	2.82	128

*Depth below original surface.

During water application, despite the central well open to the atmosphere, the air pressure buildup in the profile was considerable (between 0.4 and 10.4 kPa). The pressure buildup in the caisson 2 spoil was greater than in topsoiled caisson 1 since infiltrating water moved faster in the spoil alone and entrapped air could not exit. An analogous situation existed with regards to oxygen concentrations. In Table 3.3 we compare oxygen concentrations at three depths in the two caissons. Preliminary data showed that oxygen concentrations in topsoiled caisson 1 did not recover to the initial concentration as did those on spoil alone in caisson 2. The data, however, were not sufficient to conclude that the topsoil layer impeded oxygen movement. Oxygen concentration in the profile after caisson 1 was uncovered (17 days) and raked (23 days) showed only a slight increase over previous readings.

TABLE 3.3. OXYGEN CONCENTRATION AT SELECTED DEPTHS AFTER WATER APPLICATION

	Caisson 1, depth, m				Caisson 2, depth, m		
Time	0.30	1.22	2.44	Time	0.38	1.30	2.52
days	percent oxygen			days	percent oxygen		
0	14.8	8.4	12.9	0	17.1	9.8	11.3
1	1.9	5.7	6.7	1	19.8	19.0	water
2	1.9	4.8	7.6	4	17.6	19.0	water
3	1.1	3.1	7.1	5	16.9	17.7	water
6	2.1	4.0	11.4	6	18.1	19.0	water
7	1.2	3.5	8.1	7	19.1	18.9	water
8	1.9	2.8	7.6	8	18.0	18.8	17.7
9	1.7	2.7	8.4	12	20.7	19.9	20.2
13	4.7	4.5	10.5	14	20.8	19.6	20.5
15	4.1	4.5	9.5				
16	4.6	6.9	11.8				
17	5.0	7.1	12.7				
20	3.2	4.6	11.5				
21	5.0	3.4	6.0				
22	3.6	4.1	6.1				
23	5.0	3.9	9.9				
25	5.1	8.3	9.6				
27	8.1	7.7	4.2				

Infiltration and redistribution of applied water and wetting-front passage in the spoil profiles were monitored with the neutron moisture probe and gamma two-probe density probe (Table 3.4) supplemented by thermocouple readouts. Since neutron probe measures water content in a relatively large spherical volume of material changes in water content associated with a wetting-front passage in caisson 1 (Table 3.4) were not particularly informative. However, rapid changes

TABLE 3.4. DEPTH OF WATER INFILTRATION WITH TIME AFTER APPLICATION

Caisson 1

Depth* m	Time† min	Water content‡ m^3/m^3 Before	After
0.30	22	0.1227	0.1223
0.61	31	0.0924	0.2032
0.91	35	0.1089	0.1372
1.22	49	0.1007	0.1336
1.83	56	0.1099	0.1085

Caisson 2

Depth m	Time min	Water content§ m^3/m^3 Before	After	Wet bulk density kg/m^3 Before	After
0.30	1	0.0842	0.3942	1253	1563
2.44	54	0.1019	0.2899	1499	1687

*Below original surface.

†Time to reach given depth; beginning at the time water was first applied, pump operated during 0-70 min and 102-124 min time intervals for caisson 1 and during 0-5 min and 47-63 time intervals for caisson 2.

‡Based on neutron moisture probe readings before and after the front passage.

§Computed from changes in wet bulk density and in initial water content using gamma density probe and neutron moisture probe readings.

in wet bulk density measured with a dual gamma probe after a wetting-front passage in caisson 2 indicated a higher water content just behind the front than at a later time (2 hr later). Because of a very rapid movement of water in caisson 2, we could monitor only two depths whereas in caisson 1 where infiltration was slower, we obtained more readings. In general, the two-probe gamma density probe was better for monitoring the wetting front movement than was the neutron moisture probe, since with the former at any time only a small volume of spoil (25 mm slice) was being examined. Similar conditions are likely to prevail in the field. Direct transmission dual gamma probe could ideally be used above and below a topsoil-spoil interface to monitor the rate of seepage into the underlying profile.

Since the applied water was at a different temperature than caisson spoil, we could follow its movement by observing temperature changes. For shallow depths, particularly in caisson 1, rapid temperature changes accurately indicated the wetting front passage. However, infiltrating water appeared to reach the bottom of caissons considerably earlier than any noticeable changes in temperature at deeper depths could be observed. This indicates that preferential water flows do occur through select channels and larger pores of spoil profiles. Single measurements are unlikely to intercept the flow channels in the field. Consequently, it would seem prudent to use simultaneously a combination of measurements including moisture, density, temperature and water table elevation at a sufficiently large number of measuring sites.

Figure 3.9 shows water redistribution profiles based on neutron probe measurements. Redistribution profile 2 on topsoiled caisson 1 represents water content values immediately after the wetting front has passed a given depth. Redistribution profile 3 on caisson 1 measured a day later corresponds more closely to what may be expected under field conditions following a heavy rain. While the topsoil in caisson 1 was draining, the water content of the spoil below the 1-m depth remained relatively constant.

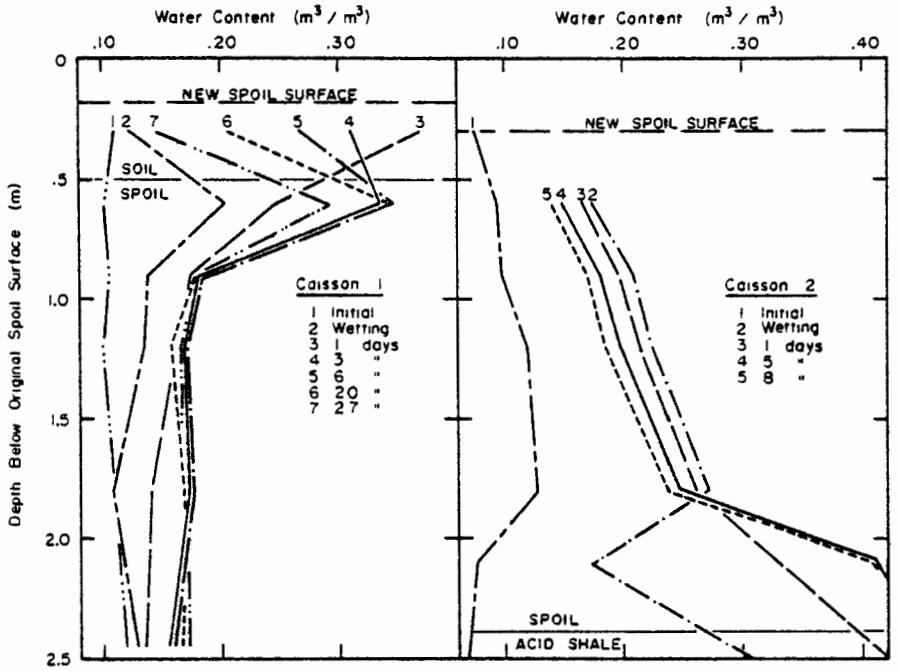

Figure 3.9. Water redistribution profiles for caissons 1 and 2 for indicated times.

For caisson 2 on spoil alone redistribution profiles showed the water content to increase gradually with depth up to 1.80 m. Below that depth, and in an acid shale layer of lower density and higher porosity, the water content increased more rapidly (redistribution profiles 3, 4 and 5) after a slower initial wetting (redistribution profile 2). Coarse spoil layers in the field may initially act as impeding layers and may not begin to fill with water until overlying spoil becomes saturated.

In caisson 1 the redistribution was slow. After initial drainage (profiles 2 to 4), water redistribution took place over a period of one month with little change in water content below the 1 m depth (profiles 4 to 7). At the same time we observed considerable drying of topsoil. In caisson 2, however, water continued to drain freely and relatively fast from the coarse grained spoil profile that has not been topsoiled. This could be ascribed to smaller retentivity and lower air entry value of spoil compared with topsoil.

Redistribution profiles on caisson 1 and 2 in Figure 3.9 cover the same time period as the tensiometer readouts in Figure 3.10. We obtained our best readings

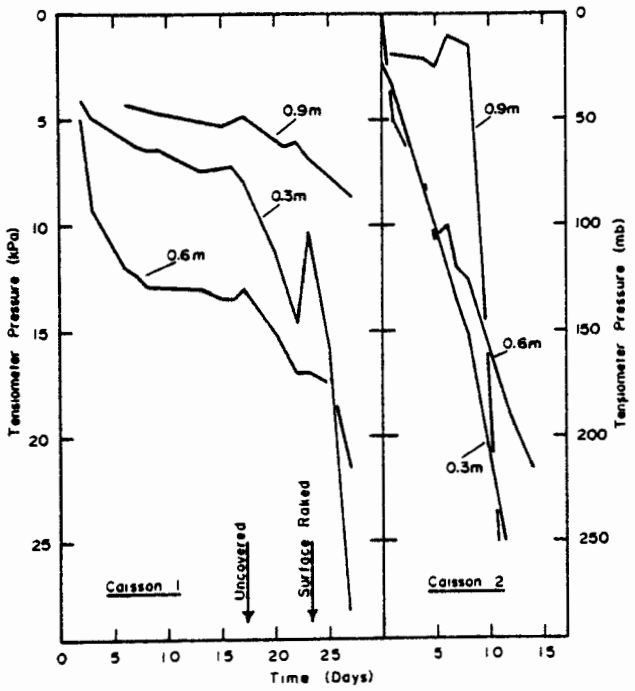

Figure 3.10. Comparison among tensiometer pressures at 0.3-, 0.6- and 0.9-m depths on caissons 1 and 2 for 27 and 15 days after water was applied.

with individual porous cup tensiometers at the 0.3-, 0.6- and 0.9-m depths, inserted into the spoil profile from the surface. Tension in caisson 2 began to decrease in the 0.3-m depth tensiometers 5 min after water was applied, and in the 0.6-m depth tensiometers 10 min after application. After a pause (42 min), and 8 min after restarting water application, tensiometers at 0.9-m depth began to change. In contrast, two-probe data on caisson 2 indicated the wetting front passing the 0.3- and 2.4-m depths at 1 and 7 min after water application was started and restarted respectively, suggesting a several minute tensiometer response delay in the spoil. In caisson 1 tension increased gradually until the surface was uncovered and raked, it then registered a sharp increase at the shallower depths. However, in caisson 2

marked increases in shallower values of tension could already be observed shortly after water application ceased. This suggests droughty environment for plants growing on nontopsoiled spoils in the field.

Figure 3.11 shows hydraulic properties of spoil material determined in the laboratory. Large differences between water retentivity curves (Figure 3.11a) corrected and uncorrected for coarse fragments may pose a problem when water flow in strip mine spoils is studied. Materials used in topsoiling are likely to have a water retentivity curve similar to the uncorrected curve in Figure 3.11a, while underlying spoil materials may have curves similar to the corrected curve. The

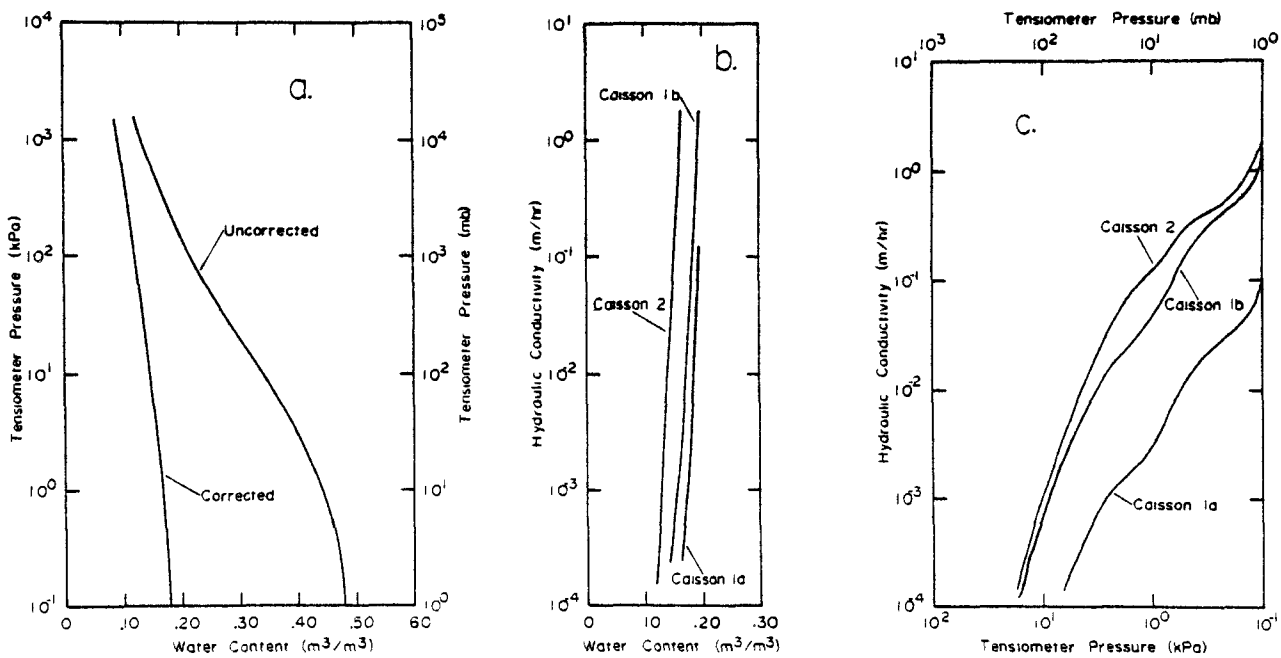

Figure 3.11. (a) Water retentivity curves averaged for all depths for spoil profile corrected and uncorrected for coarse fragments and specific retention; (b) matched (Green and Corey, 1971) hydraulic conductivity values as a function of water, corrected for coarse fragments and specific retention; (c) hydraulic conductivity as a function of tensiometer pressure; curves labeled 1a refer to caisson 1, they were matched at K_{sat} = 0.13 m/hr, curves labeled 2 were for spoil material in caisson 2 and were matched at K_{sat} = 1.89 m/hr.

measured water contents and tensiometer pressures in the topsoiled layer in caisson 1 (Figures 3.9, 3.10) are somewhat larger than those expected from the uncorrected water retentivity curve, however, values for the spoil follow those for the corrected curve. In caisson 2 measured values of water content below 1 m depth appear larger than expected from the corrected water retentivity curve in Figure 3.11a, but a rapid decrease in tensiometer pressure above 1 m depth corresponds to what would be expected from the corrected water retentivity curve. The curves in Figure 3.11b show that small changes in water content can result in large changes in hydraulic conductivity of the spoil. This means that even when water content of the spoil varies little from place to place faster flows may occur through wetter zones. Compared to natural soils under the field situations larger hydraulic conductivity values (both saturated and unsaturated) could be expected at lower water contents and higher values of tensiometer pressure on minesoils derived from materials similar to those studied.

Table 3.5 shows the distribution of water in caissons with depth and accounts for both the residual, and applied water. The water content values are based on neutron moisture probe measurements, before and 1 day after water was applied to the caissons. Since we could not integrate the values continuously throughout the profile, we selected the depth intervals on the basis of similar porosity (TPS). After the water was applied, we could account for both residual and applied water in caissons 1 and 2 within 2- to 4% (98- and 104%). In caissons 1, the topsoiled layer, except for the saturated zone, retained the most water, percentage of saturation decreasing with depth. In caisson 2, the percentage of saturation increased with depth. Such contrasting behavior is likely to prevail on field spoils with and without topsoil. Surface crusting on some spoil materials as a result of weathering may lead to results that are even more extreme than those shown in Figure 3.9 and listed in Table 3.5 for topsoiled caisson 1. More of the

TABLE 3.5. DISTRIBUTION OF TOTAL AVAILABLE PORE SPACE (TPS) AND OF SPOIL WATER IN CAISSONS WITH DEPTH

Caisson 1					Caisson 2				
		Water content, L					Water content, L		
Depth	TPS, L	Original	1st day	Saturation*	Depth	TPS, L	Original	1st day	Saturation
m				%	m				%
0.0-0.5	478	252	451	94	0.0-0.5	355	196	123†	35
0.5-0.8	487	146	336	69	0.5-0.8	527	130	229	43
0.8-1.8	1783	491	766	43	0.8-1.8	1585	552	952	60
1.8-2.5	1320	386	444	34	1.8-2.1	476	179	363	76
2.5-2.6	242	0	79	33	2.1-2.5	778	189	613	79
2.6-3.2	1126	0	1126‡	100	2.5-3.1	1374	22	1374	100
Applied	-	2115	-	-	Applied	-	2246	-	-
Total	5646	3390	3317	58	Total	5095	3514	3654	72

*(1st day/TPS) x 100.

†Less 0.18 m on caisson 1, and 0.31 m on caisson 2 on 1st day data, as result of settling.

‡Corrected for estimated 354 L that leaked out overnight.

total pore space is filled with water in caisson 2 than in caisson 1 (Table 3.4) because in caisson 2 on the average water is distributed differently and different amounts of total pore space are available.

Table 3.6 shows water table elevation, seepage flux, and volumes of water percolating to the saturated zone at different times. Calculations for caisson 2 indicate that 27 min after water application ceased, 38% of applied water had reached the water table, and by the next morning 59% had reached the water table. In caisson 1 where water was ponded for 140 min, initial drainage accounted for 15% of the water applied, while overnight drainage accounted for 53%, which resembled overnight drainage in caisson 2 (59%). Very rapid initial seepage flux at the water table in both caissons slowed down considerably by the following morning. Since water arrived at the water table fast and before the profiles in caisson 1 and 2 were saturated, it is likely that infiltrating water may have reached the water table through a limited number of larger channels.

TABLE 3.6. WATER DEPTH*, SEEPAGE FLUX†, AND CONTAINED VOLUME‡ IN THE SATURATED ZONE AFTER WATER WAS APPLIED TO CAISSONS

Time§	Water depth	Seepage flux	Volume
min	m	m/day	%
	Caisson 1		
72#	0	-	-
77	0.163	19.7	15
80	0.223	36.4	21
1280	0.576**	0.18	53
	Caisson 2		
60	0	-	-
67	0.205	18.6	18
90	0.436	6.4	38
150	0.464	0.30	41
1160	0.671	0.08	59
5480	0.711	0.01	63

*Water depth above caisson bottom.

†Incoming seepage flux at the water table, corrected for porosity.

‡Volume accrued as percentage of applied.

§On caisson 1 2115 L water applied for 92 min, ponded for 140 min; on caisson 2 2246 L water applied 0 to 5- and 47- to 63 min.

#Time for the first arrival of water at the bottom of each caisson.

**This value would be 0.370 m if we excluded the amount that leaked out of caisson.

MODELING WATER FLUX ON STRIP-MINED LAND

Although a slow, uniform, downward movement of a wetting front is modeled, it is not always a typical infiltration mechanism on all soil materials. In some soils infiltrating water appears to move down very rapidly through a system of macropores (Quisenberry and Phillips, 1976; Dixon and Peterson, 1971). Such behavior is particularly true in coarse textured stony materials and in soils that have a well defined system of cracks and fissures (Ritchie et al., 1972). In other soils, when a finer layer overlies a coarse textured one, instability

of the wetting front at the interface may lead to fingering (Hill and Parlange, 1972; Raats, 1973; Philip, 1975). In Appalachian minesoils, because of their coarse texture, some combination of these mechanisms can prevail.

The objective of this study was to model numerically infiltration and redistribution of water in a reclaimed topsoiled and nontopsoiled Appalachian minesoil.

Appalachian minesoils are unlike natural agricultural soils for which the numerical modeling techniques are relatively well developed and flow processes are moderately well known. In these minesoils large size fractions predominate. Particles larger than 25 mm frequently constitute more than 80% of the total (Ciolkosz et al., 1983) and boulders, large rock fragments, channels and fissures are common. Under saturated conditions, turbulent (Leps, 1973) or transitional (Gill, 1976) flows may occur, and under unsaturated conditions, water often infiltrates rapidly between large fragments and along discrete channels down to the water table without noticeably wetting the rest of a profile. In such circumstances modeling flow is very difficult. We have attempted to adapt the techniques used in numerical modeling of water flow in soils to the water flow in minesoils and then to verify model results with experimental data.

The Caissons

Figure 3.12 is a schematic diagram of the two systems modeled. It represents two 2.4-m diameter, 3.0-m high caissons assumed to be packed with twenty identical layers of spoil over sand. Layers 1 through 10 of caisson 1 are referred to as spoil 1 and layers 11 to 20 of caisson 2 as spoil 2. Caisson 1 represents a system topsoiled with 0.5 m of fine textured soil. Caisson 2 represents a system without topsoil and having a 0.4-m layer very coarse acid

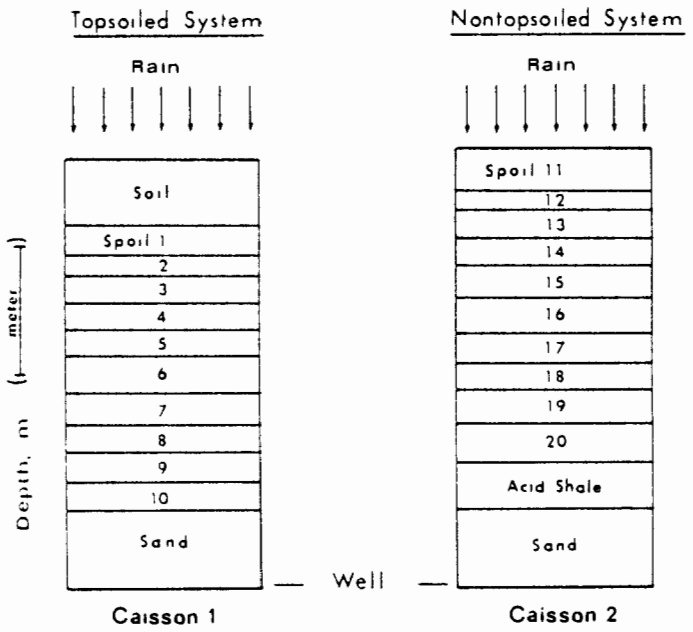

Figure 3.12. Schematic representation of the two caissons.

shale above the sand. Each caisson is thus essentially a two layer system of finer material overlying coarser material. In both cases a water table at a depth of 3 m, at the sand layer, is the lower boundary.

The actual caissons that these systems attempted to model were used to obtain experimental data on water flow and on acid generation in spoil and are described in detail in previous section. They were made from corrugated culvert pipe and were packed with two ten-layer consecutive portions of a reclaimed field profile 6-m in depth. To approximate field conditions, the first ten layers (caisson 1) were topsoiled and the second ten (caisson 2) were placed over layer of coarse acid shale. The materials in the caissons were assembled layer by layer from sequential excavations transported from a field site. Each caisson was equipped with a central well and four access tubes for monitoring the water table and profile water. Selected average properties are listed in Table 3.7 and are shown in Figure 3.13. Although the moisture characteristic curves (Figure 3.13) do not show it, comparison

TABLE 3.7. SELECTED AVERAGE PHYSICAL AND HYDROLOGIC PROPERTIES OF CAISSON MATERIALS

Caisson	Coarse fragments*	Total pore space	Specific retention†	10 kPa retention‡	Saturated conductivity
	%	----------	m^3/m^3	----------	mm/s
1					
Soil	62	0.329	0.227	0.285	0.04
Spoil 1	73	0.363	0.071	0.146	0.52
Sand	58	0.419	0.138	0.017	0.15
2					
Spoil 2	77	0.376	0.068	0.131	1.05
Acid shale	82	0.450	0.043	0.064	2.10
Sand	58	0.487	0.138	0.017	0.15

*Fragments > 2 mm.

†Water retained by the coarse fragments (ElBoushi, 1966) after drainage.

‡Water retained by fines at kPa, corrected for coarse fragments.

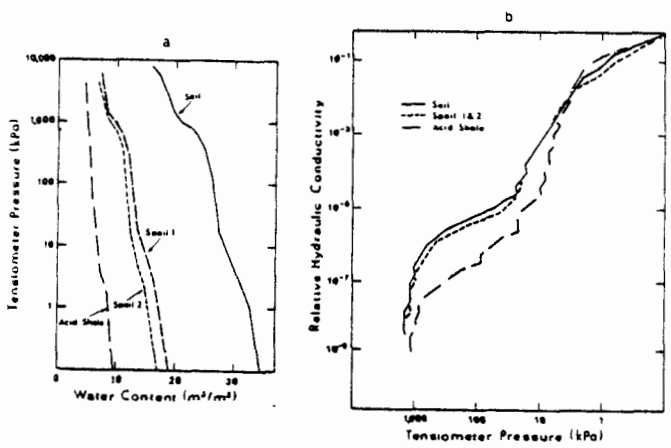

Figure 3.13. Moisture characteristic (a) and hydraulic conductivity (b) as a function of tensiometer pressure.

of the values for total pore space in Table 3.7 with anticipated water content at saturation in Figure 3.13 showed that large jumps in water content and hydraulic conductivity at saturation could be expected because of anticipated channel flow in both the spoil (1 and 2) and the acid shale. Values in Figure 3.13 were used as input to models in numerical simulation of infiltration and redistribution of water in caisson profiles.

The moisture characteristics were determined by desorption in the laboratory on the material smaller than 2 mm and were corrected for the coarse fragment content. Using these moisture characteristics and the Green and Corey (1971) model, unsaturated hydraulic conductivity values were computed and matched at the saturated hydraulic conductivity (K). Initially (Table 3.7), K values were assumed equal to the average field values in surface layers of topsoiled and nontopsoiled spoil where the caisson material originated (Pedersen et al., 1980). Subsequently, hydraulic conductivity values deduced from travel times to the water table in the caissons were also used. The ratio of hydraulic conductivities (K) in the topsoiled system ($K_{soil}:K_{spoil}$) was 1:14; the ratio in the nontopsoiled system ($K_{spoil}:K_{shale}$) was 1:2. Because the experimental moisture characteristics (Figure 3.13) represented a desorption phase; experimental values were divided by 1.6 to determine the wetting or absorption phase required for modeling infiltration (Mein, 1971, p. 49).

Flow Models

Model 1--

Using the geometry of topsoiled and spoil systems shown in Figure 3.12, a one dimensional, nonlinear, second order partial differential moisture flow equation (equation (3)) was solved numerically for infiltration and redistribution phases under variable rainfall conditions

$$\partial\theta/\partial t = \nabla \cdot (K\nabla\phi) \tag{3.1}$$

θ is the volumetric moisture content, t is time, K is the hydraulic conductivity, ∇ is the operator and ϕ is the total potential, $\phi = \psi + z$ with ψ the tensiometer pressure and z the depth measured vertically downwards. Numerical solution based on a Crank-Nicholson finite difference scheme followed Mein (1971) with some modifications and additions. These included adapting the solution to layered systems, solving for variable intensity rain, and solving for both the infiltration and redistribution phases after water application ceased. Small depth increments were taken close to the surface (Smith and Woolhiser, 1971) and at the soil-spoil and spoil-acid shale interfaces, and these increments became larger with depth. Some problems were encountered with convergence because of the low initial moisture content in the spoil, the type of moisture characteristics used (Figure 3.13), and incorporated changes in rain intensity. The program worked best if the initial water content corresponded to water content at 300 kPa or less. Under certain circumstances when convergence problems were encountered we found it useful to punch out the output on cards every 100 time steps and restart with new initial data.

In this manner moisture movement into and through the minesoils was modeled essentially in a conventional way, the output consisting of moisture profiles, wetting front positions, and pressure distributions with time. Although this approach simulated adequately the conditions expected in the natural fine grained soils adjoining the mined area and in the topsoiled minesoil represented by the geometry of caisson 1, it posed several problems on nontopsoiled spoil, which often contained as much as 80% coarse fragments. In the latter case if we used the moisture characteristic values uncorrected for coarse fragments, the program output showed unrealistically high profile water content. On the other hand, if we used the moisture characteristics corrected for coarse fragments, the program showed apparent saturation at much too low a value.

Model 2--

It could be argued that in coarse textured nontopsoiled spoil, water moved principally through a few larger channels at the rate equal to the average percolation rate, but independently of the matric potential gradient. In fact, any pressure gradients that existed were primarily local (rather than continuous), and tended to pull water from the relatively few larger channels through which it flowed to the water table.

To model this type of flow we used the following simple procedure. First, hydraulic conductivity values in Table 3.7 obtained in the laboratory were compared with the seepage flux rates in Table 3.8. Since the seepage rates, calculated from travel time through a 3-m profile, appeared to be similar in magnitude to the hydraulic conductivity, they were taken to represent flux rates for different runs. The profile was then arbitrarily divided into approximately sixty 0.05-m-thick layers. Their properties such as percent coarse fragments, surface retention on coarse fragments, total pore space and water retention at 10 kPa by fines were interpolated from the available data for each of the 11 thicknesses (11 through 21) in Figure 3.12. Water application at a known rate (Table 3.9) was then assumed to start and continue for a prescribed time (Table 3.8). We further assumed that as water went from layer to layer enough was pulled out by each layer to satisfy surface retention on coarse fragments as well as the 10-kPa retention by fines and that the rest moved on to the next layer, and so on until it reached the water table. The water table then started to rise based on the total available pore space and antecedent water content of the profile. Comparison with experimental profiles could suggest through what fraction of the total area the water moved. Model 2 is strictly an infiltration model, since both specific retention on coarse fragments and retention by fines at 10 kPa are treated as constant during

TABLE 3.8. EXPERIMENTAL VALUES OF SEEPAGE FLUX AND ANTECEDENT MOISTURE CONTENT (θ)

System	Seepage flux*	Antecedent	Illustrated in figure
	mm/s	m^3/m^3	
Soil, topsoiled (caisson 1) and nontopsoiled (caisson 2)	0.78	0.1029	5.2.3 and 5.2.4
Nontopsoiled (caisson 2)	0.96	0.0926	5.2.5
Nontopsoiled (caisson 2)	1.32	0.1633	5.2.6
	0.96	0.1962	5.2.6

*Computed as the depth to the water table divided by time required for water to arrive at the water table.

TABLE 3.9. SIMULATED AMOUNTS, DURATION AND INTENSITIES OF APPLIED RAIN AND ANTECEDENT WATER CONTENT

System	Simulated rain			Antecedent water content	Illustrated in figure
	Amount	Duration	Intensity		
	mm	min	mm/s	% by vol	
Soil	459	92	0.083	0.20	5.2.3
Topsoiled	459	92	0.083	0.20/0.10	5.2.3
Nontopsoiled	201	40	0.083	0.20	5.2.3
Topsoiled	459	92	0.083	0.20/0.10	5.2.4
Nontopsoiled	15	5	0.054	0.095*	5.2.5
	0	39	0.000	--	5.2.5
	510	16	0.525	0.100	5.2.5
Nontopsoiled	135	112	0.020	0.169	5.2.6
	0	33	0.000	--	5.2.6
	139	72	0.032	0.198	5.2.6
	0	2456	0.000	--	5.2.6
	211	146	0.024	0.254	5.2.6
	0	35	0.000	--	5.2.6
	122	11	0.177	0.338	5.2.6

*Values on this and following lines represent average profile water content.

infiltration. For redistribution, the time behavior of specific retention and retention by fines at 10 kPa also could be investigated.

Results and Discussion

Figure 3.14 illustrates a set of simulated moisture and pressure profiles using techniques of model 1 and data from Table 3.7 and Figure 3.13. Three types of systems were analyzed. Figure 3.14a shows a topsoiled system, Figure 3.14c a non-topsoiled system, and Figure 3.14b, for comparison, is a natural soil profile. The total pore space in a soil layer was adequate for simulating water profile development in a topsoiled layer, but the only way to make the incoming water move through spoil to the depth of 3 m fast enough to approximate experimental conditions was to set the total pore space to the value corrected for coarse fragments (Figure 3.13). Values almost twice that (Table 3.7) prevailed in the actual profile. If the total pore space values as given in Table 3.7 were used, the front advance was much too slow to describe the actual situation.

Figure 3.15 compares model 1 simulation with the caisson 1 experimental data. In Figure 3.15a water contents, measured during the run immediately after the wetting front had passed, are compared with a predicted (model 1) profile midway through the run. Except for the experimental point close to the surface, agreement appears good. Figures 3.15b and 3.15c compare simulated moisture profiles with caisson 1 experimental data taken the following day and the following month, respectively. Model 1 simulations agree fairly well with caisson 1 experimental results except in the soil layer near the surface. Thus, we believe that model 1 predictions of infiltration and redistribution in the profile below a 0.5-m depth can be realistic enough on a topsoiled minesoil. The low experimental value of water content near the soil surface in Figure 3.15a may be either an error or it may represent a location that did not wet well during water application. Bulk

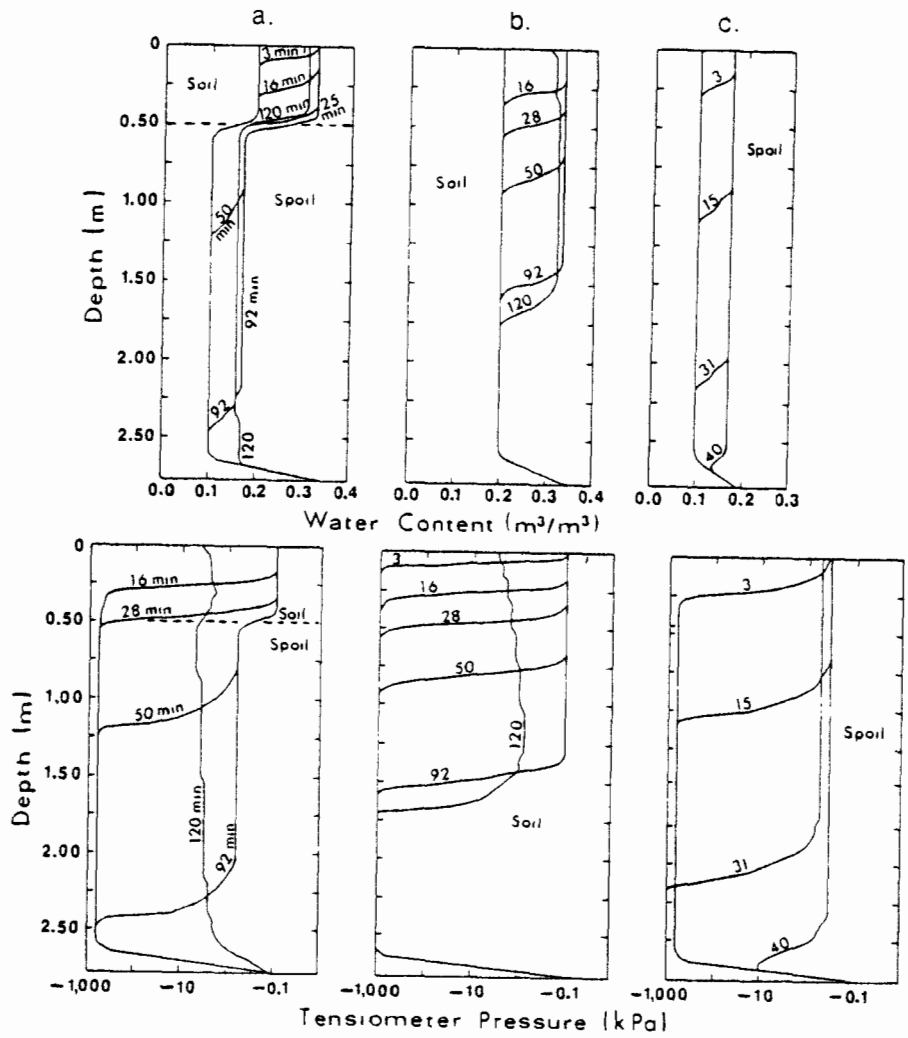

Figure 3.14. Moisture and pressure profiles simulated with model 1 on a hypothetical topsoiled spoil (a), natural soil (b), and non-topsoiled spoil (c). The numbers on the curves indicate time in minutes from the beginning of water application at the surface.

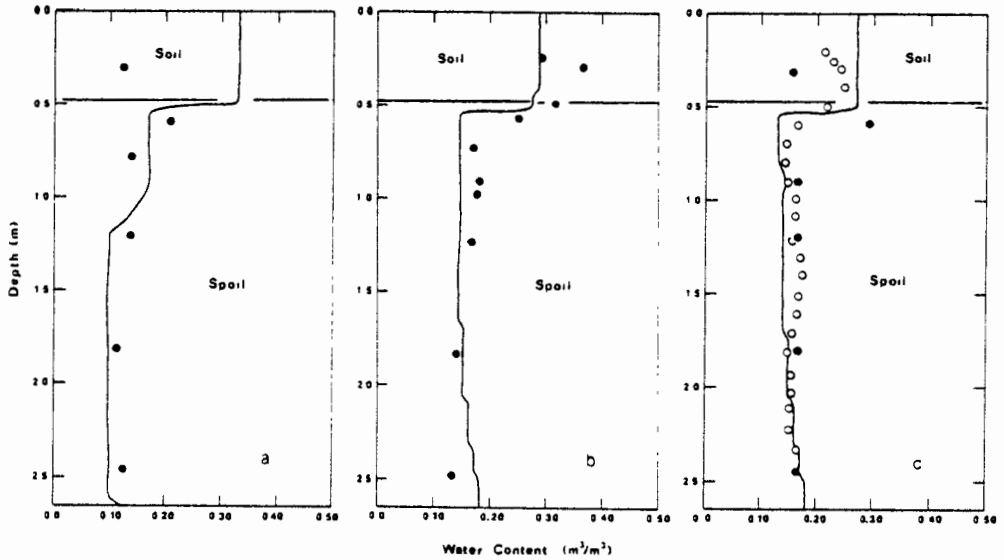

Figure 3.15. Comparison of experimental (caisson 1) water contents obtained on a topsoiled minesoil during the run with a moisture profile at 0.8 h predicted by model 1 (3.15a); comparison of experimental water contents taken 1 day (3.15b) and 1 month after the run (3.15c) with moisture profiles at 1 day and at 1 month predicted by model 1. Solid circles (●) are experimental (caisson 1) values at indicated times; open circles (○) in (3.15c) show profile water content 44 days after the run.

density data for caisson 1 (not shown) suggested that at the depth of 0.3 m a layer of somewhat lower density was present (80% of the density above and below it). Since the model assumed homogeneous conditions, this could possibly account for the discrepancy. Higher caisson 1 experimental values near the surface than predicted in Figure 3.15b may be due to a similar measurement error or may reflect higher retention than the model can account for during the redistribution phase. In Figure 3.15c the lower experimental value near the surface at 1 month may reflect evaporation losses that occurred during that month and were not accounted for by model.

In Figure 3.16 we compared simulated results for model 1 and 2 with caisson 2 experimental values taken immediately after the first run. For model 1 the agreement between the experimental (caisson 2) and simulated values got progressively worse with depth. Although model 2 in general approximated the shape of experimental profile reasonably well, it seemed to over- or underestimate caisson 2 experimental values. Table 3.10 lists matching factors necessary to correct model 2 predictions to the values observed after rain application and their reciprocals. The discrepancy between the observed (caisson 2) and simulated values may be due to errors. However, the reciprocals may also represent the fraction of an area through which the flow takes place. In addition, Figure 3.16 shows experimental (caisson 2) values at 1 month following the first run to demonstrate that in the spoil materials studied relatively little redistribution took place after the initial infiltration ceased. Consequently, expressing specific retention and retention of 10 kPa during simulation as constants may not introduce excessive error.

Next we used model 2 methodology to illustrate a specific situation: a filling up of the mined out area. Figure 3.17 illustrates progressive stages of this process. The first dashed curve on the left shows initial water content distribution in the profile in caisson 2. After the two bursts of rain (Table 3.9) experimental water contents were determined and expected moisture profile was simulated. The profile discussed here (caisson 2) is shorter (by 0.31 m) than the profile of caisson 2 shown in Figure 3.16. This is because of the settling that occurred following initial application of rain during the first run.

Simulation results (next solid curve) down to 2 m appear to reflect the experimental values well. However, below the 2 m depth simulated values seem to exceed the experimental. The reason may be that at higher initial profile water contents more water is retained by the profile than the model allows, and consequently the water table does not rise as high as projected.

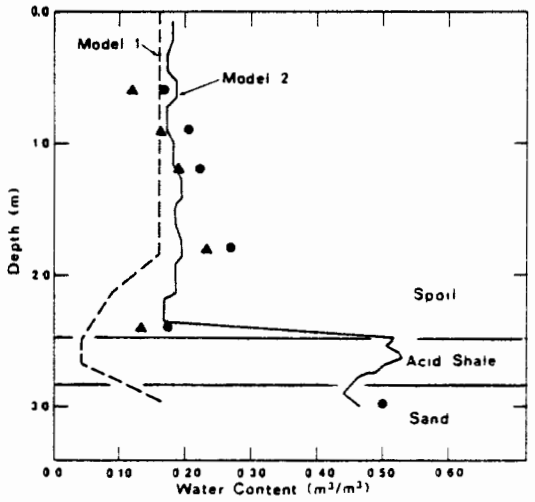

Figure 3.16. Comparison of experimental water contents obtained on nontopsoiled spoil profiles 2 h (●) and 30 days (▲) after the water application ceased with simulated profiles.

TABLE 3.10. EXPERIMENTAL AND SIMULATED* PROFILE WATER CONTENT VALUES, MATCHING FACTORS AND THEIR RECIPROCALS

Depth	Water content		Match factor	Reciprocal
	Experimental	Simulated		
m	m^3/m^3			
0.6	0.175	0.186	0.94	-
0.9	0.209	0.174	1.20	0.83
1.2	0.224	0.199	1.12	0.89
1.8	0.269	0.192	1.40	0.71
2.4	0.174	0.161	1.08	0.93
3.0	0.514	0.464	1.11	0.90

*Model 2.

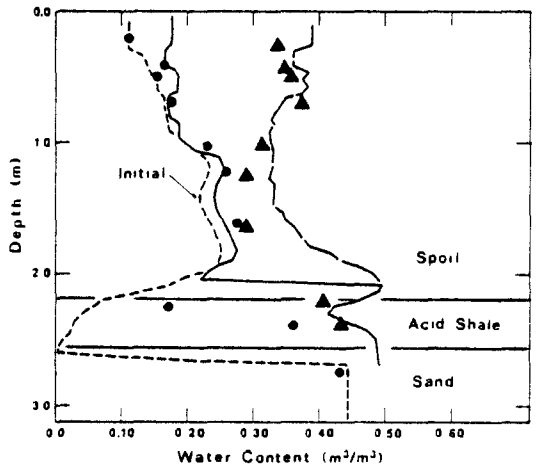

Figure 3.17. Comparison of experimental water contents on nontopsoiled spoil for two intermittent rain periods (● and ▲) 41 h apart with water content profiles simulated using model 2.

On the right hand side of Figure 3.17 a curve and (▲) data points reflect the last two bursts of rain (Table 3.9) following a 41 h pause (Table 3.9). The curve describes simulated values, the points experimental (caisson 2) measurements. Simulated values correspond to the distribution of total available pore space. Experimental values (caisson 2) are again generally somewhat lower in the 0- to 0.5-m depth and below 1 m but higher above the acid shale, suggesting a possible discrepancy between estimation of the total available pore space based in four access holes and actual pore space as reflected by caisson 2 experimental values. It is also possible, as mentioned previously, that the amount of water retained by coarse fragments is larger at higher soil water contents.

Model 2 could probably be extended to larger areas. Necessary profile properties, such as percent coarse fragments (> 2 mm) and total pore space, as well as water retention by fines and coarse fragments could be ascertained from test borings. Continuous well and rainfall records might provide adequate

data to compute seepage flux. For example, we have found that values of seepage flux obtained at our field site (Pedersen et al., 1980) compare well with those listed in Table 3.8. Subsequently, using methods outlined in Rogowski (1980), contour maps of pertinent properties over an area and with depth can be developed. If the rain and infiltration capacity distributions at a given site are known, model 2 could be used to predict profile water contents and water table accretion for a rain event.

CHEMICAL CONSIDERATIONS

In here we present and discuss the chemical properties of the spoil, spoil extracts and percolate observed in the caissons and in the laboratory, if closely coordinated and related to the caisson study. A main laboratory study included here, examined the processes potentially controlling salt and acid losses to percolate or groundwater on the spoil particle scale. The individual objectives were: 1) to identify the source of chemically degraded percolate, 2) to identify and contrast the basic chemical properties which control chemical concentration and character of percolate, 3) to compare caisson results with lab-based leachings, 4) to select a chemical parameter as an indicator of other chemical parameters, 5) to determine the potential of trace metal contamination of groundwater and 6) to identify and compare processes that potentially dominate acid production and loss at the spoil particle scale.

Analysis, Sampling and Storage Methods

The analytic methods used were as follows.

For each spoil layer, total S was determined by a high temperature combustion, while standard tests (ASTM, 1971) were used to determine sulfate, pyritic and organic-S content of the spoil matrix.

On spoil extracts and percolate, the chemical analysis included electrical conductivity (EC), total acidity, pH, SO_4, Ca, Mg, Mn, Al, ferrous Fe, total soluble Fe, Cd, Cu, Zn, Pb, Hg.

Total acidity to pH 7.3 and 8.2 were determined by NaOH titration and a glass-calomel electrode. The sample was first pretreated with 30% H_2O_2 and boiled (EPA, 1974). Electrical conductivity (EC) was determined at ~25C by a Yellow Springs instrument Model 31 conductivity meter equipped with a Beckman VS01 conductivity cell of 0.1 cell constant.

All metals, except ferrous iron were analyzed with an instrumentation Laboratory (IL) 351 Atomic Absorption (AA) Spectrophotometer using a background correction where possible. Al, Ca, Mg, Mn, total soluble Fe, Cd, Cu, and Zn were analyzed by flame AA (Emmel, 1977). Hg, Pb, and Cr were analyzed with and IL 555 carbon furnace AA using the method of known addition (Emmel, 1976). Because the background was too high for some lead samples when using standard methods, a slower atomization rate was employed. Sulfate concentrations were determined by AA measured loss of added barium due to $BaSO_4$ precipitation (Borden and McCormick, 1970). Ferrous and total soluble Fe were determined spectrophotometrically as the orthophenanthroline complex on a Coleman Model 14 Universal Spectrophotometer (APHA, 1965).

The spoil percolate was obtained from caisson lysimeters whereas spoil extracts were basically the result of lab-based spoil leaching procedure.

The sampling methods were as follows.

The spoil material analyzed was subsampled from the spoil used to reconstruct the caisson profile.

Extract sampling was done in two closely related ways. For Table 3.12 a 10-kg subsample of each spoil layer was placed in a 20 cm diameter PVC cylinder

and leached with 1000 ml of water and the leachate was filtered. For trace metals in Table 3.15 (total soluble Fe, Mn, Ca, Zn, Cd, Cr, Pb, Hg), approximately 80 g of each spoil layer was placed in a glass bottle and reciprocally shaken with distilled water (80 ml) no less than 8 hr/week over 4 weeks. The sample was centrifuged and the clear supernatant was analyzed.

The spoil percolate in the caisson was sampled from lysimeters. Three 50 x 610 mm lysimeters with a catch area of 0.0305 m^2, added during the winter of 1977-78 to augment the original system described in the previous section, were placed at three levels in each caisson (positions H, M. L). The lysimeters were operated and percolate sampled continually through all runs. When the lysimeters outflow rate exceeded one sample every 10 minutes, the sampling frequency was reduced to one sample/10 minutes. Sampling ceased upon cessation of lysimeter outflow or extensive flooding of the lysimeter due to a rising water table. In subsequent tables and figures, samples from the water table maintained in the 60 cm thick bottom sand layer are "well analysis" whereas those labeled "water supply" refer to the added rain water. Well and water supply samples were taken immediately prior to the initiation of each run.

Sample storage was usually not a problem except for caisson percolate which could generate large numbers of samples. Other samples were refrigerated at $3^{o}C$ and analyzed within a few days. Caisson percolate samples were collected in polyethylene bottles, centrifuged and part of the supernatant was analyzed on site for pH, ferrous Fe, redox potential, total acidities at pH's 7.3 and 8.2. The remainder of the sample, was immediately placed in air tight plastic bag, refrigerated ($3^{o}C$) for transport, frozen within 48 hours and usually analyzed within one week after collection. Samples selected for trace metal analysis were treated similarly except for storage up to 12 weeks before analysis.

There was no significant effect of storage on the total acidity and total soluble iron concentrations as determined experimentally.

Chemical Properties of the Spoil

The chemical properties of the spoil are determined in two ways. One way is to measure the pyrite, sulfate and organic sulfur content of the 21 spoil layers and one soil layer. The sulfate is a measure of the potential salt content which could be lost to percolate waters and the pyrite is a measure of the potential acid production. Another way is to measure the solutes extracted in a water-spoil equilibration or leaching, usually at a low water to spoil ratio. In this case, primarily acidic salts (iron, manganese and aluminum sulfates), neutral salts (calcium, magnesium, or sodium sulfates), or sulfuric acid analyzed in the extract represent maximum concentrations due to a lack of dilution, extensive contact or long equilibration times. The spoil and water extract properties are presented in Tables 3.11-3.13.

The pyrite, sulfate and organic sulfur content range between two extremes (Table 3.11), the lowest set by the soil (layer 0) and the highest by a black shale (layer 21). Sulfate or pyrite-S concentration of the other layers, appear to be in about the range of 0.05 to 0.15% and would be expected to exert a somewhat similar impact on these concentrations in percolate.

Extracts of each spoil layer contain substantial total acidity, total salts, and sulfates. Spoil layer 21 potentially dominates the system with by far the highest concentrations of the chemical parameters (Table 3.12). Extracts of spoil layer 8 contains a surprisingly high total acidity content compared to the sulfate content of the spoil layer. In fact, there is substantially more variability in the total acidity or total SO_4 extracted among spoil layers 1-20, then would be expected on the basis of the pyrite S or sulfate S concentration taken from Table 3.11.

TABLE 3.11. SPOIL PYRITE ANALYSIS

Caisson	Layer	Total soluble Fe	Pyritic-S	Sulfate-S	Organic-S	Total
		mg/ℓ	---------- % by weight ----------			
1	0	7.4	.012	.012	.012	.045 soil
	1	26.3	.076	.065	.047	.188 spoil
	2	32.7	.095	.082	.033	.210
	3	38.7	.112	.079	.070	.261
	4	46.8	.136	.089	.065	.290
	5	33.8	.098	.066	.063	.227
	6	43.1	.125	.066	.052	.243
	7	54.0	.157	.076	.056	.289
	8	24.4	.071	.094	.036	.201
	9	30.4	.088	.070	.048	.206
	10	43.0	.125	.053	.053	.231
2	11	49.2	.143	.054	.051	.248 spoil
	12	45.1	.131	.062	.050	.243
	13	49.1	.143	.053	.051	.247
	14	36.6	.106	.066	.043	.215
	15	42.8	.124	.049	.043	.216
	16	28.2	.082	.059	.041	.182
	17	22.2	.064	.056	.032	.152
	18	29.2	.085	.049	.040	.174
	19	20.7	.060	.077	.111	.248
	20	22.8	.066	.055	.033	.154
	21	677.5	1.967	.738	1.095	3.800 black shale

TABLE 3.12. VALUES OF pH, ELECTRICAL CONDUCTIVITY (EC), TOTAL ACIDITY CA, MG, AND SO_4 FOR TWENTY-ONE LAYERS OF RECONSTRUCTED SPOIL PROFILE

No	Depth	pH	EC	Total acidity	Ca	Mg	SO_4
	m		µmhos/cm	meq/ℓ			
					Caisson 1		
0	0	3.91	410	2.89	1.71	0.53	0.88
1	0.51	3.35	275	1.03	0.71	0.34	2.63
2	0.74	3.29	740	5.09	1.96	2.96	8.87
3	0.91	3.10	800	5.12	1.73	0.02	8.77
4	1.12	3.17	995	6.62	3.08	4.07	11.87
5	1.32	3.37	660	3.10	1.63	1.98	6.57
6	1.55	3.18	620	3.45	1.81	1.95	6.79
7	1.83	3.05	445	2.90	0.66	0.57	4.50
8	2.08	2.35	3400	45.44	5.25	6.98	54.85
9	2.29	3.17	998	8.04	3.11	3.40	11.89
10	2.52	3.35	870	5.86	2.78	3.23	9.69
Sand	2.74						
					Caisson 2		
11	0	2.97	905	6.68	3.08	3.40	11.09
12	0.28	2.98	820	6.22	2.65	3.15	10.19
13	0.48	3.21	900	5.92	3.98	3.60	10.89
14	0.69	2.56	2000	15.72	4.44	4.16	20.88
15	0.91	3.42	280	1.00	0.84	0.34	2.80
16	1.17	3.14	1280	8.72	6.02	4.41	14.90
17	1.44	3.19	660	3.78	2.55	2.08	7.70
18	1.68	3.21	845	5.38	3.29	3.26	9.70
19	1.89	3.36	2050	14.24	10.30	9.67	33.38
20	2.15	3.37	1100	6.86	4.90	3.80	12.80
21	2.45	2.79	6000	67.08	23.33	24.58	134.81
Sand	2.82						

TABLE 3.13. TRACE METAL CONCENTRATION OF SPOIL EXTRACT*

Layer	pH	Cd	Cr	Cu	Fe	Hg	Mn	Pb	Zn
Blank	-	<.004	<.001	<.02	<.2	<.02	<.02	<.001	<.02
1	4.02	<.009	<.001	<.02	<.2	<.02	35.4	.003	.65
2	3.67	<.004	<.001	<.02	<.2	<.02	28.3	.003	.75
3	3.40	.012	.002	.08	<.2	<.02	64.6	.012	1.95
4	3.46	.012	<.002†	.30	.4	<.02	39.4	.009	2.75
5	2.86	.029	.013	.84	4.5	.06	161.	.020	5.13
6	3.49	.022	.001	.48	.4	<.02	83.8	.015	4.00
7	2.80	.010	<.001	.10	.4	<.02	59.6	.009	2.70
8	3.69	<.004	<.001	.08	<.2	<.02	27.3	.010	1.22
9	2.90	.026	.006	.64	1.0	<.02	128.	.018	5.00
10	3.77	<.009	<.001	.02	<.2	<.02	32.3	.003	1.15
11	3.08	.015	.005	.45	1.6	<.02	85.8	.027	4.30
12	3.41	.016	.004	.46	1.2	<.02	79.8	.013	3.80
13	3.41	.015	.001	.28	.3	<.02	56.6	.011	3.50
14	3.57	.010	<.001	.10	<.2	<.02	40.4	.003	1.65
15	3.28	.010	.001	.20	.3	<.02	61.6	.011	3.15
16	3.58	.005	<.001	.12	<.2	<.02	40.4	.008	2.05
17	4.03	<.004	.003	.04	<.2	<.02	29.3	.007	1.65
18	3.41	.006	<.001	.10	.3	<.02	40.4	.006	2.10
19	3.77	.019	<.001	.10	<.2	<.02	69.7	.007	2.75
20	3.40	.011	<.001	.19	<.2	<.02	63.6	.012	2.85
21	2.65	.049	.240‡	.74	3700.	.05	319.	.010	26.0
§	-	.010	0.05	1.0	0.3	0.002	0.05	0.05	5.0

- = not determined.

* = concentration either mg/ℓ extractant or mg/g spoil; mass ratio of extractant to spoil equals 1:1.

† = insufficient sample.

‡ = flame analysis; rest determined by carbon furnace atomic adsorption.

§ = EPA drinking water standards.

Trace metal concentrations, Cd, Cr, Cu, total soluble Fe, Hg, Mn, Pb and Zn, in spoil were analyzed (Table 3.13). The EPA Interim Primary Drinking Water Standards (EPA, 1975) for Cd, Cr, Hg and Pb and the EPA Proposed Secondary Drinking Water Standards (EPA, 1977) for Cu, Fe, Mn and Zn are included for comparison. The trace element contents of 21 spoil extracts relative to the drinking water standards were equaled or exceeded in 14 layers for Cd, 1 for Cr, none for Cu, 11 for total soluble Fe, 2 for Hg, all for Mn, none for Pb and 3 for Zn. Because the analytic limits for mercury analyses were 10 times higher than the standard, we suspect, but cannot prove that the mercury standard was exceeded more than twice. Again, spoil layer 21 extract provided the highest concentrations.

Chemical Properties of the Spoil Percolate

The mean values ($\bar{x}$) and standard deviation (Sd) of pH, total acidity (pH 8.2), ferrous Fe, Mn, Al, Ca, Mg and SO_4 concentrations in percolate from lysimeters (L-1, 2, 4, 6, 8, 9), water supply and well are presented for all runs (Table 3.14).

Table 3.14 shows the water quality to generally deteriorate with depth in both caissons, dramatically so at lysimeter L-9. The potentially greatest acid producing spoil layers from the previous section are: primarily spoil layer 21 located immediately above lysimeter L-9 in caisson 2, and to a lesser degree spoil layer 8, which drains into lysimeter L-8 and L-9 in caisson 1. There appear to be two processes affecting water quality degradation. First, the percolate quality gradually deteriorates from L-1 to L-6 in both caissons. Because fluctuation of potential acid products concentration in any spoil layer overlying L-1 to L-6 is not extreme, the acid product concentration in the percolate steadily increases with spoil depth. Thus, the source of the chemically degraded percolate is general and no contributary zone can be clearly delineated. Second, the percolate quality generally deteriorates dramatically from L-6 to L-9 in both caissons. Thus, if the fluctuation of acid

TABLE 3.14. CHEMICAL CHARACTERISTICS OF SPOIL DRAINAGE AT SELECTED DEPTHS WITHIN CAISSONS 1 AND 2*

Sampling depth	pH		Total acidity		Ferrous Fe		Mn		Al		Ca		Mg		SO_4	
	$\bar{x}$	S_d†	$\bar{x}$	S_d	$\bar{x}$	S_d	$\bar{x}$	S_d	$\bar{x}$	S_d	$\bar{x}$	S_d	$\bar{x}$	S_d	$\bar{x}$	S_d
			meq/ℓ		mg/ℓ											
Caisson 1‡																
Water supply	6.0	0.0	0.2	§	0.8	§	.2	§	0.0	§	2.4	§	0.1	§	13.5	§
L-1	5.8	1.0	0.2	0.9	0.1	0.1	3.5	5.0	0.1	0.1	11.0	5.8	1.2	1.0	6.8	44.
L-2	5.7	0.5	0.2	0.2	0.0	0.0	0.4	0.1	0.4	0.3	10.6	3.4	2.0	1.7	5.3	15.
L-4	4.2	0.0	0.5	0.0	-	-	-	-	-	-	-	-	-	-	-	-
L-6	4.1	§	1.4	§	1.7	§	16.	§	-	-	-	-	-	-	-	-
L-8	3.4	0.1	5.0	1.0	2.2	§	-	-	22.	§	88.	§	70	§	740	1120
L-9#	3.6	0.0	12.1	0.2	1.9	0.9	99.	6.	84.	14.	270	24.	210	28	2300	410
Well**	6.8	0.4	14.5	4.3	100.	68	330	11.	0.3	§	490	§	250	§	3800	§
Caisson 2††																
Water supply	6.3	0.4	0.9	0.1	1.7	0.8	0.2	0.1	0.0	0.0	1.8	0.0	0.1	0.0	29.	*
L-1	3.8	0.2	3.1	1.9	2.4	1.2	14.7	15.0	12.2	10.0	80	57.	41	29.	550	410
L-2	3.8	0.1	3.2	3.3	3.1	4.1	18.	23.	1.5	0.7	48	70	32	42	410	580
L-4	3.5	0.1	1.9	0.4	4.0	3.8	17.5	7.	8.1	2.1	61	17	31		310	270
L-6	3.6	0.2	6.3	4.2	2.6	1.9	43.	13.	32.	17	200	74	105	25.	1270	460
L-8	2.6	0.1	22.	18.	207.	§	117	§	68.	55.	277	49	135	25	3300	2130
L-9§	2.7	0.1	82.	50.	278.	191.	258	134.	169.	79	392	126	308	116	7000	3250
Well#	2.5	0.1	157.	33	2600	1580	456	14.	266	53	400	140	511	86	10500	1800

*Values averaged for all runs for which data was collected.

†S_d is the standard deviation.

‡Includes 7/26/77, 9/14-16/77 runs.

§One observation.

#Data available for flooding condition only.

**Water table continuously maintained in sand layer (below spoil).

††Includes 8/18/77, 10/5-7/77, 8/23/78 runs.

products concentration in selected strata is extreme, i.e., total acidity for layer 8, caisson 1 or layer 21, caisson 2, these spoil layers have the most impact and control percolate quality. Under these conditions, the contributing zones are specifically and clearly delineated.

The effect of different incubation periods and water applications associated with each run undoubtedly affected, but did not override the acid products contributing pattern for each caisson. Possibly, sufficiently extreme incubation conditions and water applications were not employed to stress the chemical system and, thus break down the pattern described here. However, the experimentally employed conditions adequately represent most of the extreme water application and incubation conditions that would be experienced in the field (see hydrology section).

A similar analysis of caisson percolate shows the same pattern of trace metal contamination (Table 3.15). The level of contamination was generally similar to that determined for the corresponding spoil extracts in Table 3.13. The results compare well for Cd, Fe, Hg, Mn at all lysimeters; Cr at lysimeter L-9, caisson 1 and lysimeters L-6, L-8, caisson 2; Pb at lysimeter L-9, caisson 1 and lysimeters L-8, L-9, caisson 2; and Zn at lysimeter L-9, caisson 2. Contamination in the remaining combinations compared to spoil extract are considerably higher, particularly for Cu and Zn. Analyses of caisson wells which accumulate all percolate during the runs, corresponded with lysimeter data for caisson 2 but not for caisson 1. The reduced solubility and chemical precipitation caused by the high pH (7.0) of caisson 1 well waters probably accounted for the reduced trace metal contamination. The cause of the high pH is likely due to acid neutralization by carbonate minerals. Note the high Ca and Mg concentrations relative to the low total acidity (Table 3.14).

TABLE 3.15. TRACE METAL CONTAMINATION OF CAISSON PERCOLATE AND WELL WATERS TAKEN FROM CAISSON 1 AND 2 FOR RUN 1

Sample	Time	pH	Cd	Cr	Cu	Fe	Hg	Mn	Pb	Zn
						mg/ℓ				
Caisson 1										
Water supply*	0820	6.1	<.004	<.001	<.02	<0.02	<.02	<0.02	†	†
L-9‡	1300	3.6	.021	.020	.25	5.4	<.02	51.	†	8.40
Well*	0800	7.0	<.004	.013	<.02	6.0§	<.02	336.	.028	0.19
Caisson 2										
Water supply*	0853	6.0	<.004	<.001	<.02	<0.02	<.02	<0.02	†	†
L-6	1000	3.6	.019	.032	.14	2.7	<.02	28.	.600	6.00
L-8	0948	2.5	.022	.150	.41	564.	<.02	118.	.012	9.40
L-9‡	0936	2.4	.061	.400	5.1	1490.	<.02	419.	.012	17.3
Well*	0800	2.7	.055	.180	2.40	1083.	<.02	459	.050	11.2

*Sampled before start of leaching cycle. Water level in well maintained at approximately a constant level within sand layer between runs.

†No reading, insufficient sample.

‡Rising water table intersects lysimeter (1st sample).

§Questionable answer due to analytic interferences from other solutes and extensive precipitate formation. Ferrous iron concentration of well determined onsite at time of sampling was 51 mg/ℓ.

Chemical Interrelationships of Spoil and Spoil Percolate

The spoil chemical properties set a potential which controls percolate quality subject to the percolation rate or volume. The spoil chemical properties can be dominant under many conditions and, thus provide a means of classifying and estimating its impact on percolate quality.

The average total acidity of percolates taken from different depths within each caisson (Table 3.14) were compared with total acidity of spoil extracts (Table 3.12) from corresponding spoil layers (Figures 3.18 and 3.19). The total pyrite and total sulfate content from Table 3.11 of each layer are included for comparison. Data analysis attempted to determine if discrepancies between the two independent measures of total acidity existed and if under certain circumstances, basic spoil

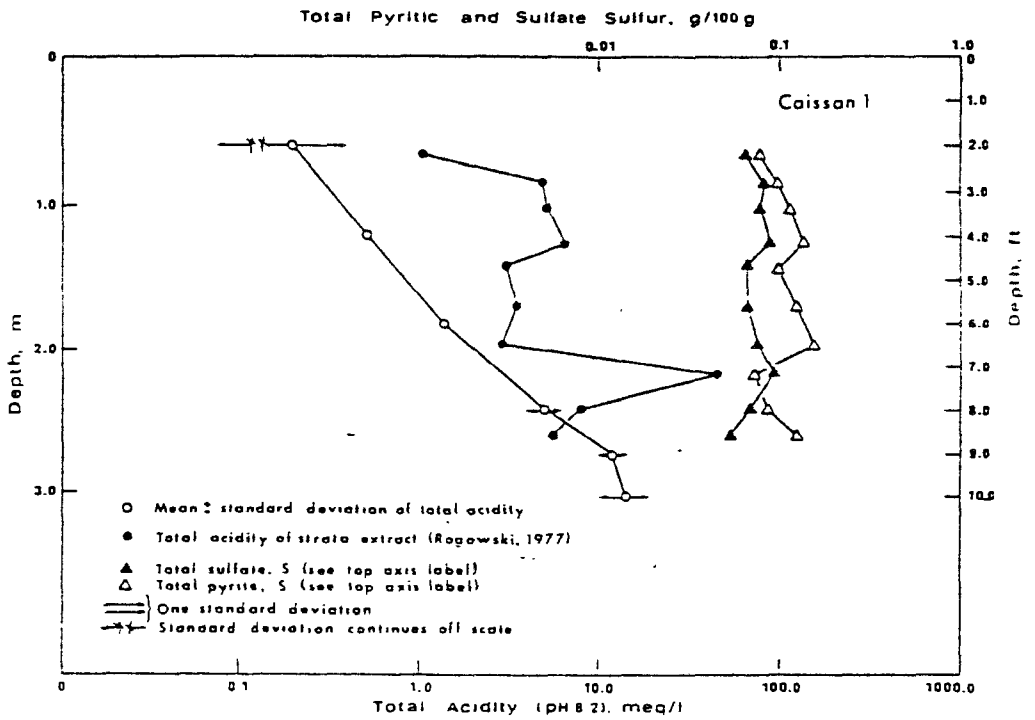

Figure 3.18. Relation of total acidity from lysimeter drainage with spoil and spoil extract analyses for corresponding spoil layers.

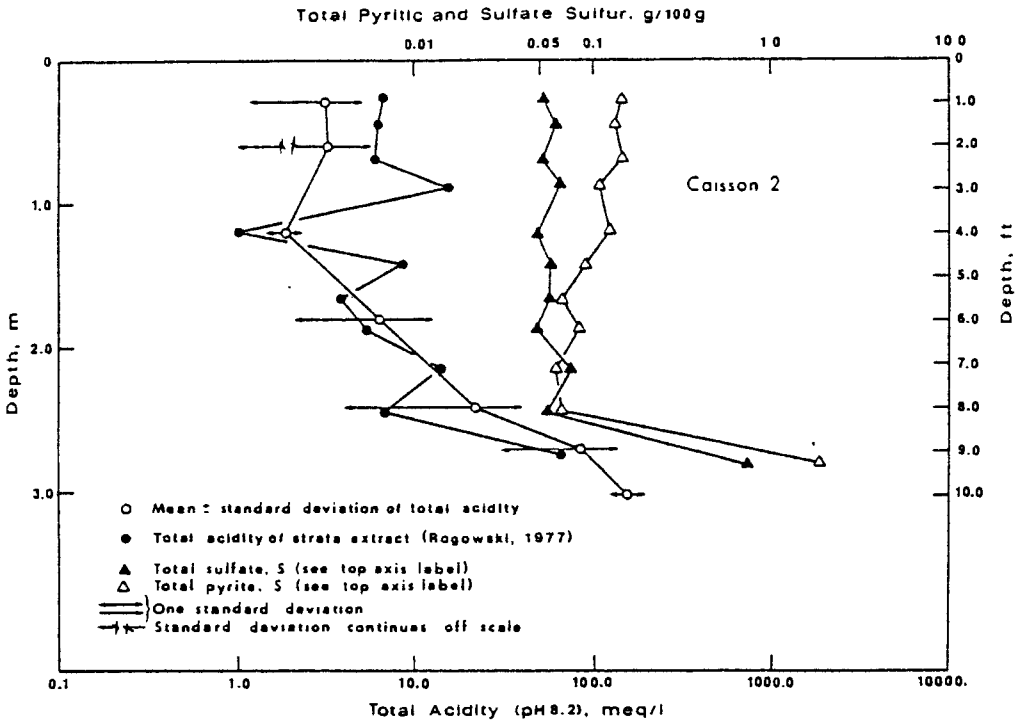

Figure 3.19. Relation of total acidity from lysimeter drainage with spoil and spoil extract analyses for corresponding spoil layers.

properties such as total pyrite content could be used to approximate the observed percolate quality.

The relationships of total acidity in percolate and spoil extracts, although initially separated at caisson 1 spoil surface, converged with depth (Figure 3.18). An analogous comparison for caisson 2 shows both relationships to be generally coincident (Figure 3.19).

The greatest divergence between these relationships in both caissons was where the total acidities were lowest, particularly less than 3.0 meq/l on caisson 1. Consistent with previous observations in Table 3.14, the total acidity in the caisson 1 percolate increased progressively with depth to the 2.3 m level (L-8), at which point the spoil extract parameter became a good measure. There appeared

to be no correspondence between the total acidity and either total pyrite or total SO_4 content other than a decrease in all parameter values observed generally within 1 meter of the spoil surface. In caisson 2, the total acidity of percolate, total acidity of the spoil layer extract, and the total pyrite and SO_4 contents clearly indicate the individual dominant influence of spoil layer 21, but not the other layers (Figure 3.19).

It should be noted that while pyrite content, as given by percent S in Table 3.11, of layer 21 is one order of magnitude greater than in overlying layers, pyrite content of layer 8 is not. However, SO_4, a pyrite oxidation product, is considerably more concentrated in layer 9 relative to overlying layers. Possibly the similarity in magnitude of acid production between layers 8 and 21 results from an originally greater pyrite availability in layer 8 due to greater exposed surface area or a greater amount of framboidal pyrite (Caruccio, 1973).

Thus, the total acidity determined for each spoil layer extract provides a good estimate of the total acidity of percolate, if the potential acid products contribution of the spoil layer is reasonably high (>5 meq/l). At low concentrations, hydrologic and spatial variability diffuse the contributions of many spoil layers. Measures of total sulfate or total pyrite appear to be useful predictions of the total acidity of percolate when great differences in sulfate content or acid producing exist, respectively. Otherwise, these two parameters appear insensitive to changes in total acidity of percolate.

The pattern, volumes and rates of flow would be expected to affect the interrelationship between spoil layer chemistry and percolate, especially under extreme conditions. Under conditions of high water application rates (0.143 mm/sec - caisson 1; 0.055 mm/sec - caisson 2), the percolate outflow quality decreased at a rapid rate to a stable level in most cases (Figure 3.20). The total acidity of sequentially sampled percolate from the H and L lysimeters followed a common

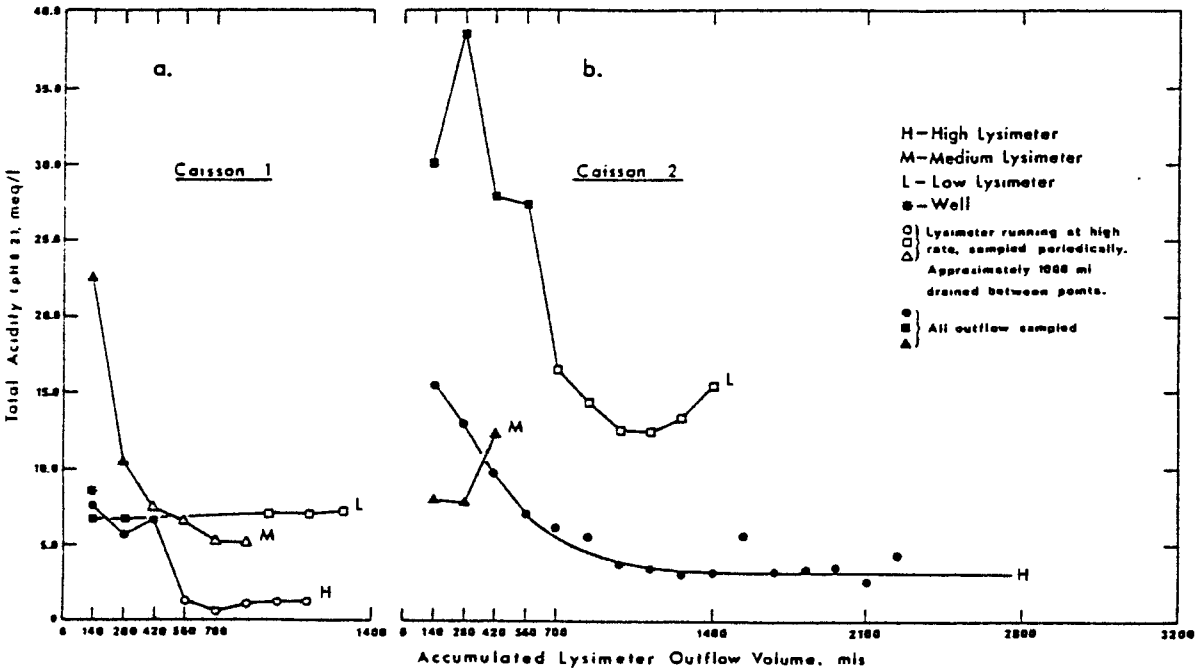

Figure 3.20. Total acidity as related to flow duration on caissons 1 (7/18/78) and 2 (8/23/78).

decreasing curvilinear relationship. At all lysimeters where sufficient samples were taken, the total acidity upon extended leaching stabilized according to lysimeter location. Expressed in meq/l, these were approximately: caisson 1, H - 1.0, M - 5.0, L - 7.0; caisson 2, H - 3.5, M - Unknown, L - 12.5 to 15.5. Although considerably higher than the stabilized total acidities, the initial total acidity values for the H and L lysimeters also relate to lysimeter location. The amount and the rate at which rainwater is applied (Rogowski, 1978) does have substantial impact on the total acidity of strip mine spoil percolate during the initial part of the run. However, the total acidity of the percolate quickly stabilizes relative to its position in the spoil or the presence of a dominating spoil layer. The common curve shape for different depths suggests that the same processes control total acidity concentration in percolate.

One reason for the readily discernible and, in some cases, not greatly reduced effect of spoil chemical properties on percolate quality even under high percolation rates, may be due to partial and changing leaching patterns of the overlying coarse spoil throughout the event. The results indicate that flow occurred in caisson 1 on the average through only 3% of the overlying volume, while flow occurred in caisson 2 through 30% of the overlying volume at the H level (near the surface), 2% at the M level and 6% at the L level. These values were calculated in the following way. The lysimeter depth, the time between the start of rainfall application and the first lysimeter outflow, rate of lysimeter outflow and rainwater application relative to lysimeter outflow were used to estimate the initial percolation rate and final outflow rates. The average porosity of spoil material in caisson 1 was 0.384 and in caisson 2 was 0.447 by volume. Thus, rainwater application rates corrected for porosity would be .372 (.143/.384) and 0.123 mm/sec for caissons 1 and 2, respectively. Outflow rate/application rate ratio for H and L lysimeters, caisson 1, becomes then .04 and .02. Similarly, for H, M and L lysimeters in caisson 2, the ratio becomes .30, .02 and .06, respectively. For these lysimeters to produce outflow, saturated flow must have occurred over some portion of the porosity immediately above the empty lysimeter cavities.

These computations support a hypothesis (Rogowski, 1978) that flows in coarse spoil materials occur only through a portion of available pore space. A word of caution, under unsaturated flow conditions some divergence of flow in the vicinity of lysimeters cavities is likely.

Another reason high percolation rates did not mask the expected percolate quality based on spoil chemical properties, is that acid product concentrations at or near the spoil particle surface are in excess of flow transport capacities. Under the most extreme leaching conditions simulating a rapidly moving saturated flow system, spoil layer 21 was leached in the laboratory (Figure 3.21). The

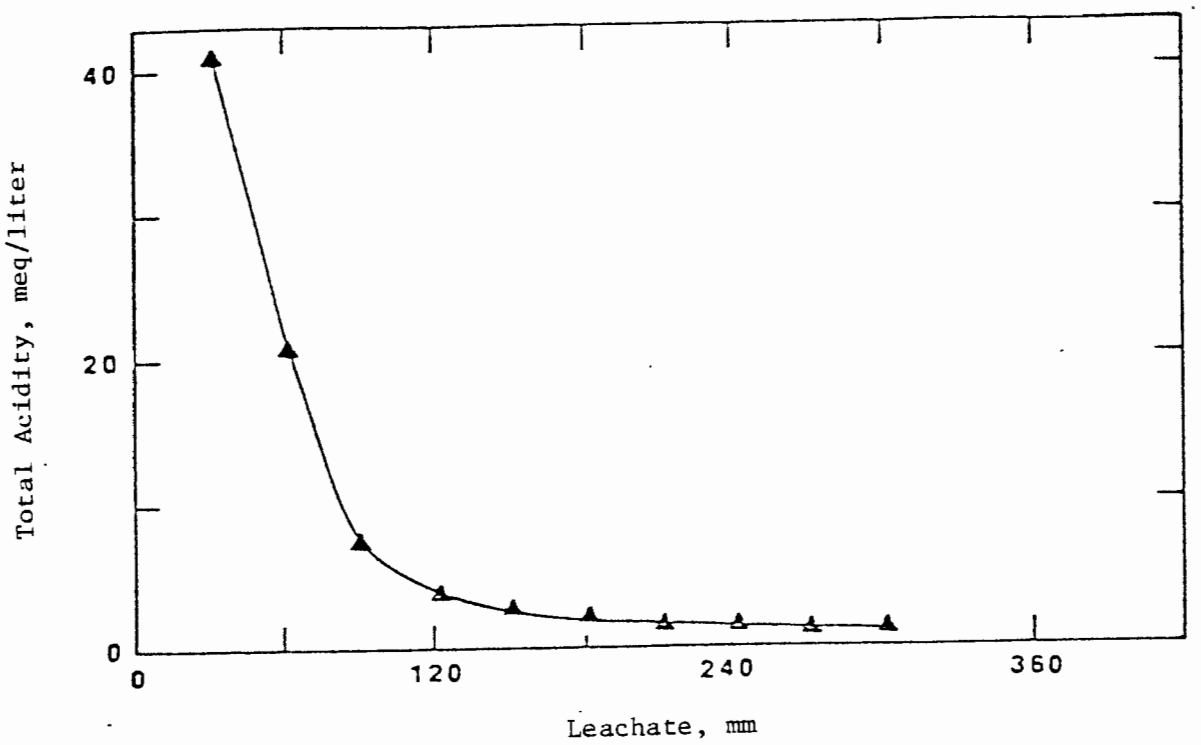

Figure 3.21. Total acidity as related to quantity of leachate under saturated conditions for spoil 21.

flow rate was 12.5 ml/min for an 85 g sample, with a pore volume of 25 mls. Incubating the column under an oxygen-free (N_2) atmosphere for two weeks and repeating the leaching step essentially regenerated an approximately equivalent amount of acid products, implying that diffusion of acid products from the particle interior to the surface is an important process.

Processes Controlling Acid Product and Acid Losses from the Spoil Particle

If a single spoil particle from the worst spoil layer can be considered to represent the behavior of that layer, we would probably observe the following. Immediately following particle formation due to the mining process, the spoil particle would probably have pyrite and pyritic reaction products distributed with some degree of ordered uniformity throughout the particle. Initially and rapidly, acid products at and close beneath the particle surface would be lost

to percolating or surrounding waters due to the short diffusion distance. If extensive ongoing pyrite oxidation was the primary source of acid products, that lost to drainage waters would likely be controlled by the kinetics of the pyrite oxidation reaction (we assume percolation is not limiting if the spoil particle is in an unsaturated zone). After the pyrite or indigenous acid products at or near the particle surface are removed, the accumulation rate of acid products at the particle surface would likely become progressively more diffusion controlled, i.e., controlled by O_2 diffusion in and/or acid products diffusion out. We would expect acid products lost from the particle, or the spoil to be initially high and then reduce over time to some base level. This behavior has been observed for stripmine drainage (Vimmerstedt and Struthers, 1968). Thus, the acid products contribution to percolating or surrounding waters would initially be controlled by reaction kinetics but would gradually shift to diffusion control.

The specific objectives of this section are to: 1) determine at the spoil particle scale if the diffusion processes potentially control acid product movement to the particle surface or O_2 diffusion to the reaction sites; and 2) compare some of the published acid production rates for spoil based on pyrite content to the observed rate of pyrite oxidation.

The basic approach was to alternatively leach and incubate spoil-containing columns in the laboratory under oxygen free (N_2) or atmospheric (20% O_2) conditions. The rate of acid production and acid product regeneration during these incubations, and the leaching curve characteristics during the leaching step, provided the data which was either used directly for comparing the importance of acid production versus acid products leaching or indirectly as input into a diffusion equation.

Laboratory Setup and Procedure

The physical setup consisted of 13 columns, each being continuously incubated at room temperature (~25C) for periods of 5.5 - 3305 hours. Either water saturated air (20% O_2) or N_2 gas, was passed through these incubation columns. The long-term gas-flow rate through these series connected columns following the preliminary high rate purging step for the N_2 incubation, was 5 ml/min for N_2 and a 40-80 ml/min for air. Both rates were measured at the exhaust of the last column in the series. In the N_2 incubation system, a 10 cm water-pressure equivalent head was maintained using a manostat bottle. This, in addition to the 5 ml N_2/min flow rate through the system prevented air entry. Because the total void volume of 7 columns (most ever run in a series) was less than 0.5 liters, the total air volume was replaced at least once every 12.5 minutes at the air flow rate. Each column was incubated from one to seven times with each incubation being followed by a leaching cycle. In some cases, the treatments (air or N_2) were switched between incubations (Table 3.16).

The columns are polyethylene cylinders of 3.2 cm internal dia x 30 cm length, stopped with neoprene stoppers and end packed with glass wool. These columns were series connected by tygon tubing with gas inflow at the bottom and exhaust at the top.

The columns were filled with approximately 75 gms of sieved, washed spoil 21. Spoil 21 characteristics and source areas were described earlier in this section and the hydrology section. Spoil 21 was taken from previously undisturbed shale strata immediately overlying the coal and contains 2% pyritic sulfur, 0.7% sulfate sulfur and 1.7% organic sulfur. Before packing the columns, the spoil has been sieved to remove the fractions less than 2.0 and greater than 8.0 mm. The wash procedure was used to remove most of the surface associated salts and acid products before N_2 and air incubations were initiated. The wash step consisted of

TABLE 3.16. INCUBATION SEQUENCES, TIME AND COMPOSITION OF ELUANT GAS BY COLUMN*

Column no.	Sequence 1 hrs/gas	Sequence 2 hrs/gas	Sequence 3 hrs/gas	Sequence 4 hrs/gas	Sequence 5 hrs/gas	Sequence 6 hrs/gas	Sequence 7 hrs/gas
1	43/N	268/N	310/N	16/N	-	-	-
2	137/N	25/N	19/N	6/N	745/A	-	-
3	1482/N	2523/N	-	-	-	-	-
4	46/N	115/N	20/N	4/N	763/N	-	-
5	1484/N	3305/N	-	-	-	-	-
6	67/N	123/N	17/N	409/A	6/A	15/A	7/A
7	21/A	1100/A	1969/N	-	-	-	-
8	139/A	790/A	1968/N	-	-	-	-
9	25/A	115/A	22/A	6/A	954/N	-	-
10	1463/A	-	-	-	-	-	-
11	47/A	122/A	17/A	408/N	6/N	16/N	7/A
12	45/A	245/A	310/A	15/A	-	-	-
13	70/A	100/A	16/A	-	-	-	-

*Time = hours incubation; N = 100% N_2 atmosphere; A = ambient atmosphere (~20% O_2).

sequentially leaching (every two minutes) one retention volume (~25 mls) with distilled water until the leachate was less than 125 µmhos/cm electrical conductivity (EC). This was the starting point for the first incubation. The starting point for subsequent incubations was at the end of the extraction cycle described as follows.

The column was bottom filled with distilled water to the top of the spoil, immediately distilled water was added to the top of the column, then 25 mls were drained from the column. This removed the water contained in the column void space below the spoil which had not contacted the spoil material. The draining of the first 25 mls was the zero or starting time. Following this, one retention volume (25 mls) was drained from the column every two minutes and chemically analyzed. The time to drain the 25 mls was approximately 5 seconds. The retention volume, i.e., void space within the spoil, ranged from 22-25 mls/column. The two minute sampling frequency was carried out until the EC was less than or equal to 125 µmhos/cm. Once collected, the 25 ml leachate sample was immediately analyzed for EC and pH. In excess of 50 composited samples, each composite taken from different columns at different stages of elution, were analyzed for Ca, Mg,

Mn Al, total soluble Fe and SO_4. Two or three individual samples, taken in series from the same column and of approximately the same value, were composited to provide sufficient sample for analysis and a more stable result. These data were used to develop: 1) an EC - total salts relationship (sum of the Ca, Mg, Al, Mn, total soluble Fe and SO_4 concentrations) with equation and appropriate statistics (Figure 3.22, 3.23) and 2) an EC - SO_4 relationship with the equation and appropriate statistics (Figure 3.24, 3.25). Figures 3.23 and 3.25 provide an expanded scale to observe the low values in these relationships. The SO_4 or total salts concentrations predicted by either equation below 850 EC was sufficiently close so that only the equations in Figures 3.22 and 3.24 were used.

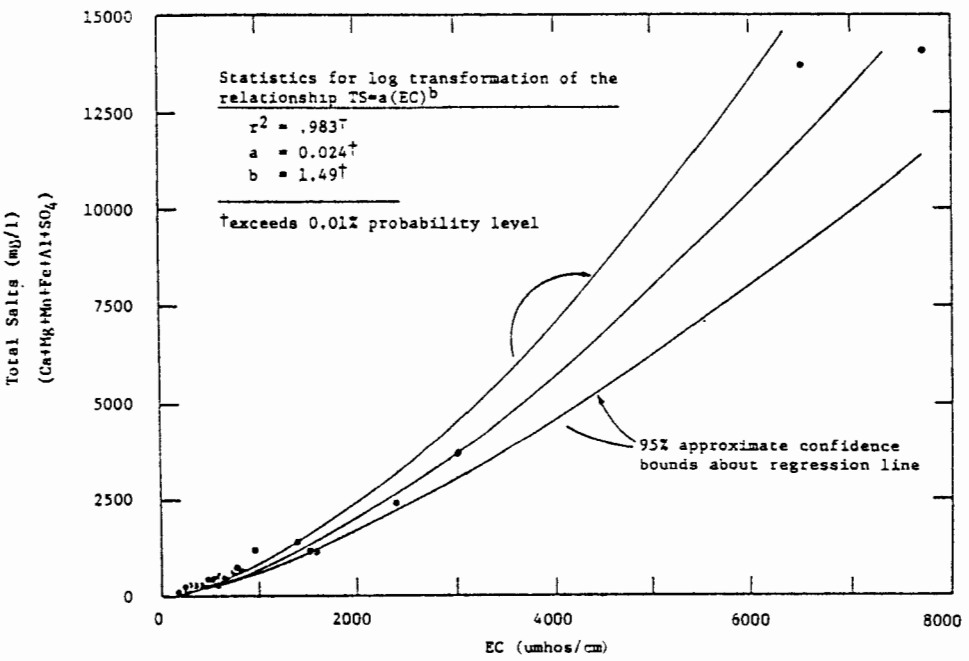

Figure 3.22. Relationship of total salts (TS) with electrical conductivity (EC) for selected column leachates.

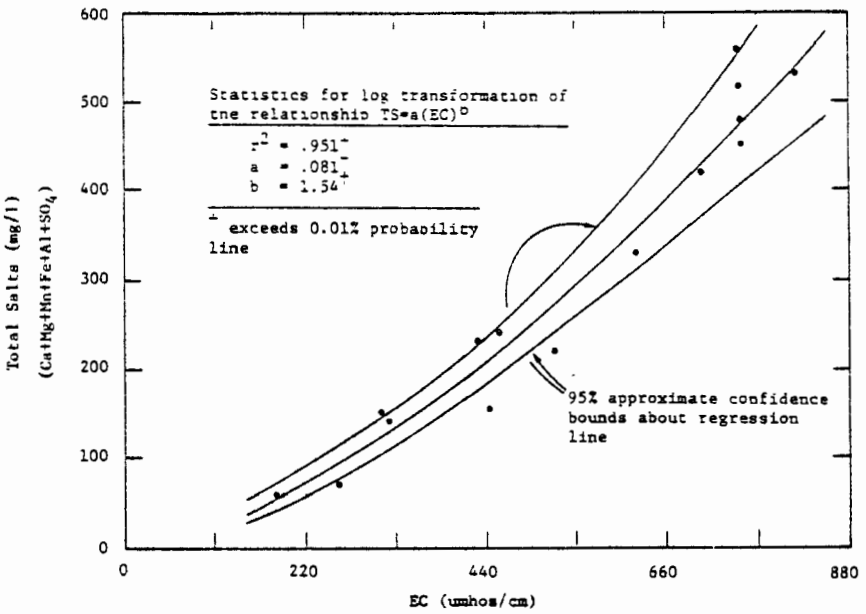

Figure 3.23. Relationship of total salts (TS) with electrical conductivity (EC) for selected column leachates (expanded).

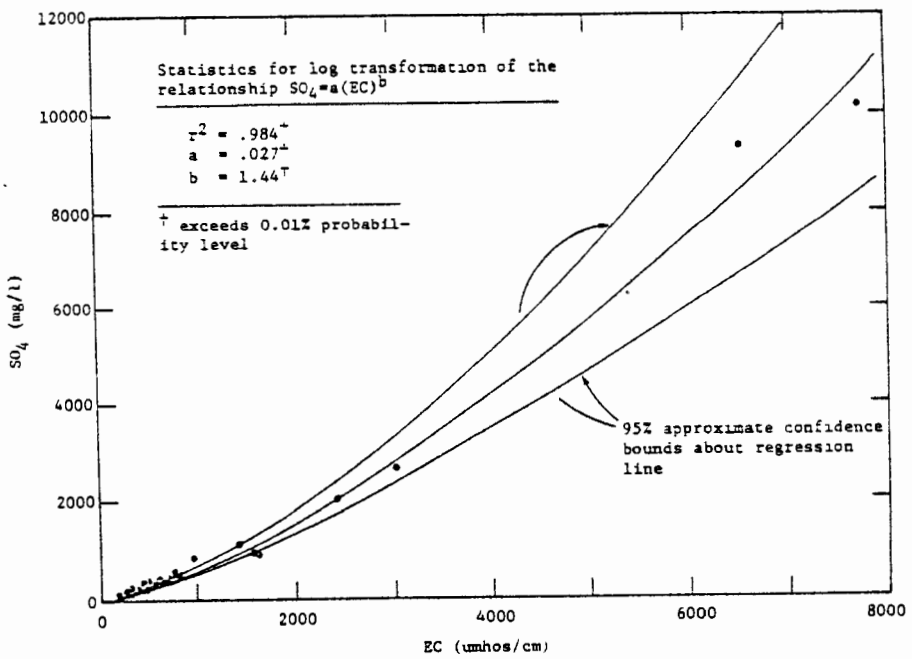

Figure 3.24. Relationship of SO_4 with electrical conductivity (EC) for selected column leachates.

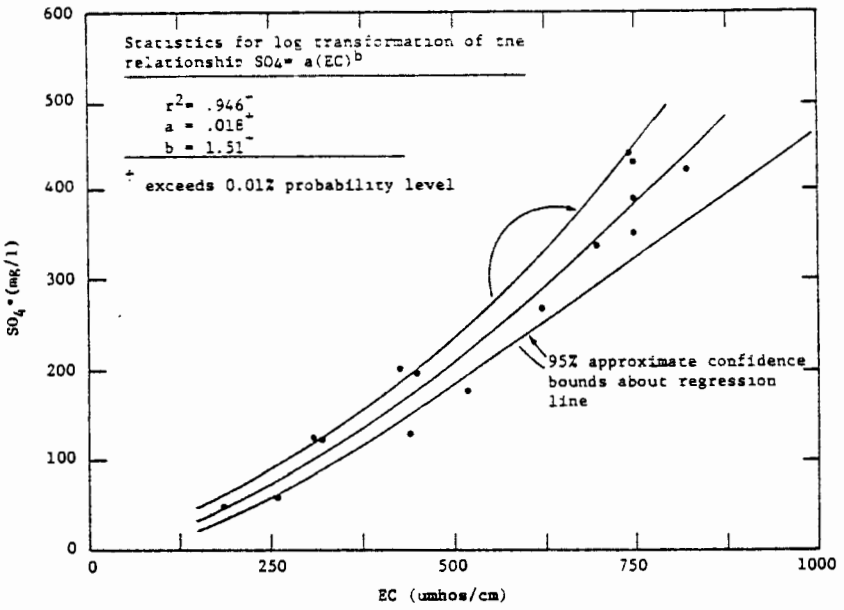

Figure 3.25. Relationship of SO_4 with electrical conductivity (EC) for selected column leachates (expanded).

The water-filled porosity for spoil layer 21 was determined on spoil samples that were stored prior to use under a water saturated condition in excess of one year. These were drained, rinsed with distilled water, rolled in absorbent towels until the reflected sheen of free surface water from the particle surface disappeared, then subjected to a weighing-drying-weighing sequence. Drying was at 105C until a stable weight loss was achieved, followed by drying at 125C as a check. The water-filled porosity was calculated by dividing water-lost volume (105C) by dry spoil volume where dry spoil equals spoil mass divided by 2.63, the measured particle density. The water-filled porosities of replicates were 11.5% and 11.9%, providing an average 11.7% (v/v).

Calculation Method

The basic equation used to delineate the acid salt source and acid producing zones in a water saturated spoil particle is a previously published diffusion

equation (Crank, 1964). The assumed geometry is a cylinder in which diffusion proceeds in the x and y along the cleavage between planes but not z direction perpendicular to the planes (Figure 3.26). The spoil particle is considered isotropic in the x, y directions and the system at steady state ($dQ_t/dt = 0$).

$$Q_t = \frac{2\Pi Dt(C_a - C_b)h}{\ln (r_b/r_a)} \tag{3.1}$$

Q_t = total mass (mg) of salt lost per particle and is measured during extended leaching (where $dQ_t/dt = 0$) following column incubation (Figure 3.27). The measured salts leached from the column times .257 gms/total column mass provide the salt leached from the individual particle. The individual particle mass of 0.257 gm is based on a cylinder of 0.5 cm dia and height (sieved fraction of 2-8 mm) and a measured spoil particle density of 2.63 gms/cc. The total-salts loss rate on a per particle basis for two columns containing spoil 21 averaged 1.41×10^{-5} mg/sec (one result was 1.62×10^{-5} mg/sec for a 2500 ml solution ranging in 94-76 EC delivered in 3000 secs from 222 gms spoil and the other was 1.20×10^{-5} for a 200 ml solution ranging from 91-72 EC delivered in 840 secs from 75 gms spoil.

t = time interval (equals one where Q_t is expressed on a per sec basis).

h = cylinder height (0.5 cm).

D = is 6×10^{-7} cm^2/sec and is a composite diffusion coefficient (D) for total salts based on the published D values for the dominant SO_4 salts; $FeSO_4$, $MgSO_4$, $CaSO_4$ and $MnSO_4$. This composite D was taken as 5×10^{-6} times 0.12 (water-filled porosity). Published

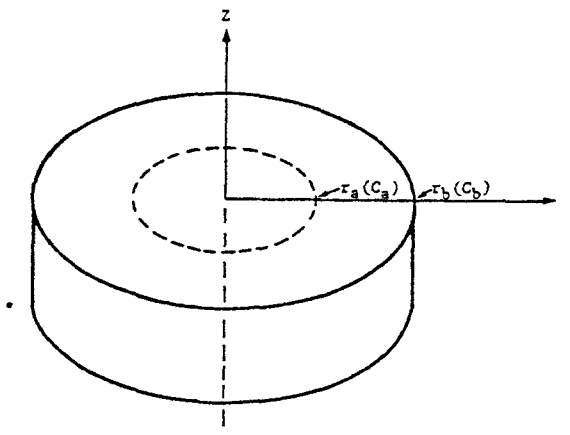

Figure 3.26. Assumed geometry and labelling of individual spoil particle.

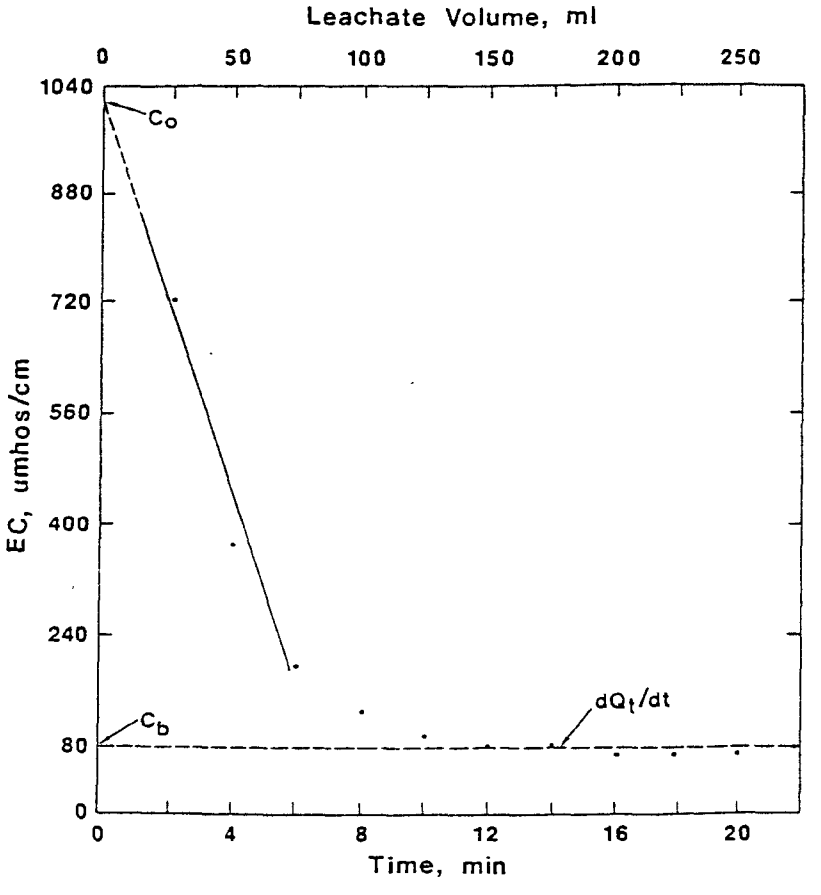

Figure 3.27. Example of column leaching sequence following N_2 incubation.

D's in free water are as follows: 3.9×10^{-6} for $FeSO_4$ at 15C (Bruins, 1929); 3.5×10^{-6} for $MnSO_4$ at 15C (Bruins, 1929); 5.1×10^{-6} for $MgSO_4$ at 20C (Bruins, 1929); 7.1×10^{-6} for $MgSO_4$ at 25C (Chemical Rubber Company, 1969). Using ion mobilities (X) at 25C, infinite dilution, and the equation $X_1/X_2 = (M_2/M_1)^{1/2}$ where M = molecular weight, D for $CaSO_4$ was calculated to be .94 times that for $MgSO_4$ (Daniels and Alberty, 1962).

r_b = total radius of cylinder (0.25 cm).

r_a = radius of noncontributing or unweathered portion (unknown).

C_b = concentration at cylinder surface (r_b) when $dQ_t/dt = 0$. This C value appears diffusion, not dilution controlled upon extended leaching (Figure 3.27) and equals 85 EC or 16 mg/l total salts.

C_a = concentration at break in the curve obtained by plotting C_o versus time of N_2 incubation (Figure 3.28 and 3.29). Break defined by extrapolating both legs of Figure 3.29 to their intersection (1000 EC or 710 mg/l total salts). The C_o (starting C for each leaching sequence representing different N_2 incubation times) was determined by 3 point linear extrapolation (Figure 3.27). The concentrations of the first 3 sequential 25 ml leachates were extrapolated back to the y axis where leaching time equals 0 or the leachate volume approaches 0, i.e., no dilution. The coefficient of determination (r^2) for this 3 point fitting ranged from 0.95-1.00 for 49 of 51 leaching sequences which included both atmospheric and N_2 incubations. For two sequences, r^2 = 0.90 and 0.62. The r^2 for 65% of the sequences equaled or exceeded .990. The raw data was plotted and found to provide very good fits in nearly all cases.

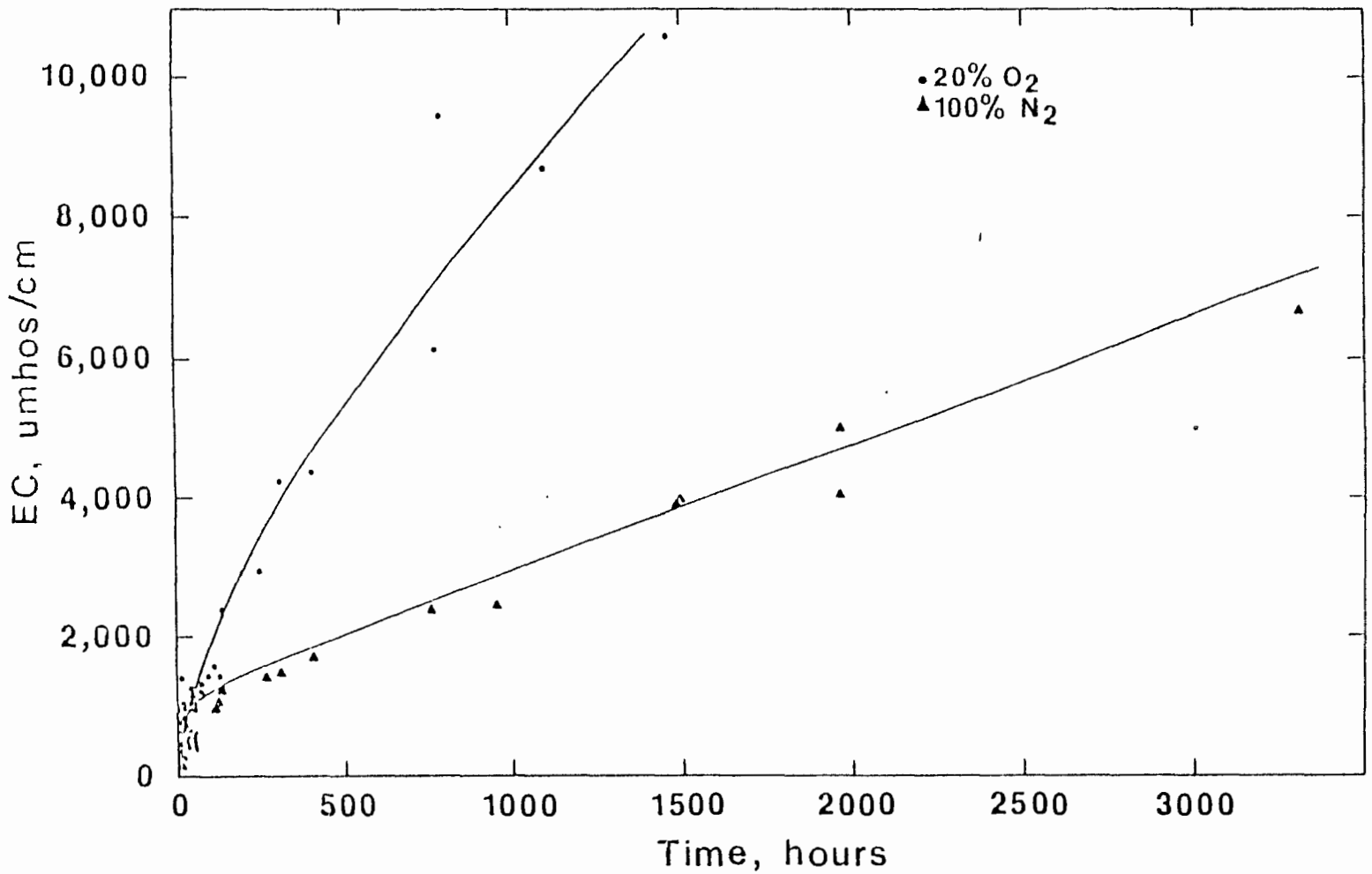

Figure 3.28. Relationship between O_2 availability, incubation time and the acid product concentration in leachate (extrapolated to zero dilution).

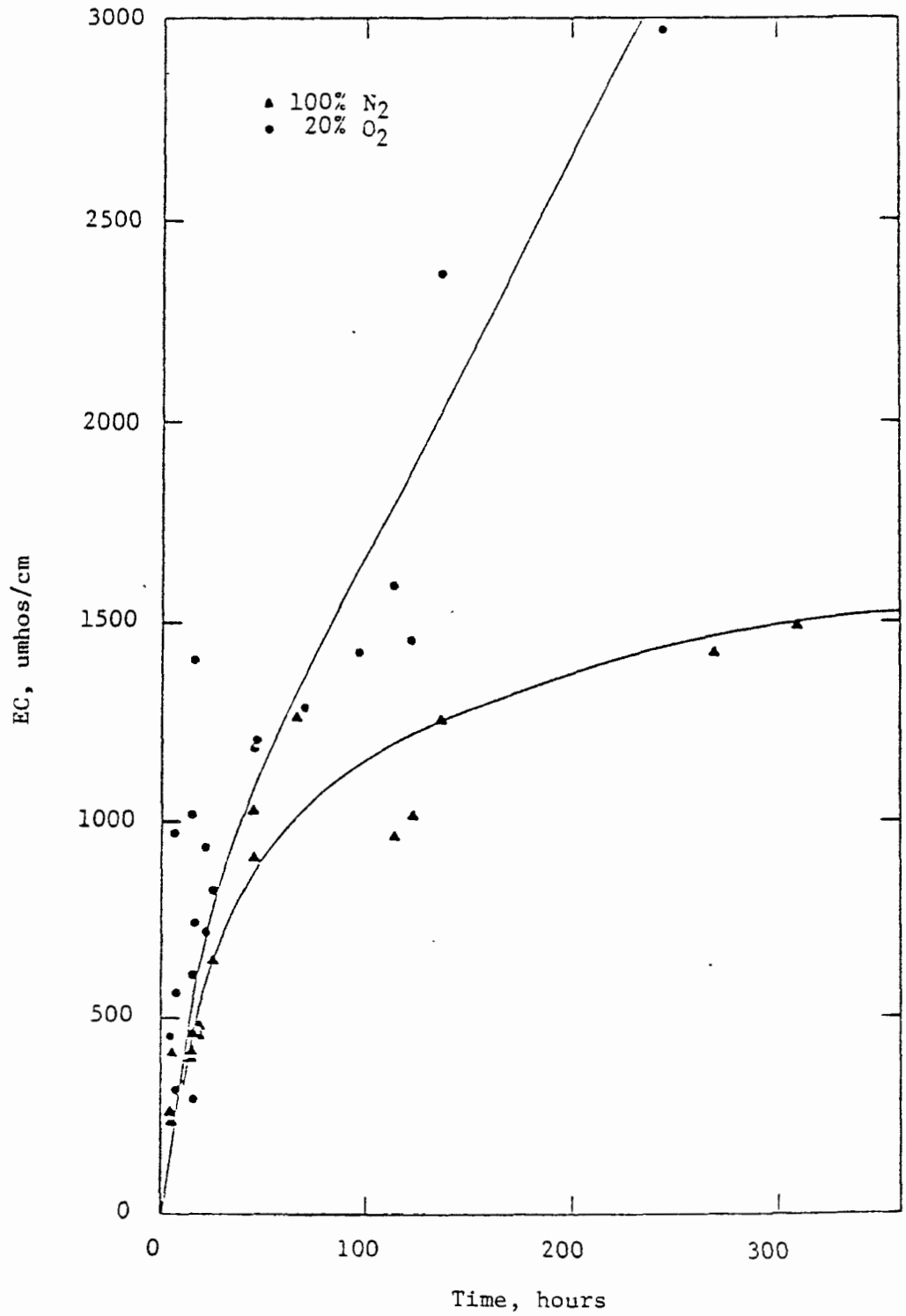

Figure 3.29. Expanded scale relationship between O_2 availability, incubation time and the acid product concentration in leachate (extrapolated to zero dilution).

The greatest depths or lower boundaries of acid producing zones of salt zones within the spoil particle were calculated by rearranging equation (3.2) into:

$$r_b/r_a = e^{3.14\ Dt(C_a - C_b)/Q_t} \tag{3.2}$$

Upon substituting,

$$r_b/r_a = e^{1.55 \times 10^5\ D\ sec/cm^2} \tag{3.3}$$

The basic equation and terms used to calculate the depth of O_2 penetration in a water saturated spoil particle in equation (3.2) with the following differences.

Q_t = 2.5×10^{-7} mg O_2 consumed per particle per second at steady state. Basic data obtained from Figure 3.30 was 0.45 mg SO_4/hr (0.50-0.05). See final paragraph, this section, for details on how Figure 3.30 was constructed. The O_2 consumed per SO_4 generated was 0.583 gms O_2/gm SO_4, a conversion factor derived directly from the assumed stoichiometry $FeS_2(s) + 3.5\ O_2 + H_2O \rightarrow 2SO_4^{-2} + Fe^{+2} + 2H^+$.

D = 2.2×10^{-6} cm^2/sec. This is the diffusion coefficient of O_2 in free water at 25C (1.8×10^{-5} cm^2/sec; OSU, 1971) corrected for the water-filled porosity (.12).

C_b = 0 mg/l.

C_a = 10 mg/l at 25C (OSU, 1971).

The total sulfate produced for each incubation used to construct Figure 3.30 was calculated by integrating a fitted equation describing the relationship of SO_4 with time or volume (curve in Figure 3.27 is a good example) between the lower limit of t = 2.0 minutes (first leaching volume of 25 mls) and the upper time limit where EC = 150 μmhos/cm (arbitrarily chosen). SO_4 was calculated from EC for each two minute intervals on the basis of the equation in Figure 3.24. The

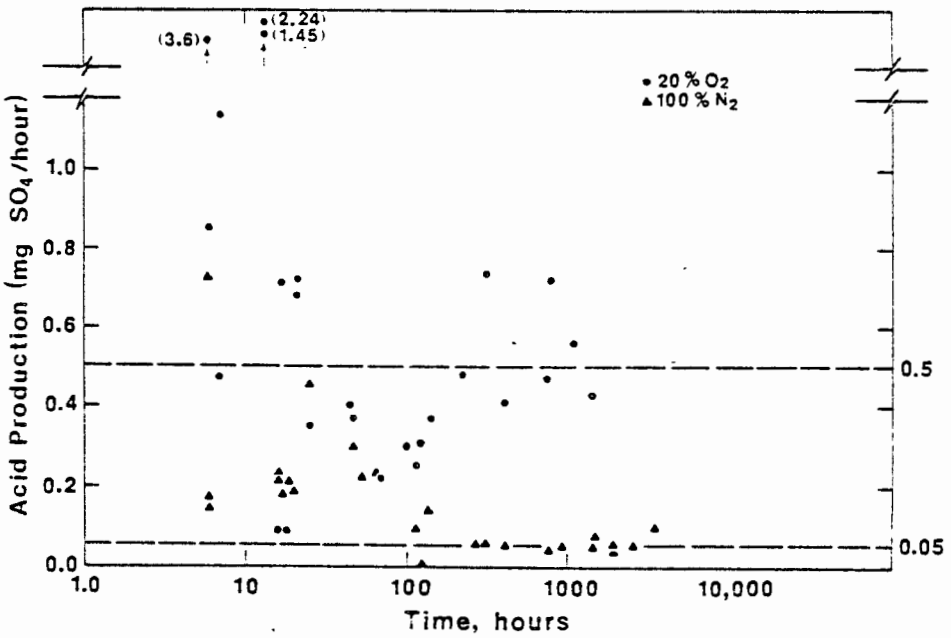

Figure 3.30. Relationship of acid production rate for different incubation periods under air and N_2 atmospheres.

The integration was performed by summing trapezoids. The coefficient of determination (r^2) for the goodness of fit of the equations ranged from 0.86-0.99 with only 2 of 51 falling below 0.90 and with over one-half equal to or exceeding 0.980. All relationships were significant at the 1% probability level with most significant at the 0.01% probability level.

Experimental Results

The experimental results show air incubation to produce substantially more acid products or salts than does oxygen-free (N_2) incubation once past the first 50 hours (Figures 3.28 and 3.29). This applies to the "starting" or undiluted concentration of the first extract (C_o) as determined by 3 point extrapolation. Before the first 50 hours or below 1000 μmhos/cm EC the two curves appear practically indistinguishable. After substantial incubation time, the curve representing the N_2 incubated system would be expected to flatten out according to mass action principle in which the

buildup reaction products at the spoil surface would depress and finally stop net movement of similar salts to that surface. This expected behavior did not happen here. Instead the EC increased slowly and linearily from the 100-3305 hour incubation period. We have no explanation and can only speculate that a slow rate of pyrite oxidation continued due to a nongaseous oxygen source or other oxidant. Apparently, this EC increase is kinetically rather than equilibrium controlled because the straight line fit implies that the relationship is independent of EC (Figure 3.28). However, this curve changes from curvilinear to linear in the range of 900-1200 EC which likely represents the equilibrium stabilized EC if the other acid-producing kinetically controlled system was not operating.

The total acid produced over each incubation period is expressed as a rate of SO_4 mass generated per hour (Figure 3.30). SO_4 was chosen because it is the product of pyrite oxidation, and can be used to measure pyrite oxidation if other sources of SO_4 are not substantial. This also assumes that SO_4 is not lost by precipitation within the spoil particle which is reasonable, considering the usually low $CaSO_4$ concentrations in spoil extracts upon extended leaching. It is apparent that there is a great deal of variability in the rate of SO_4 generated up to about 200 hours incubation time (Figure 3.30). For the long-term air incubation, SO_4 production from oxidation is 0.45 mm/hr for a 75 gm spoil. The acid production under the air system is 10 times that of the O_2-free system. The steady production of SO_4 in the O_2-free system corresponds to the slow but steady increase in EC observed in Figures 3.28 and 3.29.

We propose the hypothesis that acid production rate is likely controlling when the pyrite is exposed (the diffusion pathway length is short). As weathering progresses assuming no major physical breakdown of the particle, the diffusion pathway length increases until diffusion of either acid products out

or O_2 in is limiting. Using essentially the data of Tables 3.17, 3.18 and other parts of this study, we calculated the depth limits of the acid products source or to which O_2 penetrated. This assumes a primarily water-saturated particle so that solute diffusion can occur, and O_2 diffusion is controlled through the water rather than gaseous phase.

Diffusion of Acid Products to the Particle Surface or O_2 into the Particle as the Controlling Process

From equation (3.3) we calculated r_b/r_a as described earlier using data from the oxygen-free (N_2) incubation part of the study. The ratio of r_b/r_a is the ratio of the total particle radius to the unweathered radius (Figure 3.26). Thus, at 1.0, there is no weathered portion because the radius of the cylindrical particle and the unweathered portion are the same. Large values of r_b/r_a signify that much of the particle is weathered (or depleted) of either the more readily reactive pyrite or acid products. The unweathered and weathered volume was calculated for different diffusion coefficients (D) corrected for porosity (Table 3.17). Obviously, the depth of weathering or contributing volume is very small for those chemicals with small diffusion coefficients and is larger or total for those with large diffusion coefficients. The acid products contributing volume and weathering depth were calculated to be 0.022 cm and 17%, respectively. This was based on a corrected diffusion coefficient of 6×10^{-7}. Thus, 83% of the average spoil particle was unweathered or unleached and probably contained substantial reactive pyrite and acid product concentrations.

In a similar approach, the r_b/r_a, Δr and % contributing volume were calculated based on the penetration of O_2 into a water-saturated cylindrical spoil particle. The depth of O_2 penetration and contributing volume was calculated to be 0.06 cm and 42%, respectively (Table 3.17). This was based on a corrected diffusion coefficient of 2.2×10^{-6}. Based on these calculations, 58% of the average spoil

TABLE 3.17. THE WEATHERED VOLUME (CONTRIBUTING) AND DEPTH (Δr) AS RELATED TO DIFFERENT DIFFUSION COEFFICIENTS*

r_b/r_a	D†	r_a	Δr‡	Contributing volume§
-	cm^2/sec	cm	cm	%
2320	5×10^{-5}	.0001	~.25	~100
4.7	1×10^{-5}	.053	.197	95
2.17	5×10^{-6}	.115	.135	79
1.32	2.2×10^{-6}	.190	.060#	42#
1.17	1×10^{-6}	.214	.036	27
1.097	6×10^{-7}	.228	.022	17
1.053	5×10^{-7}	.231	.019	14
1.015	1×10^{-7}	.241	.004	3.1
1.008	5×10^{-8}	.248	.002	1.5
1.002	1×10^{-8}	.2496	.0004	0.3

*Used equation [3].

†Diffusion coefficient corrected for porosity (literature values for free water systems at 25C times 0.12).

‡(0.25 cm - r_a).

§$(r_b^2 - r_a^2)/r_b^2 \times 100$.

#Calculated depth and volume of O_2 penetration using equation (5.2).

TABLE 3.18. EFFECT OF SPOIL PARTICLE ON CONTRIBUTING VOLUME*

Individual particle volume	Height† of cylinder	r_b‡	Particle count	Contributing volume	
cm^3	cm	cm	no/m^3	cm^3/m^3§	%#
785,000	100	50	1	691	0.1
196,000	100	25	4	1380	0.2
7850	100	5	100	6908	0.9
314	100	1.0	2500	34540	4.4
3.14	100	0.1	250000	306150	39.2
.785	100	0.05	1,000,000	508680	68.6
.152	100	0.022	5,164,000	785000	100.0

*Calculated for a one $meter^3$ volume of highly ordered cylindrical particles.

†Treated as single cylinder in the z direction because no diffusion allowed through top or bottom of each cylindrical particle.

‡Particle radius.

§$\pi h\ [(r_b)^2 - (r_b - .022)^2] \times$ particle count.

#$100\ [r_b^2 - (r_b - .022)^2]/r_b^2$ where .022 calculated from equation (5.3) where $D = 6.0 \times 10^{-7}\ cm^2/sec$.

particle remained experimentally in an oxygen free system and, thus probably retained substantial reactive pyrite.

Where diffusion potentially limits the acid products contribution of subsurface spoil to groundwater, an obvious question is raised. Because the depth by diffusion is limiting and diffusion only occurs through surface area of the particle which to some degree can be manipulated, could the contributing volume of spoil be substantially decreased by increasing the size of the average spoil particle? Using $D = 6 \times 10^{-7}$ cm^2/sec, the contributing volume related to average particle size was determined (Table 3.18). Table 3.18 represents the acid product source zones rather than the depth of O_2 penetration. The contributing volume was greatly affected by particle size. Excluding extremes such as particle sizes less than .05 cm and greater than 5 cm radius, the absolute and relative (%) contributing volume change greatly. This suggests that relatively small changes in particle size can greatly alter the rate of acid production or acid products loss per unit volume spoil bank.

Rate of Pyrite Oxidation as the Controlling Process--

From the air incubated part of the study, the long term pyrite oxidation expressed as SO_4 production was found to be .45 mg/hr for a 75 gram spoil sample. Based on a 3.8% pyrite content, this converts too .16 mg SO_4 generated/gm pyrite/hr. This compares to: 0.13 mg SO_4/gram pyrite/hr reported by Braley (1954) for aerated moistened -8 + 40 mesh sulfur ball; 0.11 mg SO_4/gram pyrite/hr reported by Clark (1966) for submerged -40 + 50 mesh pulverized pyrite at 20C (calculated from Clark's equation $dSO_4/dt = 0.023\ [D.O.]^{2/3}$ where dissolved oxygen equals 10 mg/l); 0.06 mg SO_4/gram pyrite/hr reported by OSU (1970) for submerged sulfur ball at 25C (averaged 35 μg O_2 consumed/gram pyrite/hr for 8-10 mg/l dissolved oxygen converted to SO_4 basis). Although we cannot directly compare these to our results because of the different experiment conditions, pyrite sourves and physical experimental setup, our results

although high are generally in agreement. Moreover, Braley (1954) reported SO_4 production in submerged pyrite to be well below that obtained from aerated moistened pyrite which could substantially increase the rate of SO_4 production reported by Clark (1966) and OSU (1970) if subjected to our rather than their experimental conditions. On the basis of these results, acid production from this fresh spoil subjected to air incubation appears to be controlled by the reaction rate rather than O_2 diffusion into the spoil particle.

Interpretation of Results

The spoil material used in this experiment contains substantial concentrations of both pyrite (3.8%) and acid products (3.1%). If deep placed, especially where submerged or frequently flushed, the initial acid product losses to groundwater can be very large, even in the absence of O_2. In fact, the loss could be hydrologically controlled by percolation or groundwater flow rates rather than chemically controlled. Subsequently, as leaching progresses, diffusion quickly becomes potentially limiting because of the very low diffusion coefficient of these acid products.

Pyrite oxidation in the spoil particle appears potentially controlled by either the pyrite oxidation or O_2 diffusion rate. For new, unweathered spoil, the experimentally determined pyrite oxidation rate compared reasonably well with published values and the O_2 diffusion rates never appeared to be controlling. Thus, where O_2 is in excess supply and the particle remains water saturated, the initial, and the subsequent rate of acid production from pyrite will likely be controlled by the pyrite oxidation rate. As weathering removes the shallow pyrites, the O_2 diffusion or acid product diffusion rate should become controlling.

In cases where diffusion is limiting, the basic particle size is important in controlling the rate of acid product and acid loss to groundwaters since this reduces the contributing volumes relative to the total spoil mass.

Chemical Parameter Interrelationships

The basic thrust of this unit is to investigate interrelationships between chemical parameters that are useful for simplifying data collection. Often for a selected site or within limits, chemical parameters are intercorrelated so that one can be used as a surrogate measure for several.

Analyzing caisson percolate, total acidity at pH 8.2 was found to be linearly correlated with total acidity at pH 7.3, SO_4, total soluble Fe, Mg, Mn and Al but not with Ca, ferrous Fe or pH (Table 3.19). The relationship between total acidity determined at pH 7.3 and 8.2 is very precise with a slope near 1.0 and intercept near zero (Figure 3.31), indicating that both procedures measure the same thing in this particular system. The relationship with SO_4 is not exactly linear, but for our purposes can be considered as such (Figure 3.32). However, there are several limitations. At concentrations less than 10 meq/l, the basic relationships either change in slope and/or become more variable for SO_4, Mg, Mn, Al and total soluble Fe (Figures 3.32, 3.33 and 3.34). For Ca, the decline in concentration (Figure 3.33) with increasing total acidity, which probably results from $CaSO_4$ precipitation, precludes the use of a linear relationship. Comparison of sample pH with the log of total acidity assumes that a single disassociation constant controls the hydrogen ion concentration in solution which is not likely true over a substantial pH range. Within the aforementioned limits, the total acidity can be selected as a measure of other chemical parameters. Thus, total acidity data subsequently presented can also be interpreted in terms of SO_4, Mg, Al and total soluble Fe concentrations.

Data in Figure 3.35 shows a rough correlation between trace element concentration and pH, supported by the studies of Massey (1972) who found the log of Zn, Cr and Ni concentration to be negatively correlated with pH in aqueous spoil extracts. To establish a simple method for estimating the potential of trace metal contamination in this spoil system, selected trace metal concentrations from spoil layer

TABLE 3.19. RELATIONSHIP* OF THE TOTAL ACIDITY DETERMINED AT pH 8.2 (y) TO DIFFERENT CHEMICAL PARAMETERS (x)

Parameter	Coefficient of determination r^2	Obser. n	Standard error estimate SY	m	b
Total acidity (pH 7.3)	.995**	139	3.16	.948	.36
SO_4	.966**	65	15.5	1.36	12.9
Ca	.478**	63	6.35	.100	5.88
Mg	.914**	61	4.71	.249	4.37
Al	.960**	81	2.07	.191	1.38
Total soluble Fe	.978**	85	4.87	.620	-1.94
Fe^{+2}	.636**	59	12.0	.365	-2.20
Mn	.826**	74	2.44	.096	0.98
pH†	.634**	136	.50	-.97	4.09

*All data except pH in millequivalents/liter, y = mx + b.

†Correlation is between sample pH and log total acidity; well analysis not included.

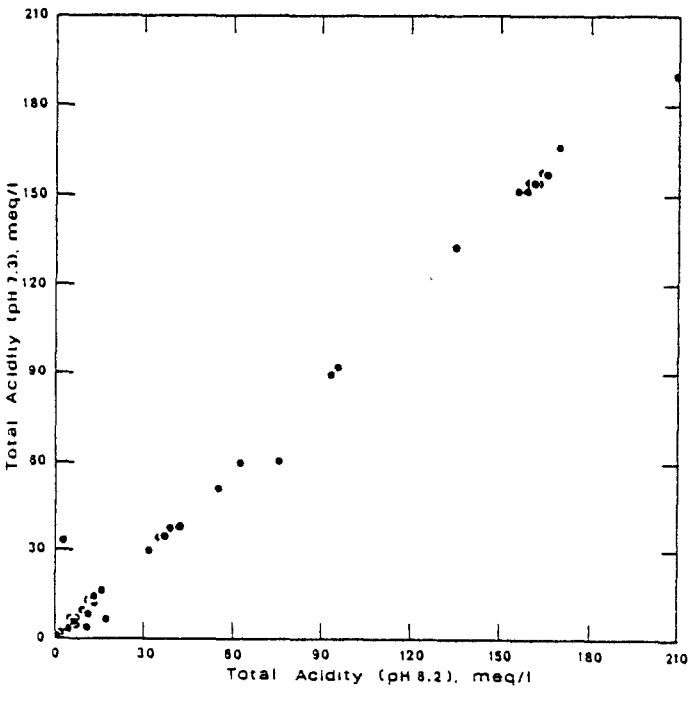

Figure 3.31. Relationship between two measures of total acidity.

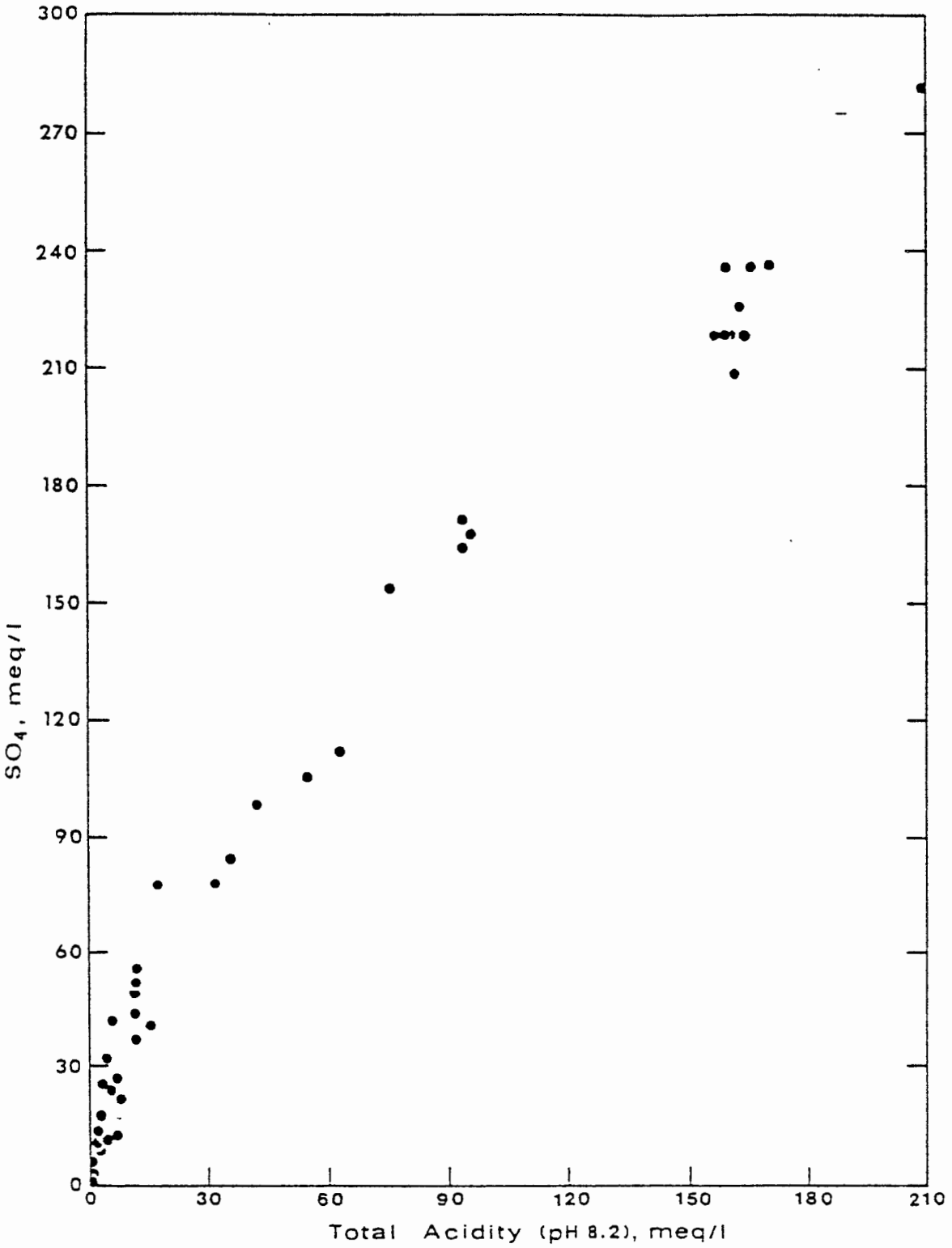

Figure 3.32. Relationship between total acidity and sulfate concentration.

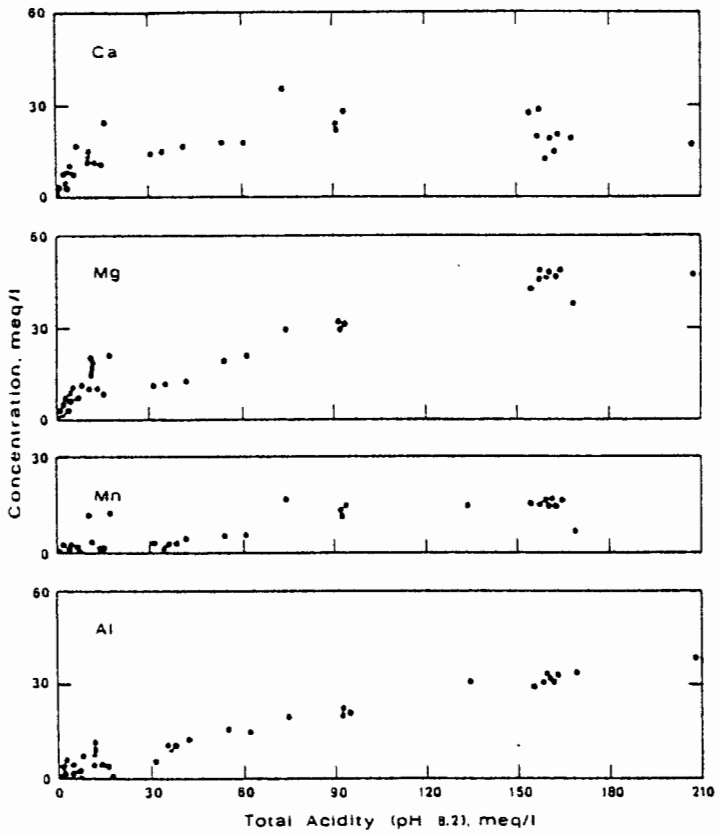

Figure 3.33. Relationship of calcium, magnesium, manganese and aluminum with total acidity.

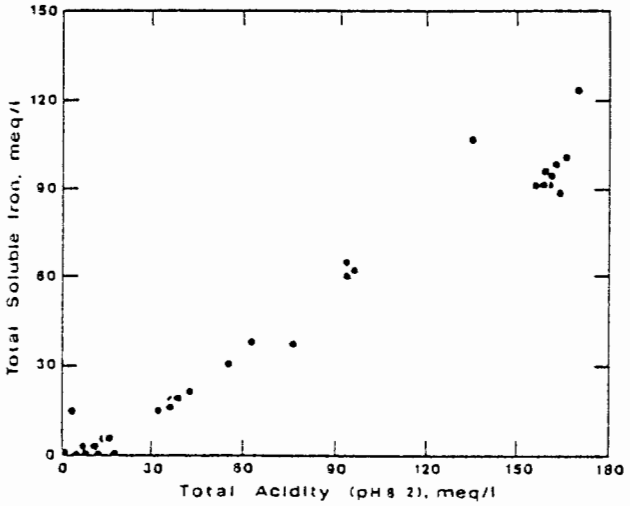

Figure 3.34. Relationship between total soluble iron and total acidity.

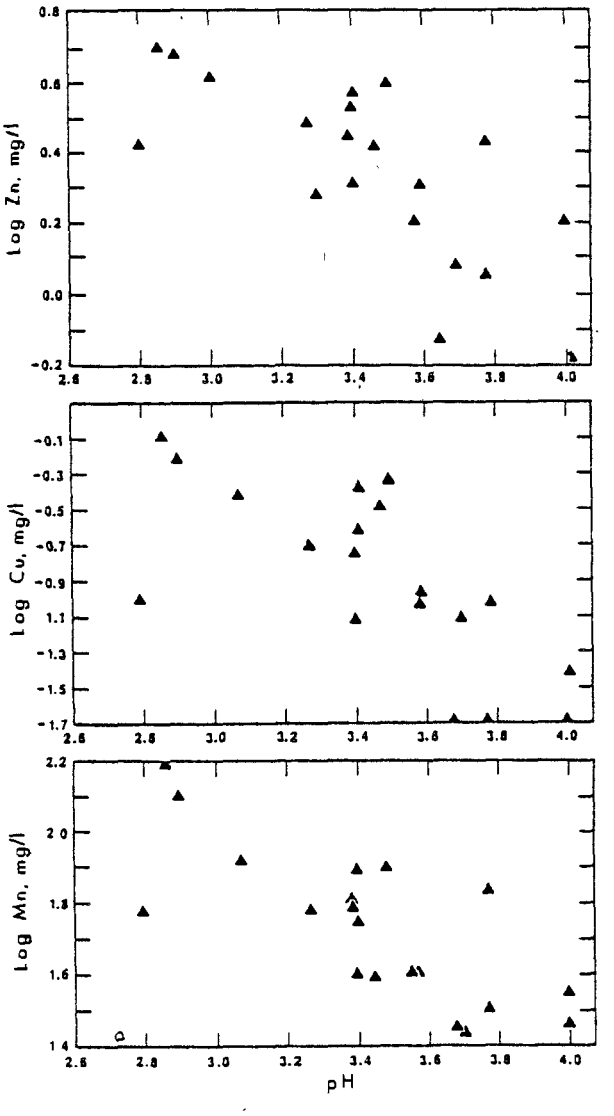

Figure 3.35. Relationship of log Zn, Cu and Mn concentrations with pH.

extracts (Table 3.13) were compared with the corresponding pH and SO_4 concentration. SO_4 concentration was chosen for several reasons. First, it correlated well with total acidity over the complete concentration range and the SO_4 loss due to $CaSO_4$ precipitation was not substantial. Second, specific conductance which could be used is not a valid measure of total salts concentration over a range where the chemical composition and ionic species change substantially. Third, pyritic

minerals which may also serve as a source of trace metals are the predominant source of SO_4 in this system. Data from spoil layer 21 was omitted because it was a single point of extreme value.

In all comparisons, the point scatter was considerable; not at all similar to the high precision achieved by Massey and Barnhisel (1972). The plots of Zn, Cu and Mn vs SO_4 concentration (Figure 3.36) showed generally less scatter than did the corresponding log Zn, Cu and Mn vs pH plots (Figure 3.35). The reader may note that the apparently similar scatter is numerically much larger on the log-log scale. The sulfate concentrations can provide reasonable estimates of the Zn, Cu and Mn concentrations provided they are not extrapolated much beyond the concentration range upon which they were tested.

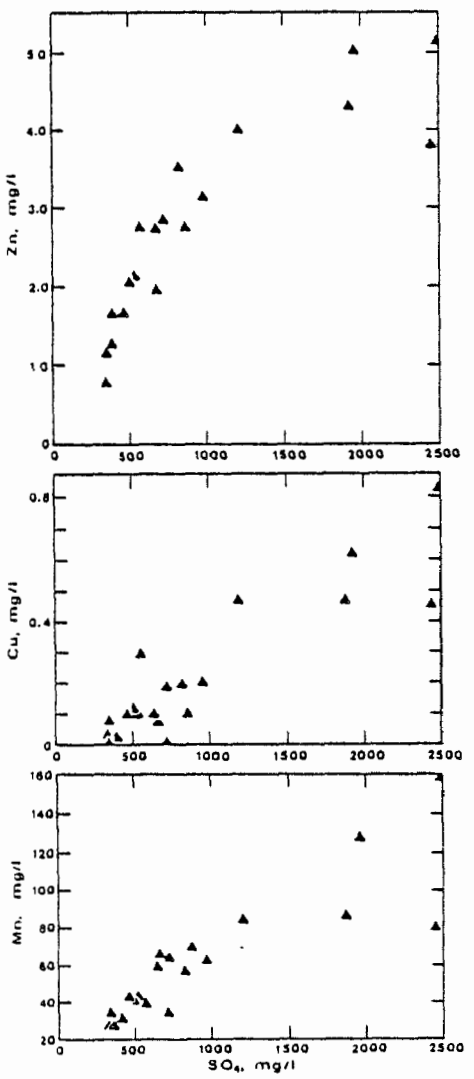

Figure 3.36. Relationship of Zn, Cu and Mn concentrations with sulfate concentrations

REFERENCES

1. Allison, L. E. Organic Carbon. In: Methods of Soil Analysis Part 2, C. A. Black, ed. American Society of Agronomy, Madison, Wisconsin. 1965.
2. American Public Health Association, Inc. Standard Methods for the Examination of Water and Wastewater. Twelfth Edition, 1965.
3. ASTM. Standard Methods of Coal Analysis. Am. Soc. for Testing Materials, Philadelphia, Pennsylvania, 1971.
4. Borden, F. Yates, and Larry H. McCormick. An Indirect Method for the Measurement of Sulfate by Barium Absorption Spectrophotometry. Soil Sci. Soc. Am. Proc., 34(4):705-706, 1970.
5. Braley, S. A. Summary Report of Commonwealth of Pennsylvania, Department of Health, Industrial Fellowships No. 1-7, August 20, 1946-September 30, 1953. Mellon Institute of Industrial Research, Pittsburgh, Pennsylvania, 1954. 279 pp.
6. Bruins, H. R. Coefficients of Diffusion in Liquids. In: International Critical Tables of Numerical Data, Physics, Chemistry and Technology, E. W. Washburn, ed., 1929. 5:63-77.
7. Caruccio, F. T. Characterization of Strip-mine Drainage by Pyrite Grain Size and Chemical Quality of Existing Groundwater. In: Ecology and Reclamation of Devastated Land, Volume I, R. J. Hutnik and C. Davis, eds. Gordon and Breach Publishers, New York, 1973. pp. 193-226.
8. Chemical Rubber Company. Handbook of Chemistry and Physics. 50th Edition, R. C. Weast, ed. The Chemical Rubber Company, Cleveland, Ohio, 1969.
9. Ciolkosz, E. J., R. L. Cunningham, G. W. Petersen, and R. C. Cronce. Characteristics Interpretations and Uses of Pennsylvania Minesoils. Progress Report 381. The Pennsylvania State University, Agricultural Experiment Station, University Park, Pennsylvania, 1983. 88 pp.

10. Clark, C. S. Oxidation of Coal Mine Pyrite. J. Sanit. Eng. Div., Am. Soc. Civ. Eng., 92:127-145, 1966.

11. Crank, J. The Mathematics of Diffusion. Oxford University Press, Amen House, London E.C. 4, 1964. 347 pp.

12. Daniels, F., and R. A. Alberty. Physical Chemistry. John Wiley and Sons, Inc., New York, 1962. 744 pp.

13. Dixon, R. M., and A. E. Peterson. Water Infiltration Control: A Channel System Concept. Soil Sci. Soc. Am. Proc., 35(6):968-973, 1971.

14. ElBoushi, I. M. Geologic Interpretations of Recharge through Coarse Gravel and Broken Rock. Unpublished Ph.D. Dissertation, Stanford University, Stanford, California, 1966.

15. Emmel, Robert H., John J. Sotera, and Ronald L. Stux. Atomic Absorption Methods Manual, Volume 1. Standard Conditions for Flame Operation. Instrumentation Laboratory, Inc. (publisher), Wilmington, Massachusetts, 1977. 80 pp.

16. Emmel, Robert H., Martha Fogg Bancroft, Stanley B. Smith, Jr., John J. Sotera, and Timothy L. Corum. Atomic Absorption Methods Manual, Volume 2. Flameless Operations. Instrumentation Laboratory, Inc. (publisher), Wilmington, Massachusetts, 1976.

17. Gill, M. A. Analysis of One-dimensional Non-Darcy Vertical Infiltration. J. Hydrol., 31:1-11, 1976.

18. Green, R. E., and J. C. Corey. Calculation of Hydraulic Conductivity: A Further Evaluation of Some Predictive Methods. Soil Sci. Soc. Am. Proc., 35(1):3-8, 1971.

19. Hill, D. E., and J.-Y. Parlange. Wetting Front Instability in Layered Soils. Soil Sci. Soc. Am. Proc., 36(5):697-702, 1972.

20. Jordan, C. F. A Simple Tension Free Lysimeter. Soil Sci., 105(2):81-86, 1966.

21. Keys, W. S., and L. M. MacCary. Application of Borehole Geophysics to Water-Resources Investigations. Techniques of Water-Resource Investigations of the U.S. Geological Survey Book 2, Chapter E1. U.S. Government Printing Office, Washington, DC 20402, 1971.

22. Leps, T. M. Flow through Rock Fill. In: Embankment-Dam Engineering, Casagnande Volume, R. C. Hirschfeld and S. L. Paulas, eds. John Wiley and Sons, Inc., New York, 1973.

23. Marshall, T. J. A Relation between Permeability and Size Distribution of Pores. J. Soil Sci., (9):1-8, 1958.

24. Massey, H. F. pH and Soluble Copper, Nickel and Zinc in Eastern Kentucky Coal Mine Spoil Materials. Soil Sci., 114(3):217-221, 1972.

25. Massey, H. F., and R. I. Barnhisel. Copper, Nickel and Zinc Released from Acid Coal Mine Spoil Materials of Eastern Kentucky. Soil Sci., 113(3): 207-212, 1972.

26. Mein, R. Modeling of the Infiltration Component of the Watershed. Unpublished Ph.D. Thesis, University of Minnesota, Minneapolis, Minnesota, 1971.

27. Millington, R. J., and J. P. Quirk. Transport in Porous Media. Int. Congr. Soil Sci., Trans. 7th, Madison, Wisconsin, 1960. 1.3:97-106.

28. Ohio State University Research Foundation. Acid Mine Drainage Formation and Abatement. Water Pollut. Control Res. Ser. DAST-42-14010 FPR-04/71, U.S. Environmental Protection Agency, Washington, DC, 1971. 83 pp.

29. Ohio State University Research Foundation. Sulfide to Sulfate Reaction Mechanism. Water Pollut. Control Res. Ser. 14010 FPS-02/70, Federal Water Quality Administration, U.S. Department of Interior, Washington, DC, 1970.

30. Pedersen, T. A., A. S. Rogowski, and R. Pennock, Jr. Physical and Hydraulic Characteristics of Some Minesoils. Soil Sci. Soc. Am. J., 44:321-328, 1980.

31. Philip, J. R. Stability Analysis of Infiltration. Soil Sci. Soc. Am. Proc., 39(6):1042-1049, 1975.

32. Quisenberry, V. L., and R. E. Phillips. Percolation of Surface Applied Water in the Field. Soil Sci. Soc. Am. J., 40(4):484-489, 1976.

33. Raats, P. A. C. Unstable Wetting Fronts in Uniform and Nonuniform Soils. Soil Sci. Soc. Am. Proc., 37(5):681-685, 1973.

34. Raney, W. A. Field Measurement of Oxygen Diffusion through Soil. Soil Sci. Soc. Am. Proc., (14):61-65, 1949.

35. Ritchie, J. T., D. E. Kissel, and Earl Burnett. Water Movement in Undisturbed Swelling Dry Soil. Soil Sci. Soc. Am. Proc., 36(6):874-897, 1972.

36. Rogowski, A. S. Hydrologic Parameter Distribution on a Mine Spoil. Symposium on Watershed Management 1980, Boise Idaho, July 21-23, American Society of Civil Engineers, New York, 1980. pp. 764-780.

37. Rogowski, A. S. Water Regime in Strip Mine Spoil. In: Surface Mining and Fish/Wildlife Needs in the Eastern United States, D. E. Samuel, J. R. Stauffer, and W. T. Mason, Jr., eds. Proceedings of a Symposium, FWS/OBS-78/81, sponsored by West Virginia University and the Fish and Wildlife Service, USDI, 1978. pp. 137-145.

38. Rogowski, A. S. Estimation of the Soil Moisture Characteristic and Hydraulic Conductivity: Comparison of Models. Soil Sci., 114(6): 423-429, 1972.

39. Soil Survey Staff. Soil Taxonomy. Agriculture Handbook 436, U.S. Department of Agriculture, Soil Conservation Service. U.S. Government Printing Office, Washington, DC, 1974. p. 469.

40. Smith, R. E., and D. A. Woolhiser. Mathematical Simulation of Infiltrating Watersheds. Hydrology Paper 47, Colorado State University, Fort Collins, Colorado, 1971.

41. U.S. Environmental Protection Agency. National Secondary Drinking Water Regulations. Federal Register, 42(62):17143-17146, 1977.

42. U.S. Environmental Protection Agency. Water Programs, National Interim Primary Drinking Water Regulations, Part IV. Federal Register, 40(248):59570, 1975.

43. U.S. Environmental Protection Agency. Methods for Chemical Analysis of Water and Wastes. EPA-625/6-74-003a, 1974.

44. Vimmerstedt, J. P., and P. H. Struthers. Influence of Time and Precipitation on Chemical Composition of Spoil Drainage. In: Proceedings, Second Symposium on Coal Mine Drainage Research, Pittsburgh, Pennsylvania. Coal Industry Advisory Commission to Ohio River Valley Sanitation Commission, 1968. pp. 152-163.

SECTION 4

FIELD STUDIES

PHYSICAL AND HYDROLOGIC SETTING

In Section 2 we have concentrated on the physical and chemical description of experimental site. In this section we will emphasize the overall response of the site to climatic influences as observed during the study period. To evaluate site response properly we need first to consider the actual physical setting and properties of a site as a whole. Figure 4.1 shows the cross section and aerial view of the site, delineating areas that have been deep mined, stripmined and left undisturbed, as well as indicating the position of wells, seep and stream relative to each other. Chronologically, Kittanning B coal was mined first from drift mines

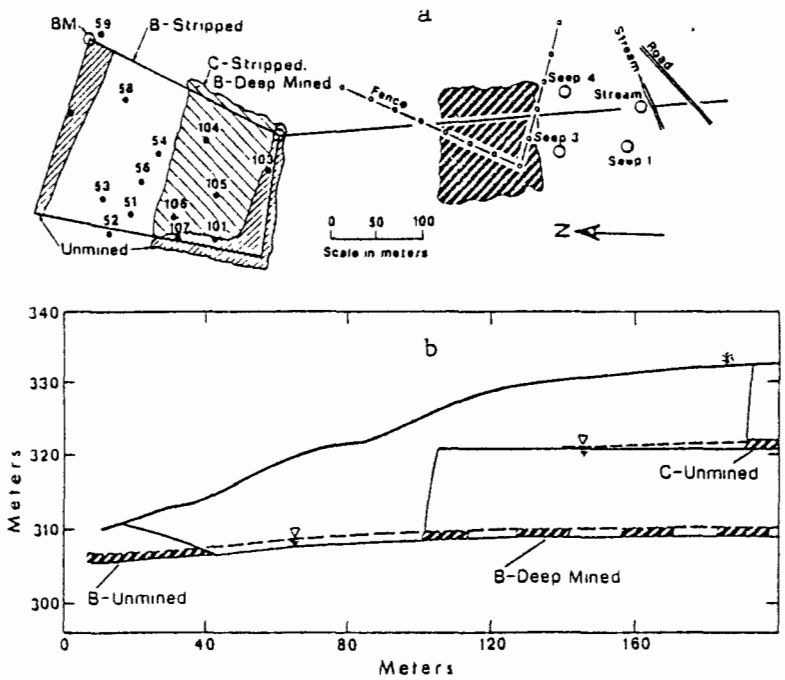

Figure 4.1. Schematic diagram of the experimental site.

extending back into the hill (Figure 4.1a). Subsequently, the northern portion of the area was stripmined. Little coal was recovered because of previous deep mining activity. This area was reclaimed in 1967 before new Pennsylvania legislation requiring topsoiling went into effect and now supports a stand of beech, pine and aspen. The area is bordered on its northernmost edge by a narrow strip of undisturbed land, and on the south by a buried high-wall. The southern portion of the site was stripmined for Kittanning C coal only. The deep mined layer was left undisturbed and the whole area was reclaimed under new regulations, topsoiled and seeded to grass. As part of farming operations the proprietor spread manure over the eastern half of the site which now supports a heavy grass and legume stand (Figure 4.2).

We have measured infiltration on the site using small and large ring infiltrometers (Rogowski, 1980). Figure 4.3 shows relative distribution of infiltration over the area with a peak in the east central portion. In general we observed that infiltration and hydraulic conductivity were quite variable both in time and in space. We have also found (Pedersen et al., 1980) that when sufficient moisture was present pan evaporation adequately represented reclaimed site evapotranspiration. At other times the evapotranspiration could be simulated using Ritchie's (1972) ET model. Figure 4.4a and b shows typical soil water variation over the area and depth, while Figure 4.4c indicates an overall shape of the water table sloping towards northeast. Figures 4.5a and b show a characteristic distribution pattern of solar radiation and precipitation over the site respectively, while Figure 4.6 illustrates site response to a spring storm.

During that storm we observed essentially no runoff until a high intensity burst of rain 18-23 hours after rain first begun. Vegetated area responded to this burst faster than the nonvegetated one, but runoff rate on the nonvegetated part was 100 times larger. Simultaneously with the occurrence of runoff, water table, 72 m below the ground surface, began to rise and continued rising for more than five days following the occurrence of this 29 mm storm.

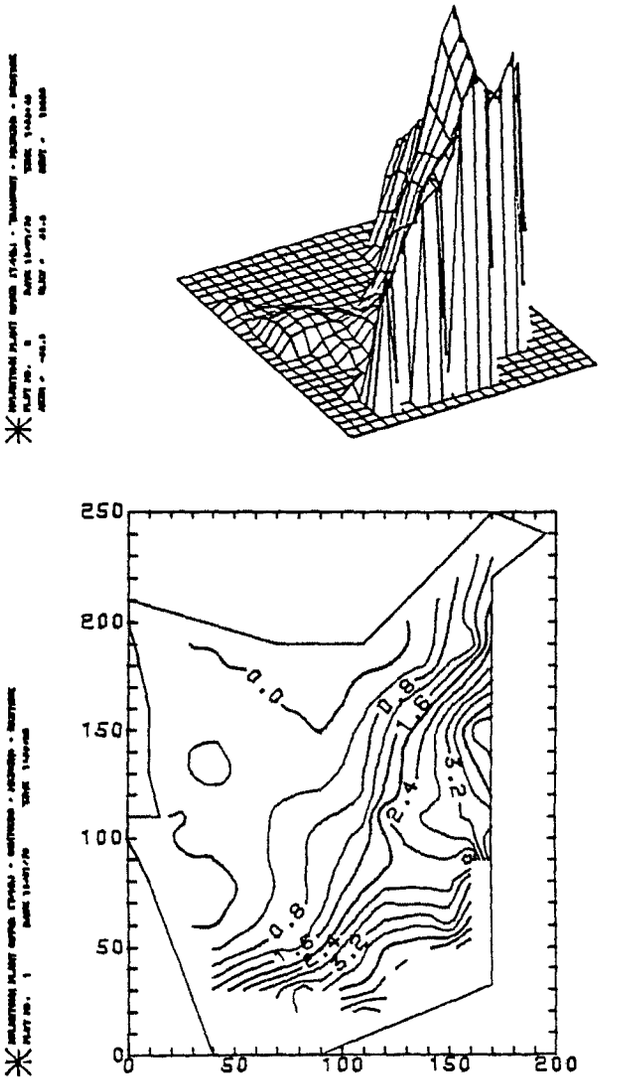

Figure 4.2. Vegetative cover density (T/ha) at the experimental site.

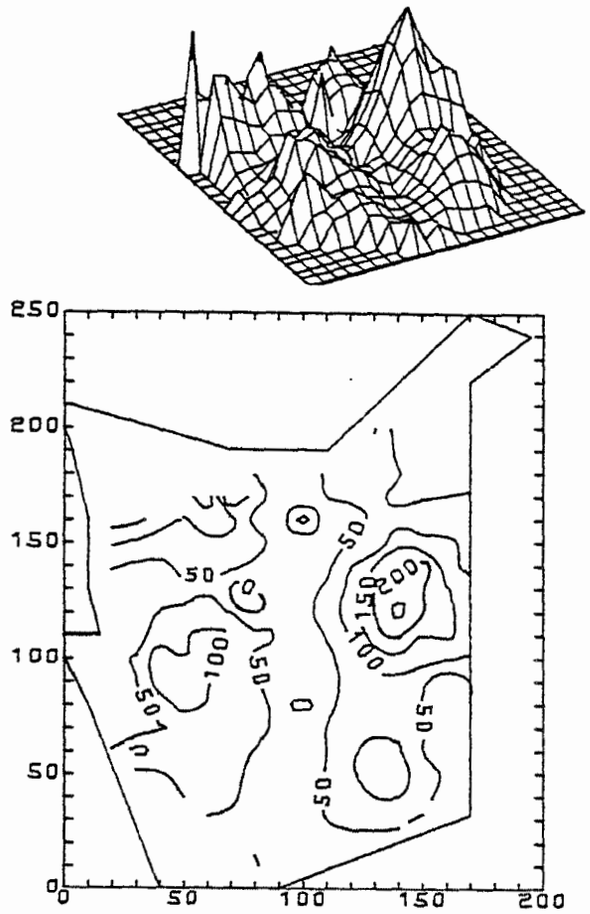

Figure 4.3. Relative distribution of infiltration at 60 minutes for a 65 mm summer storm (200 = 43 mm, 150 = 38 mm, 100 = 31 mm, 50 = 23 mm).

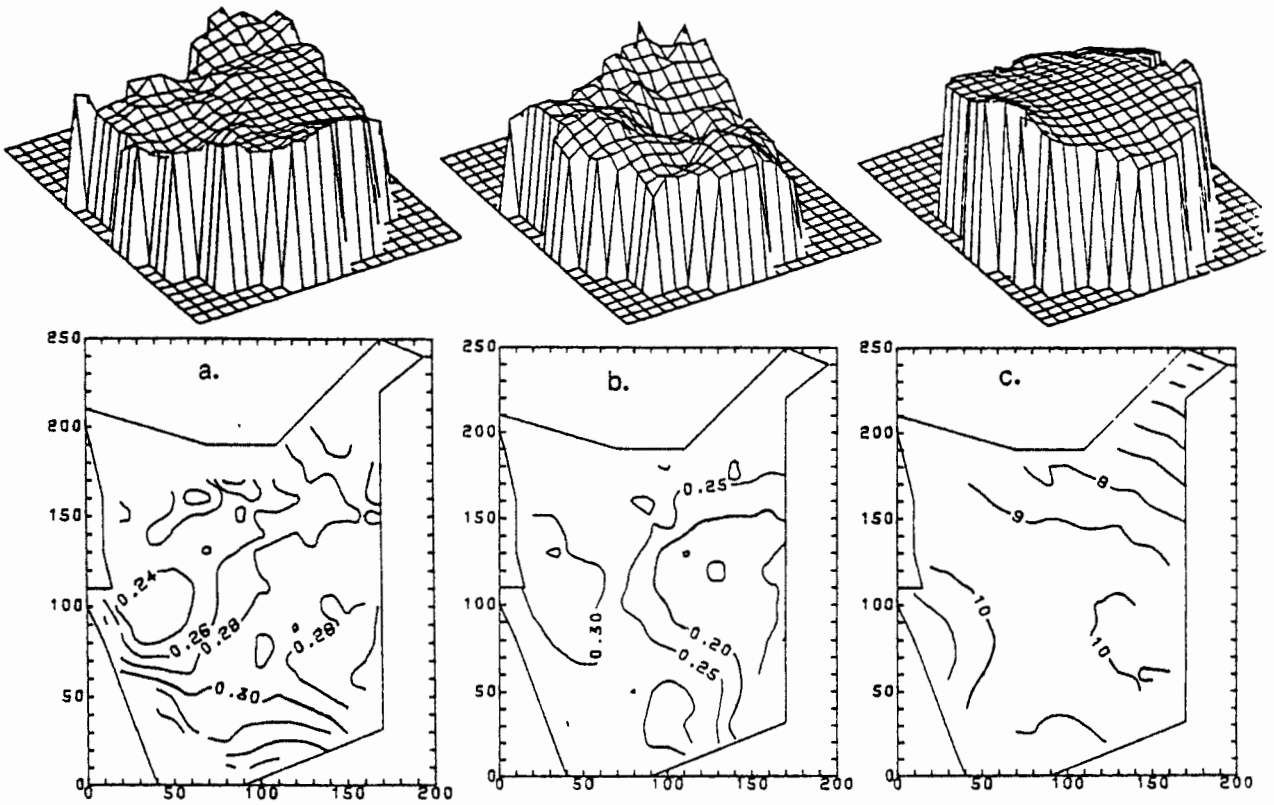

Figure 4.4. Water content at the surface (a) and at 0.9 m (b) and water table evaluations during a monitoring period in the summer, site scales are in meters.

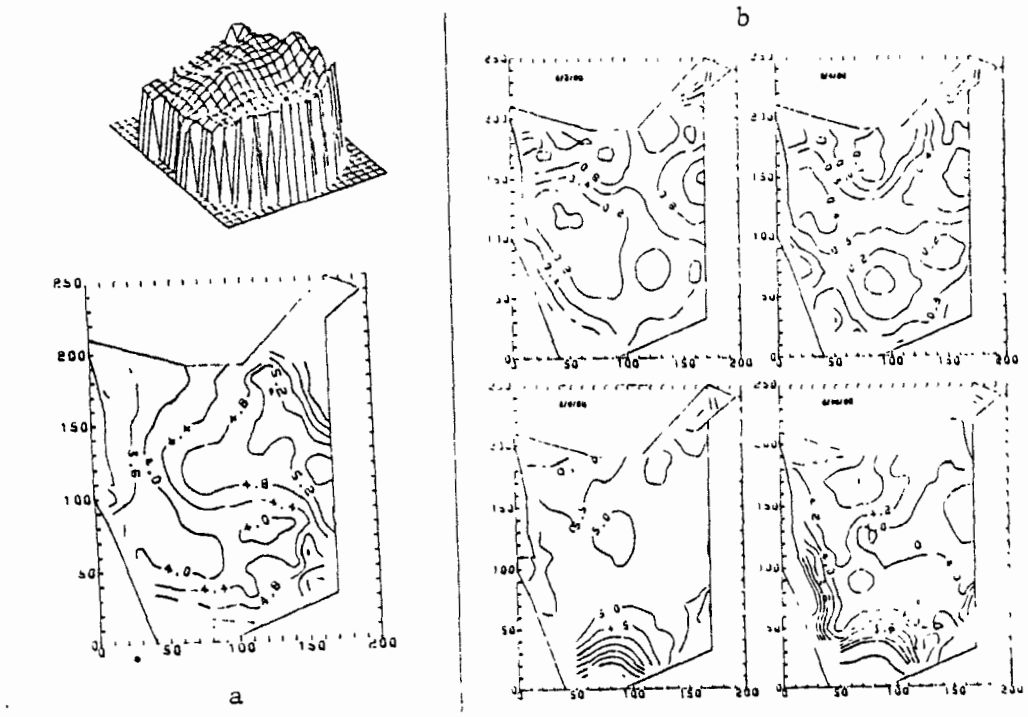

Figure 4.5. Characteristic distribution pattern of solar radiation (a) and of precipitation (b) at the experimental site.

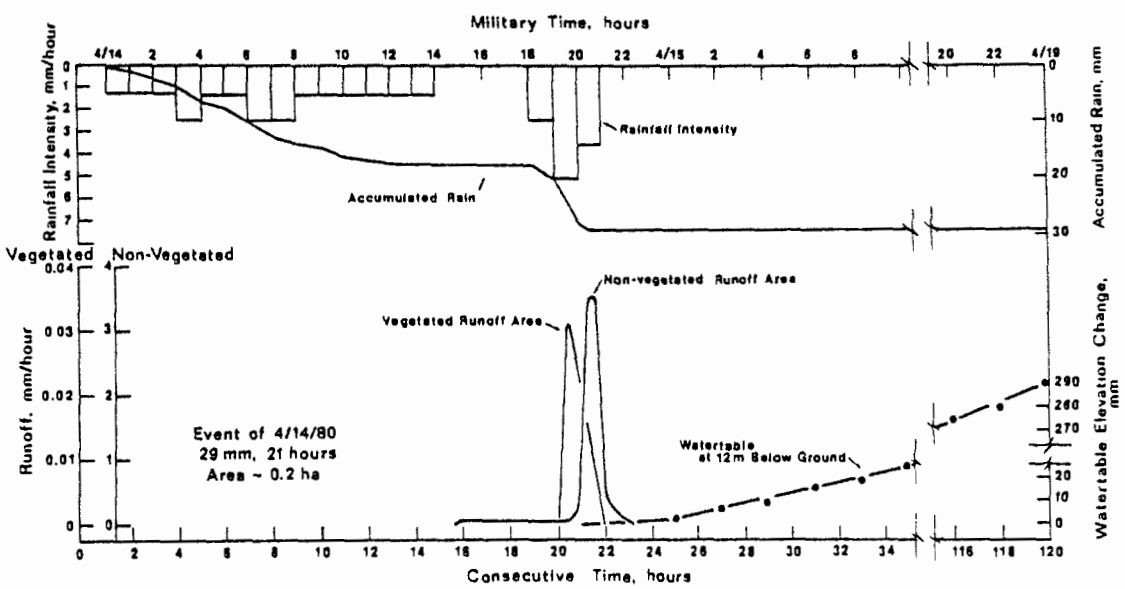

Figure 4.6. Site response to a spring storm.

In our modeling effort we observed (Rogowski and Weinrich, 1981) that on topsoiled profiles (such as spoil C in Figure 4.1) we could adequately model infiltratation and redistribution of applied water with numerical techniques using moisture characteristics corrected for coarse fragment content and hydraulic conductivities derived either from seepage flux measurements or experimentally determined values. On nontopsoiled profiles (such as spoil B in Figure 4.1) numerical techniques appeared inadequate. A better fit to experimental data was obtained by subtracting from the flux the amount of water retained by fine particles and the amount retained on the surface of coarse fragments and then considering the flux to be the function of gravity alone. However, often even this approach was not wholly satisfactory. At times when spoil was reasonably dry (water content $\sim$ 0.1 by vol) water apparently moved only through the larger channels in the coarse spoil materials without appreciably wetting the rest of the profile.

CHEMICAL SETTING

Occurrence of acid mine drainage from deep mines and strip mines, and resulting degradation of water quality in streams of a mined area, is caused primarily by the oxidation of iron sulfide mineral, pyrite. Two mechanisms for pyrite oxidation have been demonstrated. The first mechanism involves oxygen in the spoil atmosphere reacting directly with pyrite and water,

$$FeS_2 + 3.5\ O_2 + H_2O \rightarrow Fe^{2+} + 2SO_4^{2-} + 2H^+ \tag{4.1}$$

the second mechanism uses ferric iron as the electron acceptor,

$$14Fe^{3+} + FeS_2 + 8H_2O \rightarrow 15Fe^{2+} + 2SO_4^{2-} + 16H^+ \tag{4.2}$$

For this reaction to produce significant levels of acid, ferric iron must be present. Although at the normally low pH's of strip mine materials (pH <4), ferrous (2+)

rather then ferric (3+) iron is the dominant ion, certain bacteria use the ferrous-ferric oxidation reaction as an energy source. Because ferric iron is needed as input to equation 4.2, the rate limiting step for equation 4.2 may be,

$$14Fe^{2+} + 14H^{2+} + 3.5\ O_2 \xrightarrow{\text{bacteria}} 14Fe^{3+} + 7H_2O \qquad (4.3)$$

which is often considered to be bacterially catalyzed within strip mine spoils. Equations 4.2 and 4.3 can reduce algebraically to 6.1; thus, regardless of whether the reaction is bacterially catalyzed or not the final products of pyrite oxidation remain the same. Acid mine water emptying into a stream will cause a decrease in stream biota, but does not directly result in any visual degradation. It is the iron in the acid mine drainage that creates significant visual impact by precipitating in the streams to color them red or to form yellow-orange stains called "yellow-boy" on stream bottoms and sides.

We measured oxygen profiles at the experimental reclaimed stripmined site. Figures 4.7a and b illustrate a typical O_2 profile in August and October respectively approximately 700- and 800 days from the start of experiment (Jaynes et al., 1982). During this time of the year water levels in wells are dropping and increased penetration of oxygen into the spoil is generally observed. With the approach of winter the surface spoil layer cools and plant respiration slows or ceases. Thus, O_2 uptake decreases in the surface and O_2 can penetrate deeper into the spoil. The increased O_2 concentrations in the deeper parts of the spoil although slight, can apparently induce an increase in pyrite oxidation.

The results presented in Figures 4.1-4.6 illustrate a typical study site response to the climatic influences. They form the background against which we will now discuss the overall impact of mining and reclamation on quality of the groundwater at the experimental site in space and in time.

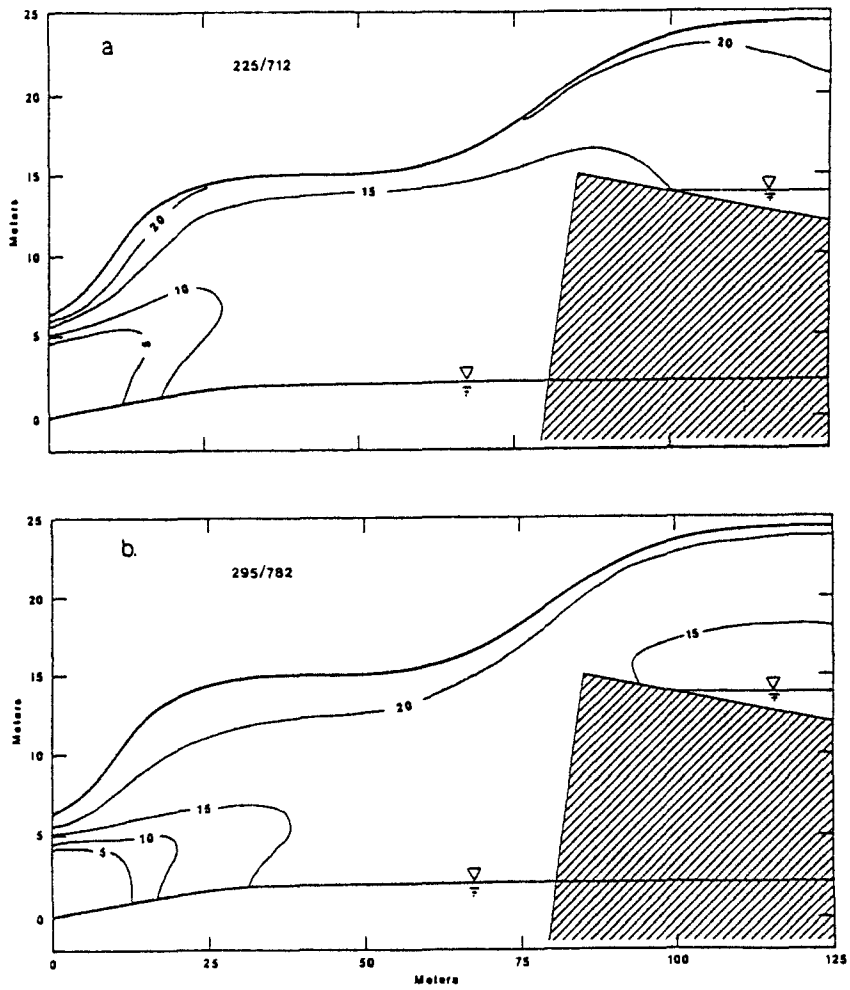

Figure 4.7. Typical oxygen profiles in August (a), and October (b) at the experimental site.

WATER QUALITY

Site Response in Time

Figure 4.8a, b, c and d shows the overall response of mined and reclaimed experimental site during the 1000-day study period. The bars in Figure 4.8a give the monthly rainfall amounts and the points indicate weekly water levels. The bars are positioned so as to reflect the maximum precipitation during a given month. For example, if a greater than 25 mm rain occurred on the 20th, the bar representing that month's precipitation would be positioned 2/3 of a way through the interval. If all

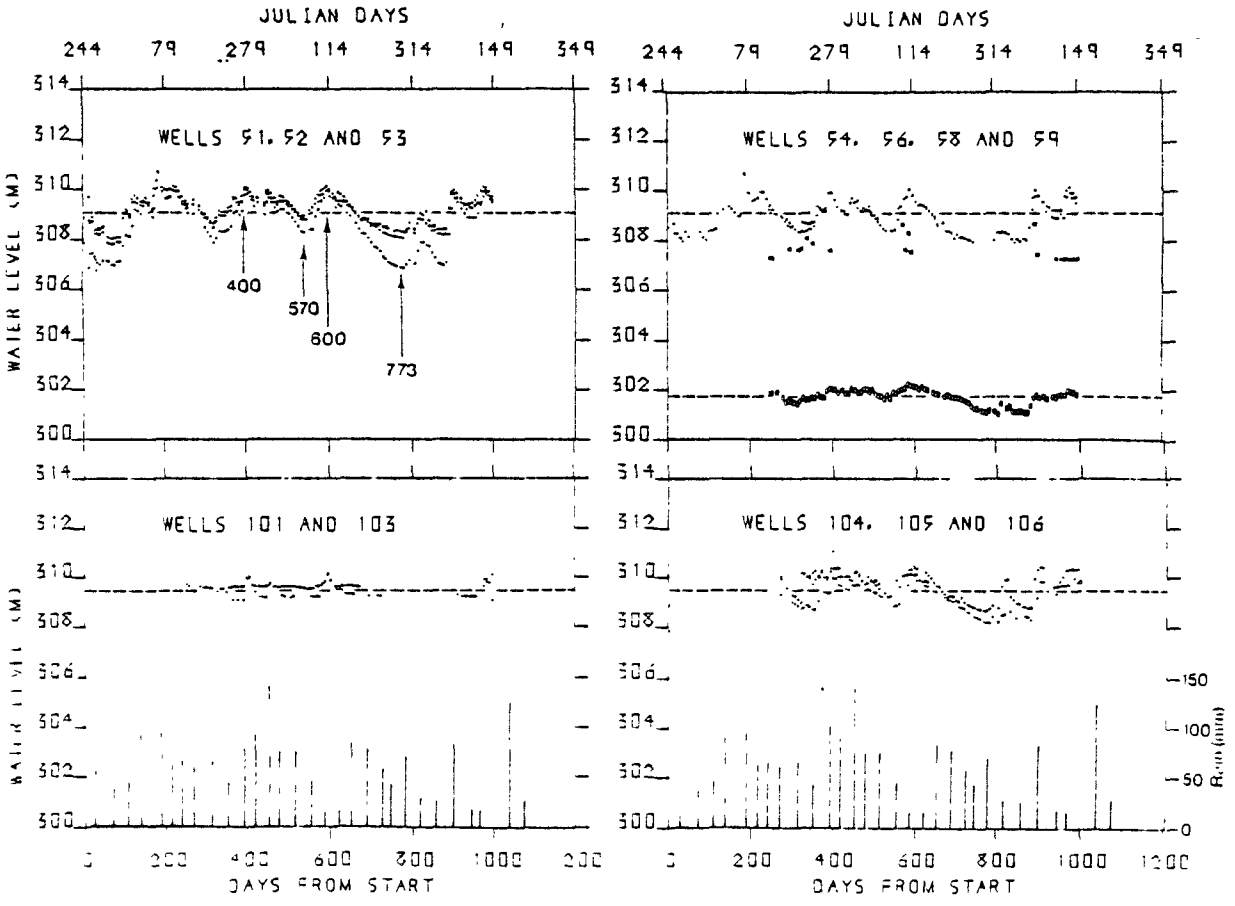

Figure 4.8a. Overall response of the experimental site during the study period: water levels.

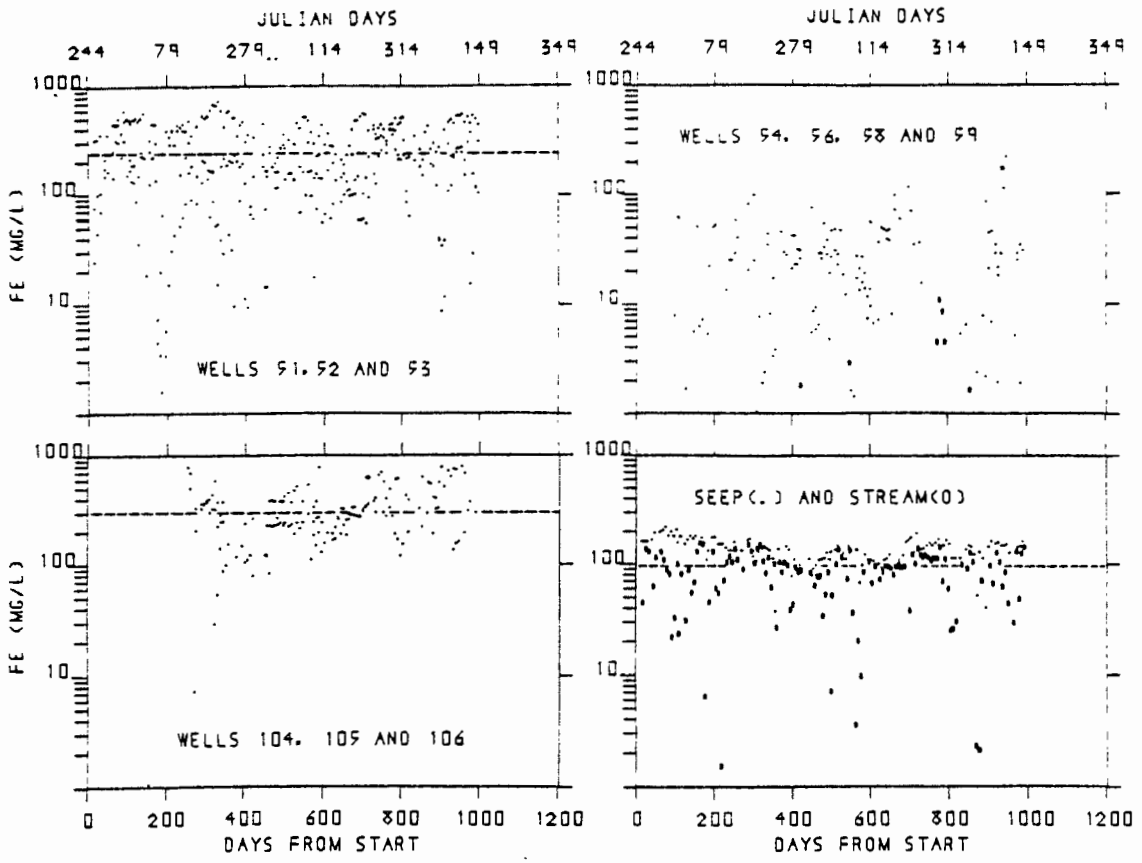

Figure 4.8b. Overall response of the experimental site during the study period: Iron (Fe) concentration.

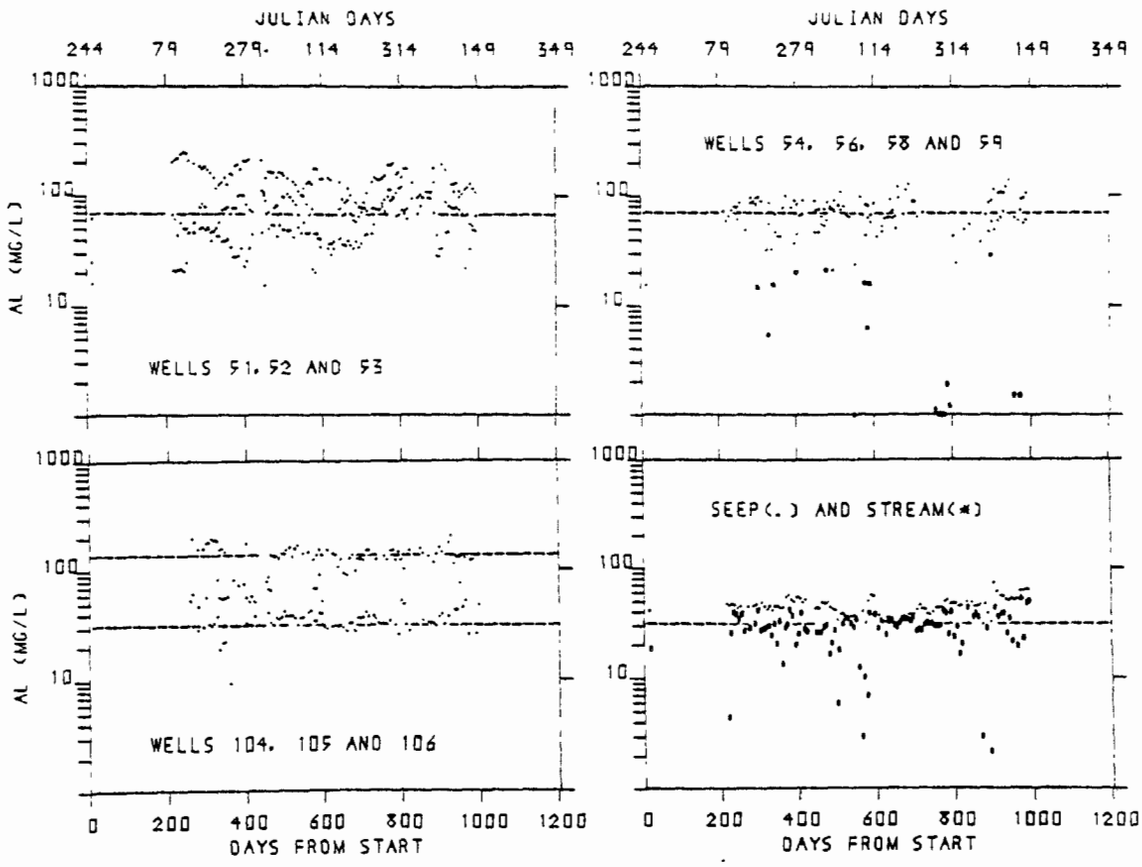

Figure 4.8c. Overall response of the experimental site during the study period: Aluminum (Al) concentration.

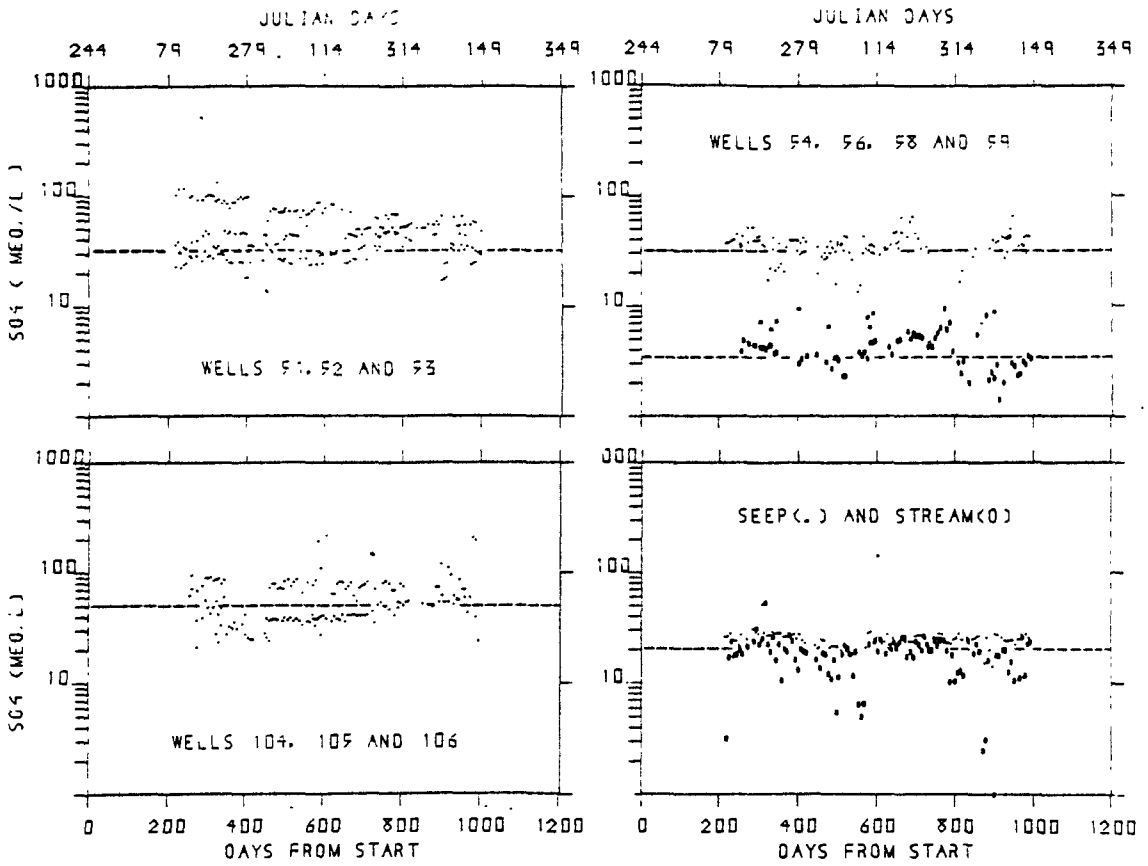

Figure 4.8d. Overall response of the experimental site during study period: Sulfate (SO_4) concentration.

rains were less than 25 mm the bar would be positioned in the middle of an interval. The points that indicate weekly water levels are grouped into four groups of wells. Wells 51, 52, 53 are located in a reclaimed area, stripmined for lower Kittanning B-coal. Wells 104, 105 and 106 are located in the area deep mined for B-coal. For wells 101 and 103, located on the fringes of deep mined area, the information is scanty, highly variable, and not included in subsequent parts of Figure 4.8. Even though water level response in wells 101 and 103 appears reasonably smooth the picture is misleading. Water level would drop during the dry period below the well bottom and would not be recorded. Thus, the results from these wells represent the response during high water periods only. Wells 54 and 56 (dots), and 58 (stars *), in the upper right hand corner of Figure 4.8a, are on the fringes of stripmined area and well 59 (•) samples water table overlying undisturbed at that point, Clarion A-seam.

In subsequent parts (b, c and d) of Figure 4.8 we show on the same scale distribution of Fe, Al, and SO_4 in the well water and in the seep and stream draining the B-coal area. In all drawings the horizontal dashed lines represent the mean distribution for a given group of wells. If more than one distribution is present two dashed lines appear. In what follows we compare the response observed in stripmined wells 51, 52, 53, 54 and 56 with that of deep mined wells 104, 105 and 106, we contrast their behavior with that of an undisturbed area (well 59), and examine probable effects of acid mine drainage on seep and stream.

Water levels in all wells, except well 59 (•) are approximately the same, and times of occurrence of minima and maxima generally coincide. In Table 4.1 days from start of experiment, appropriate dates, and times of major storms and times of occurrence of these well minima and maxima are listed. The data show that the maxima in wells both on strip and on deep mined spoil follow occurrence of major storms, while minima appear to result from 60-day or longer dry spells (rains < 25

TABLE 4.1. TIME OF OCCURRENCE OF MAJOR STORMS AND ASSOCIATED WELL ELEVATION MINIMA AND MAXIMA

Day	Month	Date				
		Calendar	Julian	Rain ≥ 25 mm	Well Min (Julian)	Well Max
5	Sept	090678	249			
100	Dec	121078	344	286,343	323	66
200	Mar	032079	79	24,57,69		
300	June	062879	179	144		
400	Oct	100679	279	204,249,271,278	205	284
500	Jan	011480	14	330,359		
600	April	042380	114	105	65	112
700	Aug	080180	214	133,199		
800	Nov	110980	314	299	293 (large)	335 (small)
900	Feb	021781	48		33	60
1000	May	052881	148	61,81	90 (small)	147

mm). The response appears to be more dependent on the presence or absence of rain than season of the year. In that sense the spoil-deep mine system appears to respond faster to weather extremes than does the natural system. The fast response of mined area is not altogether surprising since the spoil can hold only about one-fourth as much water between 10 and 1500 kPa as the undisturbed materials it replaces. In contrast, the response of the undisturbed well 59 (solid •) is considerably damped, while that of well 58 (stars *) which is on the very fringe of stripmined area and quite shallow, occurs immediately after the major storms possibly in a form of interflow from mined area just above it.

In Figure 4.8b we observe behavior of Fe at a point. Generally the highest concentration of Fe both in wells and in the seep and stream occurs during the time when water level is at the minimum. The concentration of Fe appears highest in the deep mined area (104, 105, 106), followed by that of stripmined area (51, 52, 53). Concentration of iron (Fe) in the fringe wells (54, 56, and 58) is less than or equal to that in seep and stream, while the concentration in the undisturbed well 59 (•) is the lowest. The most significant aspect of Fe behavior is the large variability observed in the response. Concentration in the stream tends to be lower than in the

seep, most likely because of dilution by less contaminated waters derived from drainage above the seep. The lowest values of Fe concentration in the stream at times (i.e., ∿ day 200) related to dilution by precipitation, at other times (i.e., ∿ day 500) they occur during low water level and reflect low effluent concentrations.

Figure 4.8c shows the Al response of the site. Al levels in the undisturbed well 59 (●) are quite low on the order of 1 or 2 mg/l. The highest concentrations occur in parts of the deep mined area (well 105--upper dashed line in the lower left hand corner of Figure 4.8c) and in the stripmined area (51, 52, 53). Little or no lowering in Al concentration on the fringes of mined area (54, 56, 58) is evident except perhaps at well 58 where thick soil overburden is present. The seep and stream effluent appear to have Al concentrations similar to those found in well 106 (lower dashed line in the left hand corner of Figure 4.8c). The overall response, compared to Fe shows less variability, where less well defined maxima and minima follow the water level maxima and minima.

Finally in Figure 4.8d gives sulfate (SO_4) concentrations for the same three groups of wells, the seep and the stream. The sulfate concentrations show the least scatter and smallest variability compared to Fe and Al. The highest average concentrations are observed in the deep mined area (wells 104, 105, 106) concentrations are identical in the stripmined area and on its fringes (wells 51, 52, 53, 54 and 56) and concentrations decrease markedly in well 58 (*) and particularly in well 59 (●) on undisturbed material. Interestingly, the seep and stream effluent concentrations of SO_4, while lower than the deep- and stripmined water table concentrations are substantially higher than concentrations in the undisturbed area (59). Sulfate concentrations appear more nearly constant with little or no tendency to follow water level minima and maxima.

In summary therefore, Figure 4.8 shows that the water levels in the wells at the mined and reclaimed site responded primarily to rainfall events ⩾ 25 mm. Iron (Fe)

concentrations varied most and were higher at the deep mined than at the stripmined site; aluminum (Al) concentrations varied less and were highest in parts of deep mined and stripmined areas; sulfate (SO_4) concentrations varied least and were highest in deep mined area.

Controlling Processes

The variation of chemical concentration of well water with time can result from chemical or hydrologic changes in local groundwater or from throughflow or groundwater of different composition originating elsewhere. For local groundwater hydrologic dilution or concentration would be primarily through the addition of percolate. Where the quality of added water is better than that of the groundwater, the chemical concentration decreases due to dilution, but the load stays roughly constant or may even increase. Where chemicals are being added or removed from solution, the concentrations will be correlated with load but not with total volume. Because the water levels and percolate contributions are variable, it is likely that the process determining the water quality in the well may switch back and forth, depending on climate, season and even event. The gain or loss of chemicals to groundwater from diffusion, resolution or chemical precipitation proportionately increase or decrease both concentration and load independent of changes in groundwater volume. Separating these effects from increases due to the addition of highly contaminated percolate depends mostly on the rate of the process. In strip mined systems, rates of increase due to percolate inflow are usually rapid and short term, being basically a response to a hydrologic event. The chemical processes such as those controlled by diffusion or pyrite oxidation kinetics are much slower and steadier. Diffusion of salts contained in spoil materials can cause a steady chemical contribution to a groundwater, thus increasing both concentration and load, simultaneously. Similarly, in cases where solubility, redox or other chemical additions or

subtraction processes largely independent of volume or flow rate are operating, the load and concentration plots versus time should provide similar relationships. One difficulty with this interpretation is that apparent accretion or drainage of groundwater at a point can seemingly increase or decrease the load over time before the system attains an equilibrium. Table 4.2 summarizes the controlling processes by looking at the concentrations, water volume, or percolate flux to the well and load relationships, and assuming that water through flow is not controlling unless stated otherwise.

TABLE 4.2. CONTROLLING PROCESSES AFFECTING GROUNDWATER QUALITY ON STRIPMINES

System	Concentration (C) $[SO_4]$	Water Level (H) or Flux (Q)	Δ Load Correlates with ΔC	ΔQ	Process
1	(A1) Increasing	Stable	Yes	No	Acid produced without water addition, e.g., pyrite oxidation or salt diffusion.
5	(B2) Decreasing	Increasing	No	No	Dilution effect, direct inflow of good quality percolate.
2	(A2) Increasing	Increasing	Yes	Yes	Substantial percolate inflow with acid products to the groundwater.
8	(C3) Stable	Decreasing	No	Yes	Groundwater draining out of system.
3	(A3) Increasing	Decreasing	1/	1/	Acid products added from spoil matrix while waters draining away.
4	(B1) Decreasing	Stable	Yes	No	Acid product loss, e.g., chemical precipitation.
6	(B3) Decreasing	Decreasing	-	-	Groundwater through flow.
7	(C2) Stable	Increasing	No	Yes	Groundwater through flow and/or variations of A1 or A2.

1/ If Δ Load correlates with ΔC, then (A1) is the type of system present, excluding drainage loss. If it correlates with ΔQ, drainage loss must be dominant.

In general, we can measure concentration experimentally by taking a sample of the well water at a given time and infer the load by assuming similar concentration throughout the water column of unit area and of height equal to that of the water table at a well point. To do this properly we must know accurately the lower well boundary at each point and be able to estimate accurately the absolute height of the

water table above its lower boundary. Where water table is sloping, or where concentrations vary with depth, considerable errors can be made by assuming the wrong depth. Fortunately, coal seams in western Pennsylvania are approximately level over short distances such as our study site, and spoil materials are sufficiently porous so that we can apply uniform concentration and constant depth lower boundary assumptions. Under these conditions Load = Concentration x Depth, where depth is expressed on a volume basis.

For the stripmined wells (51, 52, 53) and the deep mined site (wells 104, 105, 106) iron, aluminum, and sulfate loads appear to follow the pattern of concentrations shown in Figure 4.8b, c and d respectively. When concentrations increase the loads increase as they decrease the loads decrease. The system appears quite dynamic, signifying ongoing leaching, weathering and oxidation of pyrite.

In Figure 4.9 we look closer at the 500 to 700 day segment of SO_4 concentrations and water table elevations in Figure 4.8 for three of the wells. We took well 106 to represent the deep mined area, well 51 to represent stripmined area and well 59 to represent undisturbed area. In an attempt to find the controlling mechanism of acid generation, we compared changes in the water table elevations (solid line) with changes in concentration of SO_4 (dashed line) using criteria set out in Table 4.2. At each of the main time segments shown in Figure 4.8 we listed a possible operating system (A1 through C3). The letters above the line designate a more likely system, those below a less likely one. The analysis suggested that on a deep mined portion of the site we have acid products added to the groundwater as it drains away followed by an influx of acid percolate during accretion. On a stripmined site we can assume either a stable concentration of $[SO_4]$ suggesting groundwater throughflow and/or drainage, or, more likely, an acid percolate influx during accretion accompanied by a groundwater throughflow during decline. The most likely situation on the undisturbed

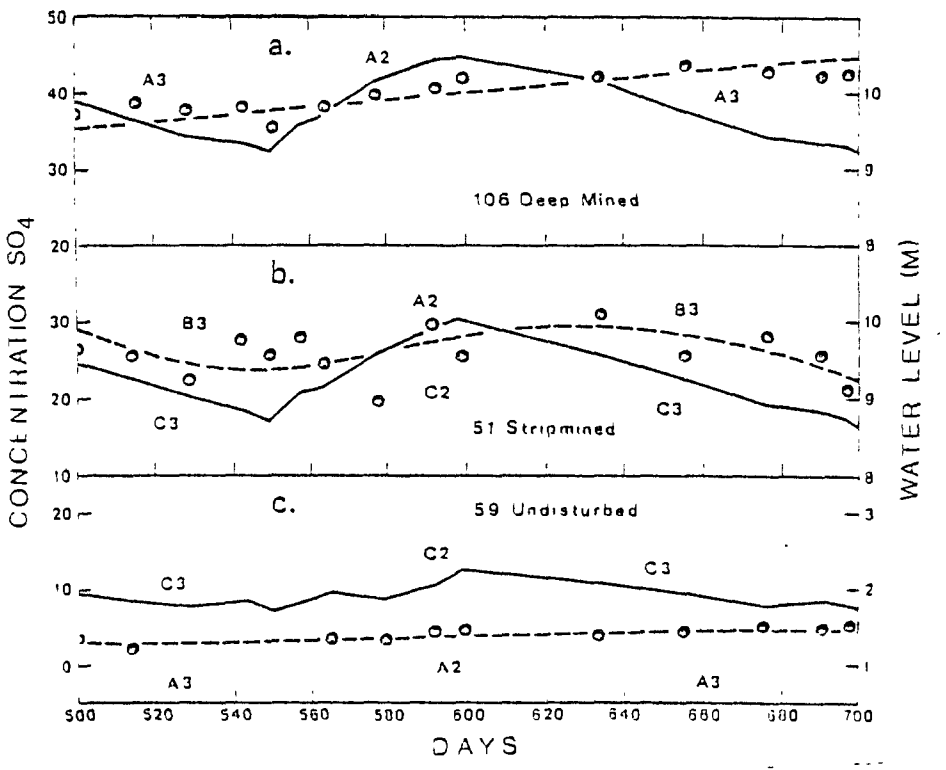

Figure 4.9. Water table elevations (solid line) and SO_4 concentrations (dashed line) during 500-700 day time segment, points represent experimental values of SO_4 concentration.

site is a groundwater throughflow and drainage with a hint of acid products arriving via percolate or from the adjacent matrix.

Site Response in Space--

Mean values--Figure 4.10 shows the distribution of mean values associated with some of the chemical constituents of groundwater at the study site. The orientation of the site in relation to North and to monitoring wells is shown in the upper left hand corner map in Figure 4.10. In general, all the maps show that lowest values of pH and highest for acidity and chemical concentrations center around wells 105 and 106 in the deep mined area. The steepest gradient appears to exist for pH and Fe, the least steep for acidity at pH 8.2, SO_4 and Mn; the gradient for Ca, Mg, and Al

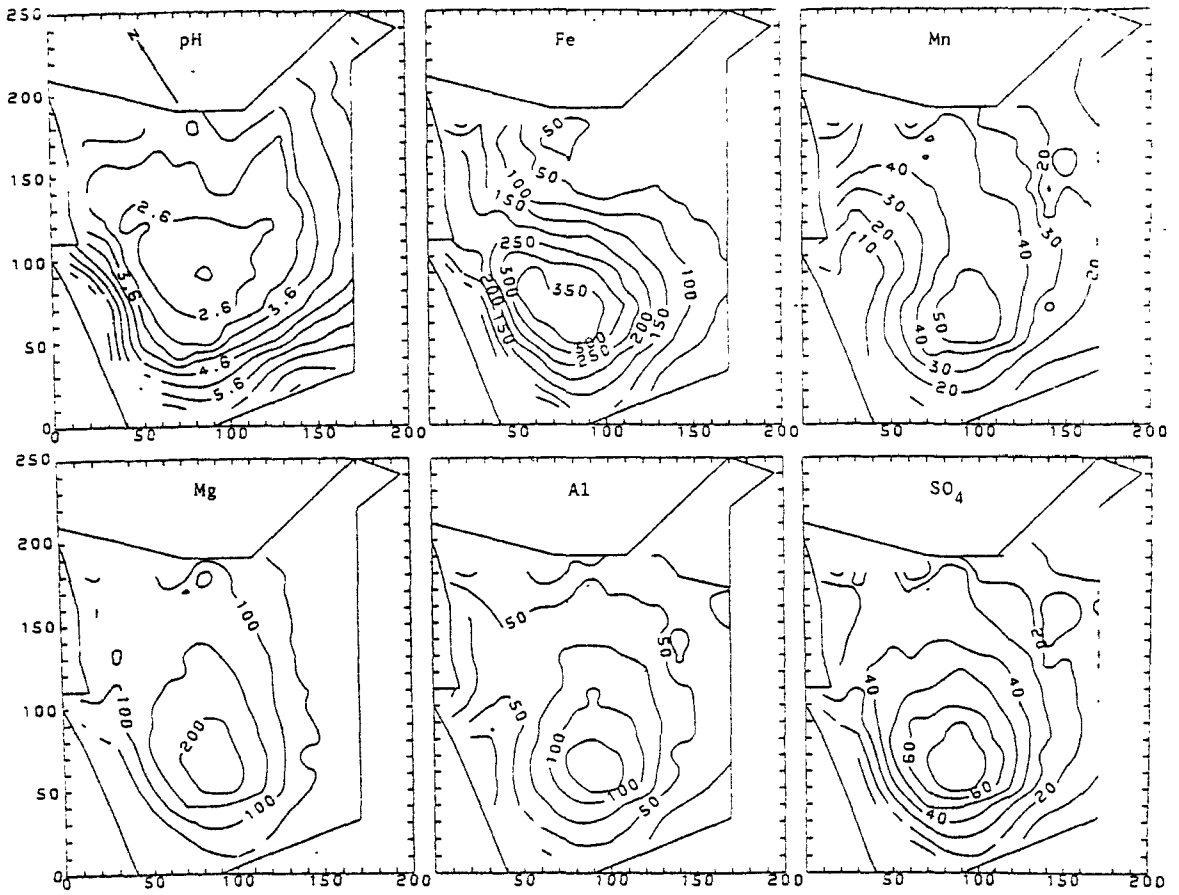

Figure 4.10. Average changes in pH (units), and iron (Fe), manganese (Mn), magnesium (Mg), aluminum (Al), and sulfate (SO_4) in mg/l, outside scale is in meters.

is intermediate between these extremes. Although largest variance values (not shown) (standard deviations ± 90 meq/l) were observed for Fe in the deep mined area, values almost as large for Mg centered around the highest infiltration zone in the northeast part of the area shown in Figure 4.3. Several of the chemical variables such as Mn and Al show an increase in variance towards plot borders, for others (SO_4, pH) variance increases from North to South in the deep mined area.

Another way of assessing spatial behavior is to examine chemical concentrations in wells on specific dates during low and high groundwater levels. Table 4.3 shows

TABLE 4.3. ACIDITY*, pH, AND CONCENTRATION OF SELECTED CHEMICAL CONSTITUENTS IN WELL WATER† ON A MINE AND RECLAIMED SITE MEASURED DURING HIGH AND LOW WATER LEVELS‡

Well No.	Water level (m)								Acidity (meq/ℓ)				Fe (mg/ℓ)				Mn (mg/ℓ)			
	1	2	3	4	1	2	3	4	1	2	3	4	1	2	3	4	1	2	3	4
51	10.08	9.51	10.20	8.18	2.96	2.99	2.92	3.05	6.4	12.1	8.32	30.8	11.7	100.0	57.5	405.0	25.0	23.0	30.6	27.0
52	10.19	9.70	10.23	8.41	2.81	2.95	2.97	2.92	49.3	36.1	36.9	41.7	317.5	388.0	450.0	415.0	105.0	79.8	55.6	111.3
53	9.87	8.99	10.02	6.96	2.97	2.92	3.46	3.40	22.8	18.9	12.7	32.3	130.6	169.0	143.0	455.0	60.2	57.1	41.8	32.6
54	10.02	8.97	10.47	-	2.84	3.10	3.08	-	16.5	11.7	12.2	-	43.5	28.5	12.2	-	44.4	47.4	38.2	-
55	10.03	9.46	10.19	-	2.66	-	2.70	-	16.3	-	-	-	34.4	-	56.3	-	27.5	-	13.8	-
56	10.06	9.41	10.19	-	2.97	3.03	3.12	-	10.9	15.3	9.4	-	22.1	18.1	7.8	-	43.3	53.6	34.7	-
57	10.07	-	10.18	-	-	-	4.14	-	-	-	2.8	-	-	-	-	-	-	-	12.2	-
104	11.16	10.12	10.57	-	2.81	-	2.85	-	16.9	-	15.4	-	108.5	-	135.0	-	29.6	-	27.5	-
105	10.05	9.28	10.18	8.31	2.20	-	2.41	3.19	127.9	-	90.9	37.8	860.0	-	1255.0	345.0	105.6	-	61.2	62.7
106	10.44	10.16	10.48	8.76	2.55	2.95	3.12	2.97	19.8	19.0	15.6	27.5	250.0	117.0	255.0	515.0	5.1	4.6	4.6	7.6
58	7.64	-	7.57	-	3.64	-	-	-	4.0	-	-	-	0.2	-	-	-	13.8	-	-	-
59	2.10	2.01	2.21	1.19	5.94	6.23	5.80	5.13	0.5	0.2	0.4	0.8	0.2	0.2	0.7	4.5	1.3	0.4	0.4	2.5
101	10.03	9.72	10.16	-	-	6.56	-	-	-	2.6	-	-	-	0.2	-	-	-	1.0	-	-
103	10.08	9.29	10.24	-	7.17	-	7.88	-	-	-	-	-	-	-	-	-	0.4	-	-	-
107	11.96	12.67	13.12	-	7.34	-	6.82	-	-	-	2.1	-	-	-	-	-	-	-	1.7	-
Stream (2)					2.72	2.79	2.71	2.80	15.4	12.7	14.9	16.1	80.4	141.0	116.0	163.0	17.8	11.2	13.8	10.7
Seep (1)					2.93	2.91	2.77	2.78	7.8	3.96	13.1	12.9	42.8	19.9	105.0	112.0	7.1	3.4	11.5	8.0
Seep (3)					-	2.98	2.75	2.85	-	14.2	30.7	16.9	-	175.0	161.0	221.0	-	10.2	13.3	10.2
Seep (4)					-	2.77	2.63	2.78	-	19.0	18.6	21.5	-	231.0	207.0	271.0	-	6.1	6.1	8.2

Well No.	Ca (mg/ℓ)				Mg (mg/ℓ)				Al (mg/ℓ)				SO_4 (mg/ℓ)			
	1	2	3	4	1	2	3	4	1	2	3	4	1	2	3	4
51	104.5	127.0	116.0	173.0	85.4	87.0	93.3	109.0	24.0	48.0	36.0	120.0	19.0	25.0	25.5	53.2
52	351.7	310.0	217.0	255.0	-	297.0	206.0	164.0	217.5	141.0	148.0	203.0	102.0	77.0	74.0	73.2
53	162.8	137.0	92.5	207.0	150.0	126.0	101.0	128.0	104.0	70.5	42.5	104.0	47.0	37.0	31.0	54.7
54	182.9	185.0	175.0	-	156.0	149.0	130.0	-	95.0	71.0	10.1	-	40.5	31.0	35.5	-
55	125.6	-	66.3	-	119.0	-	58.4	-	68.0	-	44.0	-	33.0	-	25.0	-
56	152.8	223.0	121.0	-	145.0	204.0	133.0	-	39.0	102.0	60.0	-	33.0	44.5	31.0	-
57	-	-	137.0	-	-	-	138.0	-	-	-	12.0	-	-	-	22.0	-
104	114.6	-	84.4	-	60.1	-	49.0	-	59.0	-	54.0	-	29.0	43.5	28.5	-
105	287.4	-	259.0	350.0	348.0	-	264.0	275.0	184.0	-	143.0	157.0	68.0	80.0	127.0	82.5
106	132.7	170.0	169.0	249.0	168.0	150.0	158.0	119.0	35.0	44.0	42.0	36.0	44.0	37.0	42.0	48.6
58	68.3	-	-	-	40.0	-	-	-	20.1	-	-	-	9.4	-	-	-
59	44.2	46.2	36.3	88.4	28.5	31.6	22.1	52.2	-	0.6	-	1.0	3.0	3.8	4.8	9.3
101	-	10.0	-	-	-	3.0	-	-	-	-	-	-	-	1.0	-	-
103	56.3	-	60.3	-	11.1	-	5.1	-	-	-	-	-	-	-	-	-
107	48.2	5.3	14.1	-	21.5	3.0	7.2	-	1.2	-	-	-	-	0.4	0.5	-
Stream (2)	102.5	110.0	92.5	113.0	52.2	47.4	49.8	49.0	57.5	42.1	38.0	46.5	26.0	21.5	27.5	28.5
Seep (1)	64.3	52.3	87.4	90.4	31.6	16.1	43.4	40.2	25.1	10.1	37.2	41.0	13.0	6.5	23.5	24.0
Seep (3)	-	90.4	110.0	108.0	-	45.8	50.6	49.0	-	43.0	51.0	48.0	-	25.0	27.5	27.5
Seep (4)	-	48.2	66.3	94.5	-	41.1	33.2	45.0	-	57.0	44.0	58.5	-	30.0	27.5	31.0

* Acidity at pH 8.2 in meq/l $CaCO_3$.

† Water level given as height above (or below-negative) a 300 m benchmark.

‡ Water levels given for: 1 - 400 (10/8/79), 2 - 570 (3/24/80), 3 - 600 (4/21/80), 4 - 775 (10/13/80 days from start.

water table elevations, pH, acidity and chemical concentrations in all the wells for four dates. Dates 1 and 3 correspond to relatively high water levels; dates 2 and 4 correspond to low water levels (Figure 4.8a). For the purposes of analysis the results were grouped into those for spoil wells (51, 52, 53, 54, 55 and 56), deep mine wells (104, 105, 106), undisturbed material wells (57, 59, 101 and 103), the seep, and the stream. When missing values were encountered it meant that insufficient water was present to obtain a sample.

Average values for selected concentrations of SO_4, Fe, and Al at high and low water levels are shown in Table 4.4. The results are not conclusive. While concentrations of SO_4, Fe and Al in undisturbed wells are generally low, higher values on the average of acidity, SO_4, Fe and Al occur during low water levels on spoil wells. In contrast on deep mine wells the average values of acidity and average concentrations of Fe, Al and SO_4 are either lower or about the same at lower water levels. Based on the results of this study we have concluded that both the stripmined and deep mined areas respond similarly to major storm events ($\geqslant$ 25 mm). Although on the average little or no difference is apparent between results at high and low water levels in the wells, iron concentration appears considerably higher during high water level in the deep mined wells, while acidity, SO_4, Fe and Al are all higher at low water levels in spoil wells.

CONCLUSIONS

Distribution of groundwater elevations in time at the experimental site showed that highest levels on both the stripmined and deep mined areas generally follow the occurrence of major storms, while lowest levels appeared to result from 60-day or longer spells with rains $\leqslant$ 25 mm. Iron (Fe) data showed most scatter. Highest concentrations of Fe on stripmined wells and in the stream occurred when water level was at the minimum. Aluminum (Al) and SO_4 were less variable and showed at times

TABLE 4.4. AVERAGE WATER LEVELS, ACIDITY AND CONCENTRATIONS OF SO_4, FE AND AL AT HIGH AND LOW WATER LEVELS FOR GROUPED WELLS

	Well Bottom	Water Level		Acidity		SO_4		Fe		Al	
		High	Low	High	Low	High	Low	High	Low	High	Low
		(m)		(meq/l)		(mg/l)		(mg/l)		(mg/l)	
Spoil	7.7	10.1	8.8	18	25	41	50	107	247	74	107
Deepmined	8.1	10.5	9.3	48	28	56	58	477	326	86	79
Undisturbed	7.0	8.8	7.0	2	1	4	4	<1	2	11	1
Seep		-	-	18	15	23	24	172	167	58	44
Stream		-	-	15	14	27	25	98	152	39	43
MEAN		9.8	8.4	20	14	30	32	171	178	54	55

some tendency to follow water level maxima and minima. We have found that despite much scatter and variability in the data, SO_4 concentration was most highly correlated with other variables and could be used to estimate each of the other chemical parameters for selected sampling sites. Closer scrutiny of 500 to 700 day SO_4 data suggested that on the deep mined site the controlling mechanism of acid generation was addition of acid products during groundwater drainage followed by an influx of acid percolate during groundwater accretion. On stripmined portion of the site the most likely mechanism of acid product gain and loss were acid percolate influx during groundwater accretion accompanied by the groundwater throughflow during decline.

REFERENCES

1. Jaynes, D. B., A. S. Rogowski, H. B. Pionke, and E. L. Jacoby, Jr. Atmosphere and Temperature Changes within a Reclaimed Coal Strip Mine. Soil Sci., 136(3): 164-176, 1983.
2. Pedersen, T. A., A. S. Rogowski, and R. Pennock, Jr. Physical Characteristics of Some Minesoils. Soil Sci. Soc. Am. J., 44:321-328, 1980.
3. Ritchie, J. R. Model for Predicting Evaporation from a Row Crop with Incomplete Cover. Water Resour. Res., 8(5):1204-1213, 1972.
4. Rogowski, A. S. Hydrologic Parameter Distribution on Mine Spoil. Watershed Management Symposium, ASCE Irrigation and Drainage Division, July 21-23, Boise, Idaho, 1980. pp. 764-780.
5. Rogowski, A. S., and B. E. Weinrich. Modeling Water Flux on Strip-Mined Land. Trans. ASAE, 24(4):935-940, 1981.

SECTION 5

RECOMMENDATIONS

INTRODUCTION

Potentially there are several chemical and hydrologic problems associated with placement of acid spoil materials. The rationale for a deep placement well below the soil surface, and preferably below a water table, is to prevent or minimize oxidation of pyrite to sulfuric acid and associated salts by reducing the supply of oxygen. If, however, substantial sulfuric acid or associated salts are already contained within the spoil because of present or previous mining, handling and reclamation operations (or if large supplied of indigenous salts exist, placement below a water table) may actually increase the rate of acid and salt leaching. Specific placement of acid- and salt-containing spoil should be aimed at preventing contact with percolating water or rising water tables. We recommend placement based on chemical and physical spoil properties that may affect water percolation and O_2 diffusion rates in the profile. Both the deeper placement of acid spoil and coarser particle size can substantially reduce the amount of acid drainage. Placement above the water table with emphasis on percolate control may be better for high sulfate spoils, while placement below the non-fluctuating water table may be better for pyritic spoils.

Acid generation from pyrite oxidation is common in many mining wastes world wide. Although such materials may occur anywhere in the overburden profile, they are frequently composed of shales overlying the coal layer.

Present federal regulations in the United States require that acid- and toxic-forming materials be covered during the backfilling process with a minimum of 1.2 m

of the best available non-toxic and non-combustible material. Other requirements are that the acid- and toxic-forming materials (1) be placed so as to minimize contamination of onsite or offsite groundwater systems, and (2) be placed so as not to pose a threat of water pollution.

In the State of Pennsylvania, the acid- or toxic-forming spoil must be placed either below the water table if the water table does not fluctuate substantially, or on a clay layer above the zone of highest anticipated water level and covered with a soil or soil-like material. The type of placement is usually written into the mining permit, depending on the projected position and behavior of the post-mining water table.

The purpose behind specific placement of the acid- and toxic-forming spoil is to keep it out of the plant root and surface runoff zones and simultaneously to reduce its potential impact on the groundwater. Techniques for reducing this impact on groundwater generally rely on atmospheric or hydrologic isolation. Isolation from the atmosphere (atmospheric isolation) attempts to reduce the O_2 resupply rate, thus slowing down pyrite oxidation that ultimately results in acid mine drainage. One method of atmospheric isolation is placement of acid spoil several meters below the ground surface but still in an unsaturated zone, i.e. increasing the pore length for O_2 diffusion. The diffusion coefficient of O_2 through the atmosphere at 25°C is 20.6 $mm^2\ s^{-1}$ (Ohio State University, 1971). The effectiveness of increasing the pore length depends on the O_2 resupply rate relative to the pyrite oxidation rate. Atmospheric isolation is better achieved by submerging highly pyritic materials below the water table. This type of placement is effective because the diffusion coefficient of O_2 in water is about 4 orders of magnitude less than in air. In contrast, isolation from flow (hydrologic isolation) emphasizes control over transport of acid products rather than the rate of acid production. Methods such as clay enveloping have been used to isolate extremely acid spoil. At times, a clay envelope is

deliberately constructed in the unsaturated zone above the water table to minimize leaching even further.

Once the spoil is reclaimed, the system undergoes rapid change. Within a short time after backfilling and reclamation, the spoil may subside causing an increase in density (Rogowski and Jacoby, 1979), plant growth begins and the spoil undergoes external and internal erosion, weathering and changes in outflow. It is usually during this initial short-term period that the loss rates of acid products (Vimmerstedt and Struthers, 1968) and sediment are the highest. After this period (usually less than a year), flow parameters stabilize and the system seems to gradually approach a steady state (or as much of a steady state as can exist in a system subject to climatic variability). To minimize the potential impacts, both the short- and long-term effects should be considered.

Our objective was to evaluate how spoil placement may potentially affect the quality and quantity of drainage and groundwater. To do so, we will consider the effects of spoil placement and spoil particle size on oxygen and acid product movement through a prototype spoil system consisting of two 3-m high caissons filled with field sampled spoil. In addition, we will draw on our previously published work so that acid leaching can be more completely discussed.

WHAT WAS DONE

The profiles described in this section serve as illustrative examples, they were sampled near Kylertown, Pa., on a reclaimed spoil site derived from the Pennsylvanian System (Allegheny Series) materials. The prototype profiles were instrumented for monitoring water content and sampling of leachate (Rogowski and Jacoby, 1979; Pionke et al., 1980a). One profile was topsoiled to simulate field conditions, and in second profile a 0.4-m layer of acid shale obtained from just above the coal layer was placed 2 m below the spoil surface. The coarse nature

of the spoil materials, and the properties of both the topsoil and spoil are discussed in detail in Rogowski (1977) and Pedersen et al. (1978, 1980).

The profiles were leached with rainwater, simulating conditions in the field. Between leachings, the contained materials were exposed to ambient atmospheric and temperature conditions for different periods of time. Water content was monitored using a neutron probe and leachate samples were analyzed for pH, total acidity, total salts, SO_4, Ca, Mg, Mn and Fe (Pionke et al., 1980a).

Chemical leachate data used in this paper are from published data by Rogowski (1977) and Pionke et al. (1980a,b). Leachates from different layers were analyzed by Rogowski (1977) and Pionke et al. (1980a) for pH, soluble salts and sulfate content. Results represent several runs at different water application rates interspersed with variable-length incubation periods. The work of Pionke et al. (1980b) consisted of a laboratory study on sulfate salt diffusion and leaching mechanisms at the spoil particle scale. Data from Lovell et al. (1978) provide the sulfate and pyrite contents of the overburden layers sampled from active highwalls. Sulfate and pyrite sulfur were analyzed by standard methods (ASTM, 1971) Sulfate S was extracted in HCl followed by pyrite S extraction in HNO_3. Sulfur analysis was done gravimetrically by precipitation as $BaSO_4$.

SUBSIDENCE OF MATERIALS AND CHANGES IN DENSITY AND POROSITY

We found that bulk spoil density increased following the first water application to the newly reconstructed spoil profiles. The topsoiled profile subsided 6 and the nontopsoiled profile 10% on average. The density change decreased with depth, being largest near the spoil surface. Some topsoil moved by internal erosion into the underlying spoil profile (Rogowski and Jacoby, 1979); this affected the hydrologic behavior of the topsoiled spoil. Infiltrating water did not move as a front but rather in cracks. A partially impeding soil layer formed at the interface of soil

and spoil led to unsaturated conditions in the underlying spoil during subsequent water applications. When the percolating water reached the bottom of the profiles, the water table began to rise flooding the spoil. Thus under topsoiled conditions, the properties of the surface layer and the rising water table determine the water regime in the lower profile (Rogowski, 1978).

Changes in porosity, assuming constant particle density of 2.65 g cm^{-3}, are related to changes in bulk density (Baver et al., 1972, p. 185).

$$\text{Pore space (\%)} = \left[1 - (\text{bulk density/particle density})\right] \times 100 \qquad (5.1)$$

Thus, changes in bulk density following water application calculate out to as much as a one-fourth reduction in the spoil pore space. This in turn would lead to less pore space being available for oxygen diffusion and water flow.

Compaction of the surface topsoiled layer, especially when coupled with successful revegetation, may limit the amount of water transferred to deeper-placed materials. If deeper-placed materials are coarse, a denser, less coarse layer immediately above a coarse acid layer will further inhibit water percolation and oxygen diffusion. Internal transfer of fines, known as piping which affects the profile hydrologic behavior, can be controlled by judicious selection of the spoil particle size most suitable for each layer. In reclamation work, it may be desirable to use the standard filter design criteria (Cedergren, 1967, p. 175)

$$\frac{D_{15}\ \text{(of spoil)}}{D_{85}\ \text{(of soil)}} < 4\text{-}5 < \frac{D_{15}\ \text{(of spoil)}}{D_{15}\ \text{(of soil)}} \qquad (5.2)$$

Restated in words, this means that: a 15% size (D_{15}) of spoil should be less than 4-5 times the 85% size (D_{85}) of the topsoil, and also the 15% size (D_{15}) of spoil should be more than 4-5 times the 15% size of the topsoil. The soil and spoil materials used in the caissons were highly susceptible to internal erosion. In the

field, piping and surface erosion of fines leads to large amounts of coarse fragments left on the surface; a common sight at many mines.

WATER MOVEMENT IN THE PROFILE

On the topsoiled spoil we readily ponded the water, applying 500 mm in 2.3 h. On nontopsoiled spoil water did not pond even when applied at rates in excess of 1000 mm h^{-1}. We therefore applied 536 mm of water intermittently with garden sprinklers in 51.6 h. The amounts of water applied represented about half of the average annual precipitation at the field site.

Figure 5.1 shows initial water content in the topsoil spoil profile during wetting, 0.5 h after water application started, and water content profiles at 24, 72, 144, 480 and 648 h. Water movement into the spoil during infiltration appeared to be controlled by the fine/coarse interface between the topsoil and

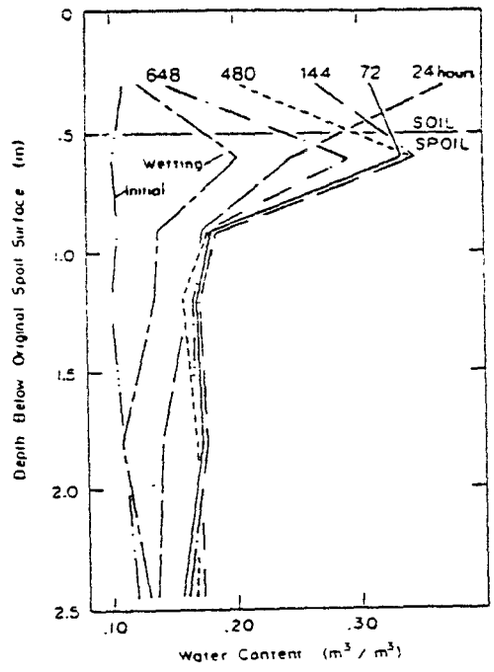

Figure 5.1. Water profiles in the topsoiled spoil prior to and following ponding.

spoil layers. Subsequently, during the redistribution and evaporation phases, little change occurred in the profile water content below 1 m depth. Most of the changes resulting from evaporation occurred initially at the surface and in the layer immediately below. It appears, therefore, that topsoiled spoils, such as these studied by us, may have lower infiltration rates, may store more water in the finer soil materials in the immediate plant root zone, and may greatly influence both the underlying spoil water content and the rate of seepage of water to the water table. The behavior is not unlike that of a much-studied phenomenon in natural soils where finer-texture layers overlie coarser ones (Miller, 1973).

In contrast, infiltration on nontopsoiled spoil can proceed very rapidly. Water percolated directly to the water table, which began to rise very shortly after the water application started (0.6 h). Figure 5.2b shows the response of the water table to water application and the times, indicated by arrows, corresponded to similarly identified water content profiles in Figure 5.2a. The general shape of these profiles, particularly in the surface layers, suggests rapid water percolation, probably by gravity alone (rather than as a wetting front) and through the larger pores and cracks between the coarse fragments. The vertical lines with hash marks in Figure 5.2 (a and b) describe the layers in which the field profile was sampled and reconstructed in the caissons. The first layer from the bottom consisted of sand and the second of coarse acid shale fragments.

Comparison of the "Flooded" curve at 51.6 h with the "Redistributed" curve at 144 h in Figure 5.2a illustrates an interesting feature. It appears that during flooding, percolating water did not completely fill all the voids possibly trapping some air. Subsequently, during the redistribution phase, water from large voids in the acid shale drained into the underlying layer. However, the finer-textured layer above the coarse acid shale could not release enough water to fill the large voids in the shale. This suggests that such coarser lenses situated within a finer matrix

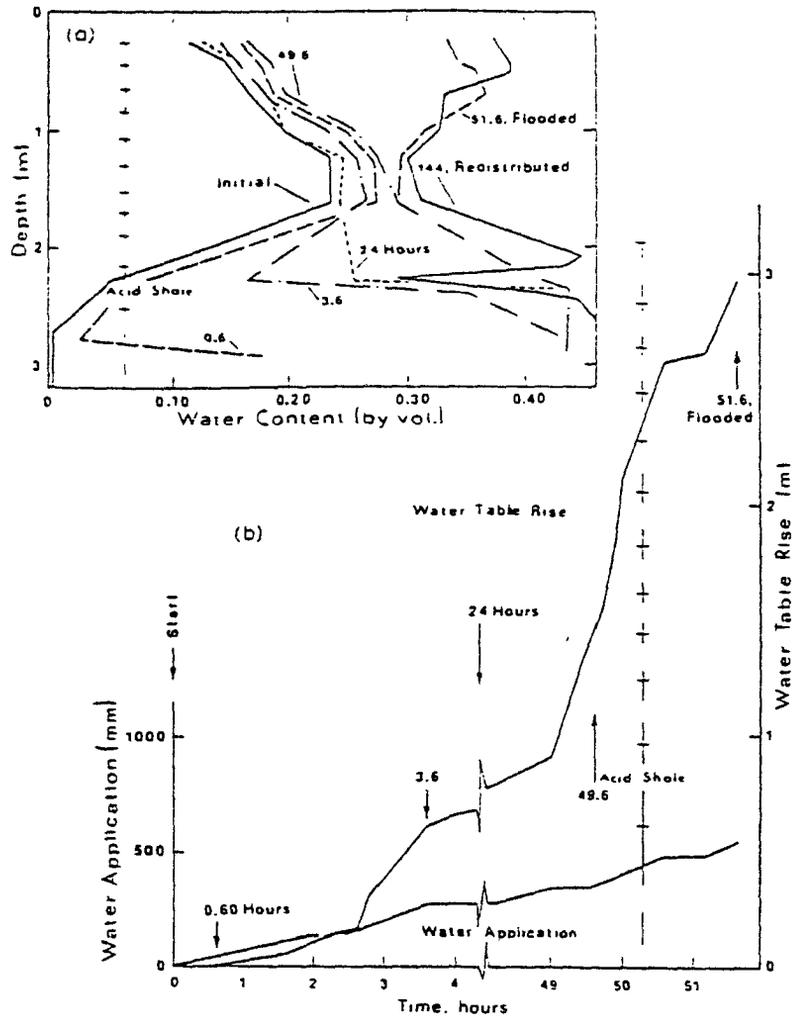

Figure 5.2. Water profiles (a) in nontopsoiled spoil following wetting, and (b) corresponding elevations of water table and amounts of water applied.

may at times become dewatered during the water redistribution phase, particularly if they connect through larger cracks and pores with the outside air at the spoil surface. We may speculate that if the coarse fragments consist of acid-producing materials, such dewatering may induce preferential mass-air movement into such spoil pockets enhancing oxidation. However, the amount of potential acid drainage generated this way would also depend, as will be seen later, on the relative size of the coarse fragments.

High permeability of the spoil can lead to a rapid build-up of the water table and subsequent rapid discharge of acid mine drainage. To moderate or prevent such

rapid build-up and discharge, we can employ selective placement of less permeable materials in specific portions of the profile to produce less permeable layers and reduce both the percolation and the discharge rates. However, a reduction in discharge can be offset by a build-up of acid products which, when eventually flushed out, may be quite concentrated. At times, coal is not mined completely to the edge of an outcrop. A certain width of it may be left, forming a natural internal barrier. Such an internal dam, when coupled with a less permeable layer, may submerge the acid layer and reduce the potential of pyrite oxidation. Current regulations in the United States, requiring topsoiling, revegetation and a stipulation that coal should not be stripped to the edge of deposit, reflect these types of practices. It appears that on materials similar to those studied, acid mine drainage potential will lessen through judicious placement of spoils, attention to particle size distributions, topsoiling, revegetation, and some control of flow rates.

CHEMICAL EFFECTS OF ATMOSPHERIC AND HYDROLOGIC ISOLATION

Placement of acid spoil below the water table can often reduce both the initial and the long-term acid loss. When submerged, the diffusion rate of O_2 is extremely low ($D = 1.8 \times 10^{-3}$ mm^2 s^{-1} in water) (Ohio State University, 1971). The low diffusion coefficient exerts a dominant control on the pyrite oxidation rate by limiting the O_2 input to reactions 5.3 and 5.4. This is the single most accepted reason given for placing acid spoil in a saturated zone.

$$FeS_2(s) + 3.5\ O_2 + H_2O = 2SO_4^{2-} + Fe^{2+} + 2H^+ \qquad (5.3)$$

$$Fe^{2+} + 0.25\ O_2 + H^+ = Fe^{3+} + 0.5\ H_2O \qquad (5.4)$$

Submergence is a sound approach, assuming that almost all of the sulfur in the acid spoil is pyritic or organic. However, this is not the case when the spoil contains substantial amounts of acid products and salts resulting from atmospheric exposure, either during previous or present mining activities, or contains salts indigenous to the formerly-intact strata. Note the high concentrations of SO_4 in unweathered and slightly weathered unmined coal overburdens in Table 5.1. The

TABLE 5.1. THE SULFATE, SULFIDE AND ORGANIC SULFUR CONTENT FOR UNMINED COAL OVERBURDEN

Geographic location	Lithology*	Sulfur content (%)†			Weathering‡
		Sulfate	Sulfide	Organic	
Somerset County, Pa.,§ near Somerset	B-1X, Lower Kittanning	0.01	1.64	0.17	S
	B-8X, Middle Kittanning	1.87	3.20	5.12	S
	B-11X, Middle Kittanning	2.13	8.08	1.68	U
	B-16X, Upper Kittanning	0.18	3.10	1.22	S
Clarion County, Pa., near West Freedom	A-3X, Upper Clarion	5.39	13.17	7.04	U
Clearfield County, Pa., near Westover	C-1X, Upper Freeport	0.03	0.24	0.06	S
	C-6, Upper Freeport	0.05	1.85	2.42	S
	C-8, Upper Freeport	1.02	1.18	0.03	S
Clearfield County, Pa., near Kylertown	B-1X, Lower Kittanning	0.74	1.98	1.10	N

*The number-hyphen-letter combinations, e.g. B-1, refer to lithologic position in the overburden strata. X refers to shale strata immediately overlying coal.

†Percent sulfur by weight.

‡From visible physical evidence: U = unweathered; S = slightly weathered; N = not classified.

§The first 8 spoils are from Lovell et al. (1978), the last one is from Pionke et al. (1980b).

dissolved SO_4 resulting from pyrite oxidation and subsequent secondary relations will generally be in the form of $FeSO_4$, $CaSO_4$, $MgSO_4$, $Al_2(SO_4)_3$ and $MnSO_4$, with the $CaSO_4$ being dominant, especially in the presence of limestone. All strata designated X in Table 5.1 represent strata immediately overlying coal. Based on the 3 western Pennsylvania sites studied by Lovell et al. (1978), these contain the highest pyritic and sulfate concentrations found in any strata except for the coal itself. In the absence of limestone, Pionke et al. (1980b) have observed the Fe^{2+}, Ca, Mg and Mn concentrations to be dominant and approximately equal in the leachates from the most acidic spoil layers. Assuming a 1:1 Fe to Ca mix of sulfates in layer C-8 of

Table 5.1 (1.02% SO_4-S, 1750 kg m^{-3} density, 0.30 m thickness), 1 ha of C-8 material would contain 127 metric tons of $FeSO_4$ and 114 metric tons of $CaSO_4$. In the extreme case of layer A-3X of Table 5.1 this would amount to 673 metric tons of $FeSO_4$ and 602 metric tons of $CaSO_4$. Within solubility limits, placing sizable quantities of this type of material below the water table would introduce large quantities of both acidic ($FeSO_4$, $Al_2(SO_4)_3$, $MnSO_4$) and non-acidic ($CaSO_4$, $MgSO_4$) salts directly into the groundwater system. This would also be true for spoils containing relatively low sulfate concentrations. For example, a 0.1% SO_4 concentration would yield about 24 metric tons of combined $FeSO_4$ and $CaSO_4$ per ha. The placement of SO_4-containing spoil below a water table, even in a slowly-moving groundwater system, may cause initially rapid leaching losses of SO_4 followed by a decrease according to a leaching-type curve (Figure 5.3a). In such a system, sulfate leaching losses, initially controlled by the hydrologic transport, become progressively more controlled by diffusion as the spoil-particle exterior is leached (Pionke et al., 1980b). Consequently, the initial SO_4 losses would be major and the long-term losses probably minor. Thus, the decision whether to place the most acid spoil layer below the water table may depend on the spoils' sulfate content and the type of control (short-term or long-term) desired.

Placement of the acid spoil below a soil surface but above the water table potentially exposes this spoil to a more rapid O_2 resupply rate and greater acid production, according to the reactions given in equations 5.3 and 5.4. However, it reduces the direct hydrologic exposure because of unsaturated conditions, intermittent flows, and only partial contact of flowing water with affected zones. This may reduce the expected high initial sulfate losses, but can increase the long-term losses due to increased atmospheric exposure and the reduced rate of leaching efficiency.

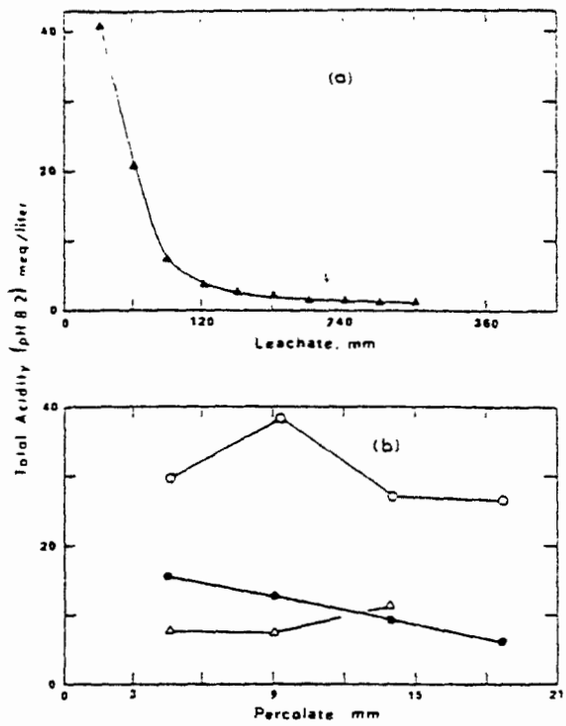

Figure 5.3. Total acidity as a function of (a) leachate, and (b) percolate quantity at 1.2 m (●), 2 m (△), and 2.5 m (○) below the spoil surface.

The O_2 resupply rate in spoil results primarily from O_2 diffusion. The usual exception is a thin mixing zone caused by temperature changes and wind profile near the surface. Within the O_2 diffusion zone, the oxygen resupply rate will depend on the diffusion path length and the porosity of overlying materials. Assuming a constant diffusion coefficient, D, in the diffusion equation, $F = D\ \partial C/\partial x$ where F is the transfer rate of diffusing substance per unit area, and $\partial C/\partial x$ is the concentration gradient normal to the surface, we can estimate both the effects of increasing the path length (depth of placement) or decreasing porosity (spoil settlement). The 6-10% volume reduction described earlier approximately translates into a 25% decrease in pore volume and cross-sectional pore area. The F values, or potential O_2 resupply rates, would thus decrease accordingly. Changing the path length has potentially an even greater effect. Spoil placement at a depth of 9 rather than 3 m

would decrease the $\partial C/\partial x$ by increasing the ∂x value. Assuming uniform spoil bank porosity and that only one spoil layer consumes O_2, the greater depth of placement would potentially decrease the O_2 resupply rate to approximately one-third the original rate. However, this rate could still exceed the O_2 consumption rate according to equations 5.3 and .4, and thus the deeper placement would not reduce acid production. Deeper placement, if effective, would probably provide a long-term rather than a short-term control. Rapid spoil settling, changes in density and reduction in pore volume would probably cause the greatest short-term changes. Moreover, the reclaimed spoil would initially contain a reservoir of approximately 20% O_2 in the pore space air. Assuming all O_2 consumed within 6 months by reaction 5.3 to form a 47% $CaSO_4$-53% $FeSO_4$ (1:1) mix, 28 metric tons ha^{-1} of the $CaSO_4$-$FeSO_4$ mixtures would be produced by a 9-m thick spoil profile, with a 50% initial pore volume.

Perhaps the most effective control on acid loss to groundwater from spoil placed above the water table may be the water flux rather than oxygen flux control. This assumes a certain type of chemical-hydrologic relationship. If we plot concentration of acid products in leachate versus leachate or percolate volume, we can get 2 basically different relationships, which are exemplified in Figure 5.3 (a and b).

The leaching-type curve (Figure 5.3a) can characterize a moving groundwater system. This curve was generated by measuring the acid product content in leachate from a spoil-filled column subjected to rapid, saturated throughflow (Pionke et al., 1980b). Decreasing the leachate volume within the linear part of the curve, e.g., from about 90 to 30 mm, would provide an approximately constant acid product load (concentration X water flow) delivered to groundwater. Thus, the acid product load lost to the groundwater system would be controlled by the resupply

rate of acid products from spoil to the surroundings, which appears to be diffusion controlled.

Figure 5.3b is the observed relationship between the amount of percolation under unsaturated flow conditions and total acidity of that percolate taken from lysimeters placed at different depths in Caisson 2 (Pionke et al., 1980a). In contrast to Figure 5.3a, reducing the percolate in Figure 5.3b would greatly reduce the acid product load delivered to the water table. For example, reducing the percolate to one-half (12-6 mm) substantially reduces the acid product load delivered to each lysimeter, and reduces it to about 1/2 the original load in 2 of the 3 lysimeters. This relationship characterizes the field situation where the load would be controlled by the percolation or flow rate.

The reason for the apparently stable percolate quality of Figure 5.3b is not known. We speculate that as percolation proceeds, the pathways of water flow through the spoil change, thus continuously leaching a percentage of fresh spoil. More likely, acid salt concentrations at or near the spoil particle surface are in excess of the flow transport capacities. Percolate control in the unsaturated system might therefore be particularly useful for treating spoils that contain high acid product concentrations. Its impact would probably be both initial and long-term.

INTRAPARTICLE DIFFUSION PROCESSES AFFECTING ACID PRODUCTION AND LOSS

Up to this point, we have considered either deep placement of the acid spoil en masse to reduce pyrite oxidation, or changes in percolation to control initial and long-term impacts on groundwater quality. Turning now to the individual spoil particle scale, where the particle is partially weathered, diffusion processes can potentially control acid production in situ or acid product loss to percolating or surrounding waters. Pionke et al. (1980b), using spoil B-1X (at the bottom of Table 5.1) and the published diffusion coefficients for the common SO_4 salts,

calculated the depth of the SO_4-salt-contributing zone within a spoil particle. This approach differs from that of Caruccio (1975) or Geidel (1979) in that we postulated a cylindrical model of spoil particle and applied to it diffusion theory to explain observed results. In contrast, the work of Caruccio (1975) and Geidel (1979) is based on experimental data from selected crushed (to pass 2-mm sieve) spoil materials, without an attempt at a theoretical development.

Assuming a cylindrical particle (Figure 5.4), conceptually, a boundary (r_a) exists within this particle that separates the weathered outer zone from the unweathered interior zone. Inside this boundary, the SO_4 concentration with depth is relatively uniform. Outside this boundary, SO_4 and O_2 gradients exist that control the transport rate of SO_4 to the particle surface, or of O_2 to the pyrite-containing interior. The weathered outer zone, of depth (r_b-r_a), was calculated using a diffusion equation and experimentally-collected input data. Converting the depth (r_b-r_a) to volume for different-sized cylindrical particles, the effective SO_4-contributing volumes in Figure 5.5 are readily calculated. Figure 5.5 shows that the effective SO_4-contributing volume to total spoil particle volume (%) decreases rapidly with increasing particle size. The considerably faster

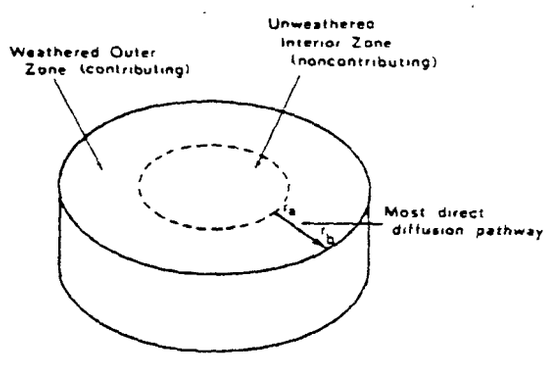

Figure 5.4. Assumed structure of cylindrical spoil particle.

diffusion of O_2 into the particle would shift the curve to the left but still provide the same basic relationship.

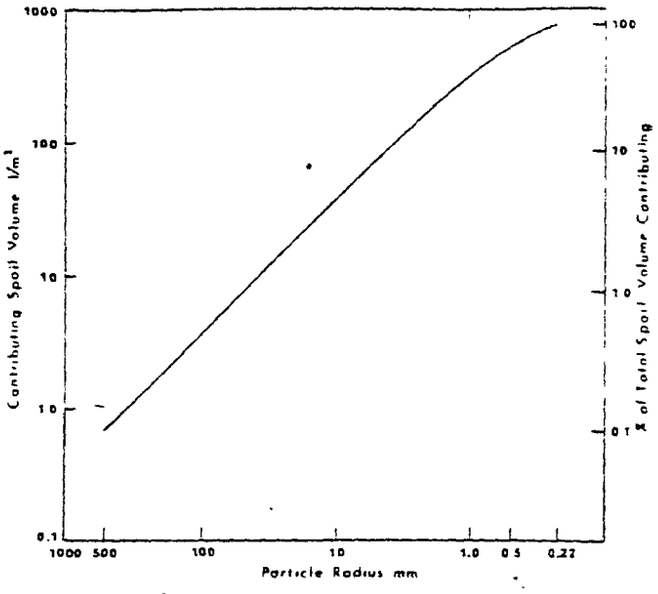

Figure 5.5. Contributing spoil volume as a function of cylindrical particle radius.

The values in Figure 5.5 apply strictly to spoil B-1X of Table 5.1 under submerged conditions. However, similar relationships would be expected for other spoils provided that diffusion processes were controlling, i.e. the mass movement-rate of water through the spoil particle was not significant. The impact of increasing the particle size, and thus decreasing the percentage of contributing volume, is basically a long-term one because the outer portion of the particle must become partially weathered and leached. The initial impact would probably be minor, because both the indigenous acid products and pyrite in the freshly fractured spoil would be in abundant supply at or near the particle surface.

The effectiveness of diffusion control was not studied for the unsaturated condition. In this case, the total pore space within the particle would be likely to contain both water and air. Potentially, the O_2 would diffuse much faster into the particle because of the far greater diffusion coefficient of O_2 in the air.

In contrast, the diffusion coefficients of SO_4 salts would be much less due to the lower water content. However, other conditions such as mass movement of water into the particle upon wetting, or out of the particle upon drying, with concomitant air entry and the continuity of air or water filled pores, could greatly alter the relationships between the spoil particle size and percent effective contributing volume.

We conclude that a number of spoil properties need to be considered before deciding how to handle acid spoils. Generally, these properties relate to, and often control, percolation and O_2 diffusion rates into the spoil bank. These include porosity, water retention, and particle size distribution of the topsoil, the layer below the topsoil, and the most acid spoil layer. Depth below the surface and differences in particle size distributions can substantially reduce the amount of percolate or slow the amount of O_2 delivered. Analysis of both SO_4 and pyrite concentrations in overburden can identify the most acid strata for subsequent isolation and can indicate whether placement should be above or below the water table. Placement above the water table, with emphasis on percolate control, may be a better method for highly SO_4-contaminated spoil, whereas placement below a nonfluctuating water table may be best for highly pyritic spoils low in SO_4. In addition, the rate of acid production and loss from spoil can potentially be managed by controlling the spoil particle size.

REFERENCES

1. ASTM. Standard Methods of Coal Analysis. American Society for Testing Materials, Philadelphia, Pa., 1971.
2. Baver, L. D., W. H. Gardner, and W. R. Gardner. Soil Physics. Fourth Edition, John Wiley and Sons, Inc., New York, 1972. 498 pp.
3. Caruccio, F. T. Estimating the Acid Potential of Coal Mine Refuse. In: The Ecology of Resource Degradation and Renewal, M. J. Chadwick and G. T. Goodman, eds. Blackwell Scientific, London, 1975. pp. 197-205.
4. Cedergren, H. T. Seepage, Drainage, and Flow Nets. John Wiley and Sons, Inc., New York, 1967. 489 pp.
5. Geidel, G. Alkaline and Acid Production Potentials of Overburden Materials: The Rate of Release. Reclam. Rev., 2(3/4):101-107, 1979.
6. Lovell, H. L., R. R. Parizek, D. Forsberg, M. Martin, D. Richardson, and J. Thompson. Environmental Control Survey of Selected Pennsylvania Strip Mining Sites. Final Report, Argonne National Laboratory, 9700 S. Cass Ave., Argonne, Ill. 60439, Contract No. 31-109-38-3497, 1978. 468 pp.
7. Miller, D. E. Water Retention and Flow in Layered Soil Profiles. In: Field Soil Water Regime. Spec. Publ. No. 5, Soil Science Society of America, Madison, Wis., 1973. pp. 107-117.
8. Ohio State University Research Foundation. Acid Mine Drainage Formation and Abatement. Water Pollution Control Research Service, DAST-42-14010 FPR-04/71, U.S. Environmental Protection Agency, Washington, D.C., 1971. 83 pp.
9. Pedersen, T. A., A. S. Rogowski, and R. Pennock, Jr. Comparison of Morphological and Chemical Characteristics of Some Soils and Minesoils. Reclam. Rev., 1:143-156, 1978.
10. Pedersen, T. A., A. S. Rogowski, and R. Pennock, Jr. Physical Characteristics of Some Minesoils. Soil Sci. Soc. Am. J., 44:321-328, 1980.

11. Pionke, H. B., A. S. Rogowski, and C. A. Montgomery. Percolate Quality of Strip Mine Spoil. Trans. ASAE, 23:621-628, 1980a.

12. Pionke, H. B., A. S. Rogowski, and R. J. DeAngelis. Controlling the Rate of Acid Loss from Strip Mine Spoil. J. Environ. Qual, 9:694-699, 1980b.

13. Rogowski, A. S. Acid Generation within a Spoil Profile: Preliminary Experimental Results. In: Seventh Symposium Coal Mine Drainage Research, NCA/BCR, The Coal Building, 1130 Seventeenth St., N.W., Washington, D.C. 20036, 1977. pp. 25-40.

14. Rogowski, A. S. Water Regime in Strip Mine Spoil. In: Surface Mining and Fish/Wildlife Needs in the Eastern U.S., D. E. Samuel, J. R. Stauffer, C. H. Hocutt, and W. T. Mason, Jr., eds. Proceedings of a Symposium, December 3-6, Morgantown, West Va., 1978. pp. 137-145.

15. Rogowski, A. S., and E. L. Jacoby, Jr. Monitoring Water Movement through Strip Mine Spoil Profiles. Trans. ASAE, 22:104-109, 114, 1979.

16. Vimmerstedt, J. P., and P. H. Struthers. Influence of Time and Precipitation on Chemical Composition of Spoil Drainage. In: Proceedings, Second Symposium Coal Mine Drainage Research, May 14-15, Pittsburgh, Pa., Bituminous Coal Research, Monroeville, Pa. 15146, 1968. pp. 152-163.

TECHNICAL REPORT DATA
(Please read Instructions on the reverse before completing)

1. REPORT NO. EPA-600/7-84-044	2.	3. RECIPIENT'S ACCESSION NO.
4. TITLE AND SUBTITLE Hydrology and Water Quality on Stripmined Lands		5. REPORT DATE March 1984
		6. PERFORMING ORGANIZATION CODE
7. AUTHOR(S) A. S. Rogowski and H. B. Pionke		8. PERFORMING ORGANIZATION REPORT NO. 8
9. PERFORMING ORGANIZATION NAME AND ADDRESS Northeast Watershed Research Center, USDA-ARS, 110 Research Building A, University Park, Pennsylvania 16802		10. PROGRAM ELEMENT NO.
		11. CONTRACT/GRANT NO. EPA-IAG-D5-E763
12. SPONSORING AGENCY NAME AND ADDRESS Office of Environmental Processes and Effects Research, Office of Research and Development, U.S. Environmental Protection Agency, Washington, DC 20460		13. TYPE OF REPORT AND PERIOD COVERED FINAL
		14. SPONSORING AGENCY CODE EPA/600/16

15. SUPPLEMENTARY NOTES
This project is part of the EPA-planned and coordinated Federal Interagency Energy/Environment R&D Program.

16. ABSTRACT

Studies were conducted to evaluate physical properties of spoils resulting from surface-coal mining and reclamation operations. Physical properties were determined at 10 sites randomly located within a 4-ha experimental area. Microlysimeter data indicated that evapotranspiration (ET) on minesoil could be approximated by class-A pan evaporation or by model results.

Two large caissons were also used to measure water movement in reconstituted spoil profile. Settlement was considerable and changes in temperature and bulk density were good indicators of water movement within the spoil and topsoiled spoil profiles. Flow through larger channels did contribute significant amounts of water to the water table.

Total acidity provided a reasonable estimate of other major chemical parameters contained in spoil drainage.

The concentrations of Cd, Cr, total soluble Fe, Hg, Mn and Zn in spoil extracts exceeded EPA water quality drinking standards from one (Cr) to all (Mn) spoil layers. The standards for Pb and Cu were not exceeded.

Specific placement of acid- and salt-containing spoil should be aimed at preventing contact with percolating water or rising water tables.

17. (Circle One or More) KEY WORDS AND DOCUMENT ANALYSIS

a. DESCRIPTORS			b. IDENTIFIERS/OPEN ENDED TERMS	c. COSATI Field/Group
Ecology Environments Earth Atmosphere Environmental Engineering Geography Other	Hydrology, Limnology Biochemistry Earth Hydrosphere Combustion Refining	Energy Conversion Physical Chemistry Materials Handling Inorganic Chemistry Organic Chemistry Chemical Engineering	Health Effects Materials Assessment	6F 8A 8F 8H 10A 10B 7B 7C 13B

18. DISTRIBUTION STATEMENT	19. SECURITY CLASS *(This Report)*	21. NO. OF PAGES
	20. SECURITY CLASS *(This page)*	22. PRICE

EPA Form 2220-1 (9-73)